10-5-2017

MIXING AND REACTIVITY CONTROL WITH BUTANOL AND ETHANOL IN COMPRESSION IGNITION ENGINES

Tongyang Gao
University of Windsor

MIXING AND REACTIVITY CONTROL WITH BUTANOL AND ETHANOL IN
COMPRESSION IGNITION ENGINES

by

Tongyang Gao

A Dissertation
Submitted to the Faculty of Graduate Studies
through the Department of Mechanical, Automotive and Materials Engineering
in Partial Fulfillment of the Requirements for
the Degree of Doctor of Philosophy at the
University of Windsor

Windsor, Ontario, Canada

2017

MIXING AND REACTIVITY CONTROL WITH BUTANOL AND ETHANOL IN
COMPRESSION IGNITION ENGINES

by

Tongyang Gao

APPROVED BY:

_____
M. Xu, External Examiner
Institute of Automotive Engineering, Shanghai Jiaotong University

_____
X. (Iris) Xu
Department of Civil and Environmental Engineering

_____
D. Ting
Department of Mechanical, Automotive and Materials Engineering

_____
J. Tjong
Department of Mechanical, Automotive and Materials Engineering

_____
M. Zheng, Advisor
Department of Mechanical, Automotive and Materials Engineering

_____
G. Reader, Co-advisor
Department of Mechanical, Automotive and Materials Engineering

September 11th, 2017

DECLARATION OF ORIGINALITY

I hereby certify that I am the sole author of this dissertation and that no part of this dissertation has been published or submitted for publication.

I certify that, to the best of my knowledge, my dissertation does not infringe upon anyone's copyright nor violate any proprietary rights and that any ideas, techniques, quotations, or any other material from the work of other people included in my dissertation, published or otherwise, are fully acknowledged in accordance with the standard referencing practices. Furthermore, to the extent that I have included copyrighted material that surpasses the bounds of fair dealing within the meaning of the Canada Copyright Act, I certify that I have obtained a written permission from the copyright owner(s) to include such material(s) in my dissertation and have included copies of such copyright clearances to my appendix.

I declare that this is a true copy of my dissertation, including any final revisions, as approved by my dissertation committee and the Graduate Studies office, and that this dissertation has not been submitted for a higher degree to any other University or Institution.

ABSTRACT

The objective of the research reported in this dissertation was to achieve clean and efficient combustion in a compression ignition engine. Previous research and literature have indicated that the control of the in-cylinder mixture preparation and charge reactivity are critical to improve combustion performance and to reduce emission formations. This research work hence focused on the exploration of the desired fuel mixing process and charge reactivity to reduce the emissions of nitrogen oxides and smoke while maintaining the high engine efficiency. Neat n-butanol, ethanol, and ultra-low sulfur diesel were used as the representative fuels to demonstrate the potential of using the significantly different physical and chemical properties to achieve the targets of combustion performance and emissions. Various fuel delivery strategies, assisted with intake boosting and EGR, were examined for the active control of charge mixing and reactivity.

Extensive experiments were performed on the two compression ignition engine platforms to systematically study the effectiveness of various engine control parameters on the regulation of ignition, combustion rate, and emission formation. The insufficient mixing of the diesel injection was observed as the primary cause for the high smoke emissions with the application of exhaust gas recirculation, while the high peak pressure rise rate in the n-butanol combustion is the main constraint for the high load applications. A promising approach to tackle the emission challenge is using inert premixed fuel to substitute the direct injection fuel. The combustion with the ethanol premixed fuel demonstrated promising results in emissions and efficiency. The n-butanol combustion showed an improved control over the combustion phasing.

With the knowledge obtained from the empirical analysis, the enhanced control of the in-cylinder charge mixing and reactivity was demonstrated in the partially premixed combustion with alcohol fuels. The combustion with n-butanol direct injection and ethanol port fuel injection was found to have low smoke emissions. The combustion with n-butanol multiple injections improved the control flexibility with different fueling strategies. The optimal combustion was demonstrated with the active management of fuel delivery, intake properties, and exhaust gas recirculation in each of the fueling strategies.

The n-butanol high pressure injection was also characterized with the injection rate measurement and the optical visualization under various injection conditions. The differences between the n-butanol injection and the diesel injection were investigated. The observations potentially improve the understanding of the combustion performance with the n-butanol injections.

DEDICATION

This dissertation is dedicated to

My Parents,

My Wife, Son, and Daughter.

ACKNOWLEDGEMENTS

Finally, I want to thank my parents, my wife, my son and my daughter, for their unconditional love, understanding, and support.

Tongyang Gao
Windsor, Ontario,
Canada
August 2017

TABLE OF CONTENTS

LIST OF TABLES

LIST OF FIGURES

LIST OF APPENDICES

NOMENCLATURE

AFR	Air to Fuel Ratio	[-]
BDC	Bottom Dead Centre	[-]
bhp-hr	Brake Horsepower Hour	[bhp-hr]
CA	Crank Angle	[°CA]
CA10	Crank Angle of 10% Heat Release	[°CA]
CA5	Crank Angle of 5% Heat Release	[°CA]
CA50	Crank Angle of 50% Heat Release	[°CA]
CAI	California Analytical Instruments	[-]
$C_\alpha H_\beta O_\gamma$	General Hydrocarbon Fuel	[-]
CI	Compression Ignition	[-]
CN	Cetane Number	[-]
CO	Carbon Monoxide	[-]
CO_2	Carbon Dioxide	[-]
cSt	CentiStoke	[-]
DAQ	Data Acquisition	[-]
DI	Direct Injection	[-]
DOC	Diesel Oxidation Catalyst	[-]
DPF	Diesel Particulate Filter	[-]
ECU	Engine Control Unit	[-]

EGR	Exhaust Gas Recirculation	[-]
EOC	End of Combustion	[°CA]
EPA	Environmental Protection Agency	[-]
EVO	Exhaust Valve Open	[°CA]
FACE	Fuels for Advanced Combustion Engines	[-]
FPGA	Field Programmable Gate Array	[-]
FSN	Filter Smoke Number	[-]
GHG	Greenhouse Gas	[-]
H₂O	Water	[-]
HC	Hydrocarbon	[-]
HCCI	Homogeneous Charge Compression Ignition	[-]
HFID	Heated Flame Ionization Detector	[-]
HFRR	High Frequency Reciprocating Rig	[-]
HiMICS	Homogeneous Charge Intelligent Multiple Injection Combustion System	[-]
HP	High Pressure	[-]
HRR	Heat Release Rate	[J/ °CA]
HTC	High Temperature Combustion	[-]
IBP	Initial Boiling Point	[°F]
ICE	Internal Combustion Engine	[-]
ID	Ignition Delay	[ms], [°CA]

IMEP	Indicated Mean Effective Pressure	[bar]
Inj.	Injection	[-]
Int.	Intake	[-]
IVC	Intake Valve Close	[°CA]
KV	Kinematic Viscosity	[mm^2/s]
LAN	Local Area Network	[-]
LHV	Lower Heating Value	[MJ/kg]
LNT	Lean NOx Trap	[-]
LP	Low Pressure	[-]
LTC	Low Temperature Combustion	[-]
$\dot{m}$	Mass Flow Rate	[g/s]
MAF	Mass Air Flow	[g/s]
$\dot{m}_f$	Fuelling Rate	[g/s], [mg/cycle]
MK	Modulated Kinetics	[-]
N$_2$	Nitrogen	[-]
NDIR	Non-Dispersive Infra-Red	[-]
NO	Nitric Oxide	[-]
N$_2$O	Nitrous Oxide	[-]
NO$_2$	Nitrogen Dioxide	[-]
NOx	Oxides of Nitrogen	[-]
O$_2$	Oxygen Gas	[-]

PC	Personal Computer	[-]
PCCI	Premixed Charge Compression Ignition	[-]
PCP	Peak Cylinder Pressure	[-]
PDA	Phase Doppler Anemometry	[-]
PFI	Port Fuel Injection	[-]
PFS	Partially Fuel Stratification	[-]
p_{inj}	Injection Pressure	[bar],[MPa]
p_{int}	Intake Pressure	[bar],[kPa],[MPa]
PM	Particulate Matter	[-]
PPC	Partially Premixed Combustion	[-]
ppm	Parts per Million	[ppm]
PREDIC	Premixed Lean Diesel Combustion	[-]
PRF	Primary Reference Fuel	[-]
PPRR	Peak Pressure Rise Rate	[bar/°CA]
PWM	Pulse Width Modulation	[-]
RCCI	Reactivity Controlled Compression Ignition	[-]
ROI	Rate of Injection	[-]
rpm	Revolutions per Minute	[rpm]
RT	Real-time	[-]
SCCI	Stratified Charge Compression Ignition	[-]
SCR	Selective Catalytic Reduction	[-]

SCRE	Single Cylinder Research Engine	[-]
SI	Spark Ignition	[-]
SOC	Start of Combustion	[°CA]
SOI	Start of Injection	[°CA]
T	Temperature	[°C], [K]
T90	90% Distillation Temperature	[°C], [K]
TDC	Top Dead Centre	[-]
THC	Total Hydrocarbon	[-]
TWC	Three-Way Catalytic Converter	[-]
ULSD	Ultra-low Sulfur Diesel	[-]
UNIBUS	Uniform Bulky Combustion System	[-]
US	United States	[-]
$\mathbf{V_d}$	Engine Displacement	[m^3], [L]
VGT	Variable Geometry Turbocharger	[-]
VVA	Variable Valve Actuation	[-]
VVT	Variable Valve Timing	[-]
WSD	Wear Scar Diameter	[μm]
λ	Excess Air Fuel Ratio	[-]
ζ	PFI Fuel Ratio	[%]

CHAPTER I

INTRODUCTION

1.1 Diesel Engines

Diesel engines have been used as the primary power systems for both mobile and stationary applications. The success of diesel engines can be attributed the exceptional fuel economy, mechanical durability, and robustness [1]. The high thermal efficiency of diesel engines is mainly attributed to the typically high engine expansion ratio and the overall fuel-lean operation. Additionally, the lack of intake throttling is also advantageous for fuel economy at partial engine loads. However, the harmful pollutions emitted from diesel engines create serious environmental problems. A primary focus of modern diesel engine development is the reduction of these pollutants without compromising the high fuel efficiency.

Tremendous technical advancements in diesel engines have been made in the recent decades for cleaner combustion and better fuel economy, such as exhaust gas recirculation (EGR), intake air boosting, common rail fuel injection, and exhaust after-treatment. The application of EGR has proven to be an effective method for suppressing the formation of nitrogen oxides during the diesel combustion [2]. Intake air boosting can significantly increase the engine power density and compensate for the oxygen displacement caused by the EGR application. The common rail fuel injection system can provide a stable fuel injection pressure and facilitate a flexible fuel injection scheduling. After-treatment techniques can further reduce the engine-out emissions to satisfy the increasingly stringent emission regulations.

1

The common operating process of a modern four-stroke diesel engine is demonstrated in Figure 1-1. The three essential elements to initiate the engine combustion include the diesel fuel, the intake air, and the energy for ignition. Traditionally, only fresh air is drawn into the combustion chamber during the engine intake stroke. The diesel fuel is then injected into the combustion chamber at the completion of cylinder compression, when the temperature of the in-cylinder charge is higher than the auto-ignition temperature of diesel. An engine compression ratio higher than that of gasoline engines, can be used without the constraint of premature combustion. The load control of a diesel engine is commonly implemented through the regulation of the amount of fuel delivered into the combustion chamber. The intake air amount is in excess of what is required for the stoichiometric combustion. Hence, the diesel engine is generally operated in the fuel-lean conditions with excess oxygen left in the exhaust stream.

The reduction of NOx emissions is a challenging task in diesel engines. The application of EGR decreases the NOx formation by reducing the intake oxygen level. However, extensive EGR may also reduce the combustion efficiency due to the increased emissions of partially oxidized products, such as particulate matter (PM), total hydrocarbons, and carbon monoxide. The after-treatment techniques, such as selective catalytic reduction (SCR) and lean NOx trap (LNT), are capable of suppressing the tailpipe NOx emissions. Nevertheless, a reducing agent is frequently required in both the techniques for the NOx conversion. Furthermore, additional systems for delivering the reducing agent are also necessary for the implementation of these after-treatment techniques.

2
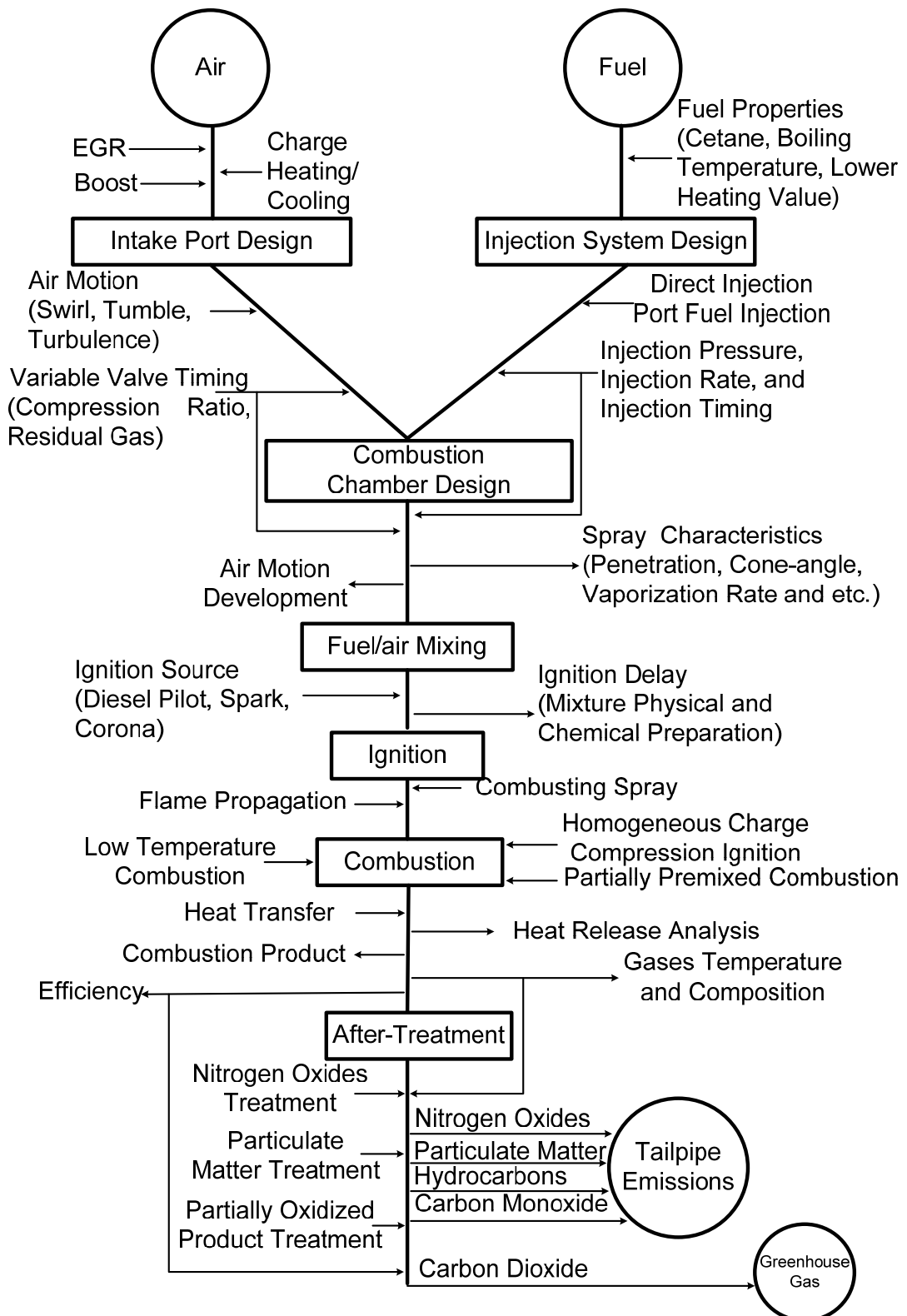
Figure 1-1 Block diagram for typical diesel engine operation, adapted from [3]

1.2 Diesel Fuel

Diesel fuel is a complex mixture of paraffinic, naphthenic, and aromatic hydrocarbons [4]. The overall diesel properties are determined by the characteristics of the individual hydrocarbons. The specific property of diesel can vary in a wide range because of the variations in the crude oil sources and the refinery processes. Various additives are also added to the commercial diesel fuel to improve the fuel quality, such as lubricity improvers and fuel stabilizers.

The selected fuel standards from ASTM D975 for the US No. 2 ultra-low sulfur diesel (ULSD) [5] are listed in Table 1-1. The critical fuel properties that often affect engine combustion and operation include Cetane number, volatility, viscosity, and lubricity. Cetane number is a measure of the fuel reactivity to compression ignition. A fuel with a higher Cetane number typically has a shorter ignition delay under various engine operating conditions. Hence, the combustion of the fuel of high Cetane number tends to be closely coupled with the fuel injection event. The separation of the combustion event from the injection event, which is often required for improved in-cylinder charge mixing and low emissions, becomes challenging in diesel engines.

The volatility of a fuel is often evaluated with T90 (the distillation temperature of 90% of the fuel by volume), if the fuel is a mixture rather than a pure substance. The minimum required T90 of No. 2 ULSD is higher than the typical engine intake temperature. The direct use of diesel port injection is thus challenging without additional intake heating. Furthermore, the diesel injections deployed early in the compression stroke may potentially lead to the wall impingement and lubrication oil dilution.

4

Table 1-1 Fuel standards for US No. 2 ULSD [5]

Fuel Property	ASTM D975	Effect of Property on Performance
Cetane Number [-], min	40	Measure of ignition quality – affects cold starting, combustion, and emissions
Flash Point [°C], min	52	Safety in handling and use – not directly related to engine performance
T90 [°C], min	282	Measure of fuel volatility – affects spray evaporation, smoke, and combustion
T90 [°C], max	338	
KV[1] [mm^2/s], min	1.9	Affects fuel spray atomization and fuel system leakage and lubrication.
KV [mm^2/s], max	4.1	
WSD[2] @ 40 °C [μm], max	520	Affects fuel injection system (*i.e.* pump and injector) wear

1. KV: kinematic viscosity @ 40 °C

2. WSD: wear scar diameter from high frequency reciprocating rig test

The viscosity of a fuel is a measure of the resistance to shear flow. This property affects the liquid film thickness in the diesel fuel systems. In a common rail fuel system, diesel fuel is the working fluid as well as the coolant and the lubricant. A thicker liquid film often provides better heat transfer and better protection between the moving metal components. Moreover, the viscosity also affects the fluid velocity through narrow gaps and orifices. A fuel with a higher viscosity often flows slower under a fixed differential pressure. The fuel jet also has a lower tendency to break up into small droplets. Therefore, the required viscosity of the ULSD is in a range of 1.9 to 4.1: the minimum threshold is

primarily required for the sufficient cooling and lubrication, while the maximum one is important for the flow performance and fuel spray atomization.

The lubricity of a fuel is a direct measure of the lubrication performance. A common way to evaluate the lubricity is using a high frequency reciprocating rig (HFRR). In the experiment, a steel ball rubs for 75 minutes on a steel plate that is submerged in the test fuel. The diameter of the wear scar on the steel plate is used to evaluate the lubricity of the fuel. A smaller diameter indicates a better lubricity of the fuel.

1.3 Combustion in Diesel Engines

A simplified reaction, as shown in Eq. (1-1), can be employed to illustrate the combustion process in diesel engines. The three essential elements for combustion, as given in Figure 1-1, are included in this equation. A generic formula of hydrocarbon is used to represent the fuel. The fresh air is considered as a mixture of oxygen and nitrogen, while other minor compositions are disregarded. The ignition energy is provided from the high temperature generated during the engine compression stroke. The fuel is fully oxidized to carbon dioxides (CO_2) and water (H_2O). Pollutants other than CO_2 are not taken into consideration due to their low concentrations, but the presence of these emissions should not be disregarded.

$$C_\alpha H_\beta O_\gamma + \lambda(\alpha + \beta/4 - \gamma/2)(O_2 + 3.76 N_2) \rightarrow$$

$$\alpha CO_2 + (\beta/2)H_2O + (\lambda - 1)(\alpha + \beta/4 - \gamma/2)\,O_2 + 3.76\lambda(\alpha + \beta/4 - \gamma/2)N_2 \qquad (1\text{-}1)$$

6
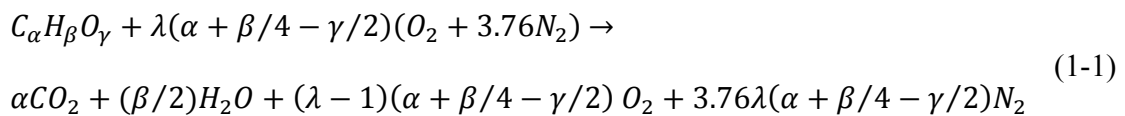
A quantitative analysis of combustion process is often conducted through the heat release estimation using the in-cylinder pressure data. A heat release rate (HRR) curve, as shown in Figure 1-2, is commonly used as the indication of the fuel energy released during combustion.
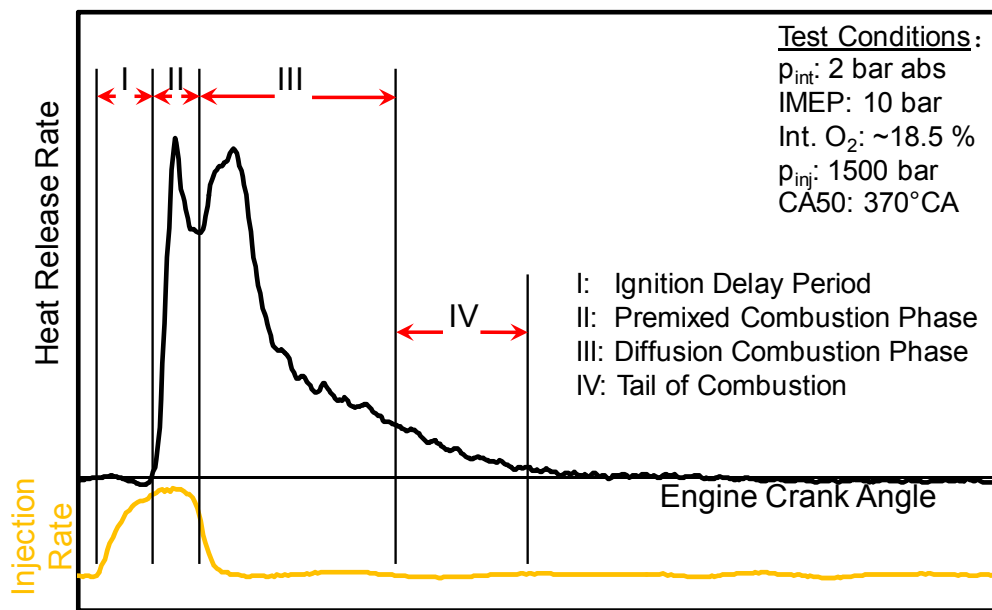
Figure 1-2 Typical HRR of combustion in conventional diesel engines

The HRR of conventional diesel combustion can often be categorized into four phases: ignition delay period (I), premixed combustion phase (II), diffusion combustion phase (III), and tail of combustion (IV) [6].

I. Ignition delay period: the ignition delay period is defined as the duration from the start of injection (SOI) to the start of combustion (SOC). The SOC is commonly determined from the cumulative heat release, while the SOI can be determined with the injection command and injection opening delay. The ignition delay period is essential for the reactants to prepare for combustion. A liquid jet needs time to atomize, evaporate, and

7

mix with the surrounding air. When the local air to fuel ratio (AFR) and the temperature are sufficient for auto-ignition, the combustion initiates at the regions with the mixed charge.

II. Premixed combustion phase: the heat released in this phase is mainly from the combustion of the premixed in-cylinder charge. The combustion can often be identified from the intense energy release. The portion of premixed combustion is primarily determined by the ignition delay and the fuel volatility. The premixed combustion often forms low smoke emissions.

III. Diffusion combustion phase: the fuel that has not been consumed during the premixed combustion phase is oxidized in this phase. The fuel is often surrounded by the burnt gas from the premixed combustion. Although the local temperature is typically higher than the auto-ignition temperature of the fuel, the reaction is limited by the diffusion of fuel into the surrounding oxygen. In this heated environment, the combustion often continues in fuel-rich regions. High emissions of NOx and smoke are formed at this high combustion temperature.

IV. Tail of combustion: the tail of combustion is identified from the lower HRR and the relatively long duration especially at a higher engine load. The majority of the fuel is burnt in the premixed and diffusion combustion phases. The partially reacted emissions may get oxidized in this phase if the in-cylinder temperature is sufficiently high and the oxygen is available for the reaction.

1.4 Exhaust Emissions from Diesel Engines

The primary exhaust emissions from diesel engines, which are regulated by the regulatory authorities, consist of nitrogen oxides (NOx), particulate matter (PM), carbon monoxide (CO), and total hydrocarbons (THC) [7]. The concentrations of these pollutants are lower compared to the primary compositions in the exhaust gas from diesel engines, such as nitrogen (N_2), oxygen (O_2), H_2O, and CO_2. However, the impacts of the emissions on the environment and human health are more significant. The primary formation mechanisms and reaction pathways of these emissions are described in the following subsections.

1.4.1 Nitrogen Oxides

Nitrogen oxides are a group of chemicals that are composed of nitrogen and oxygen. The two most common NOx emissions from diesel engines are nitric oxide (NO) and nitrogen dioxide (NO_2). NOx emissions are often regulated on a NO_2 equivalent basis because it is the most prevalent form of NOx in the atmosphere that is generated by human activities [8]. NO_2 can react in the atmosphere to form the tropospheric ozone (O_3), as shown in Reaction (1-2). The tropospheric ozone is an essential reactant for smog.

$$NO_2 + O_2 \leftrightarrow NO + O_3 \qquad (1\text{-}2)$$

The primary NOx pollutants from conventional diesel engine exhaust are NO emissions. The NO formation in the conventional high temperature combustion of diesel can be explained with the Extended Zeldovich mechanism [8], as shown in Reactions (1-3), (1-

9

4), and (1-5). This mechanism is also referred to as the thermal mechanism because the majority of NO is formed at a temperature exceeding 2000 K. The single nitrogen radical, which is generated from Reaction (1-3), is essential for Reaction (1-4) and (1-5) to proceed to the side of NO production. Reaction (1-3) requires high activation energy (high temperature) to break the strong triple bonds in N_2. Therefore, the local combustion temperature and the local flame temperature determine the formation rate of the thermal NOx. An effective emission control technique that suppresses the NOx formation during this stage, such as EGR, often reduces the combustion temperature.

$$N_2 + O \leftrightarrow NO + N \tag{1-3}$$

$$N + O_2 \leftrightarrow NO + O \tag{1-4}$$

$$N + OH \leftrightarrow NO + H \tag{1-5}$$

1.4.2 Carbon Monoxide

Carbon monoxide is produced by the incomplete oxidization of a hydrocarbon fuel. Sufficiently high temperature and available oxygen are the two essential conditions for the CO emissions to be further oxidized to CO_2 [15]. Therefore, the CO emissions, which are initially formed in the fuel-rich regions, are often further oxidized by the excess oxygen in the conventional high temperature combustion. In stark contrast, the CO emissions have a lower tendency to be oxidized in the low temperature combustion that is implemented to lower the emissions of NOx and smoke. Because of the lowered combustion temperature and the reduced intake oxygen level, the CO emissions at these

combustion modes are often higher than that from the conventional diesel high temperature combustion.

1.4.3 Total Hydrocarbon

The majority of the total hydrocarbon emissions are the unburned fuel and the light hydrocarbons from the fuel cracking reactions. The THC emissions may also include some oxygenated hydrocarbons, such as alcohol and aldehydes. A small portion of THC emissions are from the evaporation and oxidization of the engine lubricating oil.

The diesel engines operated under the high temperature combustion mode often produce low THC emissions because of the fuel-lean combustion, high combustion temperature, high compression ratio, and in-cylinder direct fuel injection. However, the THC emissions are typically higher when the engine is running under the low temperature combustion mode due to the prolonged ignition delay and the increased portion of premixed charge [15].

1.5 Emission Regulations

The emission standards from major regulatory authorities over the world have become more stringent in the recent several decades. The emission regulations for heavy-duty diesel engines from the United States (US) Environmental Protection Agency (EPA) are shown in Figure 1-3 as an example. The standards for the NOx and PM emissions have been reduced by more than 90% over the past 30 years. The emission standards for these emissions remain at the same level as the 2012 standards. The greenhouse gas (GHG) emissions of carbon dioxide have been regulated since 2014. [7, 10]

US EPA Emission Standards for Heavy-duty Diesel Engines

Engine MY	1988	1998	2004	2012	2014	2017
NO_X (g/bhp-hr)	6.0	2.4	2.0	0.2	0.2	0.2
PM (g/bhp-hr)	0.6	0.1	0.1	0.01	0.01	0.01
CO_2 (g/bhp-hr)	-	-	-	-	489	474

Technical Solutions	1988-1998 Injection Timing Turbocharging DOC	1998-2004 Common-rail EGR & Boost DPF	2004-2010 Common-rail LTC Aftertreatment	2010-present/future Renewable Fuel Lightweighting Aftertreatment

Figure 1-3 Emission standards summary for US EPA heavy duty diesel engines

The emission requirements for NOx, PM, and GHG have significantly increased the challenges in diesel engine development, because the typical emission reduction strategies for NOx and PM often have conflicting impacts on engine efficiency and GHG emissions. For example, simultaneously low NOx and smoke emissions can be achieved with a high EGR rate in diesel low temperature combustion [11]. However, the engine thermal efficiency is often reduced by the lowered combustion efficiency (high emissions of CO and THC).

1.6 Mixing and Charge Reactivity in Compression Ignition Engines

The mixing of a direct fuel injection in compression igntion engines occurs when the fuel at a high pressure is injected into the compressed air inside the combustion chamber. The injected liquid fuel atomizes, evaporates, and mixes with the surrounding air to prepare the combustible mixing [6]. The liquid fuel may evaporate completely before the onset of

combustion, as in homogeneous charge compression ignition (HCCI) [12]. The fuel evaporation and mixing may still continue during the combustion process, as in the diffusion phase of conventional diesel combustion.

The charge reactivity in compression ignition engines is mainly regulated from thermal impacts and compositional impacts [13]. The thermal impacts are mainly determined by the temperature of the in-cylinder charge that varies continuously during the engine compression and expansion stroke. The compositional impacts are primarily from the AFR gradient and the oxygen concentration [13]. Moreover, a fuel with a higher Cetane number potentially increases the overall charge reactivity [14].

1.7 Research Objective and Dissertation Contribution

The objective of the research presented in this dissertation is to achieve clean and efficient combustion in a compression ignition engine. Neat n-butanol, ethanol, and diesel are used as the representative fuels to demonstrate the potential of using the significantly different physical and chemical properties to achieve the targets of combustion performance and emissions. Various fuel delivery strategies, assisted with intake boosting and EGR, are examined for their effects on combustion characteristics and emissions.

The specific objectives of this dissertation can be summarized as follows:

1. To control the mixing process of the in-cylinder charge with direct fuel injection of diesel and n-butanol, and to investigate the trade-off between the emissions of NOx and smoke.

2. To actively modulate the reactivity in a premixed charge using port fuel injection (PFI) of ethanol and n-butanol, and to study the control effectiveness of various fuel delivery strategies under the applications of EGR and intake boosting.

3. To develop clean combustion strategies using n-butanol and ethanol, and to explore the potential engine load range with high efficiency and low emissions of NOx and smoke.

4. To examine the correlations between the injector control parameters (*i.e.* injection duration and injection pressure) and the actual injection characteristics (*i.e.* injection rate, injection opening delay, and injection closing delay) of the direct injection (DI) of n-butanol.

The dissertation contributions include:

1. Identified that the primary explanation for the emission trade-off in diesel combustion is the insufficient mixing of diesel at high fuel reactivity.

2. Enhanced the mixing process with n-butanol direct injection and demonstrated ultra-low emissions of NOx and smoke with the prolonged ignition delay.

3. Improved the ignition quality of n-butanol direct injections (DI) with a higher intake pressure and a high intake temperature on the two engine research platforms.

4. Achieved the reactivity control with direct injection of diesel in a premixed charge of ethanol. The fuel ratio between the port injected fuel and the directly injected fuel is identified as a critical factor for combustion performance and emission formations.

14

5. Conducted a detailed analysis on the effectiveness of various fuel delivery strategies on the control of mixing and charge reactivity with a high intake pressure and the application of EGR.

6. Proposed an injection strategy with multiple injections of diesel to increase the reactivity of the premixed ethanol charge, and reduce the THC and CO emissions.

7. Demonstrated the HCCI combustion with n-butanol port fuel injection, and identified the control challenges in combustion rate and combustion phasing.

8. Demonstrated combustion with n-butanol and ethanol at comparable engine loads and fuel efficiencies of diesel with considerably lower emissions of NOx and smoke.

9. Quantified the injection rate of the n-butanol high pressure injection, visualized the n-butanol high pressure injection in a constant volume chamber under a high background pressure, and measured the fuel droplet velocity and diameter with laser phase Doppler anemometry.

1.8 Dissertation Organization

The dissertation structure is schematically illustrated in Figure 1-4. In Chapter 1, the research motivations, research objectives, and primary dissertation contributions are outlined with the brief introduction of the combustion process in diesel engines and the emission regulations. A literature review is conducted in Chapter 2 for an overview of the previously published research work related to the control of charge mixing and reactivity with various engine control parameters. The research methodology and experimental setup are given in Chapter 3. These three chapters are categorized as the preparatory work for this dissertation.

The core of this dissertation is the empirical investigation of the control of the in-cylinder charge preparation and charge reactivity. Chapter 4 presents the characterization of the n-butanol high pressure fuel injections with the measurement of the injection rate, injection opening and closing delays, as well as the performance of multiple fuel injections. The differences between the diesel DI and n-butanol DI are highlighted. Chapter 5 describes the results of using direct fuel injection of diesel and n-butanol to control the mixing process. The trade-off between the emissions of NOx and smoke is overcome by the enhanced mixing of n-butanol DI. The high combustion rate and the low ignition ability in the n-butanol combustion are also investigated. The charge reactivity modulation is studied in Chapter 6 with a premixed charge formed with the port injection of ethanol and n-butanol. A systematic analysis of the fuel delivery impacts is conducted at various intake pressures and EGR levels. The HCCI combustion of n-butanol is also investigated in this chapter. Based on the knowledge gained from the previous chapters, the partially premixed combustion with n-butanol and ethanol is shown in Chapter 7.

Finally, the significant research findings are summarized in Chapter 8. The recommendations for the future work are also given in this chapter.

PREPARATORY WORK

CHAPTER 1
Introduction
- Diesel Engine Operation Principles
- Diesel Fuel Properties
- Combustion in Diesel Engines and Heat Release Rate
- Emissions and Emission Regulations

CHAPTER 2
Literature Review
- In-cylinder DI Feature and Implementation
- Engine Parameters Used for Mixing and Reactivity Control
- Low Emission Combustion Strategies: LTC, HCCI, RCCI, PPC

CHAPTER 3
Methodology and Experimental Setup
- Methodology and Research Approaches
- Advanced Research Engine Platform: Research Engines, Air Management, Implementation of EGR, Fuel Delivery Systems, and Emission Measurement
- Offline Fuel Injection Characterization: EFS Injection Bench, Bosch Long Tube, High Speed Camera, Laser, and Constant Volume Chamber

EMPIRICAL INVESTIGATION

CHAPTER 4
N-butanol High Pressure Injections
- Offline Study of the Effects of Injection Pressure, Injection Timing, and Injection Duration on Fuel Delivery and Injector Characteristics
- Multiple Fuel Injection Interactions
- Optical Visualization of the N-Butanol Spray and Laser PDA

CHAPTER 5
Mixing Control with Direct Fuel Injection
- Mixing Control with DI Diesel, Causes for NOx-Smoke Trade-off, and Effectiveness of Injection Strategies
- Mixing Enhancement with DI N-butanol, Ignition Delay, Combustion Rate, an Ignition Improvement with Intake Heating
- Comparison between Different Engines

CHAPTER 7
Partially Premixed Combustion with Butanol
- N-butanol DI with Ethanol PFI, Ignition, Combustion Phasing Control, Emissions, Load Span
- N-butanol PFI and N-butanol DI, Engine Load Extension, Fuel Ratios, Emissions
- N-butanol Multiple Injections, Improved Mixing Control, Demonstration of Clean Combustion at High Load

CHAPTER 6
Reactivity Modulation in Premixed Charge
- Combustion with Ethanol PFI, Impacts of Various Fuel Delivery Parameters at Different Intake Pressures and EGR Levels
- Diesel Micro Pilot Strategy to Increase Charge Reactivity and Reduce THC and CO Emissions
- N-butanol HCCI Combustion: Load Span, Potential and Challenges
- Combustion with N-butanol PFI, Fuel Ratios, EGR, Strong NOx-Smoke Trade-off

CHAPTER 8
Conclusions and Future Work
- Summary of Research Observations
- Future Work and Recommendations

Figure 1-4 Dissertation organization

CHAPTER II

LITERATURE REVIEW

This chapter provides a review of the previously published work related to the control of charge mixing and reactivity in CI engines with conventional diesel fuel and unconventional alternative fuels, such as ethanol and n-butanol. It covers the main techniques which have been used to achieve the combustion control, including the fuel delivery method, the management of intake gas property, and engine hardware improvement. In addition, a summary of the representative combustion strategies for simultaneous reduction of NOx and smoke emissions is also included. The salient features and limitations of each strategy are highlighted.

2.1 Fuel Delivery Technique in CI Engines

The fuel delivery technique is critical, which significantly affects the engine combustion characteristics [16]. It controls the in-cylinder fuel distribution, the mixing process, and the charge reactivity. The primary fuel delivery methods in modern compression ignition engines include port fuel injection and direct fuel injection.

2.1.1 Port Fuel Injection

Port fuel injection is a technique of delivering fuel through the intake port of an engine cylinder. A relatively simple fuel supply system working at a low pressure can be used in the application of port fuel injection [17]. The mixing of the fuel and air begins inside the intake manifold and continues in the engine cylinder. A fully premixed in-cylinder charge is often formed during the engine intake stroke and the compression stroke, before the

18

onset of combustion. Hence, the impact of PFI on the combustion event is mainly through the fuel injection quantity rather than the injection timing.

2.1.2 Direct Fuel Injection

Direct fuel injection in diesel engines refers to the process of supplying fuel directly into the compressed charge inside the combustion chamber. This injection technique has been recognized as an effective technique to generate the stratified charge and thus to broaden the engine operation limit of clean combustion [18-22]. With a common rail fuel injection system, the fuel injection timing, injection amount, and injection events can be precisely implemented to generate the reliable ignition [23, 24], to prevent the premature combustion [25, 26], and to regulate the burn rate [27].

The direct fuel injection provides the essential gradient in AFR for auto-ignition. A conceptual model for the combusting spray has been proposed by Dec [28] to explain the diesel combustion during the mixing-controlled burn (diffusion combustion). Before the onset of combustion in a diesel engine, the direct injection of the liquid fuel atomizes, evaporates, and then mixes with the surrounding air. The AFR gradient of the in-cylinder mixture can cover a wide range from fuel-rich to fuel-lean, as shown in Figure 2-1. The emission formation regions for NOx and smoke are illustrated based on the equivalence ratio and temperature (Φ-T) diagram proposed by Kamimoto *et al.* in [30]. The possible operation pathways for high temperature combustion (HTC) and low temperature combustion (LTC) are also shown in Figure 2-1. The management of the DI strategy is capable of producing the desired equivalence ratio and temperature for low emissions of NOx and smoke. The combustion with low NOx and smoke emissions has been

demonstrated with direct injection of diesel in [31-37], assisted by EGR and intake boosting.
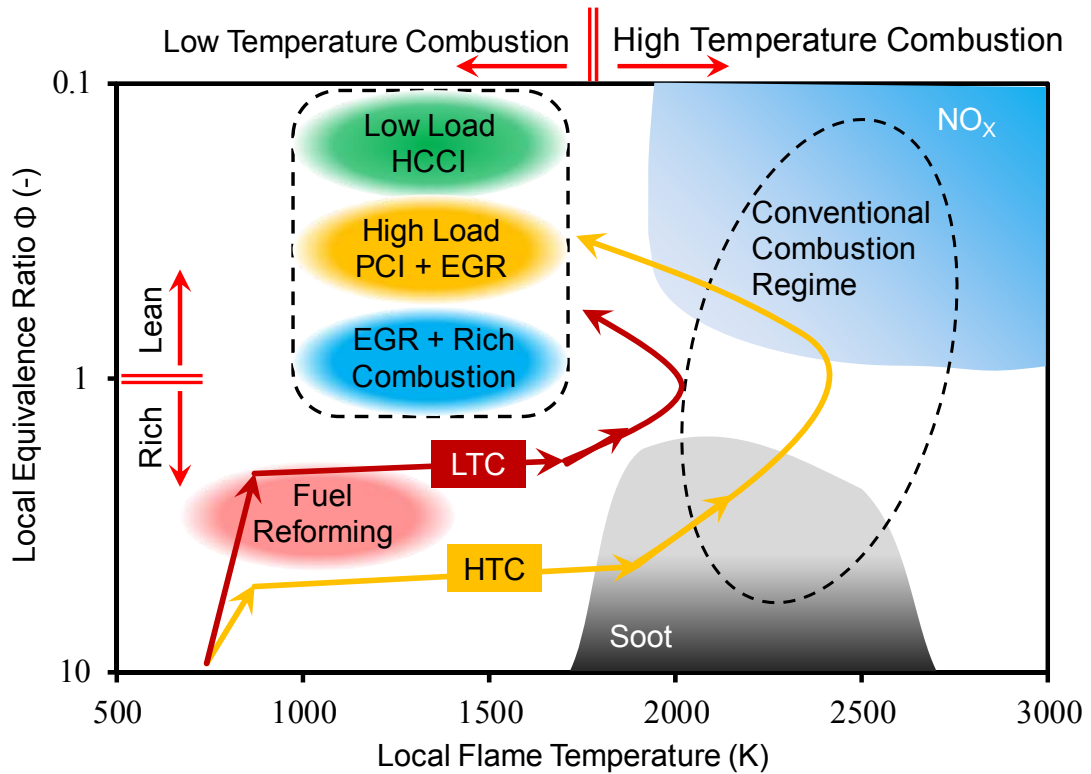
Figure 2-1 Pathways for low temperature combustion

The characterization of the DI event (*i.e.* penetration, cone angle, droplet size distribution, and injection rate) can provide important insights to interpret the combustion and emission characteristics from an engine [39], as well as valuable guidance for developing advanced injection strategies and optimizing the engine hardware [40, 41]. Offline injection measurement with the constant volume chamber [42, 43], the laser phase Doppler anemometry [44], the long tube [45], the momentum sensor [46], and the optical-accessible engines [28] have been employed in the past to study the characteristics of the direct fuel injection.

Additional fuel delivery systems can be employed to supply different fuels in the combustion research with compression ignition engines. A single fuel and the single fuel delivery system are often not sufficient to optimize the combustion performance and emissions in advanced combustion modes. Dual fueling systems have been used in the literature [18, 25, & 33]. Moreover, a single injector with dual-fuel capability [53] and dual injectors inside a single cylinder [50] have also been tested.

2.2 Fuel Property Impact on Combustion and Emissions

The primary reference fuels (PRF), such as n-heptane and iso-octane, are commonly employed to study the fuel property impacts on combustion in diesel engines. Lu *et al.* [48] have explored various combinations of n-heptane and iso-octane in a single cylinder engine under stratified charge compression ignition (SCCI). With the two-stage PFI of n-heptane and iso-octane, and DI of n-heptane, the stratification of the in-cylinder fuel is created. Thus, the heat release rate and in-cylinder temperature distribution can be controlled. Sjoberg *et al.* [50] have examined a single-stage ignition fuel (iso-octane) and a two-stage ignition fuel PRF80 (a mixture of 80% iso-octane and 20% n-heptane) in a homogeneous charge compression ignition (HCCI) engine. The combustion of PRF80 exhibits lower cycle-to-cycle variations with a retarded combustion phasing, and the combustion is more sensitive to the changes of the EGR temperature and the concentrations of hydrocarbon species in the EGR.

Alternative fuels have also been tested in CI engines to study the engine performance and emissions. Ojeda *et al.* [47] have reported nine diesel fuels for advanced combustion engines (FACE) with different fuel properties. These FACE fuels have been used as the DI fuels in a common rail fuel injection system. The empirical results have revealed that

21

a lower Cetane number (CN) is beneficial for a longer ignition delay, while a higher volatility enhances the fuel mixing. Alptekin [49] has tested the biodiesel produced from canola oil and safflower oil in a multi-cylinder diesel engine. Compared with the combustion baseline of diesel, the combustion of biodiesel emits more NOx emissions at similar operating conditions. Zheng *et al.* [51] have investigated the direct injection of neat n-butanol under the LTC strategy. The oxygen content in the fuel, the lower reactivity, and the higher volatility of n-butanol are found to be beneficial for lower emissions of NOx and smoke. McTaggart-Cowan *et al.* [52] have used a diesel pilot to ignite natural gas blended with ethane, propane, hydrogen, and nitrogen. An increased heat release rate has been observed with the enhanced charge mixing and the increased fuel reactivity.

2.3 Management of Intake Gas Properties for Clean Combustion

The enabling of clean combustion in CI engines requires the precise management of the intake gas properties. The controlled intake gas properties discussed in this section include intake pressure, intake temperature, and intake compositions.

Intake heating is a technique that can be implemented to improve the ignition consistency and control the timing of the start of combustion for the fuel with low reactivity [59]. Nevertheless, the air density and the charging efficiency are often reduced at a higher intake temperature.

The application of EGR is a widely employed technique to vary the intake compositions by introducing the burnt exhaust gas back into the engine intake. The effects of EGR on combustion have been summarized by Sjoberg *et al.* [61] as thermodynamic retarding

(specific heat capacity increase), chemical retarding (oxygen dilution), and chemical enhancing (additions of H_2O and partially oxidized species). It has been revealed that the CO_2 dilution is the most effective method to delay the start of combustion among the tested techniques.

The application of EGR is a primary technique to suppress NOx emissions in CI engines [51]. The NOx reduction is achieved mainly because of the lowered flame temperature and the diluted intake oxygen concentration. The combustion efficiency and emissions are sensitive to the EGR rate when the engine is operated the low temperature combustion mode [62]. A small fluctuation in the EGR rate at a high EGR rate (more than 50%) may increase the emissions and reduce the combustion efficiency when the EGR rate is [63]. The in-cylinder charge composition and compression temperature may also be affected by the EGR fluctuations.

2.4 Piston Bore Geometry Optimization

Piston bore geometry optimization is an indispensable aspect for CI engines to achieve the clean combustion [64]. A lowered engine compression ratio can reduce the emissions of NOx and smoke but increase the emissions of HC and CO in the premixed charge compression ignition, as reported in [65]. An open-bowl piston is preferable for premix-dominated combustion [66]. The open geometry reduces the squish volume that is beneficial to lower the HC and CO emissions, and it can tolerate relatively early fuel injections to reduce the potential wall impingement.

2.5 Clean Combustion Strategies

The reduction of NOx emissions in CI engines is challenging because of oxygen in the engine exhaust that limits the application of the Three-way Catalyst [69]. Lowering the combustion temperature is beneficial for the reduction of NO emissions, because the NO formation requires the high activation energy to break the triple bonds in N_2, as discussed in Section 1.4.1. The combustion temperature is often regulated through the modulation of the two reactants (*i.e.* oxidant and fuel) in the combustion reaction. Based on the various management techniques of the oxidant and fuel, different concepts are proposed to reduce the in-cylinder NOx and smoke emissions while maintaining the high thermal efficiency in CI engines.

2.5.1 Diesel LTC

The diesel LTC can be achieved with various fuel injection strategies assisted with high EGR rates [67, 68]. Historically, high fuel injection pressure, multiple fuel injections, high intake pressure, low intake temperature, and medium EGR rate have been applied to diesel combustion to satisfy emission standards before model year 2004 (Figure 1-3) with a minimal assistance of the after-treatment devices [70]. However, these techniques are insufficient to further reduce the emissions as the emission regulations become more stringent.

Kumar [71] has researched three strategies to enable the enhanced premixed combustion with diesel fuel: early multiple injections, EGR assisted single injection, and split combustion. Simultaneously low NOx and smoke emissions have been achieved but with a high penalty in the thermal efficiency. Kimura *et al*. [72] have proposed the modulated kinetics (MK) combustion that can be enabled with retarded injection timings and

24

reduced intake oxygen concentrations. The NOx and smoke emissions have been suppressed, but the thermal efficiency has been reduced. Similar combustion strategies have been proposed but named differently, such as uniform bulky combustion system (UNIBUS) [73], premixed lean diesel combustion (PREDIC) [74], homogeneous charge intelligent multiple injection combustion system (HiMICS) [75], and premixed charge compression ignition (PCCI) [76].

A common feature of these diesel LTC strategies is the conversion of the conventional high temperature combustion partially to premixed combustion to lower smoke emissions when EGR is applied to suppress NOx emissions. However, the diesel fuel has a high boiling temperature and high reactivity to compression ignition. A high EGR rate is typically required to withhold the onset of combustion, which also reduces the oxygen availability and limits the engine load range.

2.5.2 Homogeneous Charge Compression Ignition

The HCCI combustion has been recognized as an ideal combustion mode for both spark ignition engines and CI engines [16, 29]. This combustion mode generates inherently low NOx and smoke emissions at low to medium engine loads, and high NOx emissions at higher engine loads [16]. However, the implementation of HCCI combustion has some fundamental challenges. First, the preparation of the homogeneous charge is demanding for using the fuels with the properties similar to diesel. The fuel evaporation has to be promoted while the pre-ignition and wall impingement has to be prevented. It has been reported that the use of volatile fuels, such as ethanol, improves the charge preparation for the HCCI combustion [79]. Moreover, the generation of the reliable and controllable ignition is another challenge for HCCI operations [80]. The ignition of HCCI combustion

is mainly determined by the chemical kinetics of the in-cylinder charge, which is sensitive to the in-cylinder temperature and AFR. Therefore, unstable ignition can occur at cold start and at low engine loads in HCCI combustion, while pre-ignition and rough combustion are the potential challenges at high engine loads. When the engine is operated at low loads, the charge is often excessively lean for complete combustion of the fuel, and thus the combustion tends to form high emissions of THC and CO; while at high engine loads, the instantaneous, rapid, and intensive combustion generates excessively high pressure rise rate and combustion noise [81], which limits the high load application.

2.5.3 Reactivity Controlled Compression Ignition

The aforementioned challenges of HCCI combustion have been addressed with various strategies of fuel injections and in-cylinder charge management. Kokjohn *et al*. [33] have proposed the reactivity controlled compression ignition (RCCI) for improved controllability in the premixed combustion. The port injection of gasoline has been used to generate the majority of the engine load, while multiple injections of diesel have been employed to modulate the charge reactivity and control the ignition. Inagaki *et al*. have also reported a similar approach but using the primary reference fuels [82]. Partial fuel stratification (PFS) is another approach to control the mixing and distribution of the fuel, and thus to generate the reactivity stratification [35]. Dec *et al*. have used gasoline direct injection and gasoline port fuel injection to generate the partially stratified in-cylinder charge. The intake temperature is regulated to control the combustion phasing [35].

The common feature of RCCI and PFS is the long ignition delay (longer than 40 °CA), in stark contrast to the short ignition delay of conventional DI diesel combustion. This long ignition delay enhances the mixing of the direct injections to prevent soot formation.

Moreover, the premixed in-cylinder charge is lean and diluted, which reduces the flame temperature, resulting in low NOx emissions. However, the combustion of RCCI and PFS is still highly sensitive to the charge temperature and compositions. The variations of charge temperature, combustion chamber wall temperature, and EGR distribution between engine cycles often reduce the combustion stability [83, 84].

2.5.4 Partially Premixed Combustion

Partially premixed combustion (PPC) is developed to enhance the control of ignition using a direct fuel injection to trigger the combustion event. The feature of low emissions is maintained due to the majority of premixed combustion [85]. A fuel with similar properties as gasoline (*i.e.* high volatility and low Cetane number) is favorable for PPC [86]. The separation of the injection event from the combustion event is critical for the successful enabling of the PPC. Hence, the PPC with a single fuel injection often generates excessive pressure rise rate owing to the highly premixed combustion, which requires a high EGR rate to reduce the combustion rate [87]. The high intake pressure, high EGR rate, cooled EGR, and low compression ratio are found to be beneficial for lowering the pressure rise rate and maintaining the simultaneously low emissions of NOx and smoke [88].

2.6 Summary

In general, the mixing of the fuel with air affects the trade-off between NOx and smoke emissions. A premixed or partially premixed in-cylinder charge is essential for low emissions of NOx and smoke. To prepare this in-cylinder charge, an appropriate fuel delivery method has to be employed according to the different fuel properties. Volatile

fuels delivered through port fuel injection are beneficial to reduce the challenges in the process of charge preparation.

The controls of ignition and burning rate can be controlled with various fuel delievery strategies. The ignition can be initiated transiently with a high reactivity DI pilot as needed. The premixed fuel is then ignited by the initial flame. The premixed charge may also auto-ignite when the temperature is elevated. The burning rate of the combustion is primarily controlled by the reactivity of the premixed charge and the reactivity gradient generated from multiple fuel injections.

CHAPTER III

METHODOLOGY AND EXPERIMENTAL SETUP

The primary research methodology is schematically shown in Figure 3-1. The research motivations are identified based on the present emission regulations and the working principles of CI engines. The research approaches for high efficiency and low in-cylinder emissions are formulated from the literature review of the past research findings. The applied techniques to achieve the clean and efficient combustion are systematically studied through engine experiments. The empirical results and the effectiveness of these techniques on modulating the in-cylinder charge reactivity are analyzed with different fuels under various combustion modes.

Figure 3-1 Research methodology for mixing and reactivity control in CI engines

3.1 Advanced Engine Research Platforms

The investigation of the mixing and reactivity control is primarily conducted through the systematic engine experiments. Two fully instrumented engine research platforms are employed in this research. The critical systems of the two platforms are introduced in this section. These systems include the research engines, the air handling system, the EGR implementation and control system, the fuel delivery and injection control system, and the emission measurement system.

3.1.1 Research Engines

The major engine specifications of the two research engines are illustrated in Table 3-1. The Ford PUMA Duratorq engine is a four-cylinder four-stroke production engine. It is set up with an Eddy-current water-cooled dynamometer. The first cylinder is separated from the original inline four-cylinder engine configuration by using independent systems of intake, exhaust, and fueling for this cylinder. All the research applications are conducted with this cylinder on the PUMA engine platform, while the other three cylinders are still operated under conventional diesel high temperature combustion mode with natural aspiration. The detailed setup of this engine platform can be found in [89]. The relatively high compression ratio of 18.2:1 of this engine provides the advantage of igniting fuels of low reactivity due to the relatively high compression temperature.

The single cylinder research engine (SCRE) is a single-cylinder research engine that is connected to a direct current (DC) motoring dynamometer. This engine is designed to resemble the performance of modern medium-duty to heavy-duty CI engines. The tolerable peak cylinder pressure is higher than that of the PUMA engine. An Omega-shaped piston is installed in this engine to obtain a compression ratio of 16.5:1. This

31

compression ratio is in a similar range as the ones used in the prevalent production CI engines.

Table 3-1 Engine specifications of the research engines

Research Engine	Ford PUMA Duratorq	SCRE[1]
Displacement (liter)	1.998	0.744
Bore × Stroke (mm × mm)	86 × 86	95 × 105
Connecting Rod Length (mm)	144	176
Compression Ratio (-)	18.2:1	16.5:1
Max. Cylinder Pressure (bar)	180	200
Swirl Ratio (-)	~1.7	~1.5
Primary Injection System	Delphi Common Rail DI System	Siemens Common Rail DI System
DI Injector	Solenoid Drive 6 holes Umbrella angle 155° Hole diameter 160 μm	Piezo Drive 7 holes Umbrella angle 156° Hole diameter 200 μm
Secondary Injection System	Inhouse Low Pressure PFI[2] System	Inhouse Low Pressure PFI System
PFI Injector	Gasoline Injector 4 holes	Gasoline Injector 4 holes

[1]single cylinder research engine

[2]port fuel injection

3.1.2 Air Handling System

The air handling system on the CI engine research platform includes the intake system, the exhaust system, and the EGR system, as shown in Figure 3-2. The two employed engine platforms use similar setups. The engine intake gas is supplied from an external air source. The pressure of the intake air is regulated with an electronically-controlled gas regulator. The volumetric flowrate of the intake gas is measured with a Dresser Roots rotary meter. The intake mass flowrate is then calculated by multiplying the volumetric flowrate with the air density at the local intake pressure and temperature. Two large buffer volumes (more than 100 times of the engine displacement) are used in the intake and exhaust loops to damp the flow pulsations caused by engine valve actions [90]. An electrical cartridge heater is installed between the air flow meter and the intake surge tank on the SCRE platform. The rated power for the heater is 1500 W using 120 VAC power supply. The heater is enabled when the engine compression temperature is not sufficiently high for reliable ignitions. A series of filters and conditioning units are equipped along the intake air path to reduce dust, water, and oil contents. Manual bypass gas loops, flame arrestors, and pressure relief valves are installed to improve the safety during the engine operation.
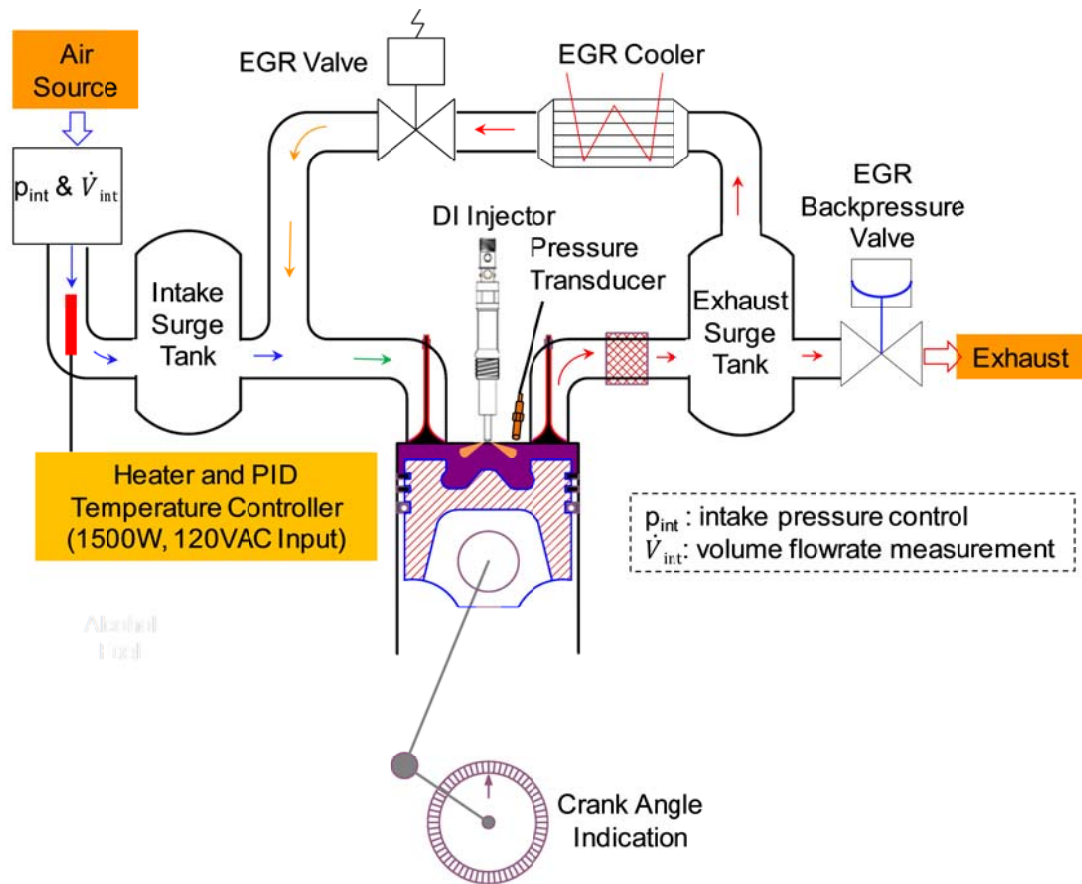
Figure 3-2 Air management schematic of the research platforms

3.1.3 EGR Implementation and Control System

The application of EGR is implemented by introducing the exhaust gas into the engine intake to modulate the intake gas properties, as shown in Figure 3-3. The main driving force for the flow of gas is typically the pressure difference between the engine exhaust and the engine intake. This pressure difference is essential for a successful EGR application. Hence, the engine exhaust backpressure is also increased for the EGR application when a higher intake pressure is used. In this setup, a pneumatic Sinclair Collins valve is installed downstream of the exhaust surge tank for the exhaust backpressure control. Compressed air at a precisely-controlled pressure is used to drive

the valve to throttle the exhaust stream and build up the backpressure. When a high EGR rate is required, the actual exhaust flow is significantly reduced. The opening area of the throttle valve in the exhaust loop may be reduced by more than 99% to obtain the desired backpressure in the case of high EGR rates (*e.g.* higher than 60% EGR).

Exhaust

- EGR Compositions
  - CO_2
  - H_2O
  - O_2
- EGR Temperature
  - Cooled EGR
  - Hot EGR

EGR

Intake

- Property Changes
  - Intake Compositions
  - Diluted O_2 Concentration
  - Increased Heat Capacity
- Mixing
  - Temperature Stratification
  - Composition Stratification
  - Reactivity Stratification
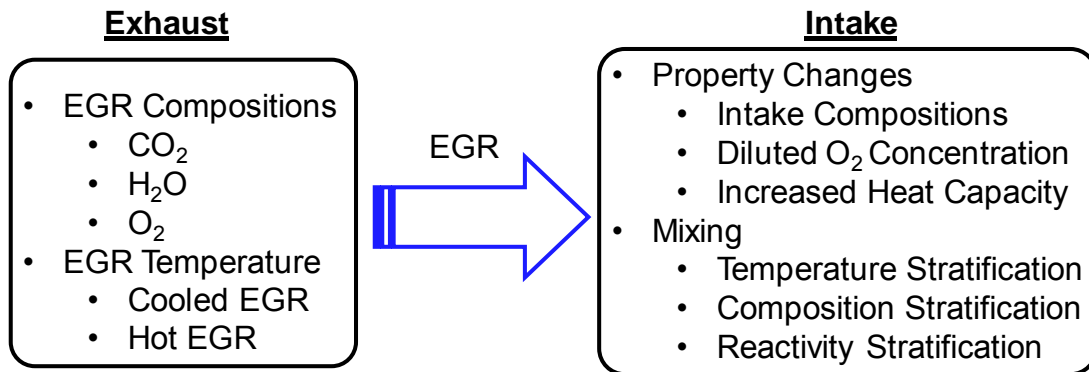
Figure 3-3 EGR application modifies the intake properties

The flowrate of EGR is determined by the pressure difference between engine intake and exhaust, and the flow resistance in the EGR loop. As shown in Figure 3-2, a production EGR valve, which has 32 discrete opening positions, is used on this platform. The EGR valve can achieve the coarse adjustment of EGR rate. However, the ultra-fine adjustment of EGR, such as a 1% increment, is typically not achievable with this valve alone. The actual EGR is implemented through the control of both the EGR valve and the backpressure valve. The flow chart of a typical adjustment of EGR rate is demonstrated in Figure 3-4. The opening position of the EGR valve is fixed at a lower percentage of opening at first. The exhaust backpressure is gradually increased to achieve the required EGR rate. If the desired EGR rate can not be achieved when the backpressure is at its maximum, the opening of the EGR valve is increased to a higher percentage. An ultra-fine increment of EGR rate is realized with the control of both the backpressure valve and

the EGR valve. The targeted pressure drop from the exhaust backpressure to intake

pressure is maintained within 10 kPa.
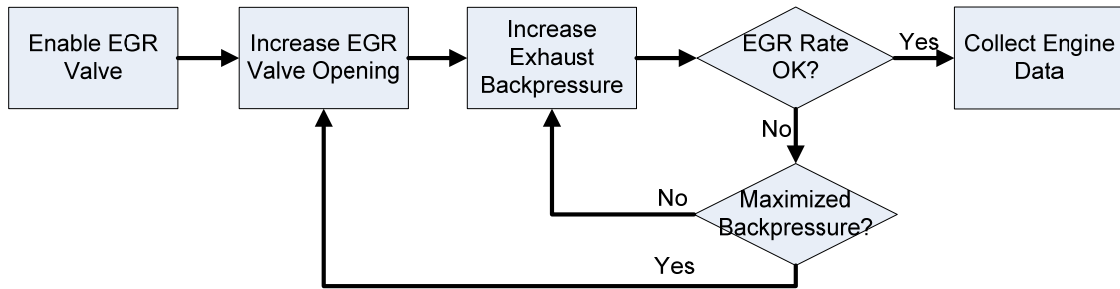
Figure 3-4 Flow chart of the EGR rate control

3.1.4 Fuel Delivery and Injection Control System

Both of the two engine platforms are equipped with dual fuel-delivery systems for the

applications of PFI and DI. The schematic diagram of the simplified system setup is

shown in Figure 3-5. For the DI system, the method of supplying fuel to the high pressure

fuel pump can be swapped between the gravity fuel feed with a raised fuel tank and the

pump feed with a low pressure fuel pump. The method of supplying fuel by gravity is

generally preferred for the relatively stable fuel flow that is critical for the fuel flowrate

measurement, especially in the single cylinder setup with a relatively low fuel

consumption. However, if the flowrate of the gravity feed is insufficient for the high

pressure pump, a low pressure pump can be used to increase the fuel flow. A series of

fuel filters are used for particle filtrations in front of the critical components (*e.g.* fuel

flow meter, high pressure pump). The filters are also served as damping plenums for the

pressure fluctuations in the fuel flow.

The PFI system is implemented on a portable cart. This system is employed to provide

low pressure fuel (about 8 bar absolute) to the port injectors. An inline gasoline pump is

used to pressurize the fuel. A mechanical regulator is employed to control the fuel pressure. The excessive fuel is returned to the fuel tank after cooled inside a heat exchanger. Certain safety measures (*e.g.* remote pressure release) are also applied in this system (not shown in Figure 3-5).
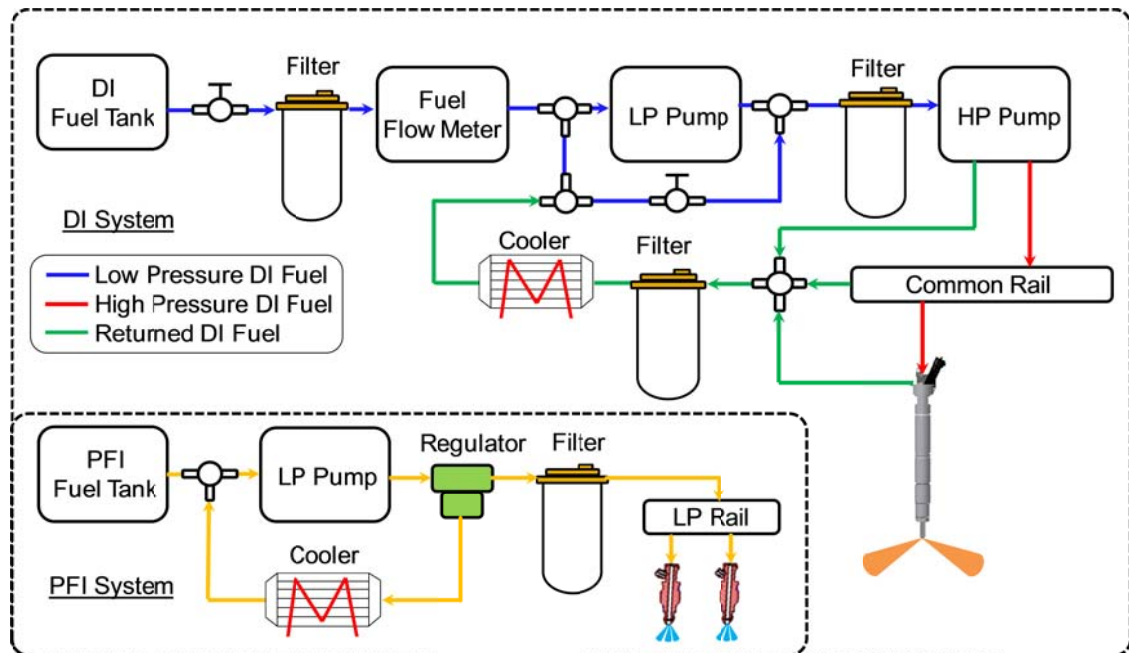
Figure 3-5 Fuel delivery system for both DI fuel and PFI fuel

The fuel injection control is implemented using the NI real-time (RT) controller with embedded field programmable gate arrays (FPGA), as shown in Figure 3-6. A personal computer (PC) is connected to the RT through local area network (LAN) and is used as the user interface of the RT. The control procedures are executed on the RT, while the FPGA is used to generate the pulse width modulation (PWM) signals to the injector drivers, based on the external trigger from the crank angle encoder and the internal system clock. The commanded injection duration is applied in the absolute time domain rather than the crank-angle domain. Hence, the potential variations in the engine rotation speed within a cycle or between cycles have no impacts on the actual injection durations.

37
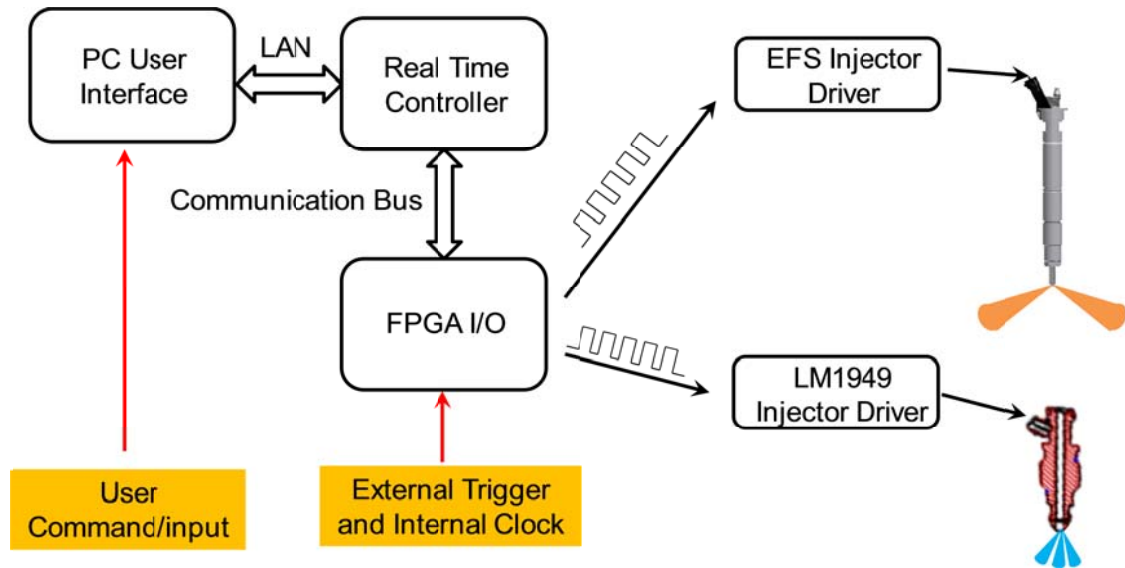
Figure 3-6 Schematic of injection control

3.1.5 Emission Measurement System

Two sets of gas analyzers from California Analytical Instruments (CAI) are used to measure the gas samples from the engine intake and exhaust, as listed in Table 3-2. The measured species in the intake flow are CO_2 and O_2. The monitored species in the exhaust stream include CO_2, O_2, CO, NOx, and THC. The gas samples pass through a conditioning unit with filters and chillers for the removal of soot and water before supplied to the gas analyzers. The smoke emissions are evaluated with an AVL smoke meter (AVL 415S). The two sets of analyzers are always used during engine experiments on both of the platforms. There are also some advanced analyzers only used in certain specially designed engine tests for the speciation of exhaust emissions. These analyzers include hydrogen analyzer (H-Sense), Fourier transform infrared spectroscopy analyzer (FTIR MKS2030-HS), Horiba PM analyzer and dilution tunnel, and Cambustion HC and NOx analyzers.

Table 3-2 Intake and exhaust analyzer systems

Intake Analyzers		
Analyzer Model	**Measurement Principle**	**Measured Species**
CAI 200	Paramagnetic	O_2
CAI 200	Non-Dispersive Infrared	CO_2
Exhaust Analyzers		
Analyzer Model	**Measurement Principle**	**Measured Species**
CAI 602P	Non-Dispersive Infrared	CO_2
CAI 300	Non-Dispersive Infrared	CO
CAI 602P	Paramagnetic	O_2
CAI 600 HCLD	Chemiluminescence	NOx
CAI 300M-HFID	Heated Flame Ionization	THC
AVL 415S	Photoelectric Blackness Measurement	Smoke

3.2 Fuel Injection Characterization

The fuel injection characterizations to be conducted in this research include the measurements of injection rate, injection opening and closing delays, and the distributions of velocity and diameter of the spray droplets. The employed instruments include the EFS injection bench, Bosch type long-tube bench [91], high speed camera, and laser phase Doppler anemometry (PDA) system.

3.2.1 EFS Injection Bench

The EFS injection bench can be used to measure the injection rate and injected mass. An important component in the EFS injection bench is the flowrate sensor, as shown in Figure 3-7. The flowrate sensor contains a micro piston. When a liquid is injected via the injector into the injection chamber that is maintained at a fixed backpressure, the increase of the volume moves the micro piston. The distance of the piston movement is proportional to the injection volume. With the measured total flowrate and the known injection frequency, the injection mass and the injection rate of an injection event can be derived. A surrogate of diesel is used in the EFS injection bench.

The EFS injection bench also includes a complete auxiliary system. An AC motor of 18 kW is installed in the EFS injection bench to drive the high pressure fuel pump. The motor speed can be precisely controlled to simulate the desired engine speed. The temperature of the fuel supplied to the high pressure pump, and the temperature of the measuring chamber are closely monitored. The backpressure inside the injection chamber is also regulated.
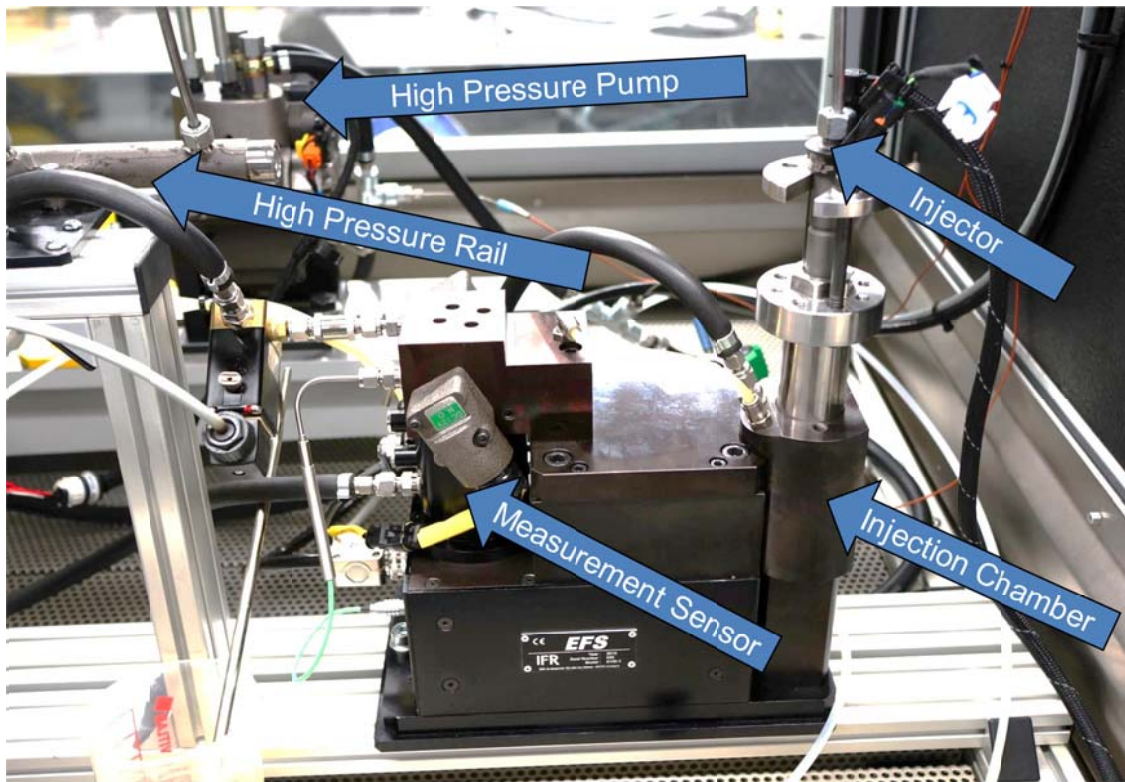
Figure 3-7 EFS injection bench system setup

3.2.2 Bosch Type Long-tube Bench

The schematic for the Bosch long-tube bench is demonstrated in Figure 3-8. The system includes three main sub-systems: the fuel injection system, the control system for fuel pressure and injection, and the measurement system for injection rate. The fuel injection system consists of a fuel cart for low pressure fuel supply, a fuel cart for high pressure fuel supply, a fuel rail, and a piezo injector. The fuel cart for high pressure fuel supply contains a common rail high pressure pump driven by an electric motor. The measurement system for injection rate is designed to measure the pressure rise caused by the fuel injection event [91]. A piezo pressure transducer is mounted near the tip of the injector nozzle. A stainless steel tube of 50 meter is connected to the injection block to collect the fuel and to substantially delay the pressure wave reflected from the end of the

41

tube. Before the measurement of injection rate is performed, the internal volumes of the injection block and the long tube are filled with the same fuel as the one used for the injection test. Several fuel injections are applied to build up the required backpressure in the system before the actual measurement. A backpressure of 20 bar was used for the results presented in this dissertation.
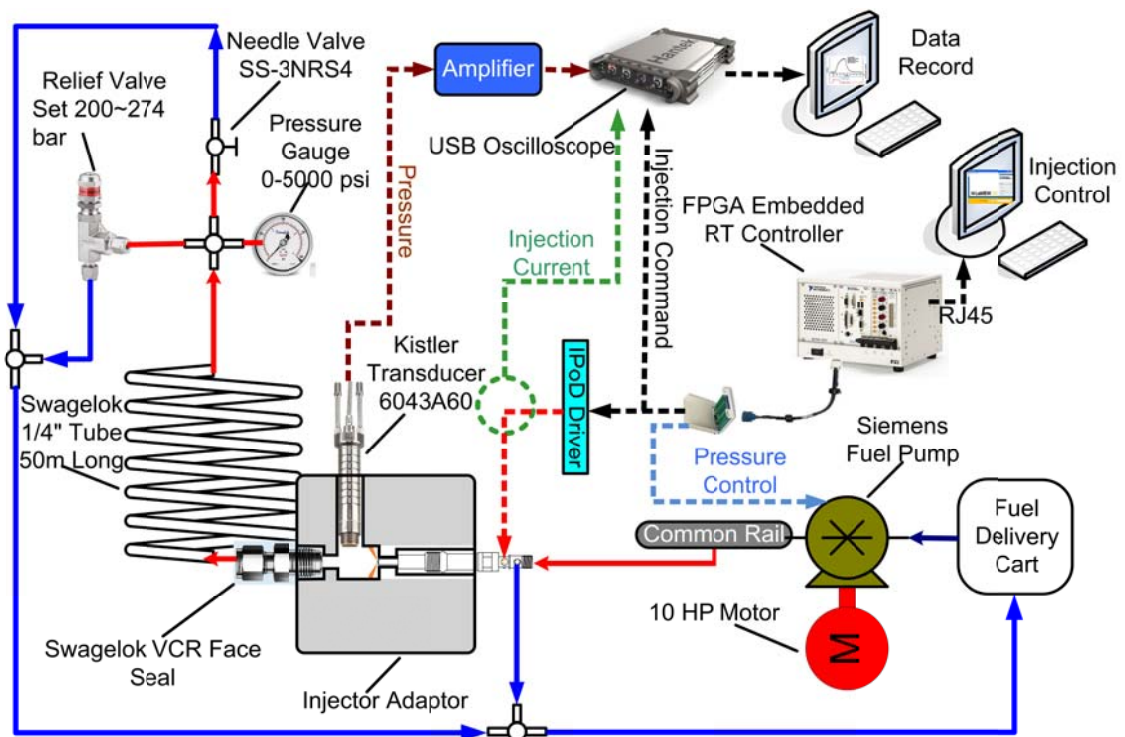
Figure 3-8 Injection rate measurement schematic

3.2.3 High Speed Camera

A high speed camera (Phantom V7.3) was employed to detect the timings of the injector opening and closing. It is also used to visualize the high pressure spray. The fuel injection system and the control system of fuel pressure and injection are the same as the ones used in the Bosch type long-tube setup. The schematic diagram for the detection of injector opening and closing is illustrated in Figure 3-9. The image recording is triggered by the rising edge of the PWM injection command. The time duration from the injection

command to the injector opening and closing can be obtained based on the image sequences. The experiment was conducted in a chamber at ambient pressure and temperature. The detailed data processing process is described in Appendix A.
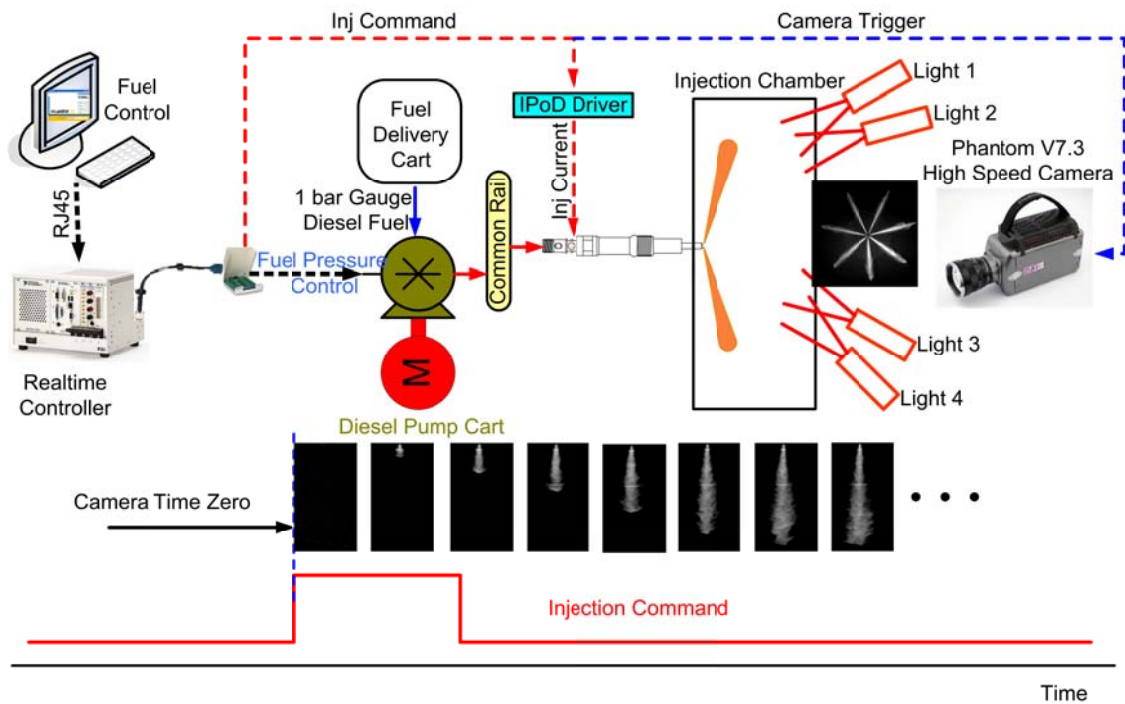
Figure 3-9 High speed imaging for detecting injector opening and closing timing

3.2.4 Laser Phase Doppler Anemometry System

The PDA system setup is illustrated in Figure 3-10. A chamber operated at ambient temperature and ambient pressure was employed for the measurement of spray droplet size and velocity. The laser used in this experiment is a continuous wave argon ion laser (Stabilite 2017 manufactured by in Year 2009 Spectra Physics). The specifications of the laser are found in [92]. The rated laser power is 5 W. The laser power measured at the exit of the laser probe is about 0.1 W for each of the two laser beams. The laser aperture was set to 2.24 mm. The intersection angle of the two laser beams was approximately 32 degrees. The wavelength of the laser is 514.5 nm.

43
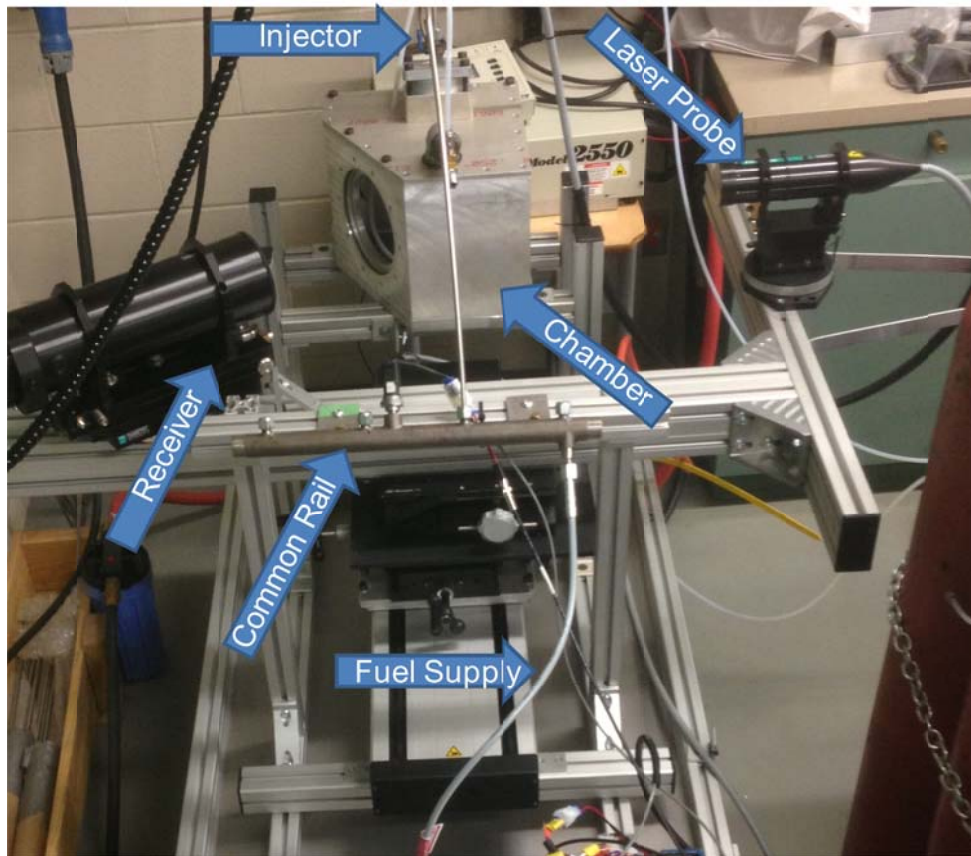
Figure 3-10 PDA system setup

3.3 Constant Volume Chamber

A high pressure constant volume chamber was used for the experiment of spray characterization. Two optical Quartz windows are assembled at the opposite sides of the chamber. The view port of the optical window is 80 mm in diameter. A single-hole injector is used in the chamber in the spray measurement. Backlight scattering is employed to visualize the injection event. The chamber is operated at ambient temperature. The internal pressure is increased to 40 bar using a high pressure nitrogen gas bottle. The schematic of the gas supply system is given in Appendix B. The Schlieren photography is also applied with two parallel parabolic mirrors to visualize the potential fuel vapor.

44

3.4 Test Fuels

The fuels used in this research program included diesel, n-butanol, and ethanol. The selected fuel properties are illustrated in Table 3-3. Diesel was delivered through high pressure direct injection, while ethanol was supplied with port fuel injection. N-butanol, due to its favorable properties, were used with both the DI application and the PFI application according to the actual requirement of combustion. Various combinations of the fuel delivery methods for the three fuels were tested. The benefits and limitations of the fuel injection strategies are discussed in the subsequent chapters.

Table 3-3 Fuel properties of the tested fuels

Fuel Properties	Diesel	n-Butanol	Ethanol
Fuel Formula	$C_nH_{1.78n}$ [93]	$C_4H_{10}O$	C_2H_6O
Density @ 15 °C, (kg/m^3)	858	813	788
Viscosity @ 40 °C, (cSt)	2.7	3.6	1.5
Speed of Sound @ 25 °C, (m/s)	1350 [94]	1239 [95]	1142 [96]
Boiling Temp @ 1 bar (°C)	Variable	117.5	78.3
Cetane Number	46.5	~25	~10
Octane Number	~25	~87	~110
Lower Heating Value (MJ/kg)	43.5	33.1	26.8
Carbon Content (% mass)	86.8	64.8	52.1
Hydrogen Content (% mass)	13.2	13.6	13.1
Oxygen Content (% mass)	0	21.6	34.8
Lubricity (μm) from HFRR	315 [97]	591 [97]	1057 [97]
Purity	-	≥ 99.7 [98]	≥ 99.5 [99]

CHAPTER IV

BUTANOL HIGH PRESSURE INJECTION

In this chapter, the characteristics of the high pressure injection of diesel and n-butanol are studied with the EFS injection bench, the Bosch long-tube bench, and the optical equipment. The tested fuel injector is a solenoid injector with the same model number as the one used in the Ford PUMA engine. The measured parameters include injection volume, injection opening delay, injection closing delay, and spray structure. The results of n-butanol high pressure injection are compared to that of diesel high pressure injection. The study in this chapter improves the understanding of the engine combustion performance with n-butanol high pressure direct injections.

4.1 Injection Rate Measurement

A high injection pressure is required for direct fuel delivery in CI engines to effectively distribute fuel inside a cylinder within a reasonable time [105]. The n-butanol fuel is used in the application of high pressure injection with a commercial common rail fuel system. A lubricity improver (OLI-9070.x) is added to n-butanol at a volumetric concentration of 500 parts per million (ppm) for the protection of moving components in the fuel system.

The fuel injection rate of n-butanol is studied with the Bosch type long tube injection bench. The measurement schematic has been given in Figure 3-8. The injection rate curves of n-butanol and diesel at the same injection pressure and injection duration are compared in Figure 4-1. The raw injection rate of n-butanol is lower than that of diesel. Based on the Bosch theory [91], the raw pressure rise should be corrected with the speed of sound and density of the fuel to show the actual injection rate. After this correction, the

47

injection rate curves are compared in Figure 4-2. It is observed that the injection rate of n-butanol is close to that of diesel. A marginal difference is that the closing time of the n-butanol injection is slightly later than the one of diesel.

The effect of the injection duration on injection rate is shown in Figure 4-3. Various injection durations were tested at a constant injection pressure of 1200 bar. As the injection duration was increased, the peak injection rate increased. The injection rate curves of different injection durations overlapped during the injector opening process. For the injection with a shorter duration, the injection rate curve shows a sharp transition from opening to closing, while the one with a longer duration displays a smooth transition. The injection pressure effect on injection rate is shown in Figure 4-4. The peak of the injection rate increased with the injection pressure. The area covered by the injection rate curve enlarged, which was an indication of an increased injection volume.
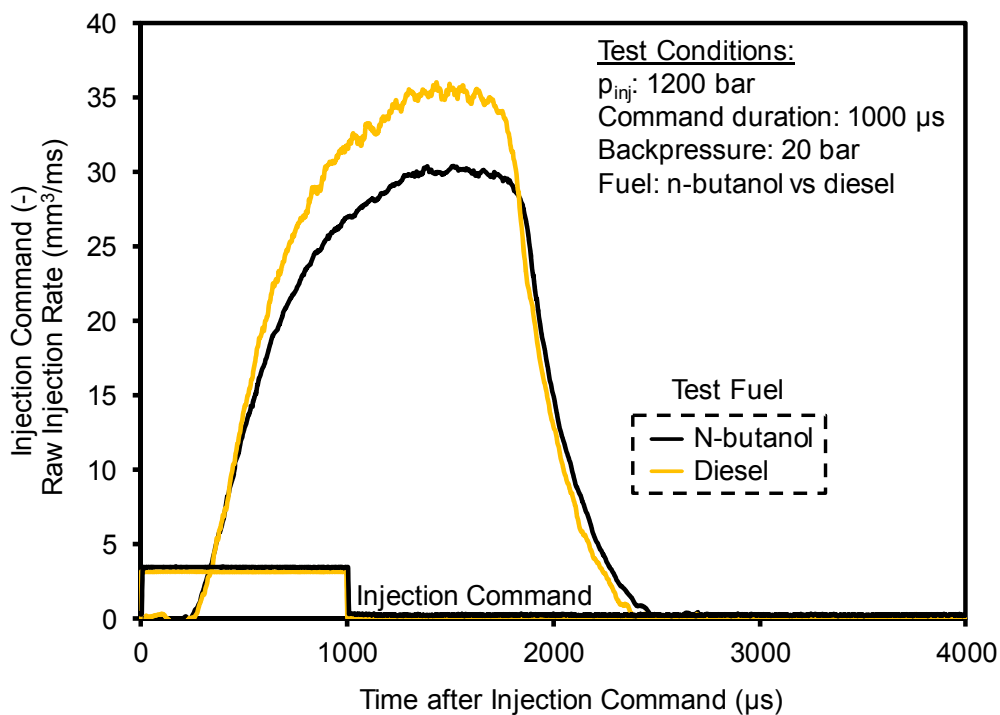
Figure 4-1 Injection rate of n-butanol: raw data
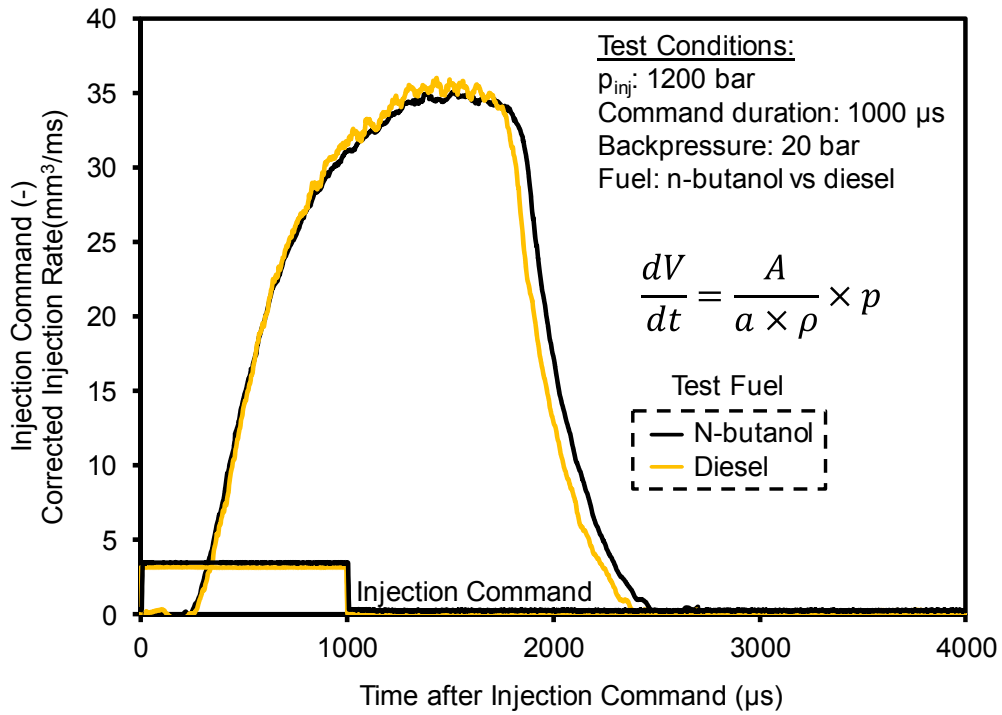
Figure 4-2 Injection rate of n-butanol: corrected injection rate
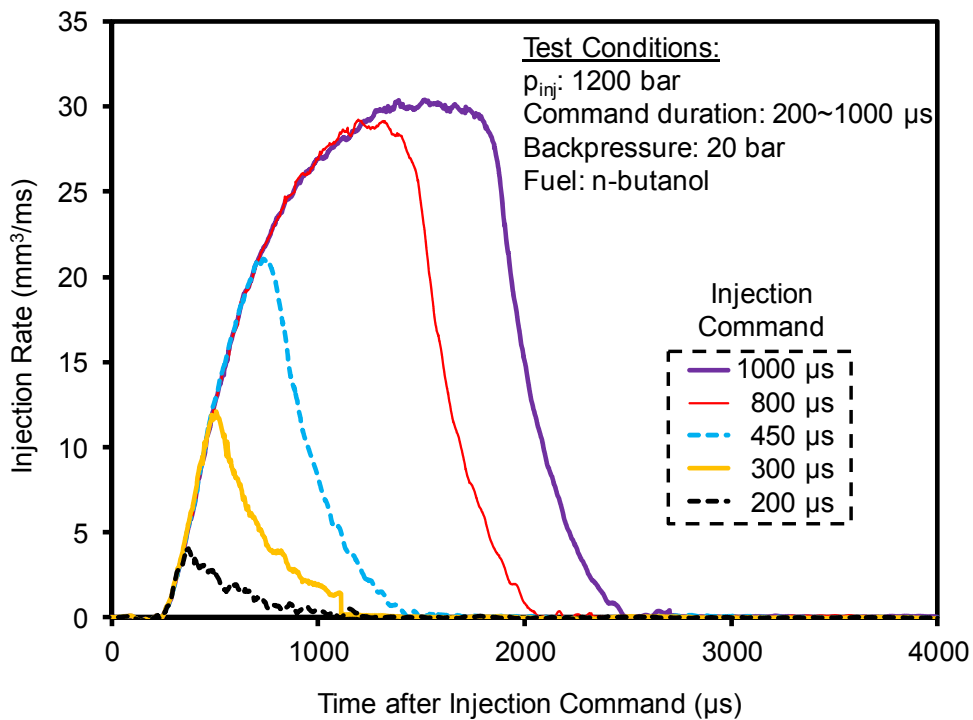
Figure 4-3 Injection rate of n-butanol: injection command effect
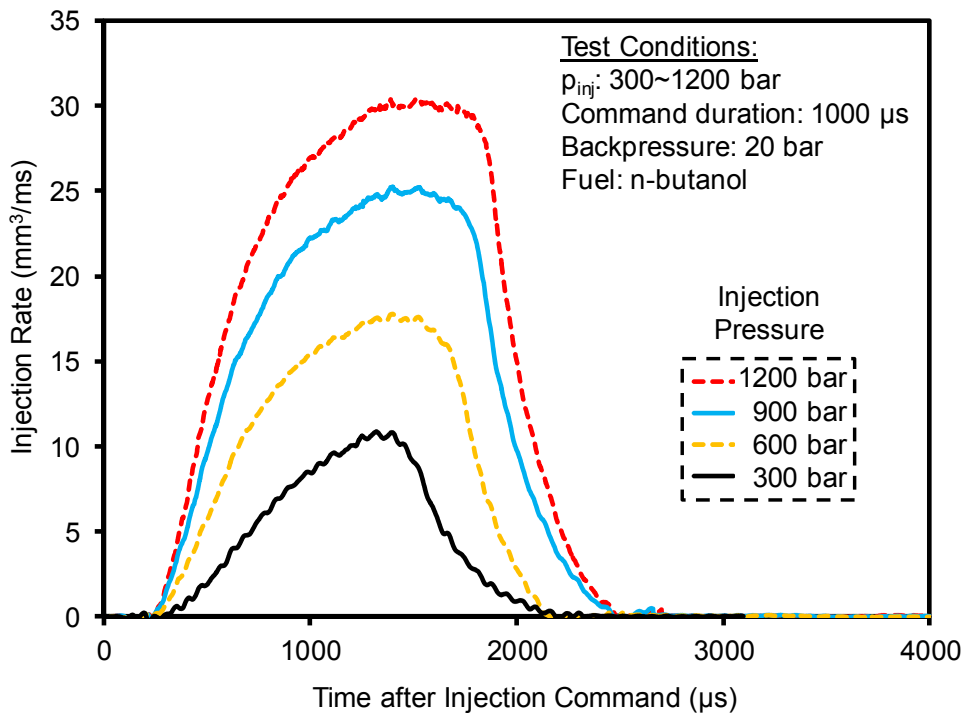
Figure 4-4 Injection rate of n-butanol: injection pressure effect

The volume of injection can be calculated from the area under the injection rate curve. The injection volume is calculated for an injection duration sweep at 900 bar injection pressure, as shown in Figure 4-5. It is observed that the relationship between the injection duration and the injection volume is not always linear for the injection duration from 200 to 2000 μs. As aforementioned, the injection volume is affected by the needle position and the injection duration. This curve suggests two different slopes between the injection volume and the injection duration. With the inflection point identified, it is relatively reasonable to conduct the duration interpolation for injection volume within the two linear portions.
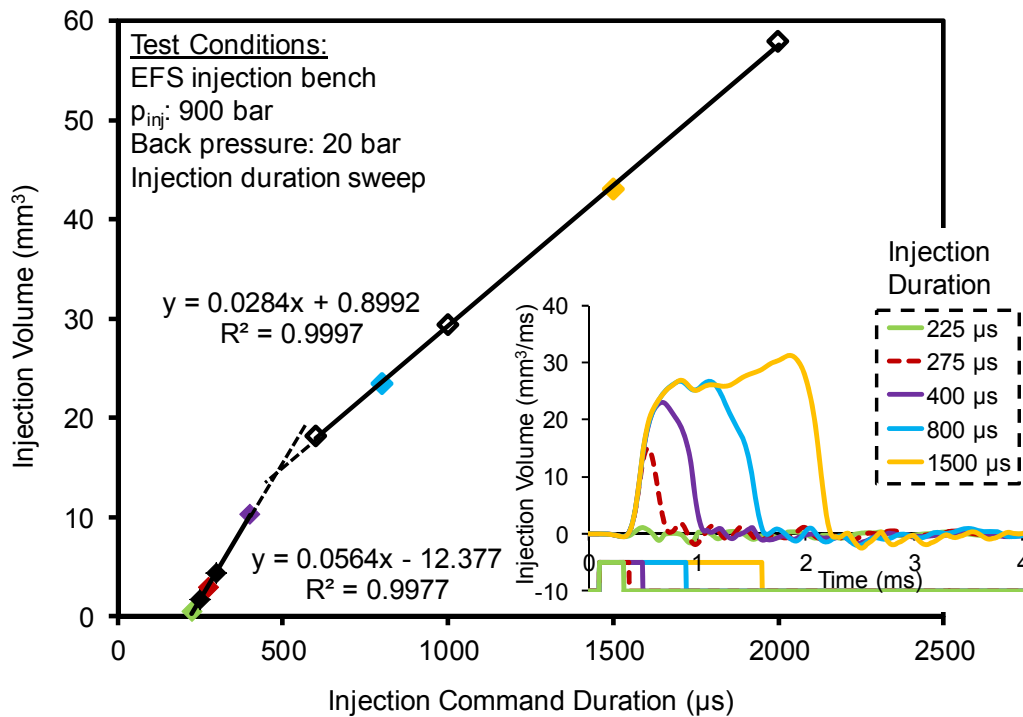
Figure 4-5 Injection volume with varied command durations

The relative injection volumes with both diesel and n-butanol are compared in Figure 4-6. All of the injection volumes presented in the figure are normalized with the volume of the diesel injection with 900 bar injection pressure and 1000 μs injection duration. It is observed that the injection volume differences between diesel and n-butanol are marginal at varied injection durations and injection pressures. Hence, it is reasonable to assume that a similar volume of n-butanol is delivered into the combustion chamber as diesel with the same injection conditions. However, because of the lower LHV (lower heating value), only approximately 80% of the energy is supplied with the n-butanol injection compared with the diesel injection at the same injection conditions.
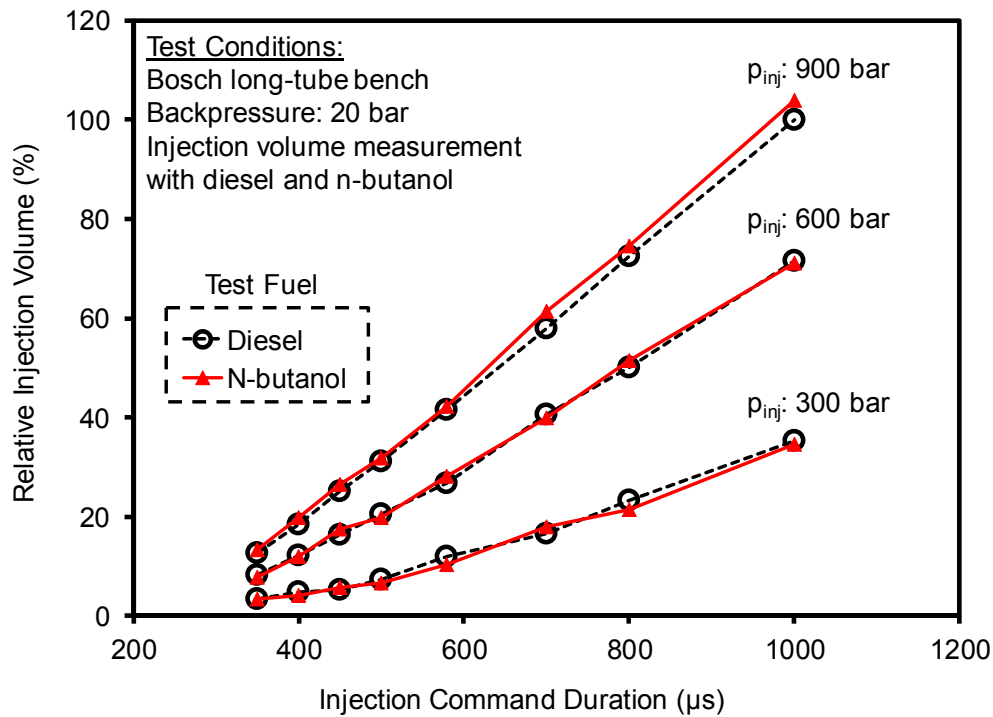
Figure 4-6 Injection volume comparison between n-butanol and diesel

4.2 Injection Opening and Closing Delays

The definitions of injection opening and closing delays are shown in Figure 4-7. Both the delays consist of the electronic delay and the hydraulic delay. The electronic delay is the duration for the injector driver to respond to the injection command. The hydraulic delay for injector opening includes the time duration required to build up the force to overcome the needle inertia and the force of the set spring for the needle, while the hydraulic delay for closing is mainly the time required for the needle to travel from certain lift to full close. The electronic delay is often neglected due to its short duration compared with that of the hydraulic delay [106].

52
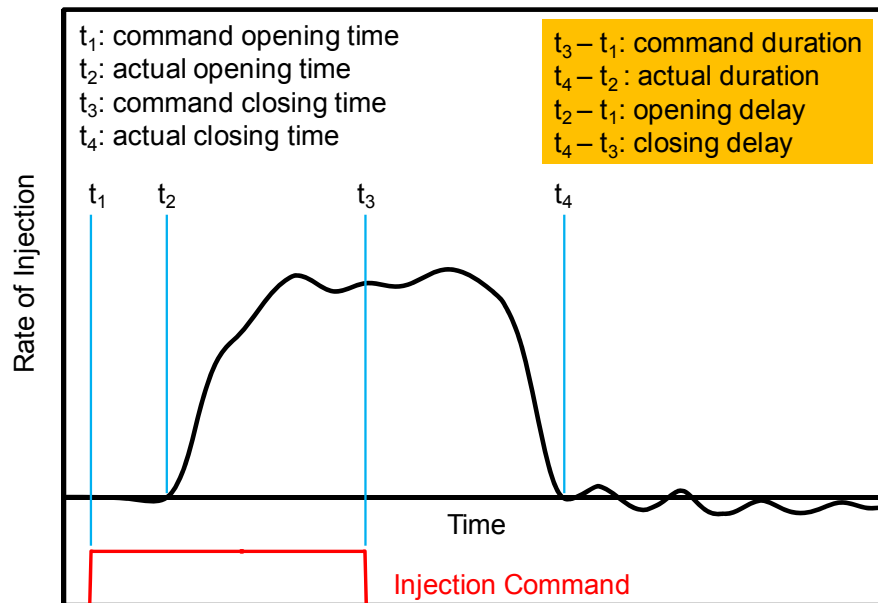
Figure 4-7 Definitions of injection opening and closing delay

The injection opening delays with n-butanol are compared with the ones with diesel in Figure 4-8. The injection opening delay remains at a constant level with a fixed injection pressure, while it varies among different injection pressures. It is observed that the opening delays at 300 bar injection pressure are longer than the ones at 600 bar and 900 bar injection pressures. The opening delays of the n-butanol injections are in similar ranges as the ones of diesel under the same injection pressures and durations. The injection closing delays with n-butanol are compared with the ones with diesel in Figure 4-9. A common trend is observed that the closing delay with n-butanol is slightly longer than that with diesel under the same injection conditions.
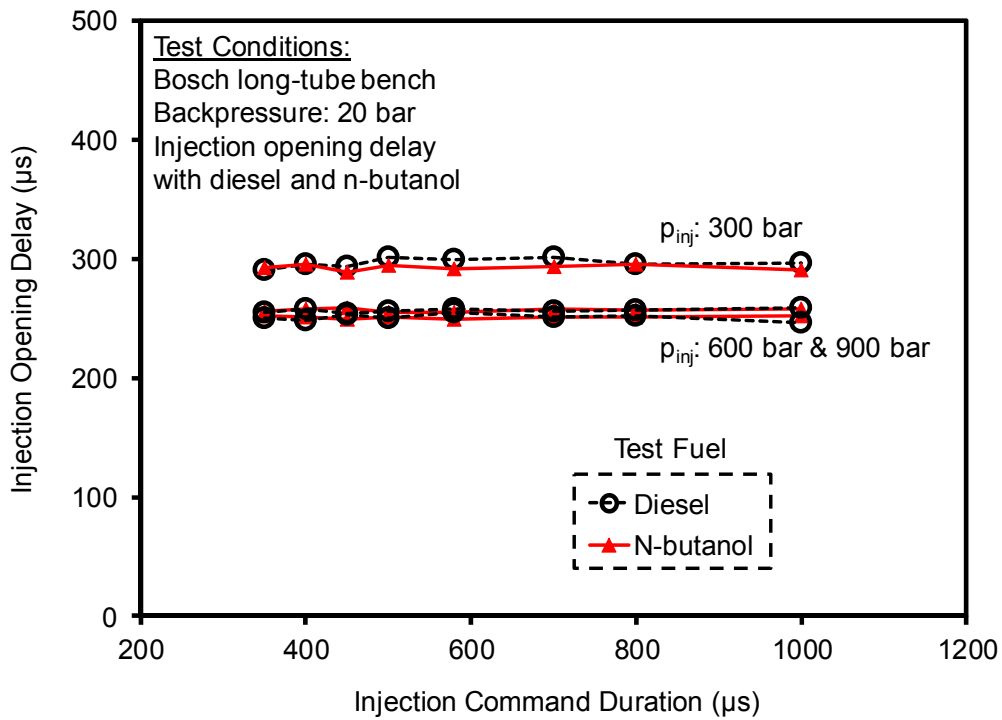
Figure 4-8 Injection opening delay comparison between n-butanol and diesel
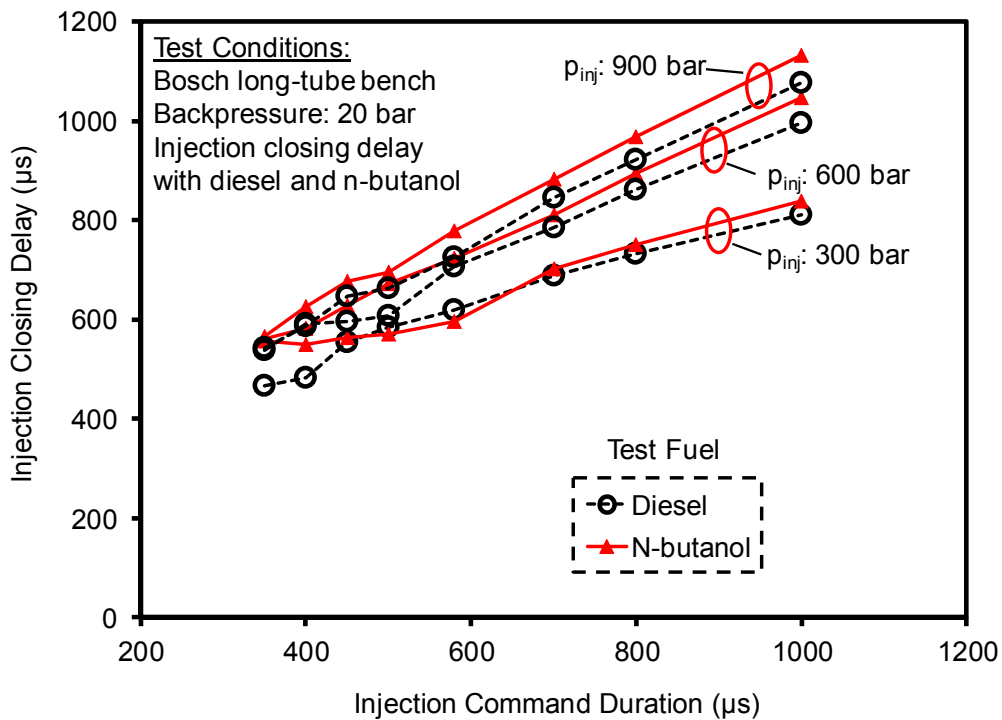
Figure 4-9 Injection closing delay comparison between n-butanol and diesel

4.3 Multiple Fuel Injections

The oscillation of the fuel pressure inside the common rail is considerably increased after a fuel injection, as shown in Appendix D. This fluctuated fuel injection pressure potentially affects the injection rate and the injection volume of the subsequent fuel injections. In this section, the effects of the dwell time between multiple injection events are evaluated based on the comparisons of the injection rate and injection volume.

The injection rate curve of two fuel injections with the same injection duration is shown in Figure 4-10. The command dwell time between the two fuel injections is defined as the time from the command of closing of the first injection to the command of opening of the second injection, while the actual dwell time is affected by the closing delay of the first injection and the opening delay of the second injection. Because of these delays, the two injection events can possibly merge into one event before the command dwell time is shortened to zero, such as the example given in Figure 4-11. The two injections start to merge when the command dwell time is reduced to about 500 μs.

The effects of the dwell time on the total injection volume are investigated in Figure 4-12 and Figure 4-13, respectively. A relatively long injection duration of 600 μs is used for both the injections in Figure 4-12, while a relatively short duration of 250 μs is used in Figure 4-13. With the longer injection duration, the total injection volume of the double injections is in a similar range of doubled the volume with a single injection at the same injection duration. In stark contrast, with a short injection duration, the total injection volume changes significantly. As shown in Figure 4-13, the injection volume is increased by more than 1500% compared with that of a single injection at 250 μs duration.

55

t_1: 1st command closing time
t_2: 1st actual closing time
t_3: 2nd command opening time
t_4: 2nd actual opening time

$t_3 - t_1$: command dwell time
$t_4 - t_2$: actual dwell time
$t_2 - t_1$: 1st closing delay
$t_4 - t_3$: 2nd opening delay

Rate of Injection

Time
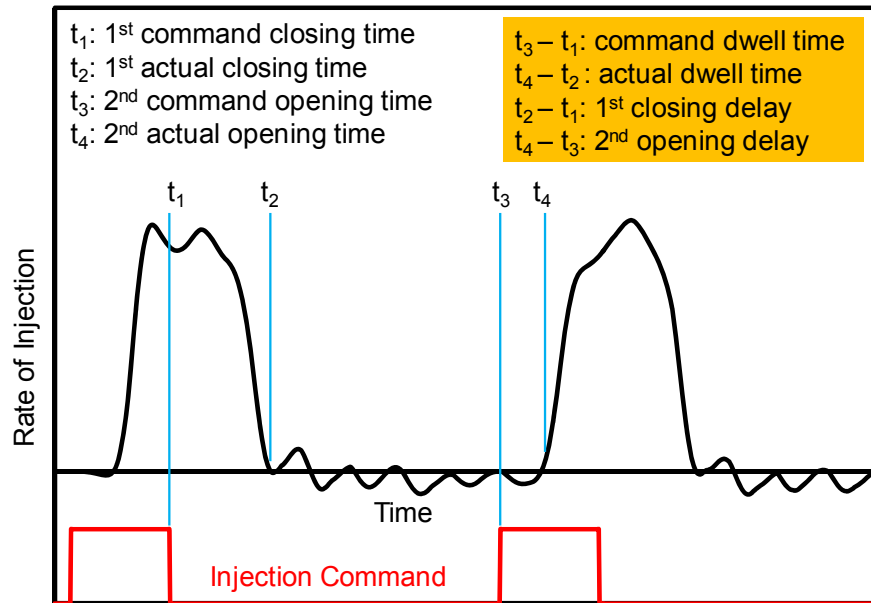
Injection Command

Figure 4-10 Comparison of command dwell time and actual dwell time

Rate of Injection (mm³/ms)

Test Conditions:
EFS injection bench
p_{inj}: 1500 bar
Back pressure: 20 bar
Inj1 duration: 600 µs
Inj2 duration: 600 µs

Dwell Time
— 300 µs
-- 400 µs
— 500 µs

Time (ms)

Injection Command
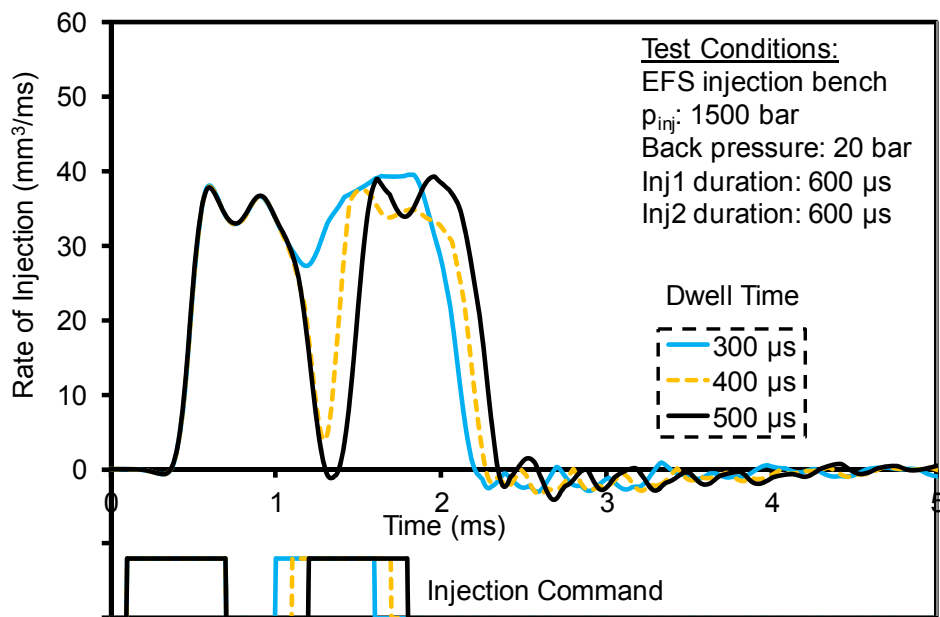
Figure 4-11 Example of double injections merging into one injection

56
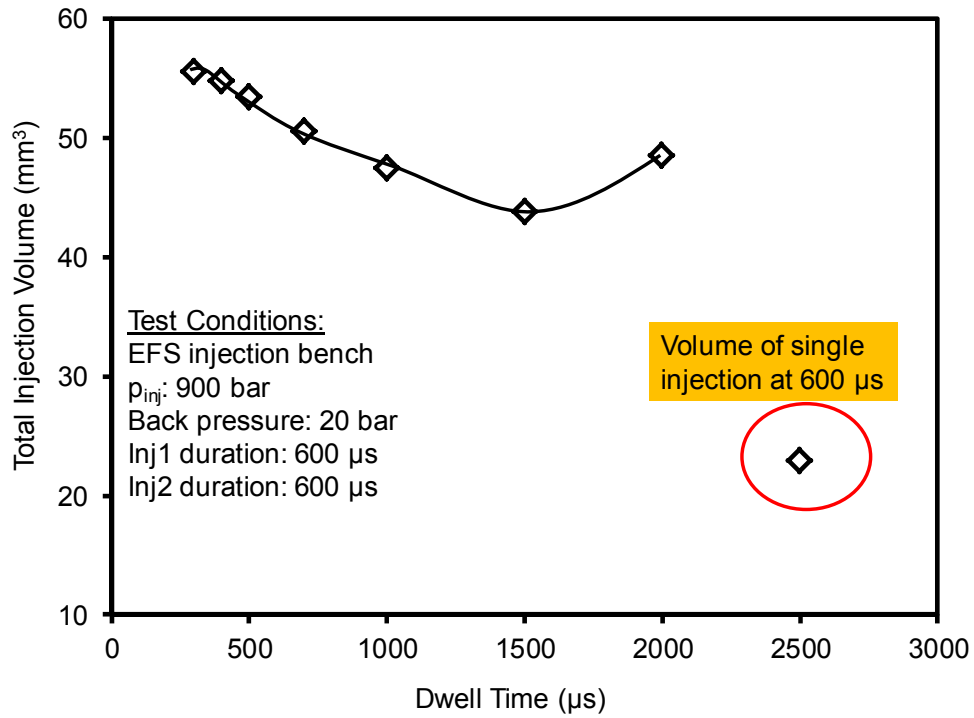
Figure 4-12 Injection volume of double injections with varied dwell time
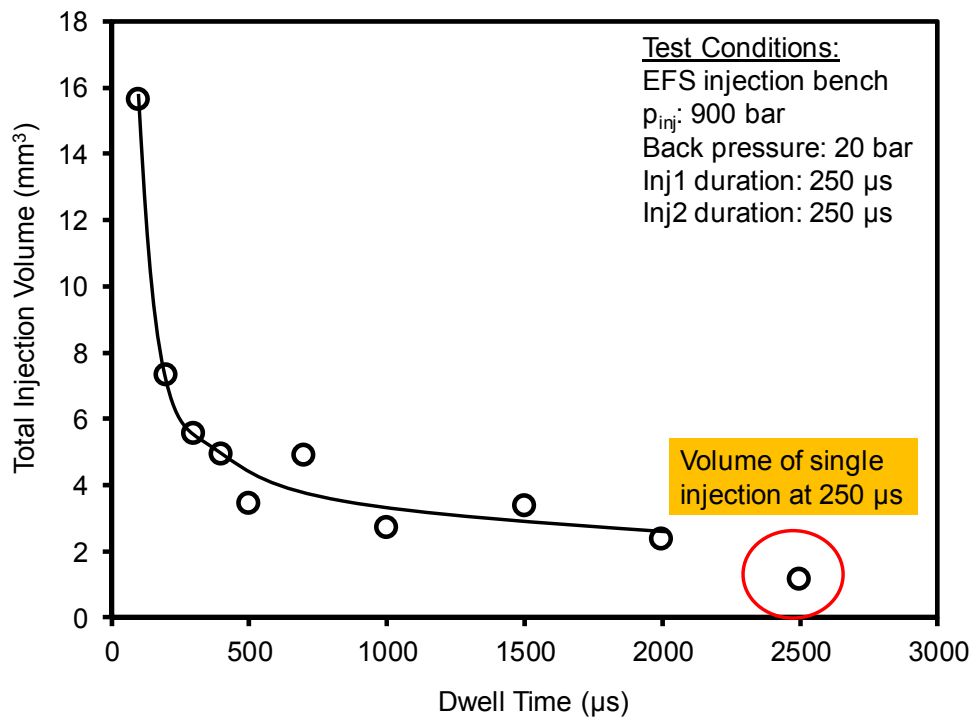
Figure 4-13 Injection volume of double injections with varied dwell time

4.4 Butanol Spray Visualization and PDA Measurement

The n-butanol high pressure spray was studied with the constant volume chamber and the high speed camera. The background gas inside the constant volume chamber was N_2 pressurized to 40 bar gauge pressure. The background temperature was maintained at room temperature. The fuel injections of both n-butanol and diesel with 1200 bar injection pressure and 1000 μs injection duration were applied to this high density background inside the constant volume chamber. The process of the spray development was recorded with the high speed camera capturing 21,000 frames per second with an image resolution of 512 × 256 pixels. Backlight shadowgraph was used. The image plane was parallel to the spray axis. A piezo injector was used in this test. The multiple nozzle orifices were pluged except one was left for the spray experiment. The orifice diameter is 140 μm. The same injector was used for both diesel and n-butanol.

Several representative images are illustrated in Figure 4-14 from the camera recording for the injections with both n-butanol and diesel. The liquid tip reached the border of the image in about 300 μs from the command of injector opening for both the n-butanol and diesel cases. The cone angle of the n-butanol injection is slightly smaller than that of the diesel injection within the image range. Overall, the spray structure of n-butanol is similar to that of diesel. The experiment was conducted at ambient temperature, thus the evaporation rate difference between the two fuels could not be revealed.
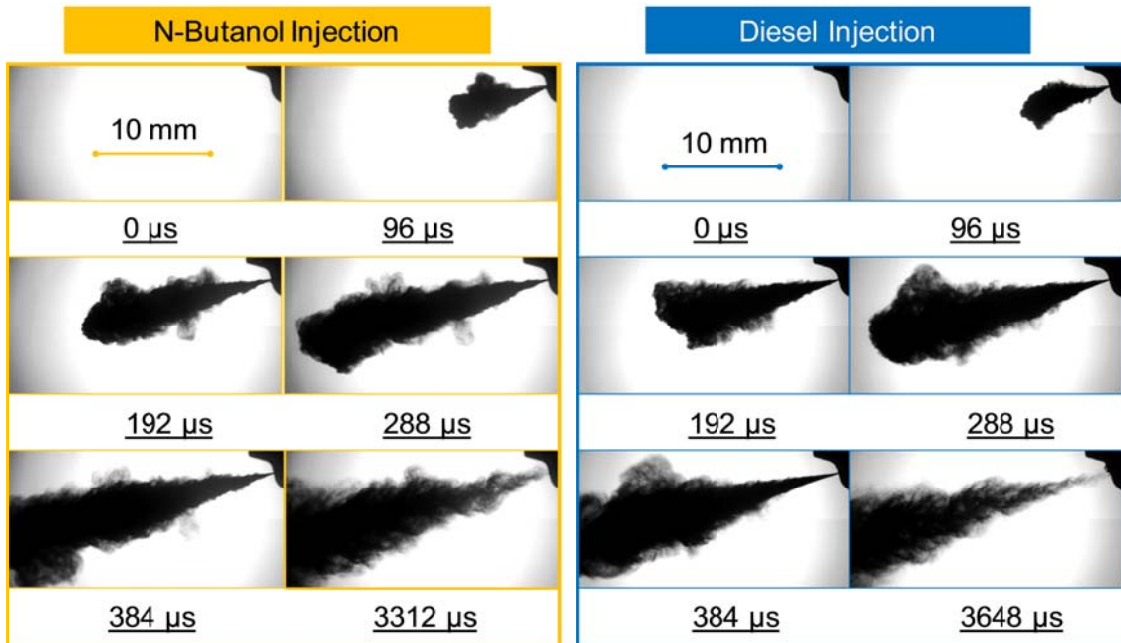
Figure 4-14 Macro spray comparison with n-butanol and diesel

The droplet velocity and size of the n-butanol high pressure injection were measured with the laser PDA. The detailed experimental setup has been described in Section 3.2.3. The droplet velocities are given in Figure 4-15 for the selected test conditions. The injection rate curve is also plotted in the same figure. The peak velocity of the droplets in the n-butanol injections was approximately 330 m/s at 10 mm and 20 mm from the nozzle hole measured by the PDA, while the velocity dropped to approximately 300 m/s for the other three measurement locations. The peak velocity quickly reduced to below 30 m/s at all the five measurement locations when the main spray traveled farther than 50 mm. The duration of the high velocity corresponds well with the duration detected from the injection rate measurement. The droplet size distribution is shown in Figure 4-16. The measurement results at different locations follow a similar trend. The most frequently detected diameters of the droplets are in the range from 10 to 20 μm.
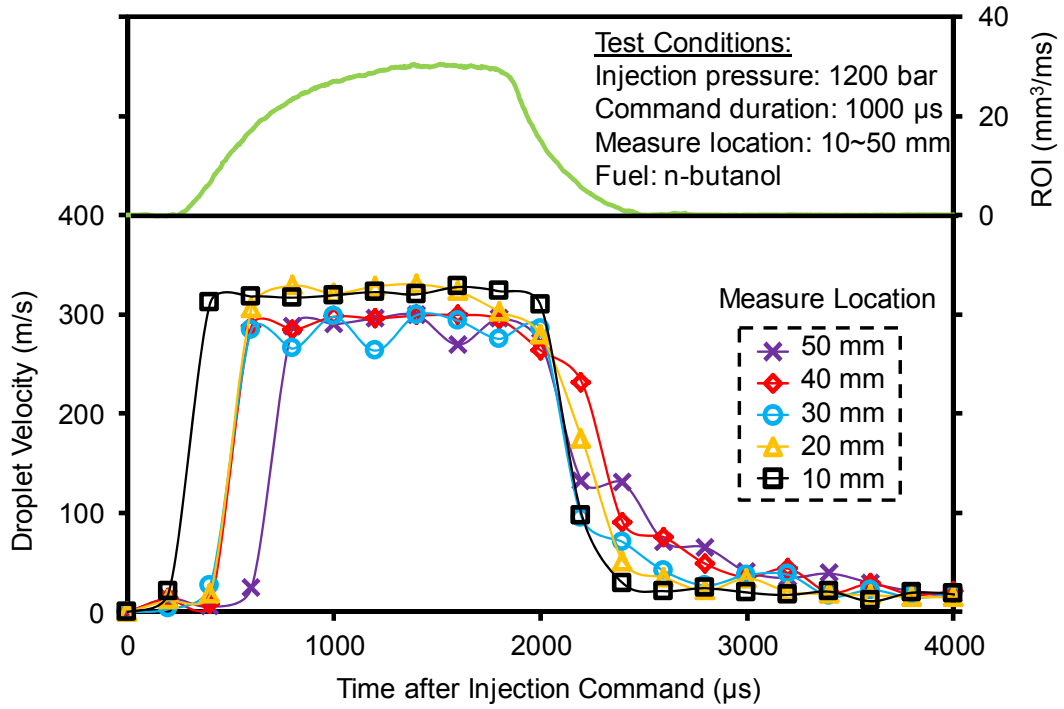
Figure 4-15 Droplet velocity at different measurement locations
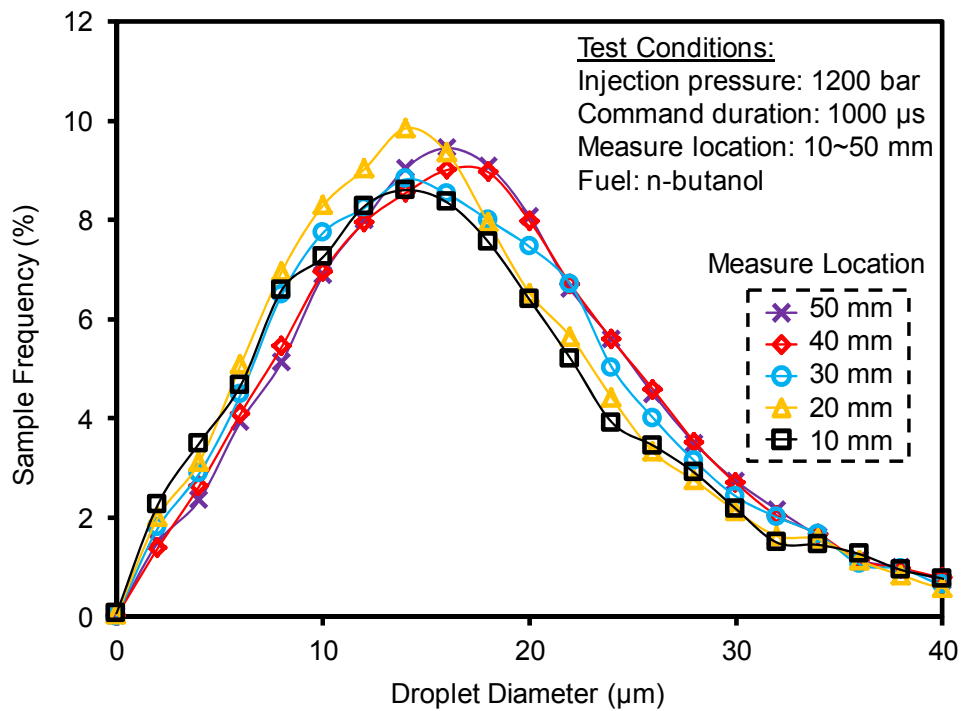
Figure 4-16 Droplet size at different measurement locations

4.5 Summary

The work presented in this chapter can be summarized as follows:

- The injection rate and the injection delays of injector opening and injector closing with the n-butanol fuel are compared with the ones of diesel. The volumetric injection rate of n-butanol is similar to that of diesel. The opening delays are at the same level for both the fuels, while the closing delays of the n-butanol injection are slightly longer than that of the diesel injection.

- The dwell time between the injection events is a critical parameter in multiple injections. A short dwell time may lead to a merged event of fuel injections. The total injection volume increases drastically when multiple injections are merged into one for the case with short injection durations.

- The macro structures of the fuel sprays with n-butanol are similar to that of diesel in the constant volume chamber. The fuel droplets close to the injector nozzle have the velocity of approximately 330 m/s detected by the PDA measurement. The majority of the droplet diameters are in a range from 10 μm to 20 μm.

CHAPTER V

MIXING CONTROL WITH SINGLE DIRECT FUEL INJECTION

The results presented in this chapter are the mixing control with diesel and n-butanol via direct fuel injections examined to determine the effectiveness of various engine parameters (*i.e.* fuel injection scheduling, intake pressure, intake temperature, and EGR). The ignition delay is used to indicate the mixing period for the direct fuel injection. Heat release rate is derived for the combustion rate comparisons. The smoke and NOx emissions are also reported at different engine operating conditions.

5.1 Mixing Control with Diesel Direct Injection

In this section, the conventional trade-off between emissions of NOx and smoke is analyzed for diesel combustion. The possible methodologies to enhance the fuel mixing are investigated. The injection strategy is limited to a single injection to eliminate the potential inferences of multiple injections.

5.1.1 NOx and Smoke Trade-off with Diesel DI

Three EGR sweeps, with different CA50 values, are conducted with diesel direct injection. The NOx emissions and ignition delays from the EGR sweeps are shown in Figure 5-1. The smoke emissions are shown in Figure 5-2. It is observed that the application of EGR is effective to suppress the formation of NOx emissions for the three EGR sweeps with different combustion phasing. As the CA50 is retarded, lower NOx emissions are observed at the same intake oxygen level. The smoke emissions at 370 °CA, reach 0.5 g/kW-hr when the intake oxygen is reduced to approximately 11.5%. In

contrast, the smoke emissions arrive at 0.3 g/kW-hr and 0.03 g/kW-hr when the combustion phasing is retarded to 375 °CA and 380 °CA, respectively.
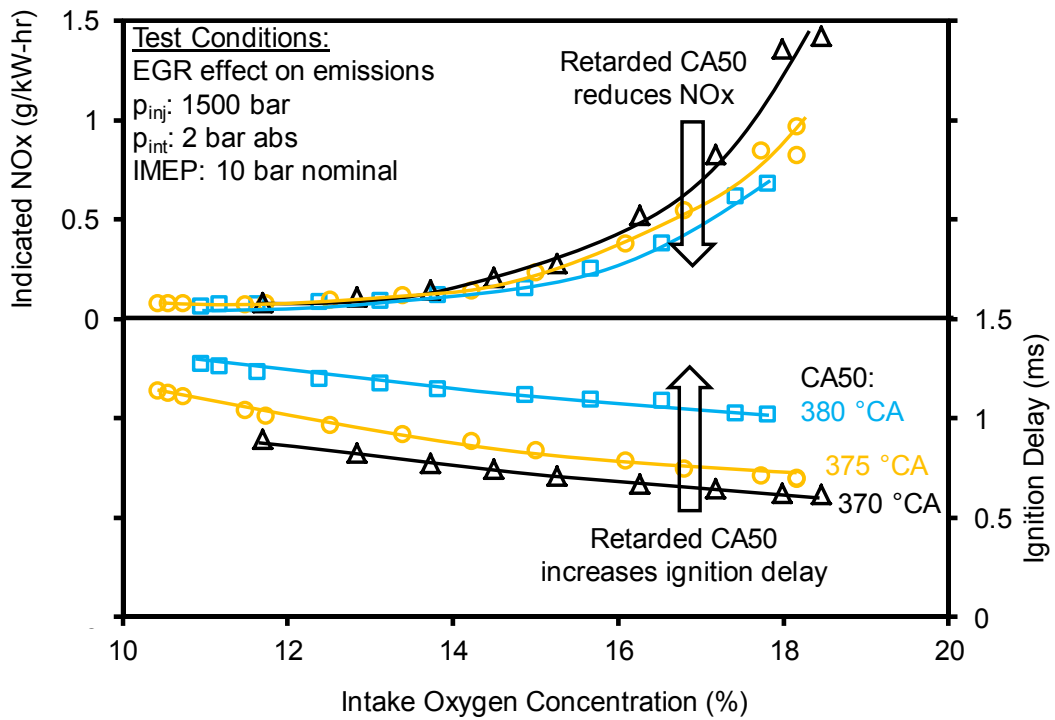
Figure 5-1 CA50 effect: NOx emissions and ignition delay in diesel combustion
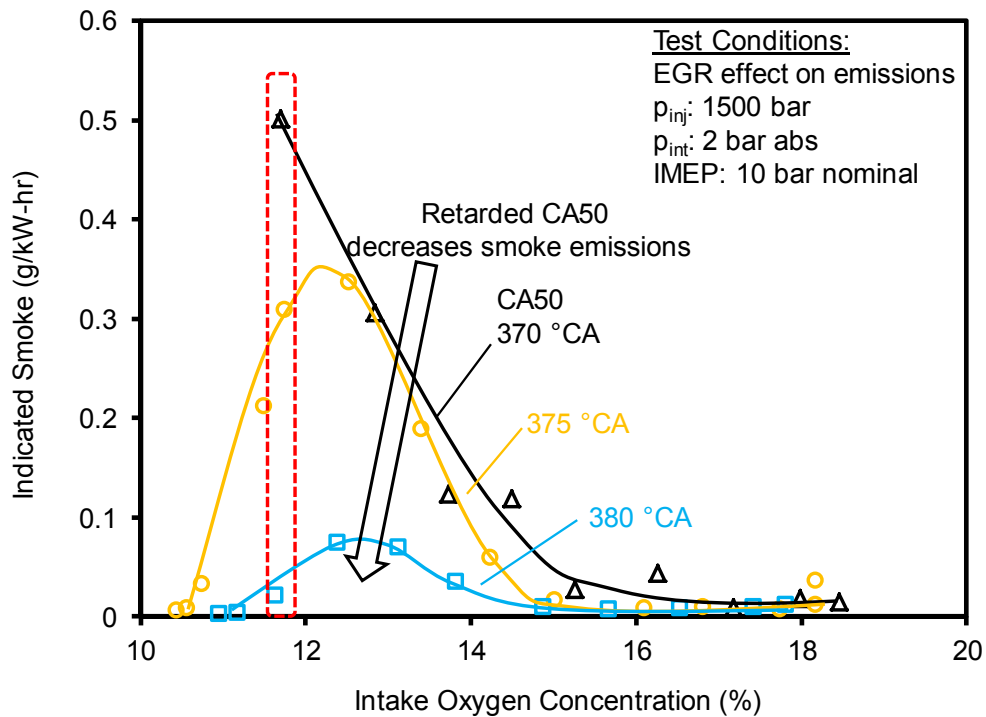
Figure 5-2 CA50 effect: smoke emissions in diesel combustion

A reduction of the indicated thermal efficiency is observed in Figure 5-3 with a retarded CA50 throughout the EGR sweep. The general trends of thermal efficiency are similar at different CA50 values. A retarded combustion phasing is beneficial to extend the ignition delay of the direct injection and enhance the fuel mixing with air. However, the delayed combustion phasing also postpones the combustion event and reduces the effective engine expansion ratio.

The CO and THC emissions are shown in Figure 5-4. The increases in the emissions of CO and THC are detected when the intake oxygen concentration is lower than 14%. The observations suggest that the increase of smoke emissions and the reduction of efficiencies (both thermal efficiency and combustion efficiency) are closely coupled.
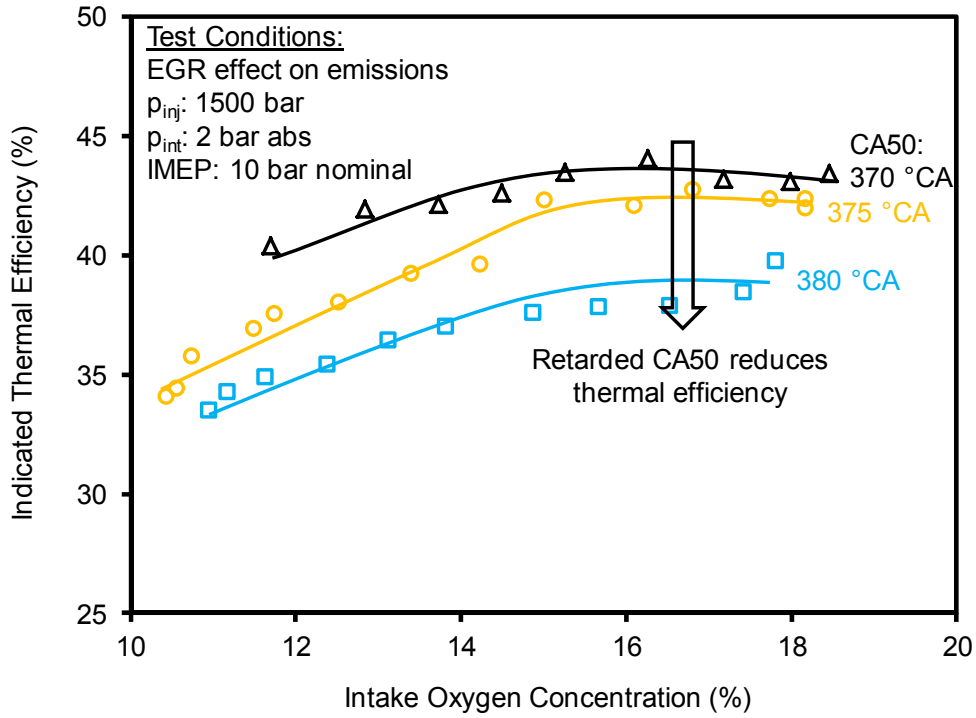
Figure 5-3 EGR effect: indicated thermal efficiency in diesel combustion
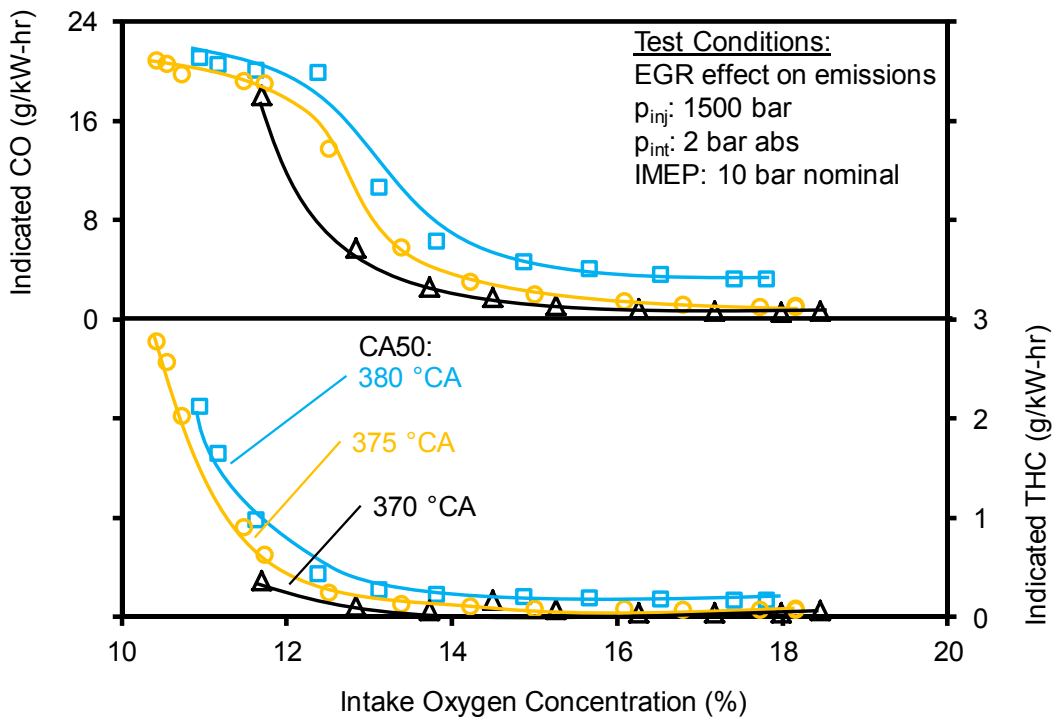
Figure 5-4 EGR effect: CO and THC emissions in diesel combustion

5.1.2 Injection Scheduling Effect on Ignition Delay and Combustion Rate

The scheduling of a direct fuel injection includes the control of injection timing, injection pressure, and injection duration. The studies of the impacts of the fuel scheduling on the mixing process are reported in this subsection.

An injection timing sweep with diesel DI is conducted at a nominal IMEP of 6.5 bar to study the effect of injection timing on ignition delay. The injection pressure is maintained at 600 bar. Natural aspiration is used in this experiment. No EGR is applied to the engine intake gas flow. The CA5 and CA50 are shown in Figure 5-5 together with the ignition delay. The CA5 is used as the indication for the onset of combustion, while the CA50 is used for the combustion phasing indication. Longer ignition delays, calculated with the injection command and CA5, are observed from the tests with both the early and late injection timings. The short ignition delays are obtained from the combustion with the CA5 close to TDC. The ignition delays are in the range from 1 ms to 1.4 ms at this engine load.
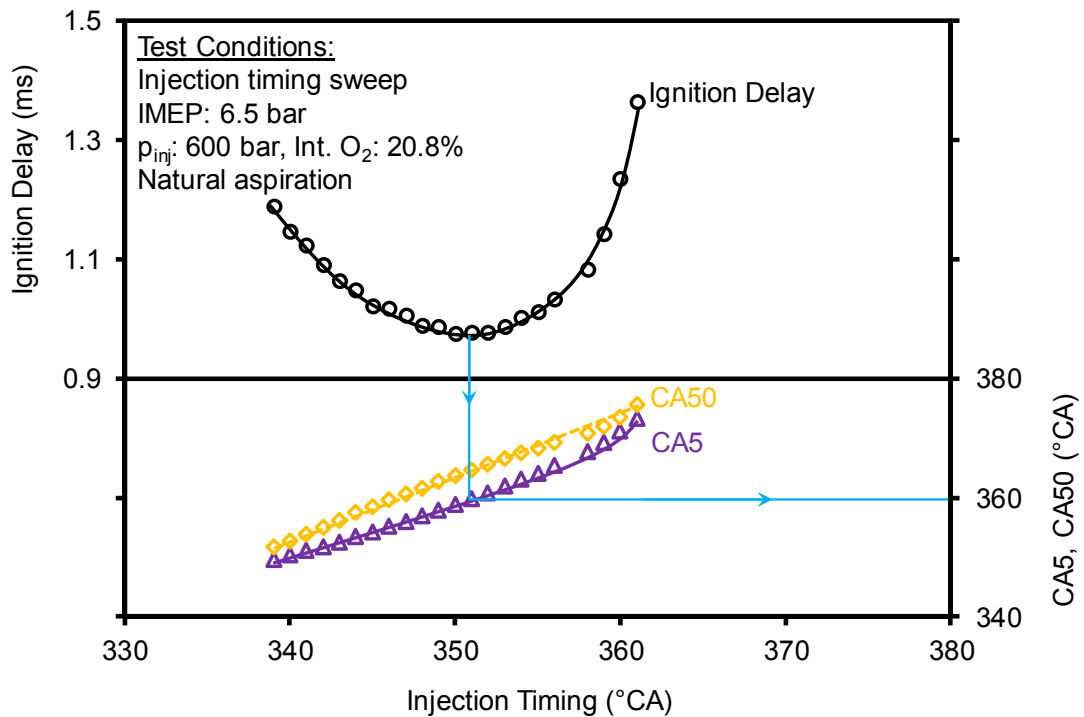
Figure 5-5 Diesel injection timing sweep: ignition delay, CA5 and CA50

A potential cause for the variations in the durations of ignition delay can be attributed to the changed in-cylinder temperature during the engine compression and expansion strokes. The estimated mean in-cylinder temperatures are shown in Figure 5-6 that are calculated using the PUMA and SCRE engine specifications, as given in Table 3-1. The heat transfer is not considered in the calculation. The peak compression temperature is estimated at about 560 °C with the compression ratio of 18.2:1. A higher engine compression ratio typically leads to a higher temperature at the TDC. The temperature profile is almost symmetric with respect to the engine TDC. However, the trend of the ignition delay values in Figure 5-5 is not symmetric. The curve of ignition delay is flatter in the compression stroke and sharper in the expansion stroke. With the increasing temperature in the compression stroke, the in-cylinder condition is more favorable to initiate combustion than that in the expansion stroke. Thus, the ignition delay is shorter in

67

the compression stroke, compared to the one at the same in-cylinder temperature in the expansion stroke.
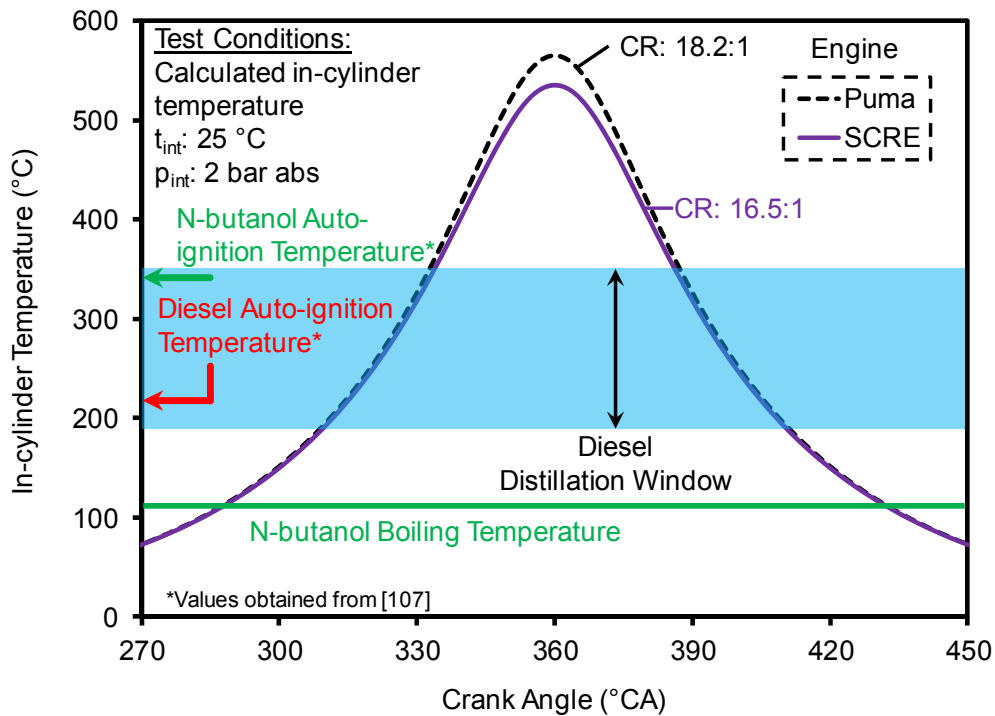
Figure 5-6 Mean in-cylinder temperature and distillation window

The evaporation of the fuel is required to generate the air-fuel mixture and start the combustion [28]. The fuel injected at a temperature lower than the minimum of the distillation temperature window, can still evaporate in the compression stroke due to the temperature rise at a later stage, but this phenomenon may not occur in the expansion stroke. This temperature window is critical for the design of fuel injection timings to prevent oil dilution and wall impingement.

It is noted that the auto-ignition temperature of diesel falls in the distillation window. The combustion can be enabled before the complete evaporation of the fuel. The combustion heat may further enhance the fuel evaporation. This phenomenon often occurs in the

diffusion combustion in conventional diesel engines. The low auto-ignition temperature of diesel can tolerate early and late timings of fuel injections. However, the relatively high ability of ignition also increases the challenge to separate the fuel injection event from the combustion event as required by the advanced combustion strategies [88].

Three data points from the EGR sweep in Figure 5-5 are selected to analyze the variations of combustion rate at different levels of ignition delay values. The cylinder pressure and heat release rate curves of the three data points are shown in Figure 5-7. The data point with the injection timing at 340 °CA has the shortest overall combustion duration among the three. The relatively low compression temperature at this injection timing enables the long ignition delay. The long ignition delay enhances the fuel mixing. Furthermore, the trend of the temperature rise in the engine compression stroke increases the rate of combustion and shortens the combustion duration.

The peak pressure rise rate (PPRR) and IMEP of this test are shown in Figure 5-8. The lowest PPRR is achieved with the injection timing at approximately 355 °CA. When the injection timing is advanced, the PPRR is significantly increased mainly due to the enhanced in-cylinder charge mixing and the temperature rise in the compression stroke. When the injection timing is delayed from 355 °CA, the combustion occurs in the engine expansion stroke. The slightly increased PPRR is primarily attributed to the longer ignition delay, as shown in Figure 5-5. The IMEP is not significantly affected within the range of injection timings from 340 °CA to 360 °CA.
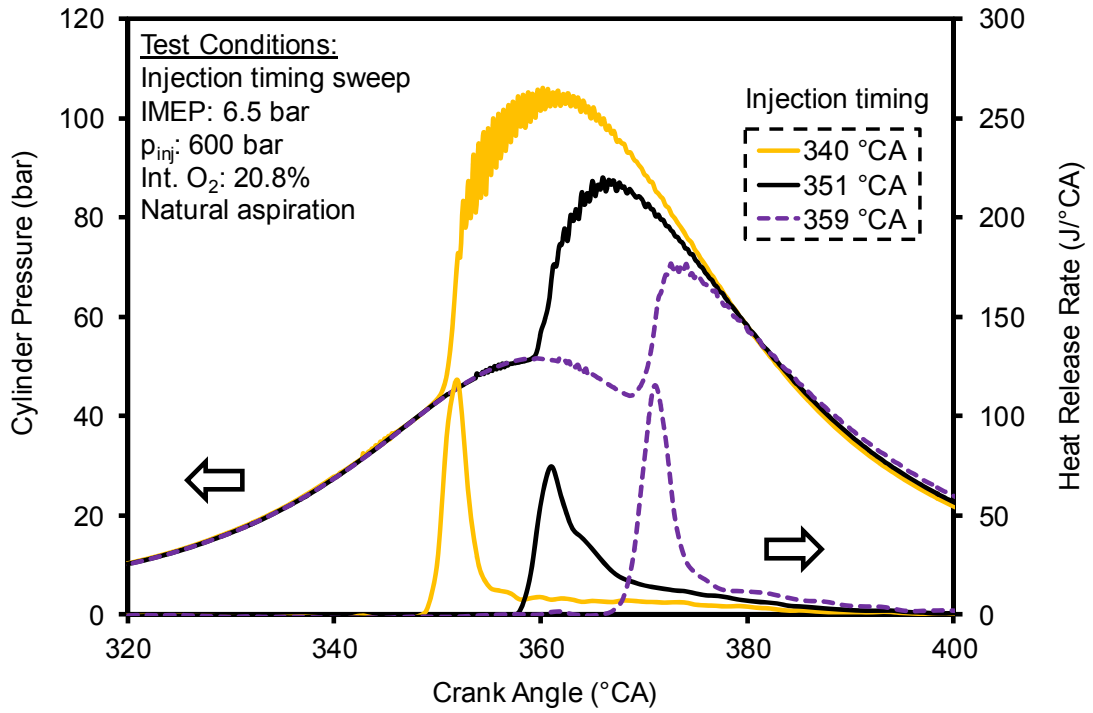
Figure 5-7 Cylinder pressure and HRR for selected injection timings with diesel
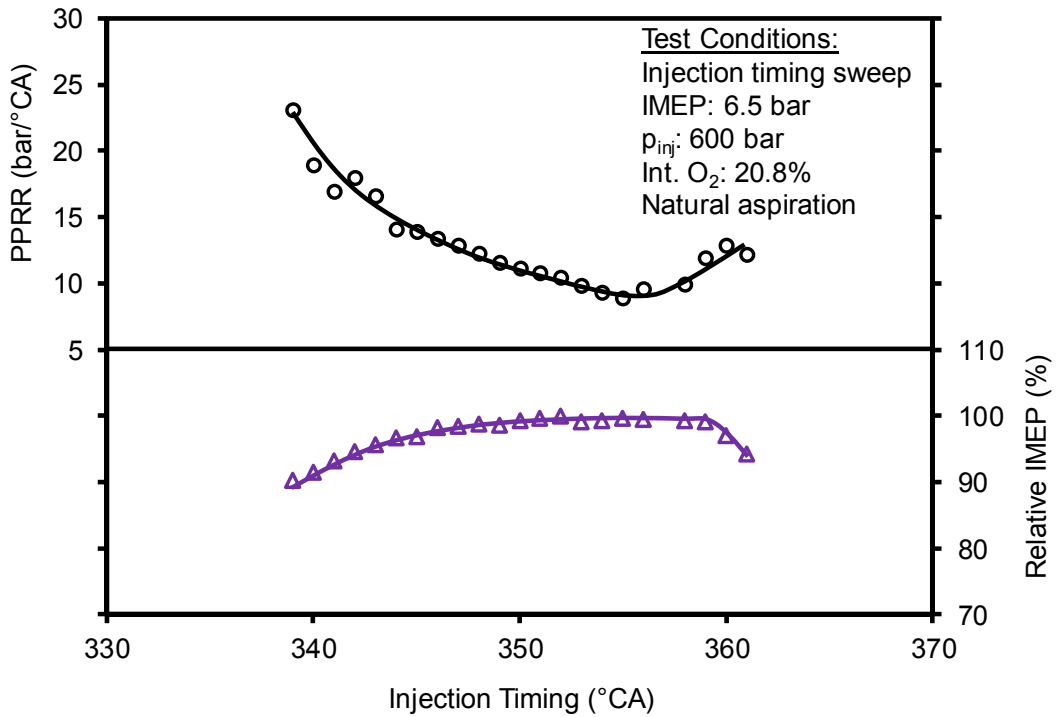
Figure 5-8 Diesel injection timing sweep: PPRR and IMEP

The effect of the fuel injection pressure on the ignition delay is shown in Figure 5-9. As the injection pressure is increased from 600 bar to 900 bar, the IMEP is maintained by using a shorter injection duration (530 μs instead of 650 μs). It is observed that the trend of ignition delay remains similarly for both the injection pressures. The ignition delays at 900 bar injection pressure are shorter than the ones at 600 bar pressure given the same injection timings. A high injection pressure increases the spray penetration and enhances the atomization of the fuel spray [42]. Hence, more small fuel droplets are typically generated at the high fuel injection pressure. The large surface area of the small droplets increases the heat transfer from hot air to fuel and accelerates the fuel evaporation process. Thus, the mixing of the in-cylinder charge can be enhanced at the higher injection pressure in diesel combustion.
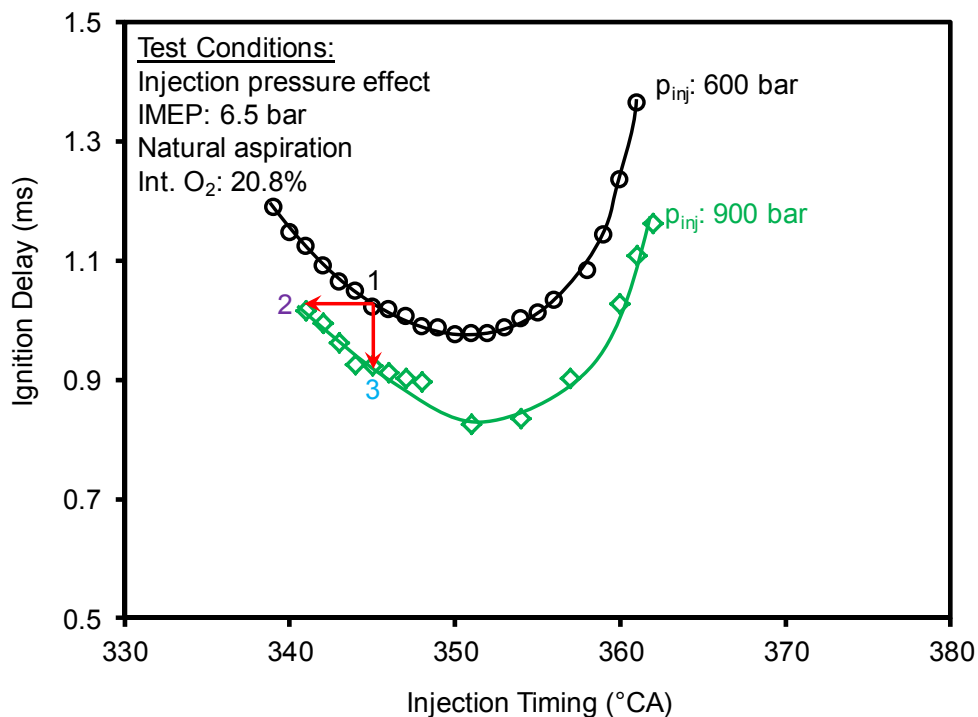
Figure 5-9 Diesel injection pressure effect on ignition delay

71

Three data points denoted as 1, 2, and 3 are selected from Figure 5-9. The ignition delay values are in a similar range for data points 1 and 2, while the injection timings are close to each other for data points 1 and 3. The heat release rate is normalized with the total heat release, to investigate the combustion rate. The normalized heat release rate curves are shown in Figure 5-10. The crank angle is shifted to align the start of combustion for the three data points. Compared to data point 1, data point 2 has a considerably higher portion of premixed combustion. Within a similar duration of ignition delay, the fuel mixing is improved with the elevated injection pressure. Data point 3 has a shorter ignition delay than data point 1, but the HRR still shows a higher portion of premixed combustion. This phenomenon suggests that a shorter ignition delay at a higher fuel injection pressure may still lead to enhanced mixing of the in-cylinder charge.
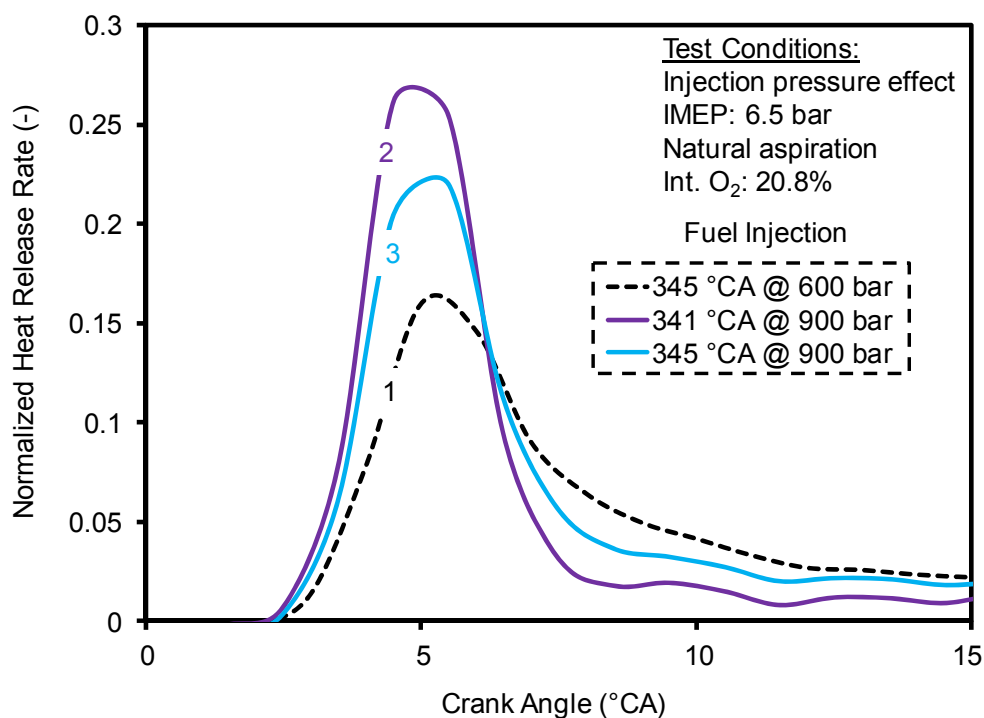
Figure 5-10 Normalized heat release rate of selected data points of diesel combustion

72

The effects of the injection duration on the combustion characteristics are shown in Figure 5-11. The duration of injection command is gradually increased from 320 μs to 880 μs while a constant combustion phasing is maintained. A higher amount of fuel is typically delivered with a longer injection duration, as shown in Figure D-1. As a result, the IMEP is increased from 1 bar to 11.5 bar. The ignition delay is only slightly prolonged (from 0.5 ms to 0.6 ms) with the considerably increased fuel amount. The diffusion burning with a longer injection duration is expected to increase due to the limited duration of ignition delay. The short ignition delay also demonstrates the mixing challenge when a large amount of fuel is employed at a high engine load.
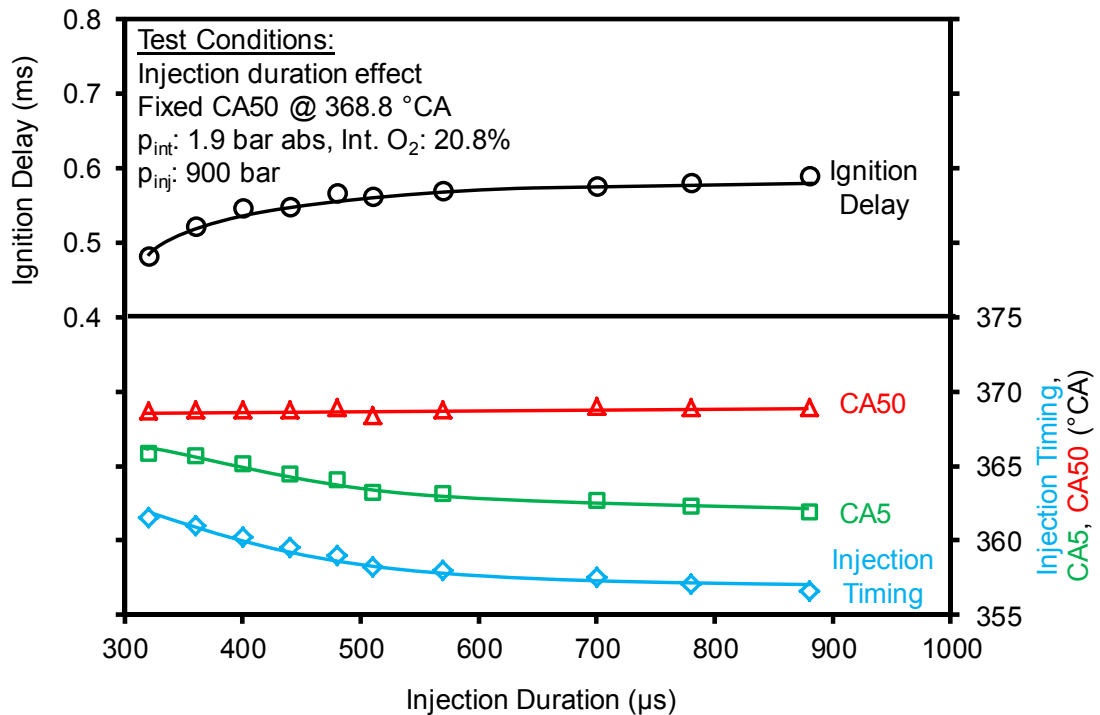
Figure 5-11 DI duration sweep: ignition delay, Injection timing, CA5, and CA50

Three engine loads are selected from Figure 5-11, and the HRR curves of the three load levels are shown in Figure 5-12. It is observed that the portion of premixed combustion reduces, while the portion of diffusion combustion increases, as the engine load is

elevated. This phenomenon supports the previous assumption of increased diffusion burning at higher engine loads.
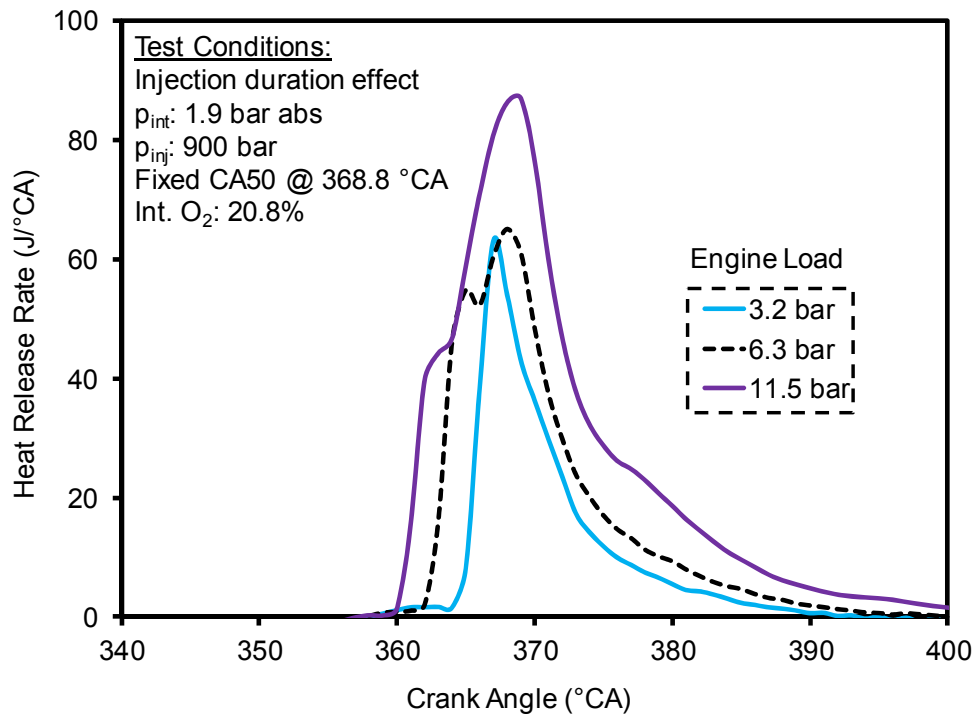
Figure 5-12 Heat release rate at varied injection durations of diesel combustion

To summarize, the trade-off between NOx and smoke emissions from diesel combustion is primarily caused by the insufficient mixing of the in-cylinder charge. Different fuel scheduling strategies, such as using the late fuel injection timing, can prolong the mixing time and reduce the emissions of NOx and smoke under the application of EGR. However, the longer ignition delay is obtained with the shortened effective expansion stroke length. Hence, both the combustion efficiency and thermal efficiency tend to be reduced with the delayed injection timing. Varied injection timings, different injection pressures, and the application of EGR have limited effects in prolonging the ignition delay due to the low volatility and high reactivity of the diesel fuel.

5.2 Mixing Control with Butanol Direct Injection

5.2.1 Ignition Delay with Butanol DI

The injection timing effect of n-butanol DI on ignition delay is studied with a fixed injection duration at 900 bar injection pressure. The nominal IMEP is at 4.5 bar. Two different intake pressures, 1.8 bar absolute (abs) and 2.0 bar abs, are used. The range of injection timing is limited by the excessively reduced engine load, the high peak cylinder pressure (PCP), and the high peak pressure rise rate (PPRR).

The ignition delay value and the CA5 are shown in Figure 5-13. Compared with the ignition delays in the diesel baseline in Figure 5-5, the ignition delays of n-butanol combustion (2~5 ms) are much longer than the ones in the diesel combustion (approximately 1 ms). The ignition delay of the n-butanol combustion increases when the injection timing is away from the timing of the shortest ignition-delay. The injection timing later than 350 °CA is infeasible due to the significant reduction in the engine load.
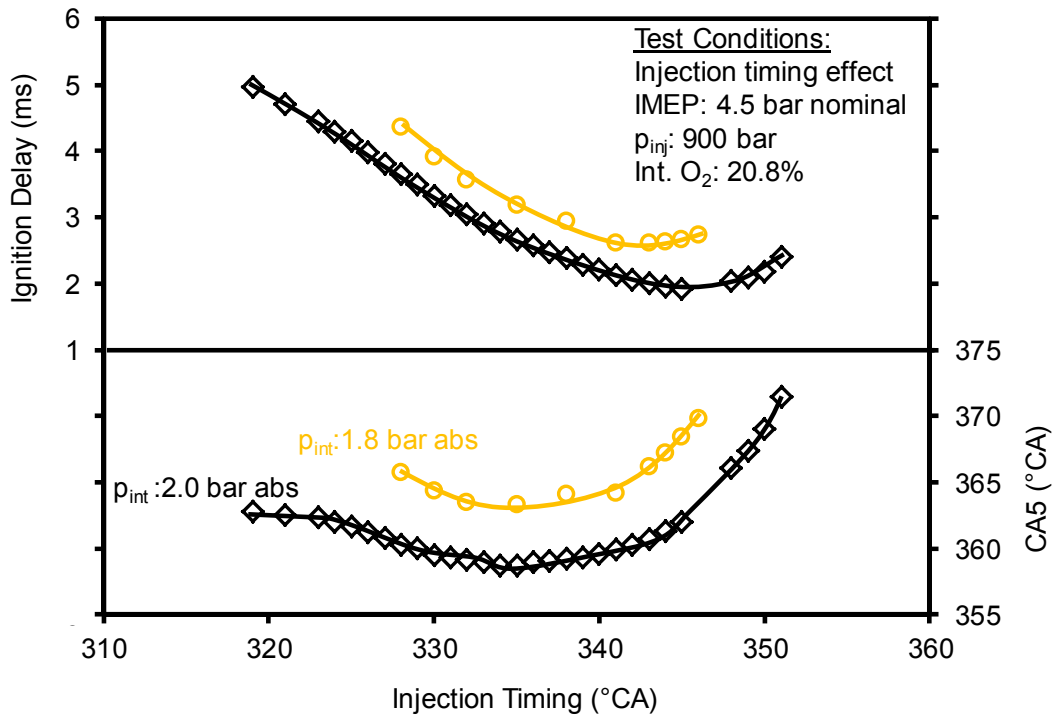
Figure 5-13 N-butanol injection timing effect: ignition delay and CA5

The long ignition delay of n-butanol is mainly caused by the low reactivity of n-butanol that requires longer chemical preparation time for the onset of combustion. Furthermore, the boiling temperature of n-butanol is lower than diesel. Together with the longer ignition delay, the mixing of n-butanol is much higher than diesel at similar engine operating conditions. Hence, the possibility of forming the in-cylinder charge excessively lean for effective combustion increases considerably. It is observed that the asymmetry of the ignition delay curve increases in the n-butanol combustion, compared with the one in Figure 5-5. This indicates that the n-butanol combustion is more sensitive to the in-cylinder temperature.

The THC and CO emissions are shown in Figure 5-14. It is observed that the THC emissions increase drastically for the early and late injection timings. The injection timing window for low THC emissions (less than 200 ppm) is approximately from

76

330 °CA to 350 °CA. The window for low CO emissions (less than 4000 ppm) is even narrower. The high emissions of these incompletely oxidized products indicate the low combustion temperature when the injection timing is excessively advanced or delayed.
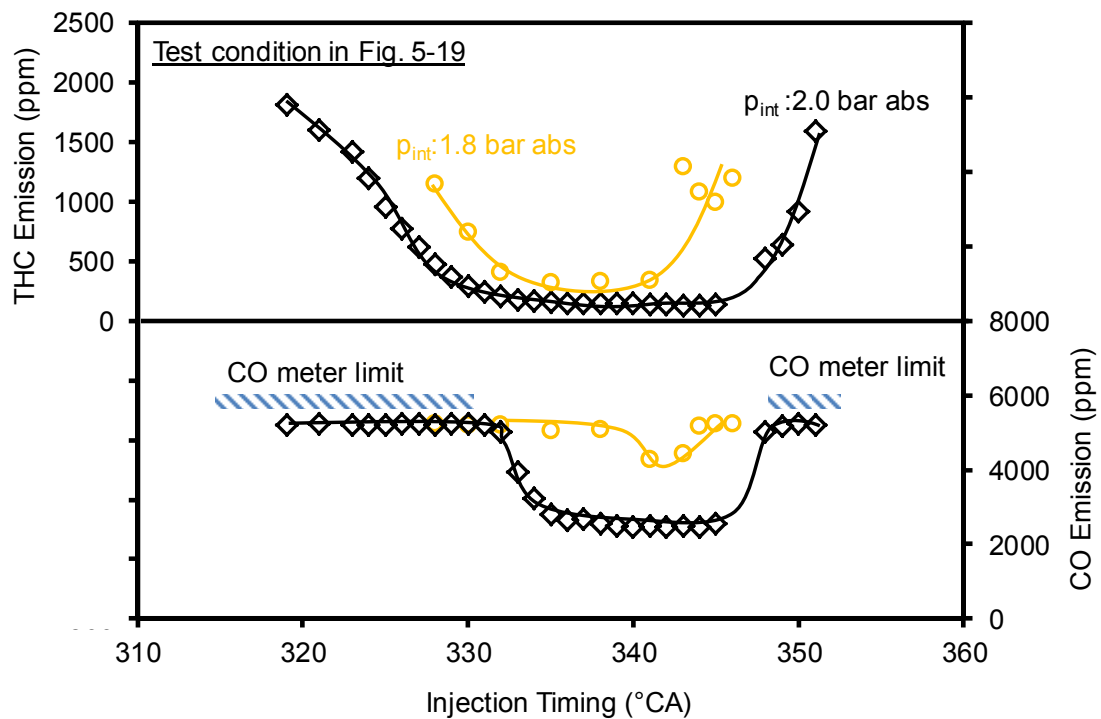
Figure 5-14 N-butanol injection timing effect: THC and CO emissions

The NOx and smoke emissions are shown in Figure 5-15. The NOx emissions remain lower than 20 ppm, while the smoke emissions are lower than 0.2 FSN for both intake pressures. The ultra-low emissions from the n-butanol combustion are primarily attributed to the long ignition delay and the enhanced mixing of the in-cylinder charge. The low fuel reactivity limits the temperature rise during combustion, which is beneficial for low NOx emissions. The assumption of low combustion temperature is supported by the high emissions of CO in Figure 5-14.
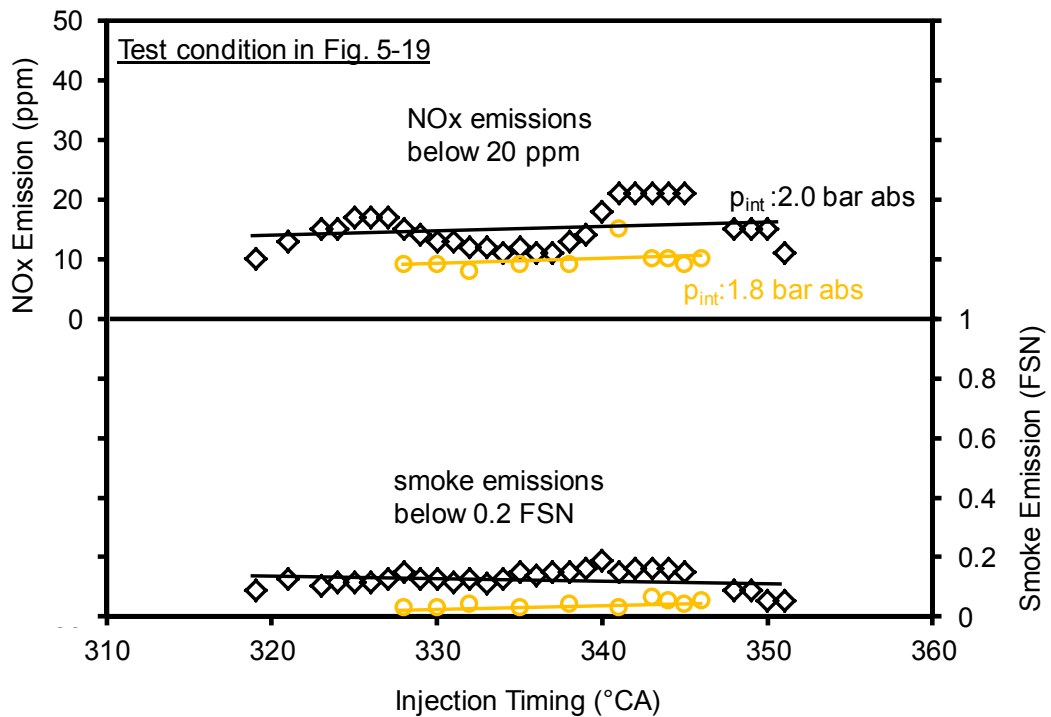
Figure 5-15 N-butanol injection timing effect: NOx and smoke emissions

With the prolonged ignition delay, the impact of injection pressure on the mixing process becomes less significant in the n-butanol combustion. The experiment in Figure 5-13 is extended by testing two more injection pressures at the same intake pressure and engine load. The ignition delays and PCP values from the test with the three injection pressures are summarized in Figure 5-16. The differences between the results of 400 bar and 600 bar injection pressures are marginal over the injection timing sweep, for both the ignition delay and CA5. Furthermore, at 900 bar injection pressure, the ignition delay is slightly shortened while the PCP is increased. Three data points at the same injection timing of 337 °CA are selected to study the impact of injection pressure on cylinder pressure and HRR, as shown in Figure 5-17. The combustion event is slightly advanced towards TDC with the increased injection pressure of 900 bar. The PPRR is increased due to the potentially higher compression temperature close to TDC.
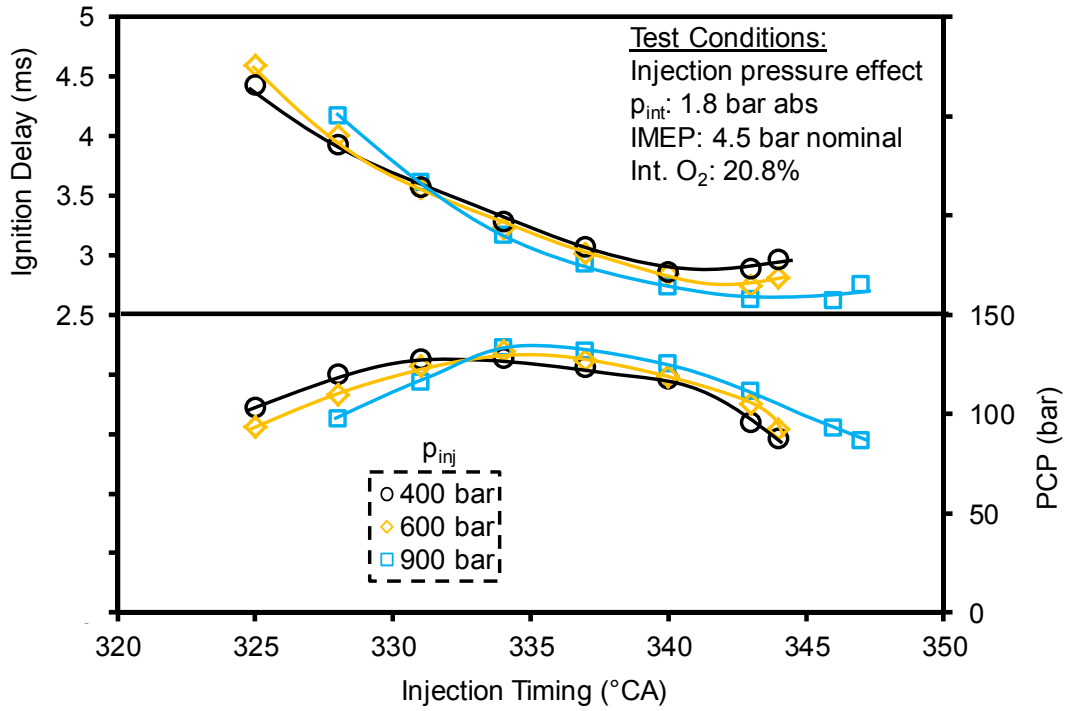
Figure 5-16 N-butanol injection pressure effect: ignition delay and PCP
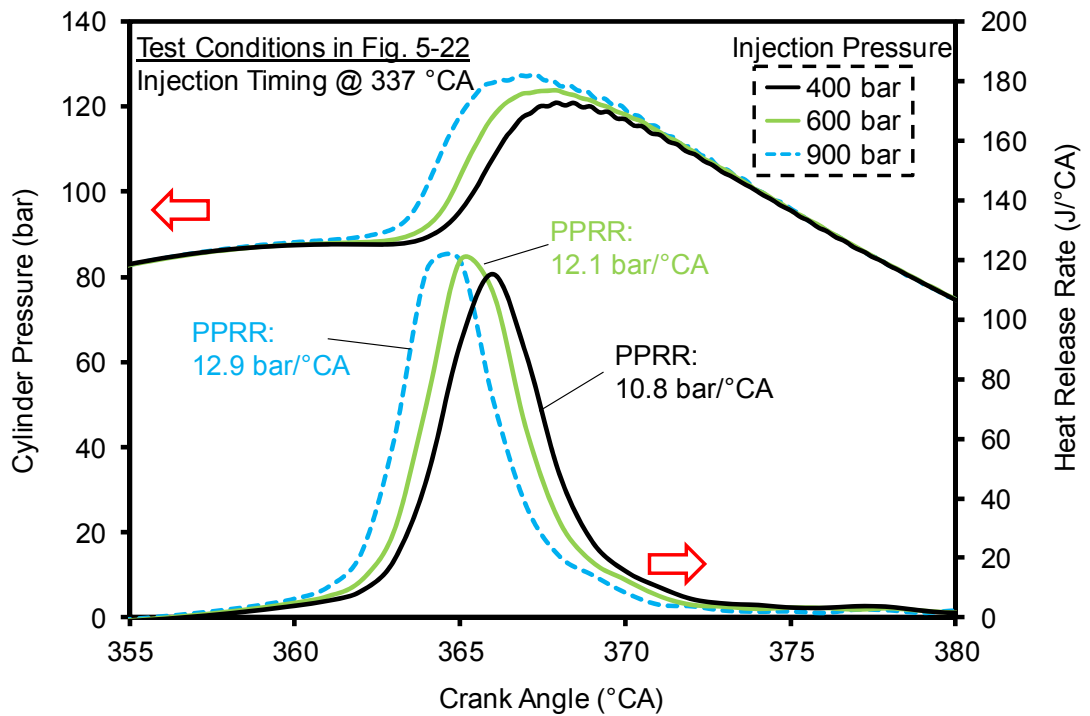
Figure 5-17 N-butanol injection pressure effect: cylinder pressure and HRR

5.2.2 Combustion Rate Control with Butanol DI

The combustion rate control is a common challenge for the combustion with premixed in-cylinder charge. A highly premixed charge is typically formed with the n-butanol DI due to the long ignition delay, at the tested conditions in the previous sub-section. Therefore, the combustion rate control of n-butanol DI is studied in this subsection.

The PPRR of the n-butanol injection timing sweep is given in Figure 5-18. It is observed that the PPRR can be reduced from approximately 15 bar/°CA to 3 bar/°CA with either advanced or retarded injection timings. However, the mechanisms for the PPRR reduction are different. With the advanced DI timing, the ignition delay is considerably prolonged. The homogeneity of the in-cylinder charge is improved. The decreased PPRR is primarily caused by the combustion with an overall leaner in-cylinder charge. In contrast, with the retarded DI timing, the change in mixing time is limited (Figure 5-13) but both the SOC and combustion phasing are significantly delayed into the engine expansion stroke due to the long ignition delay. The PPRR reduction is mainly caused by the cylinder volume expansion. The PPRR with a lower intake pressure follows a similar trend as the one at a higher intake pressure. Moreover, the PPRR at a lower intake pressure is generally lower at similar injection timings.
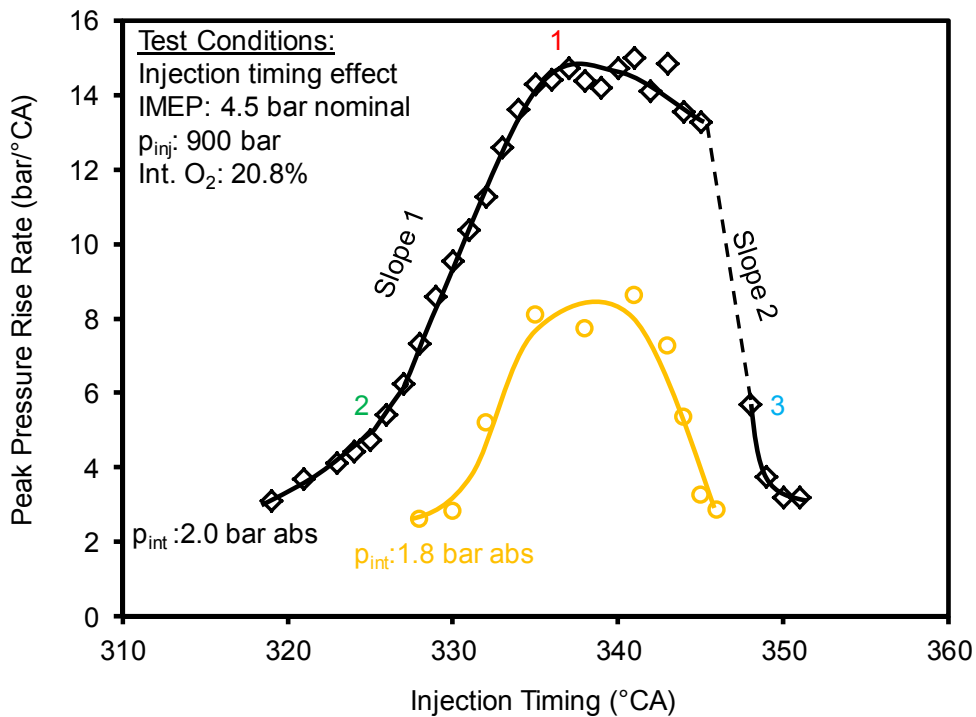
Figure 5-18 N-butanol injection timing effect: PPRR at varied injection timing

The same set of data is plotted against IMEP in Figure 5-19. The PPRR reduces with the decreased IMEP following two different slopes. The two different slopes support the aforementioned assumption of different reduction mechanisms for PPRR. When the PPRR is suppressed through the mixing control (Slope 1 in Figure 5-18), the PPRR and IMEP are closely coupled. The IMEP reduces with the decreased PPRR. In contrast, the PPRR and IMEP are decoupled when the PPRR is reduced primarily by the retarded combustion phasing (Slope 2 in Figure 5-18). This phenomenon suggests that PPRR can be drastically reduced with only slightly decreased IMEP within a certain range of injection timings (Slope 2). It is beneficial to operate the engine in this range with a low PPRR and a low loss in IMEP.
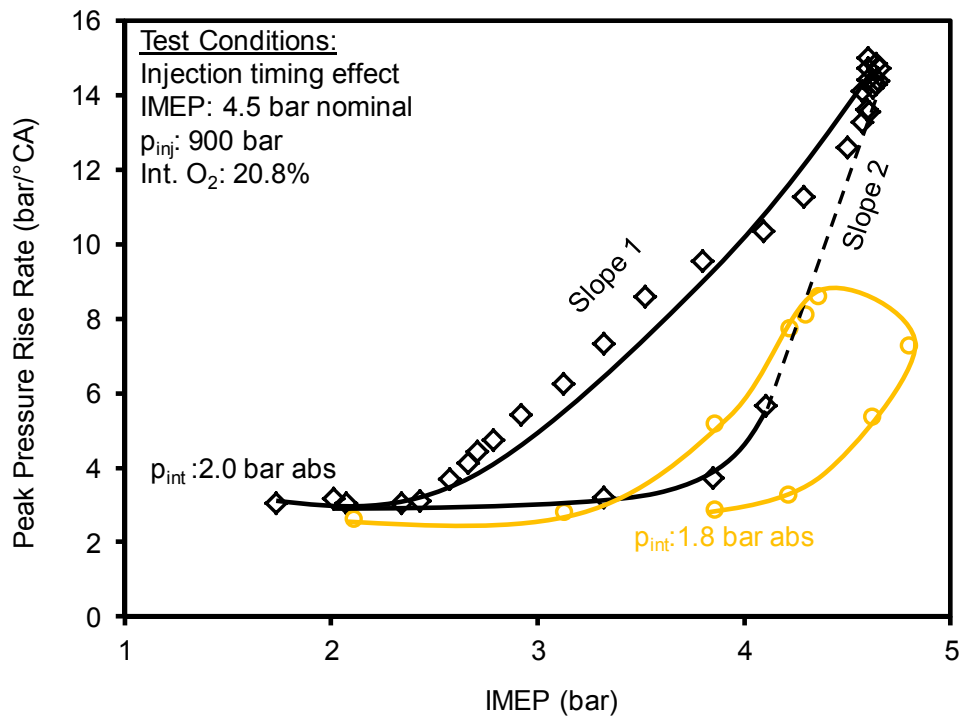
Figure 5-19 N-butanol injection timing effect: PPRR and IMEP

Three data points as highlighted in Figure 5-18 are selected from the injection timing sweep at 2.0 bar intake pressure. The cylinder pressure and HRR are compared in Figure 5-20. Data point 1 has the highest PCP and peak HRR, among the three. Data point 2 has the lowest overall HRR that is generated from the lean combustion of a highly premixed in-cylinder charge. Data point 3 has the higher HRR but retarded combustion phase. The PCP and PPRR of data point 3 are at similar levels as the ones of data point 2, but the IMEP is considerably higher than that of data point 2. The higher IMEP of data point 3 is obtained from the mixing control of the in-cylinder charge. The ignition delay of data point 3 (2.05 ms) is much shorter than the one of data point 2 (3.89 ms). The over-mixing tendency is reduced with the short ignition delay.
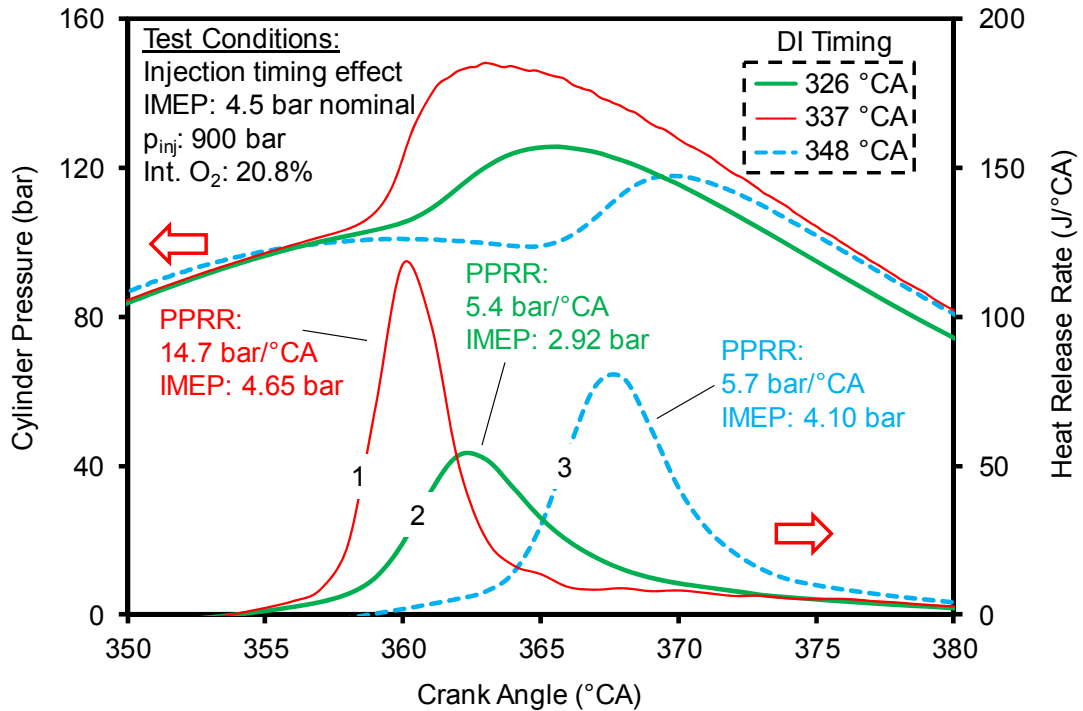
Figure 5-20 N-butanol injection timing effect: cylinder pressure and HRR

The PPRR controlled with DI timing is closely coupled with the combustion efficiency and the thermal efficiency in the n-butanol combustion. A reduction in PPRR is often associated with the reduced IMEP. The injection timing on the second slope (Figure 5-18) shows certain benefits of less reduction in IMEP. However, the combustion efficiency is still reduced by the high emissions of CO and THC (Figure 5-14). Therefore, the application of EGR is investigated for the combustion rate control.

Fixed injection timing and duration of the n-butanol DI are used to study the effects of EGR on the control of combustion rate. The nominal IMEP is 5.5 bar. The IMEP values are normalized with the peak IMEP in the EGR sweep. The IMEP is normalized with the peak IMEP in this EGR sweep, can converted to percentage. The normalized IMEP, PCP, and PPRR are shown in Figure 5-21. It is observed that the application of EGR is effective to control the PCP and PPRR in this test. However, the normalized IMEP is also

progressively reduced. A significant IMEP drop (20%) is detected when the intake oxygen concentration is reduced to approximately 18%.
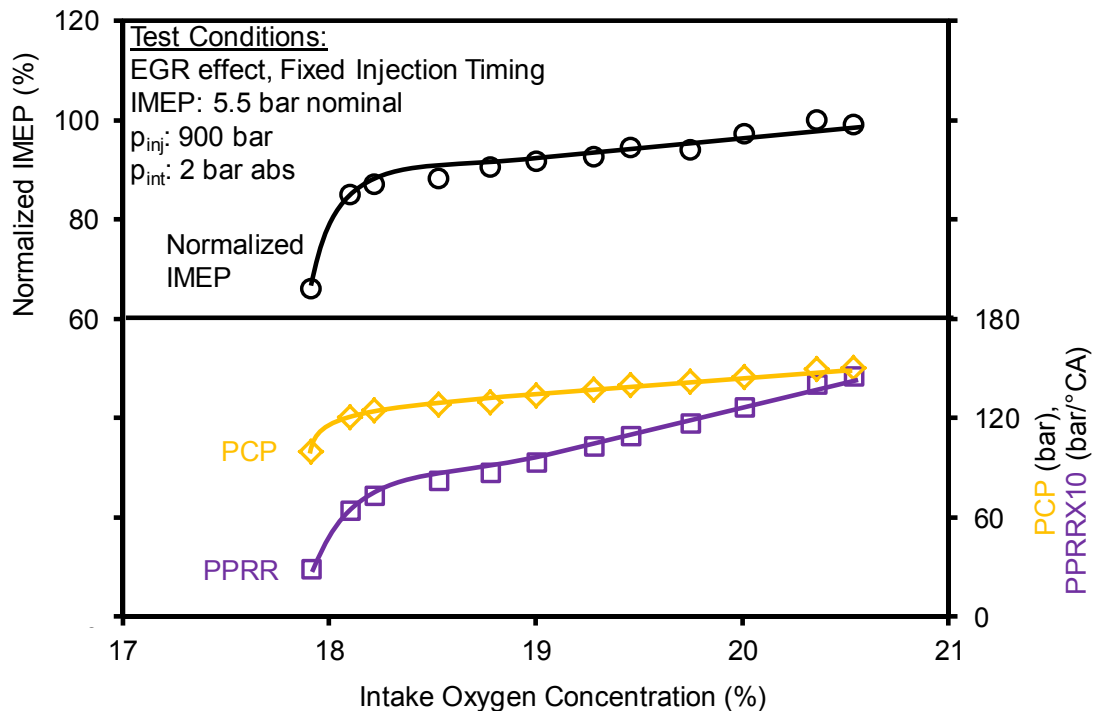
Figure 5-21 EGR effect: normalized IMEP, PCP, and PPRR in n-butanol combustion

The CA5 and CA50 of this EGR sweep are shown in Figure 5-22 together with the ignition delay. As the intake oxygen concentration is decreased, the ignition delay is prolonged. The CA5 and the CA50 are both retarded. The reductions in IMEP, PCP, and PPRR can be primarily attributed to the retarded combustion phasing.

Another experiment is conducted with a fixed combustion phasing but varied injection timings. The normalized IMEP value, PCP, and PPRR are shown in Figure 5-23. As the intake oxygen level is reduced to approximately 16% by the EGR application, the relative IMEP value, PCP, and PPRR all remain at the same levels, respectively. With a fixed combustion phasing, the PPRR is insensitive to the EGR application.
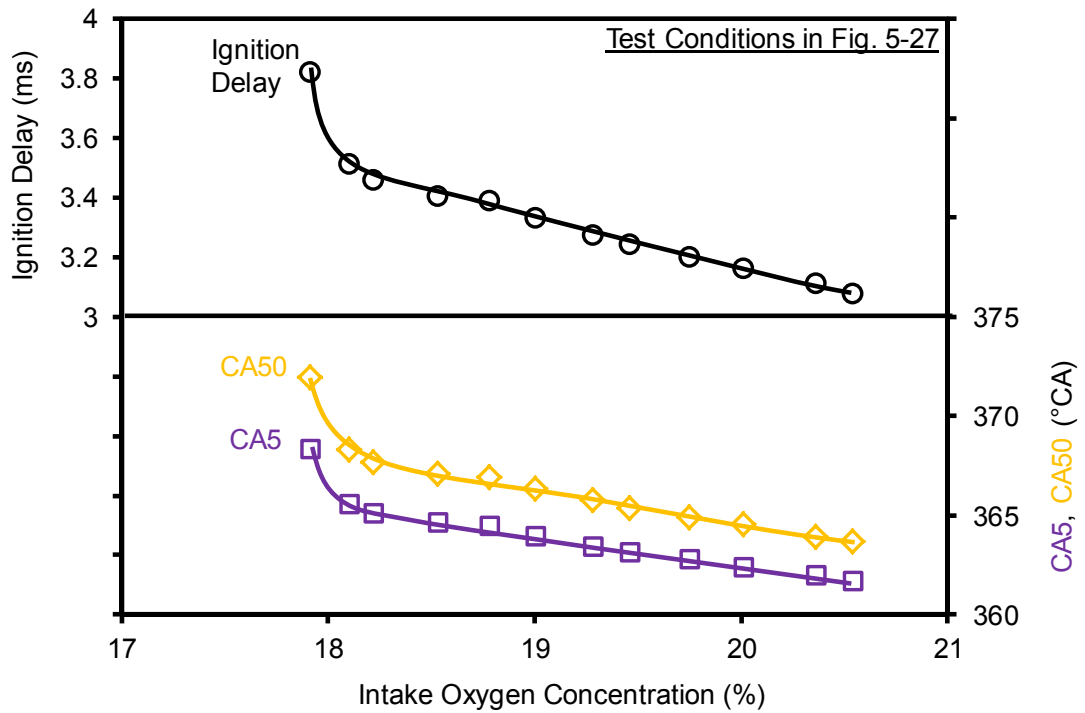
Figure 5-22 EGR effect: ignition delay, CA5 and CA50 in n-butanol combustion
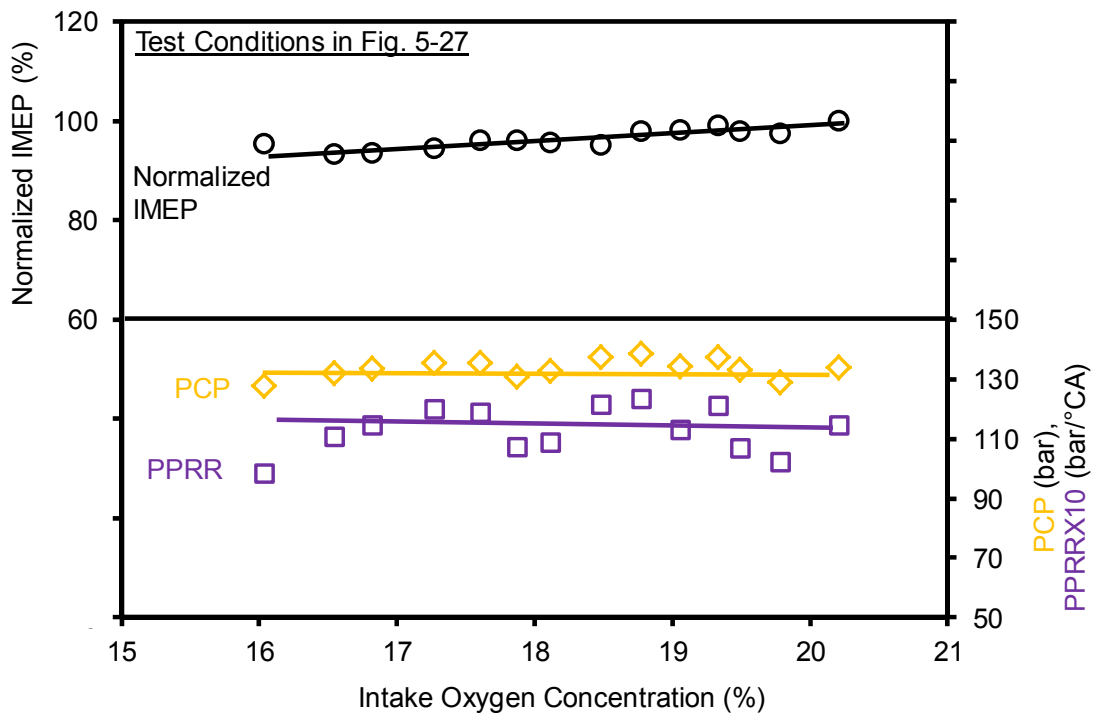
Figure 5-23 EGR effect: normalized IMEP, PCP, and PPRR in n-butanol combustion

To summarize, the control of combustion rate can be achieved via the modulation of injection timing and the application of EGR. The common mechanism is the retardation of the combustion phasing. If the combustion phasing is fixed, the effectiveness of EGR on the control of combustion rate is limited. Furthermore, a delayed combustion phasing is often associated with a lower combustion efficiency. The low charge reactivity delays the ignition, increases the combustion duration, and reduces the combustion temperature.

5.2.3 Ignition Enhancement for Butanol DI

Elevated intake pressure and intake temperature are commonly employed to enhance the ignition ability when a low reactivity fuel is used in a compression ignition engine. On the PUMA engine platform, only the increased intake pressure is required for the combustion with n-butanol DI due to the relatively high compression ratio. However, both high intake pressure and high intake temperature are needed to initiate the combustion on the SCRE engine platform. The impact of intake pressure and temperature on combustion characteristics and emissions are studied with both the engine platforms in this subsection.

The intake pressure effects on ignition delay and combustion rate have been demonstrated in the previous tests, such as in Figure 5-13 and Figure 5-18. The ignition delay is generally reduced, and the PPRR is increased, at a higher intake pressure. In this experiment, three intake pressures (1.5 bar, 1.8 bar, and 2.0 bar) are used to explore the potential operating limit of intake pressure for the n-butanol combustion. The injection pressure is fixed at 900 bar during the test. Injection timing sweeps are conducted at each of the intake pressures to examine the operating window of the injection timing.

The ignition delay and CA5 are shown in Figure 5-24 for the three intake pressure levels. Generally, a shorter ignition delay is witnessed for a higher intake pressure at the same injection timing, which is consistent with the previous observation (Figure 5-13). The ignition delays for the test at 2.0 bar and 1.8 bar intake pressures are close to each other, while the ones at 1.5 bar intake pressure are approximately 1 ms longer. The CA5 values are all in the engine expansion stroke. Hence, a longer ignition delay retards the combustion phasing further into the expansion stroke. The combustion temperature is lower and the volume expansion is higher. Both the lower temperature and faster expansion decrease the ignition ability of the charge and reduce the combustion temperature. The longer ignition delay for the 1.5 bar intake pressure case is an indication that the intake pressure approaches the low limit at this operating condition.
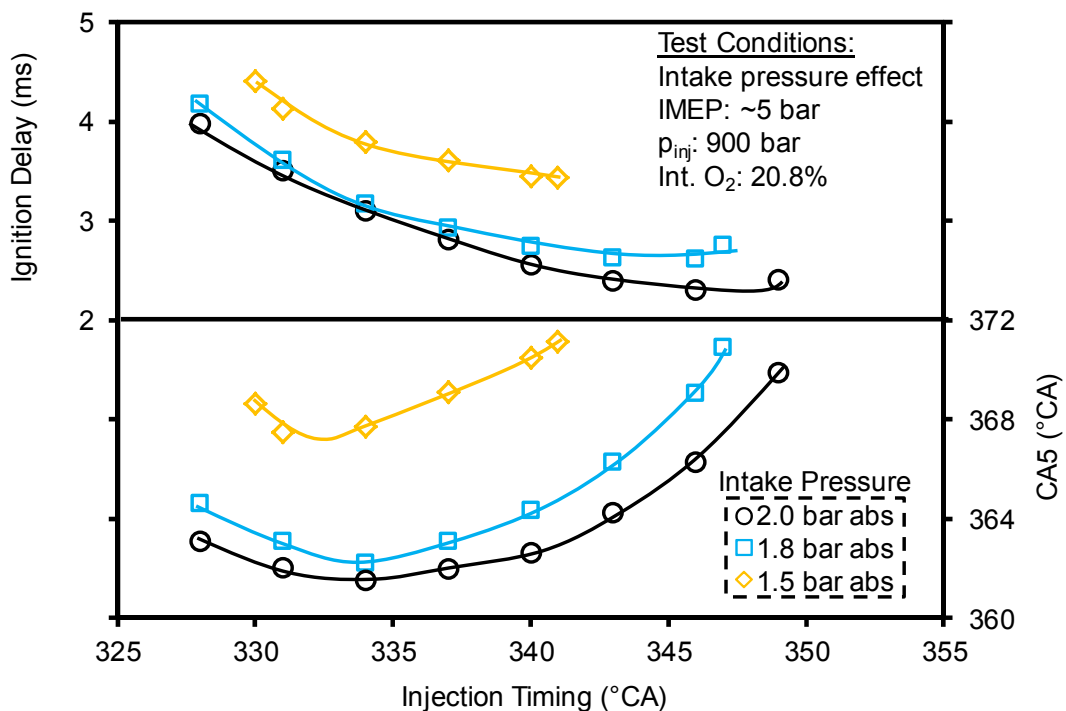
Figure 5-24 Intake pressure effect: ignition delay and CA5 of n-butanol combustion

The thermal efficiency and PCP are calculated, and the results are shown in Figure 5-25. An obvious benefit of using the lower intake pressure is the lower PCP at a similar engine load. However, it is observed that the thermal efficiency is also lower at a lower intake pressure for the combustion with n-butanol single DI. Furthermore, the window of the injection timing to reach a relatively high thermal efficiency (35%) is also considerably narrower at 1.5 bar intake pressure. Both advancing the injection timing and delaying it retard the combustion phasing and reduce the thermal efficiency.
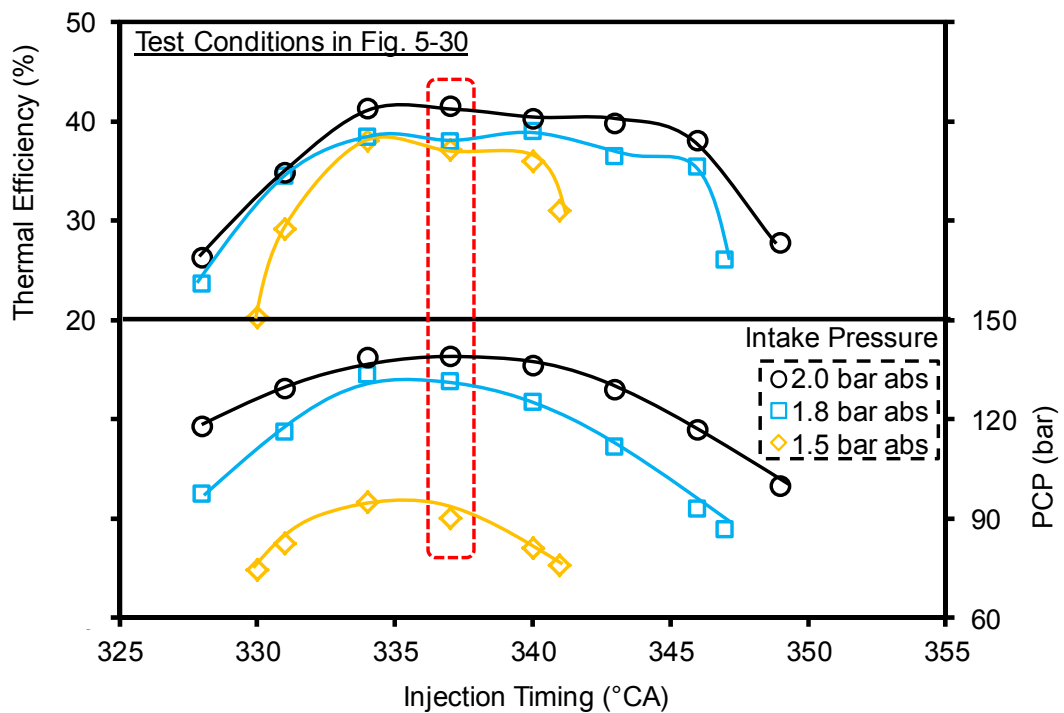
Figure 5-25 Intake pressure effect: thermal efficiency and PCP

Three data points with the same injection timing at 337 °CA are selected, as highlighted in Figure 5-25. The cylinder pressure and HRR are compared in Figure 5-26. With the fixed injection timing, the combustion event is delayed as the intake pressure is lowered. It is observed that the CA5 values for the cases of intake pressure at 1.8 bar and 2.0 bar (CA5 at 363.9 °CA and 364.7 °CA) are close to TDC, while the one for 1.5 bar case

(371.7 °CA) is away from TDC. The peak of HRR with 1.8 bar intake pressure is the highest among the three, which corresponds to the highest PPRR. The lower peak of HRR at 2.0 bar may be caused by the relatively less premixed combustion. However, the degrees of mixing for all the three cases are high due to the long ignition delays. It should be noted that the thermal efficiency at 1.5 bar intake pressure is higher than 35%, but the combustion event is excessively late to be used as an ignition source to trigger another combustion event (*e.g.* ignite a premixed charge).
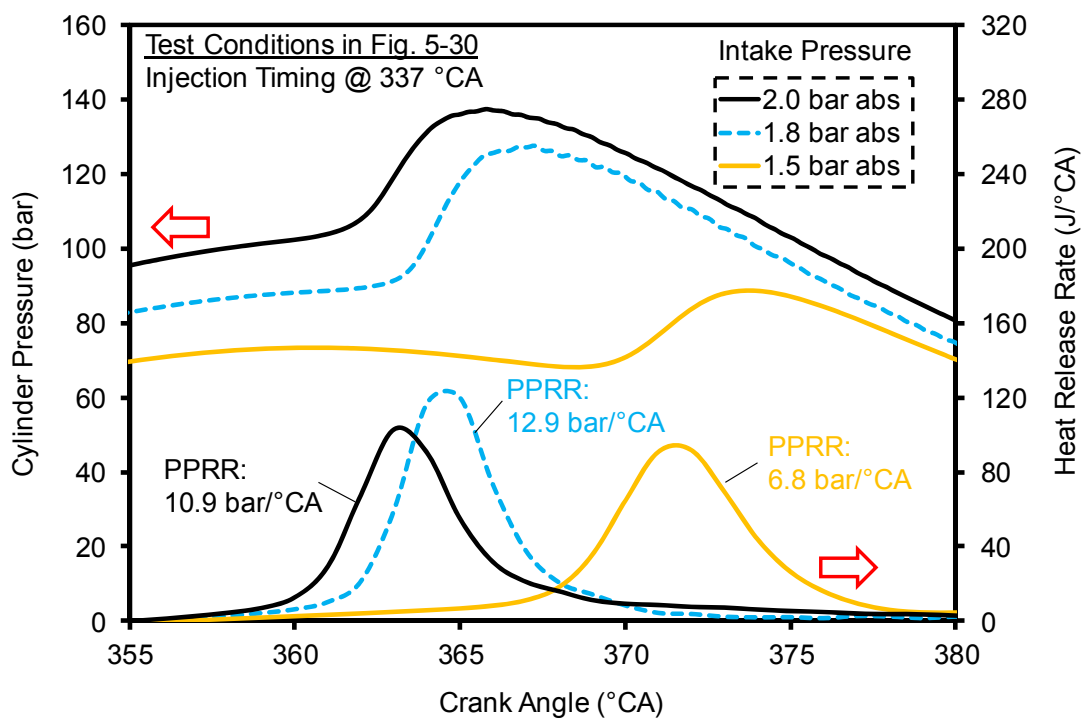
Figure 5-26 Intake pressure effect: cylinder pressure and HRR

Both a high intake pressure and a high intake temperature are used to enable the ignition of n-butanol combustion on the SCRE platform due to the relatively low compression temperature (Figure 5-6). The intake pressure effect is studied first with the constant intake temperature, fuel injection timing, and fuel injection duration. The emissions of CO and THC, combustion efficiency, and thermal efficiency are shown in Figure 5-27.

As the intake pressure is gradually reduced from 2.25 bar to 2.0 bar, the indicated thermal efficiency is decreased approximately 5%. The causes of the reduced thermal efficiency are primarily the reduced combustion efficiency with the elevated emissions of incompletely oxidized products (CO and THC) and the delayed combustion phasing as shown in the heat release curves in Figure 5-28. The heat release rate curve with 2 bar intake pressure on the SCRE platform shows a similar combustion phasing as the one with 1.5 bar intake pressure in the PUMA engine. This indicates that 2 bar intake pressure approaches the low threshold for intake pressure on the SCRE engine platform.
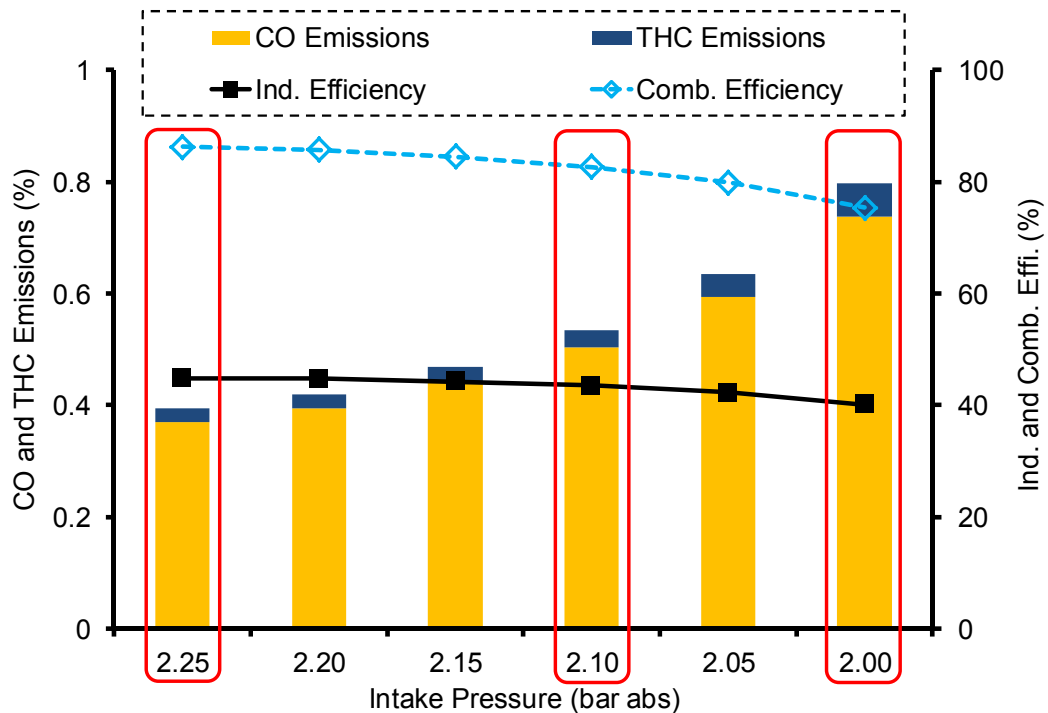
Figure 5-27 Emissions of CO and THC, combustion thermal efficiencies
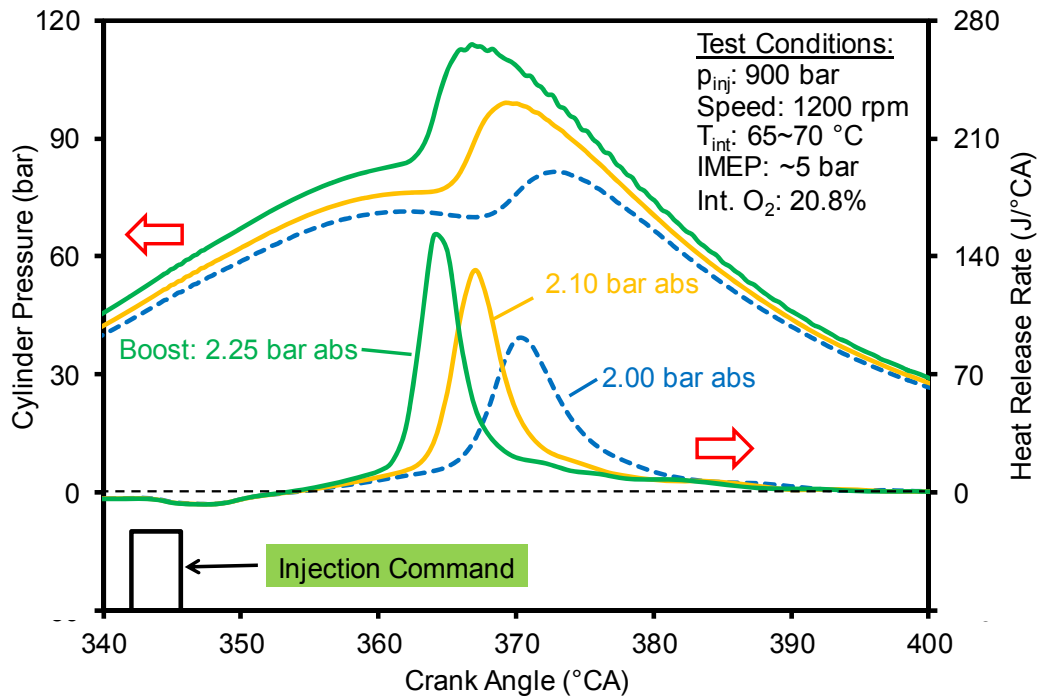
Figure 5-28 Intake pressure effect: cylinder pressure and HRR

The effect of intake temperature on the combustion characteristics is then investigated at 2.25 bar intake pressure. The cylinder pressure and HRR traces at varied intake temperatures are shown in Figure 5-29. The intake temperature is gradually reduced from 66.5 °C to 50.7 °C. No EGR is applied in this test for the relatively simple intake gas compositions and temperature distribution.

The HRR curves at various intake temperatures all display a heat absorption dip and a slow initial combustion. It is revealed that the fuel evaporation process and the actual combustion event are clearly separated. The timings of the fuel evaporation are in a similar range for different intake temperatures. However, as the intake temperature reduces, the slow initial combustion is prolonged and thus the main combustion event is progressively delayed to the engine expansion stroke. A generally longer combustion event is observed at a lower intake temperature. The combination of lower heat release

91

rate and higher in-cylinder volume expansion leads to a lower combustion temperature

that further delays the combustion phasing until misfire occurs.
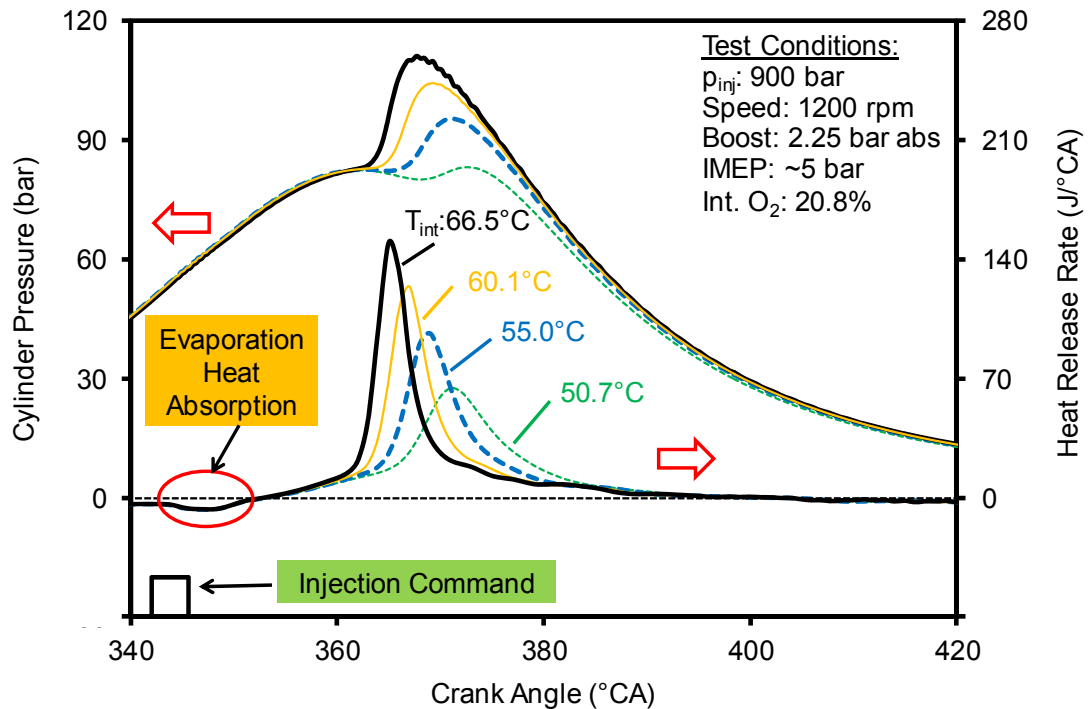
Figure 5-29 Intake temperature effect: cylinder pressure and HRR

The emissions of CO and THC, indicated thermal efficiency, and combustion efficiency

are compared in Figure 5-30 for the combustion with different intake temperatures. As

the intake temperature reduces, the combustion efficiency is significantly suppressed

because of the elevated emissions of CO and THC. The indicated thermal efficiency is

also reduced. A reduction in the intake temperature (from 66.7 °C to 50.7 °C) decreases

the indicated thermal efficiency by approximately 25%. Hence, a precisely controlled

intake temperature is required to maintain the high thermal efficiency. It should be noted

that the combustion temperature is generally low for NOx formation even with the

highest intake temperature of 66.7 °C. Lower than 10 ppm of NOx emissions and ultra-

low smoke emissions are detected in the n-butanol combustion.
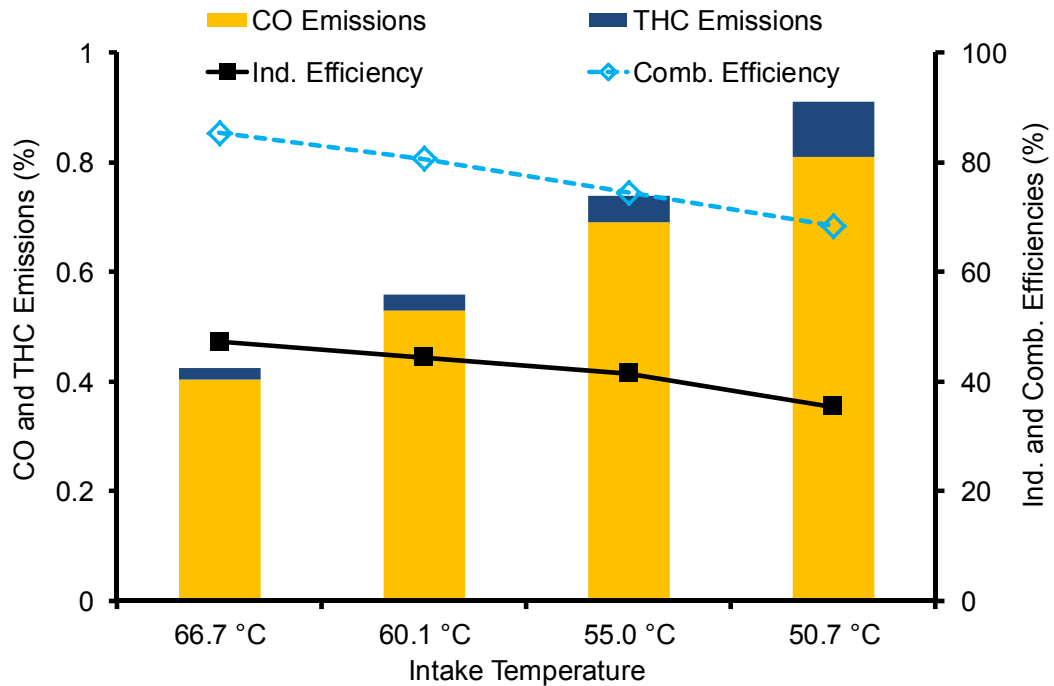
Figure 5-30 Emissions of CO and THC, combustion and thermal efficiencies

The mean in-cylinder temperatures are calculated using the measured cylinder pressures (Figure 5-29) for different intake temperature cases. The results are shown in Figure 5-31 together with the cylinder pressures for reference. With the intake temperature at 66.7 °C and the intake pressure at 2.25 bar absolute, the curve with n-butanol DI departures from the engine motoring curve at approximately 345 °CA. The liquid n-butanol fuel injection evaporates at this crank angle, absorbs the compression heat, and reduces the temperature. The intake temperature difference of about 40 °C (from 27 °C to 66.7 °C) is converted to about 80 °C temperature difference at the engine TDC (479 °C to 563 °C). The temperature increase in the engine intake compensates the lower compression temperature with a lower compression ratio, as shown in Figure 5-6.

93
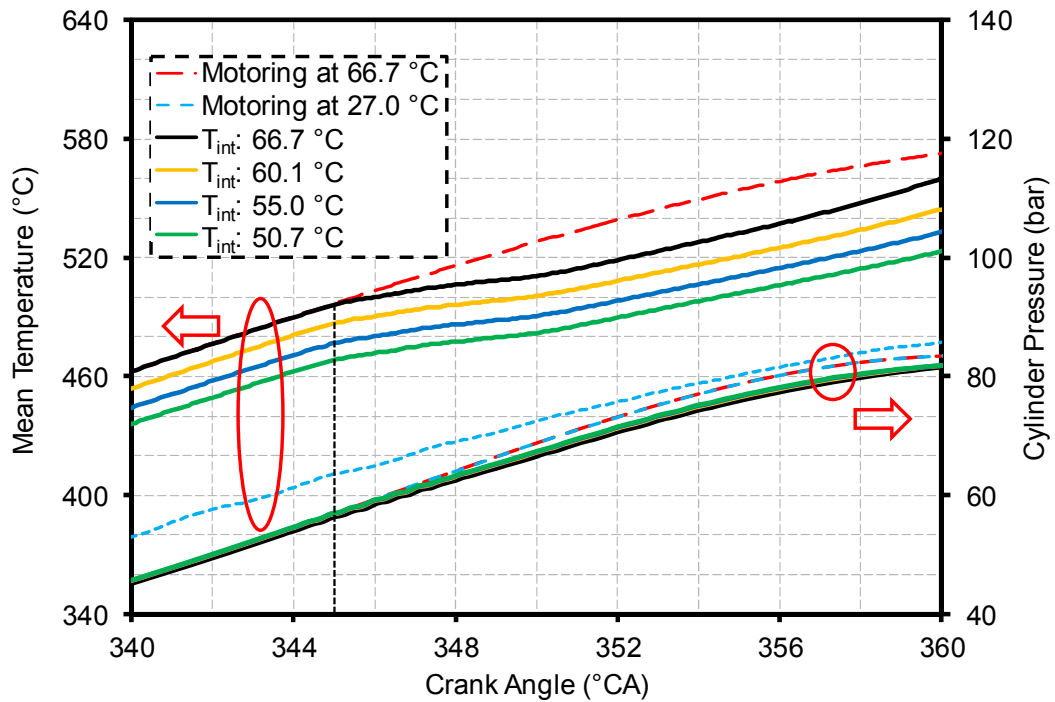
Figure 5-31 Mean in-cylinder temperature calculated with cylinder pressure

In general, both higher intake pressure and higher intake temperature enhance the charge reactivity and advance the combustion phasing. The increased charge reactivity and ignition ability by the higher intake pressure and temperature make the combustion more tolerable to higher EGR rates. A comparison test with and without intake heating are shown in Figure 5-32. The IMEP is 12 bar, which is achieved with double n-butanol injections. The strategy of double injections of n-butanol will be discussed in Chapter 7 for the high load operations. It is noted that at a higher engine load, the challenge of igniting the n-butanol charge is reduced. The n-butanol combustion can be initiated with the intake air at ambient temperature when the engine is fully warmed up.
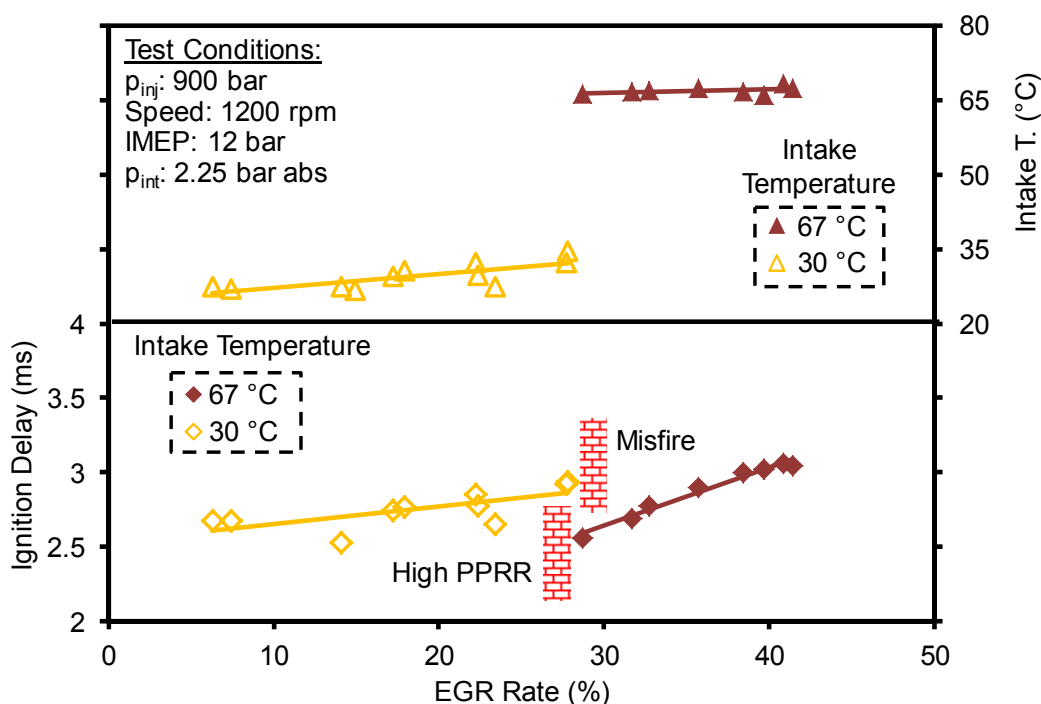
Figure 5-32 Intake temperature and ignition delay at varied EGR rate

The applicable EGR rate is limited to below 25% for the combustion with a lower intake temperature (~30 °C). Misfire occurs when the reactivity of the in-cylinder charge is excessively reduced by the EGR. When the intake temperature is elevated (~67 °C), the EGR rate can be extended to more than 40%. However, the low EGR rate becomes infeasible due to the high PPRR.

The benefit of using a higher intake temperature to enhance the reactivity is demonstrated in Figure 5-33. With the higher EGR rate, the indicated NOx emissions can be suppressed to an ultra-low level (0.08 g/kW-hr, lower than the US2010 emission standard) with ultra-low smoke emissions at this engine load. The emissions of this combustion mode are sufficiently low to fulfill the current emission requirements for NOx and smoke without after-treatment techniques.
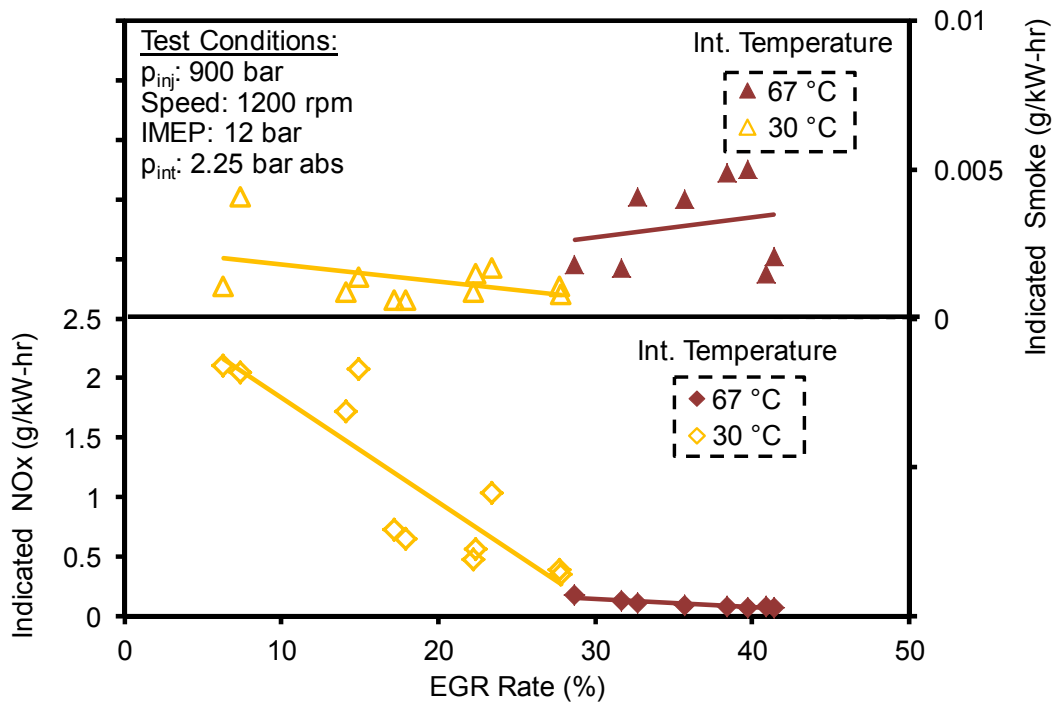
Figure 5-33 NOx and smoke emissions at varied EGR rate

5.3 Summary

The effects of various engine control parameters on ignition delay and combustion rate have been analyzed in this chapter. Both the diesel fuel and n-butanol fuel are supplied with the high pressure single DI. The following observations can be summarized.

- The ignition delay of n-butanol DI is longer than the that of diesel DI. The trend of ignition delay is related to the compression temperature.

- The DI timing has limited control over combustion phasing in the n-butanol combustion primarily due to the long mixing period. The applicable DI timing window is narrower in the n-butanol combustion than that in the diesel combustion because of the low fuel reactivity and over-mixing.

- A longer injection duration mainly increases the combustion duration in the diesel combustion, while it advances the combustion phasing and enhances the combustion rate in the n-butanol combustion, under the confined test conditions.

- With a fixed injection pressure, elevated intake pressures and temperatures enhance the charge reactivity.

CHAPTER VI

REACTIVITY MODULATION WITH PREMIXED CHARGE

The results in this chapter are used to study the effects of engine control parameters on the modulation of charge reactivity. A systematic study is performed on the fuel delivery strategies commensurate with the fuel properties. Ethanol and n-butanol are delivered through the intake port of the engine to form a premixed charge. Diesel is injected directly into the cylinder to initiate the ignition in the ethanol case and to extend the engine load in the n-butanol case, respectively.

6.1 Combustion with Ethanol Port Fuel Injection

Ethanol is injected into the intake port at the beginning of the intake stroke. The liquid ethanol droplets are tranported by the intake air flow into the cylinder. The evaporation of the liquid ethanol occurs primarily inside the cylinder. Therefore, the time for ethanol mixing with air contains the entire intake stroke and a large portion of the compression stroke before SOC. A highly premixed in-cylinder charge is formed before the diesel injection that is used as an ignition source. The potential mixing control over this ethanol premixed charge is limited to the regulation of the fuel amount that changes the AFR.

6.1.1 Diesel Injection Timing Effect on Ignition

The diesel injection timing effect is studied at 10 bar IMEP. The intake pressure is maintained at 2 bar absolute, and the diesel injection pressure is set to 1200 bar. In this test, the energy contribution from the diesel injection is about 50%. The intake oxygen concentration is at 20.8%. The CA5 and CA50 are shown in Figure 6-1 together with the ignition delay. The ignition delay remains at a similar level as that of the pure diesel

98

combustion (Figure 5-1), and prolongs gradually when the diesel injection timing is retarded. The CA5 and CA50 are delayed progressively with the postponed injection timing. This observation suggests that the diesel injection timing controls the onset of combustion and combustion phasing in this combustion mode.
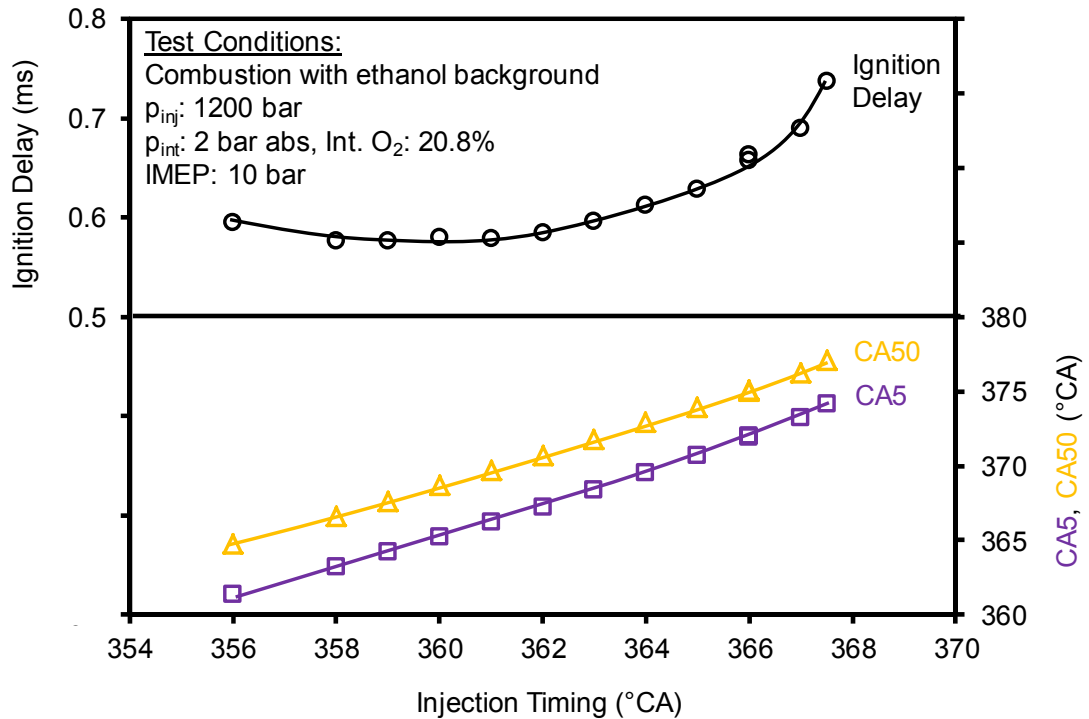
Figure 6-1 Diesel injection timing effect: ignition delay, CA5 and CA50

The burn rate in the combustion with diesel and ethanol is significantly increased over that of the combustion with diesel DI only. An example is given in Figure 6-2, in which the timing and duration of the diesel injection command are the same. A longer combustion duration is observed at a higher engine load that is achieved with a longer diesel injection duration (Figure 5-12). In stark contrast, the combustion duration remains in a similar range when the engine load is increased with the ethanol PFI (Figure 6-2). When the diesel fuel auto-ignites, multiple ignition spots are generally formed [28] to

99

burn the highly premixed charge of ethanol. Therefore, HRR, PCP, and PPRR are all increased for the combustion with the premixed charge of ethanol.
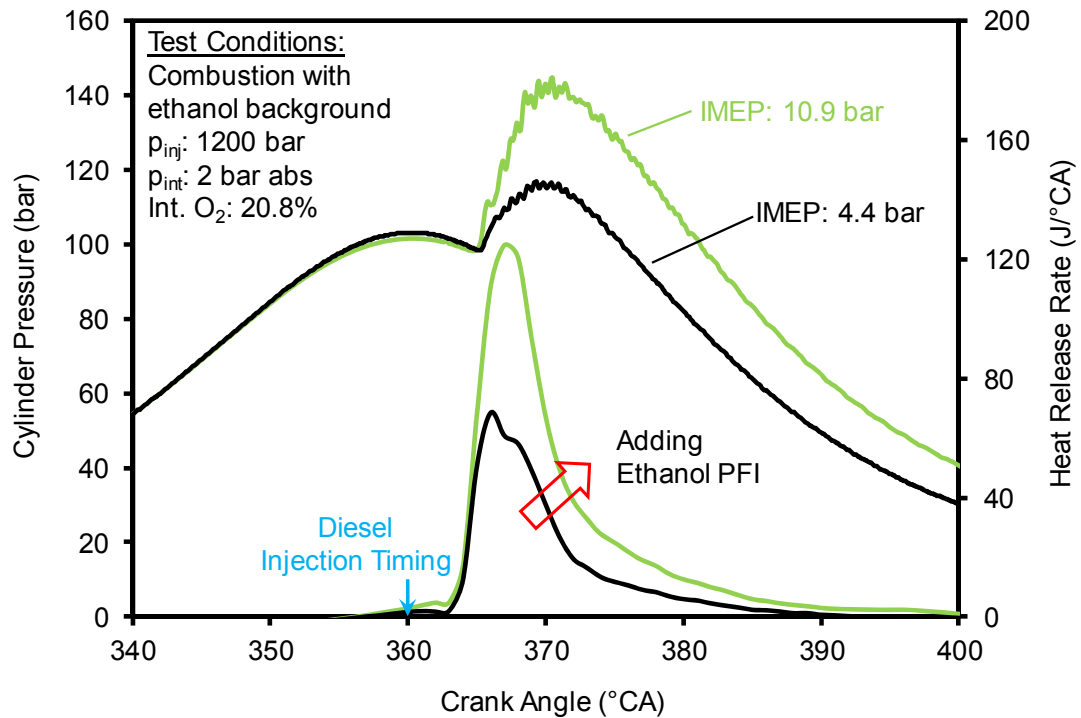
Figure 6-2 Cylinder pressure and HRR change after enabling ethanol PFI

The effectiveness of the control on PCP and PPRR with the diesel injection timing is studied at two different intake oxygen concentrations. The PCP and PPRR are shown in Figure 6-3. The overall trends for PCP and PPRR are similar for different intake oxygen levels: higher PCP and PPRR are observed with the early diesel injection timings. With a lowered intake oxygen concentration, both the PCP and PPRR are suppressed, which makes it possible to advance the diesel injection timing. However, the slopes of the PCP and PPRR curves remain at a similar level for the two intake oxygen levels.
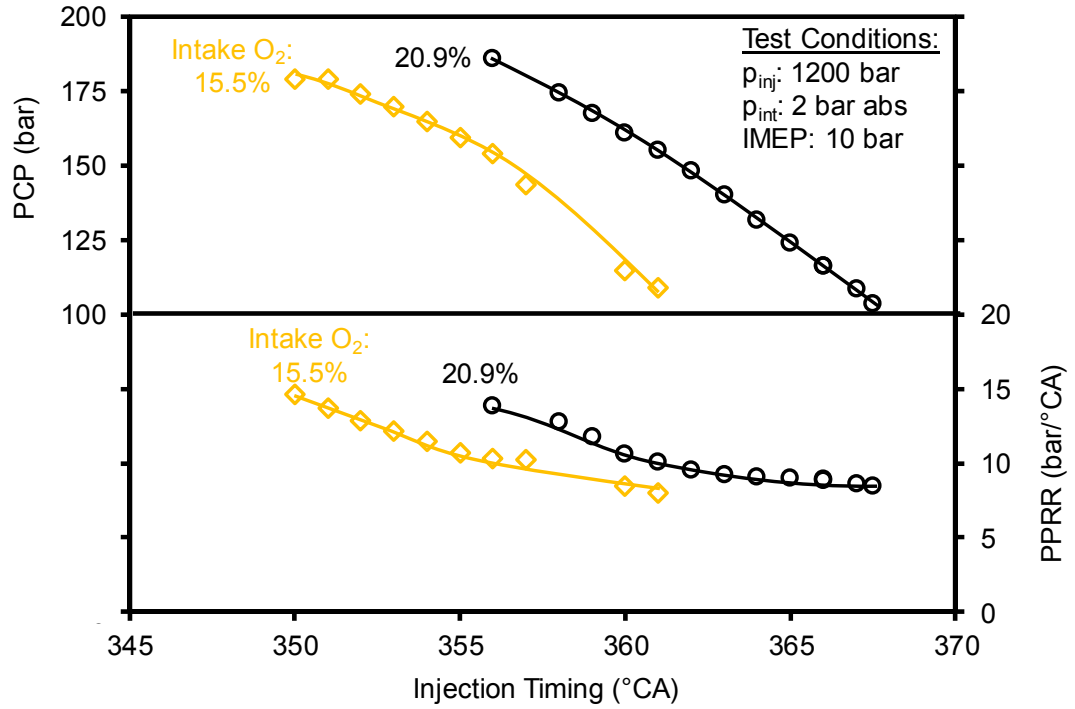
Figure 6-3 Diesel injection timing effect: PCP and PPRR at varied intake O_2

6.1.2 PFI Fuel Ratio Effect on Combustion Rate

The PFI fuel ratio (ζ) is defined in Eq. (6-1), which is based on the energy contributions from the PFI fuel and the DI fuel.

$$\zeta(\%) = \frac{\dot{m}_{PFI} \times LHV_{PFI}}{\dot{m}_{PFI} \times LHV_{PFI} + \dot{m}_{DI} \times LHV_{DI}} \times 100 \qquad (6-1)$$

where ζ, PFI fuel ratio (%); $\dot{m}_{PFI}$, PFI fuel flowrate (kg/cycle); LHV_{PFI}, Lower heating value of PFI fuel (J/kg); $\dot{m}_{DI}$, DI fuel flowrate (kg/cycle); LHV_{DI}, Lower heating value of DI fuel (J/kg).

101

The effect of the PFI fuel ratio on heat release rate is studied at a constant IMEP level. As the injection duration of the PFI ethanol increases, the diesel injection duration decreases accordingly to maintain the IMEP. The diesel injection timing and injection pressure are fixed. The cylinder pressure and HRR curves are shown in Figure 6-4 for the cases with four different PFI fuel ratios. A low EGR rate is applied to slightly reduce the charge reactivity, and to constrain the PPRR for the combustion with a high PFI fuel ratio.
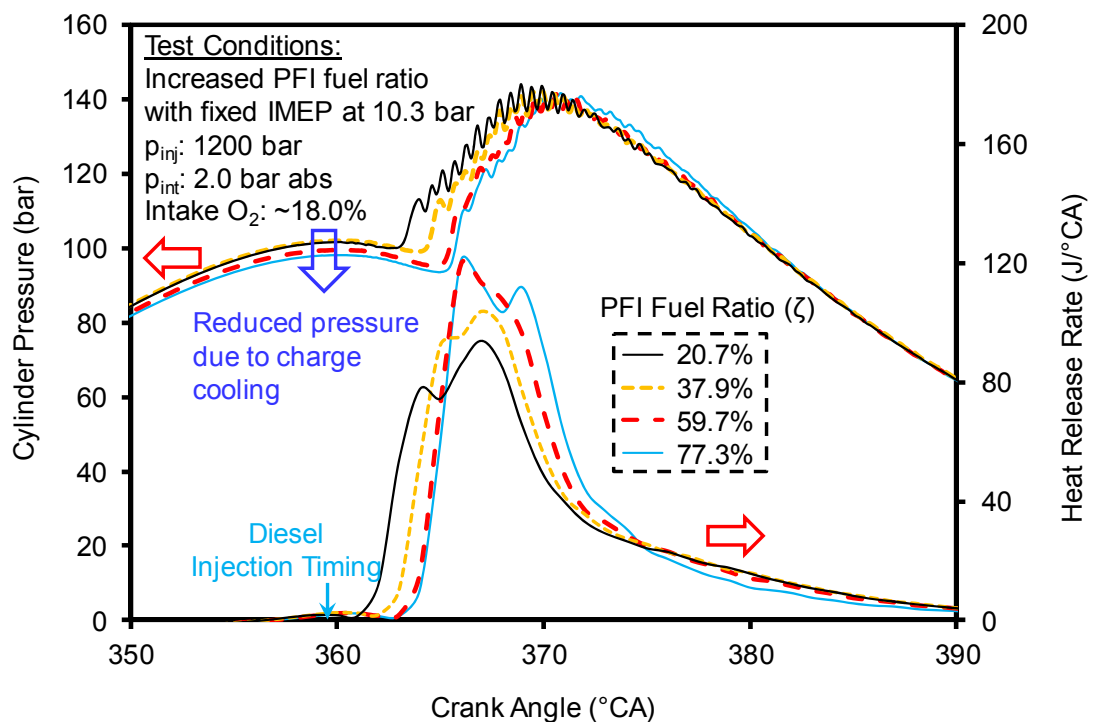
Figure 6-4 PFI fuel ratio effect: cylinder pressure and HRR with fixed IMEP

Both the cylinder pressure and HRR are affected by the PFI fuel ratio. First, the compression pressure at TDC is lowered with the high fuel ratio. This observation can be explained by the heat absorption during the ethanol fuel evaporation. The charge temperature and pressure are lower slightly when more ethanol fuel is evaporated in the engine combustion chamber. The SOC is retarded with a higher concentration of the premixed ethanol. The delayed SOC may be explained by two causes: the reduced

quantity of the diesel injection reduces the ignition ability (*e.g.* shorter penetration), and the increased ethanol quantity decreases the charge reactivity (*e.g.* lowered charge temperature caused by the evaporative cooling, and oxygen dilution with the ethanol vapor).

The HRR in Figure 6-4 shows similar dual-hump shape as the high load one of diesel (11.5 bar case in Figure 5-12). The first stage of combustion is predominantly the premixed combustion with both ethanol and diesel. The two fuels form a relatively reactive mixture through in-cylinder blending to start the initial combustion. This premixed combustion becomes more significant when a higher PFI fuel ratio is used. In contrast to the diffusion-controlled combustion of diesel, the results indicate that the second stage of combustion may be from the auto-ignition of the premixed ethanol fuel.

The PCP, PPRR, indicated NOx emissions, and indicated smoke emissions are illustrated in Figure 6-5 for various PFI fuel ratios. The PCP is maintained at the same level, while the PPRR increases considerably, as the PFI fuel ratio increases. The increased PPRR is mainly caused by the enhanced premixed combustion (Figure 6-4). The NOx emissions are slightly reduced because the amount of diesel injection is reduced. The smoke emissions remain at a low level due to the high portion of premixed combustion and the high concentration of intake oxygen.
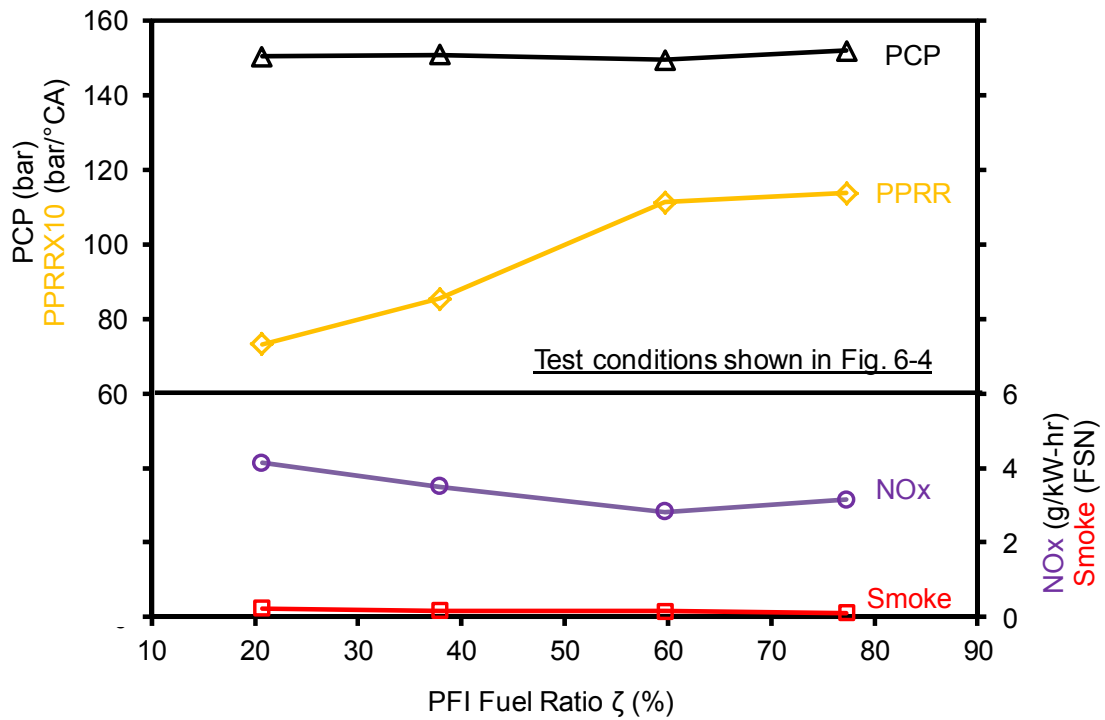
Figure 6-5 PFI fuel ratio effect: PCP, PPRR, NOx emission, and smoke emission

The effects of the PFI fuel ratio are further examined with the constant diesel injection timing and duration. The duration of ethanol port injection is gradually increased to raise the engine load. The cylinder pressure and HRR curves are shown in Figure 6-6. The initial stage of HRR overlaps on each other for different PFI fuel ratios. This phenomenon indicates that the increased ethanol concentration has a negligible impact on the SOC with the test conditions. For the HRR, the increased PFI fuel ratio significantly enhances the intensity of the second stage of combustion but only marginally increases the burning rate of the first stage. The results suggest that the second stage of combustion is primarily generated from the burning of the ethanol premixed fuel, while the first stage of combustion is mainly the burning of the DI diesel.
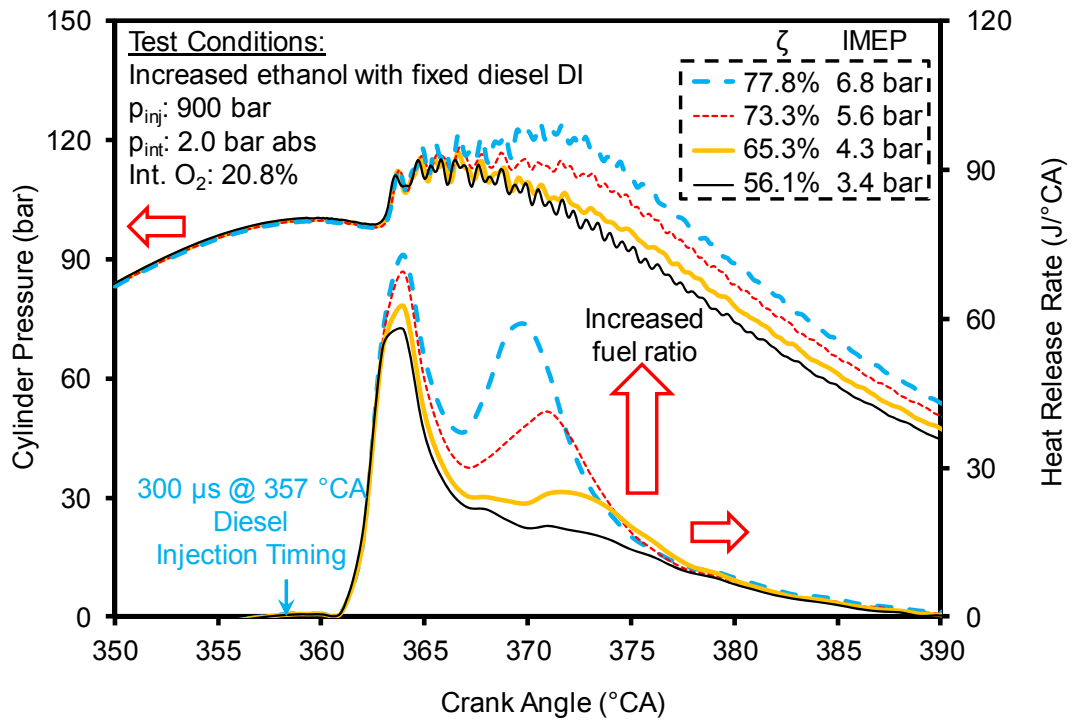
Figure 6-6 PFI fuel ratio effect: cylinder pressure and HRR with fixed diesel DI

6.1.3 Intake Pressure Effect on Ignition

The impact of intake pressure on ignition is studied with ethanol ignited by diesel. Figure 6-7 shows a comparison of ignition delay and IMEP at two intake pressures (1.5 and 2.0 bar absolute) with an increasing PFI fuel ratio. The diesel injection timing and duration are the same as the ones in Figure 6-6. Since the total energy is increasing with the increasing PFI fuel ratio, the CA5 provides an delayed SOC. Therefore, the ignition delays are calculated assuming a 50 Joule threshold for the cumulative heat release rate as the indication for the SOC. The 2 bar intake pressure shortens the ignition delay by about 0.2 ms from 1.5 bar. This difference is similar to the impact of intake pressure on the diesel combustion that has been discussed in Figure 5-9. It is also noted that the increased PFI fuel ratio has a limited impact on ignition delay at both the intake pressures, with the confined test conditions.
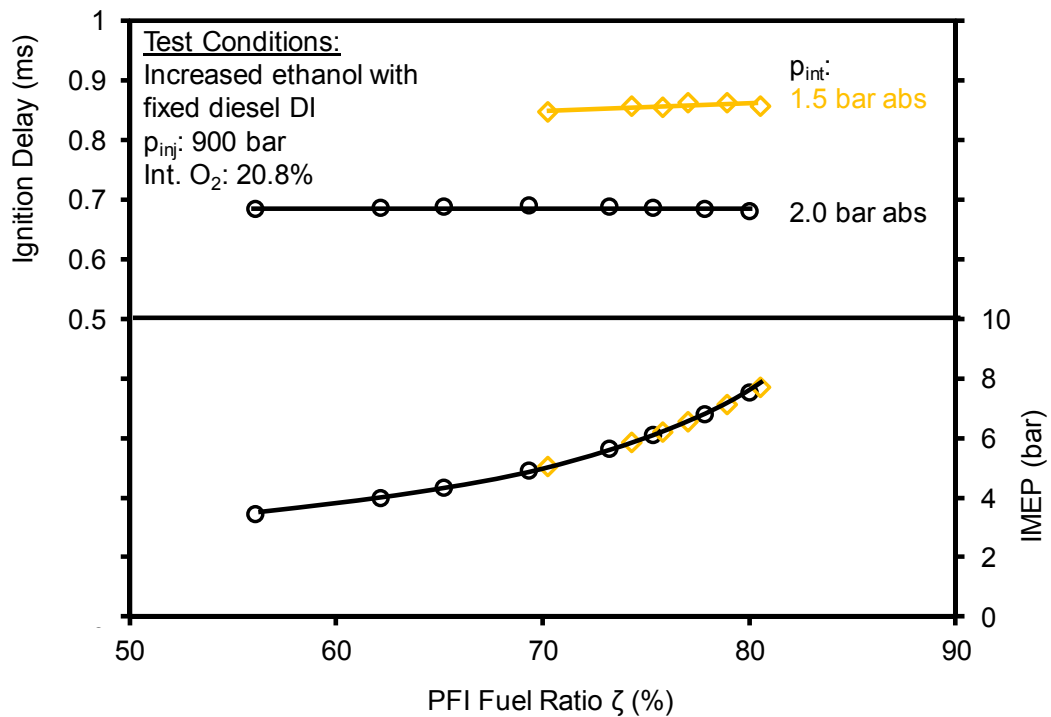
Figure 6-7 Intake pressure effect: ignition delay and IMEP

The effect of the intake pressure is further examined with a fixed PFI fuel ratio of 50%. The combustion with a single injection of diesel (without the ethanol port injection, $\zeta =$ 0%) is selected as the baseline. The intake pressure is gradually decreased from 2.0 bar to 1.2 bar absolute, while the injection timing and duration of the diesel injection are kept constant. The same sweep of intake pressure is conducted again with the same diesel injection and port injection of ethanol ($\zeta = 50\%$). The minimum tested intake pressure is 1.3 bar instead of 1.2 bar due to the high PPRR at the lower intake pressure.

The ignition delay and IMEP at various intake pressure levels are shown in Figure 6-8. The IMEP levels remain in a similar range as the intake pressure is reduced, which suggests that the thermal efficiencies are also similar for the two fuel ratios and are not affected by the varied intake pressure. The ignition delays are at the same level at high intake pressures (*e.g.* 1.8 bar and 2.0 bar), and progressively prolong as the intake

pressure is further reduced. The same trend is observed for both the fuel ratios. However, the slope of the ignition delay curve with 50% fuel ratio is steeper than that with diesel only. The results indicate that the combustion with an increased ethanol fuel ratio is more sensitive to the change of intake pressure. With the same fuel ratio, the ignition delay is more significantly prolonged at a lower intake pressure. When the intake pressure is higher than 1.8 bar absolute, further increase of intake pressure only marginally shortens the ignition delay.
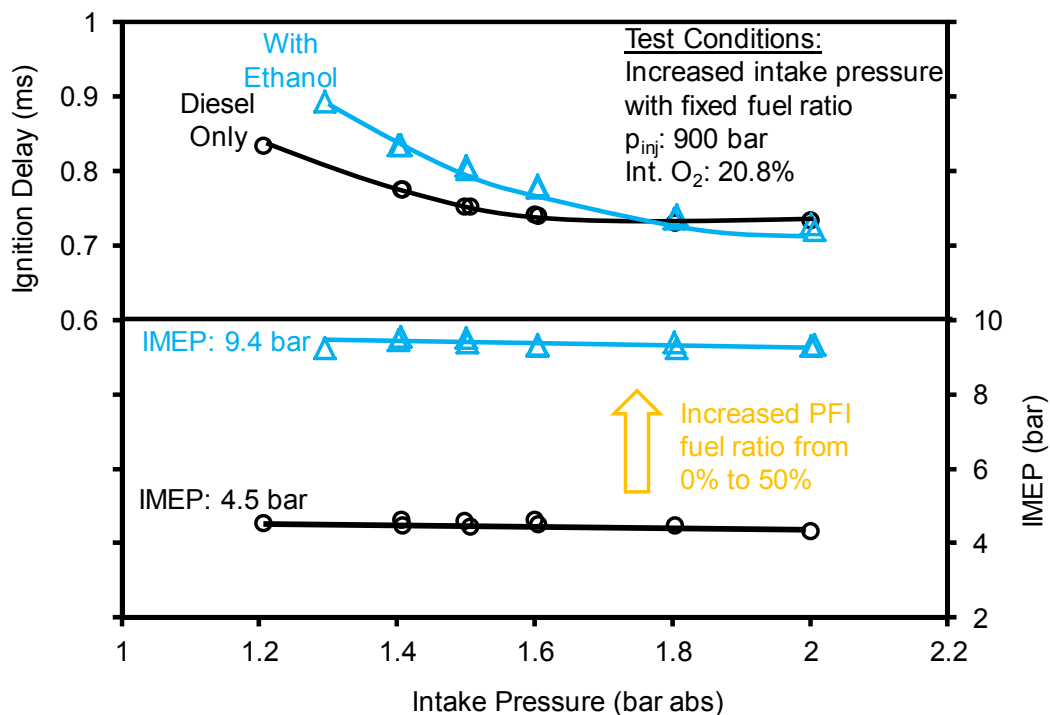
Figure 6-8 Intake pressure effect: ignition delay and IMEP

The PCP and PPRR at different intake pressures are shown in Figure 6-9. The PCP increases, while the PPRR decreases, with the elevated intake pressure levels. The increased ethanol concentration increases the peak of HRR in the premixed combustion. The engine load with the premixed ethanol charge is also considerably higher than that

with diesel only. Therefore, the PCP and the PPRR of 50% PFI ratio are higher than that of the diesel-only case.
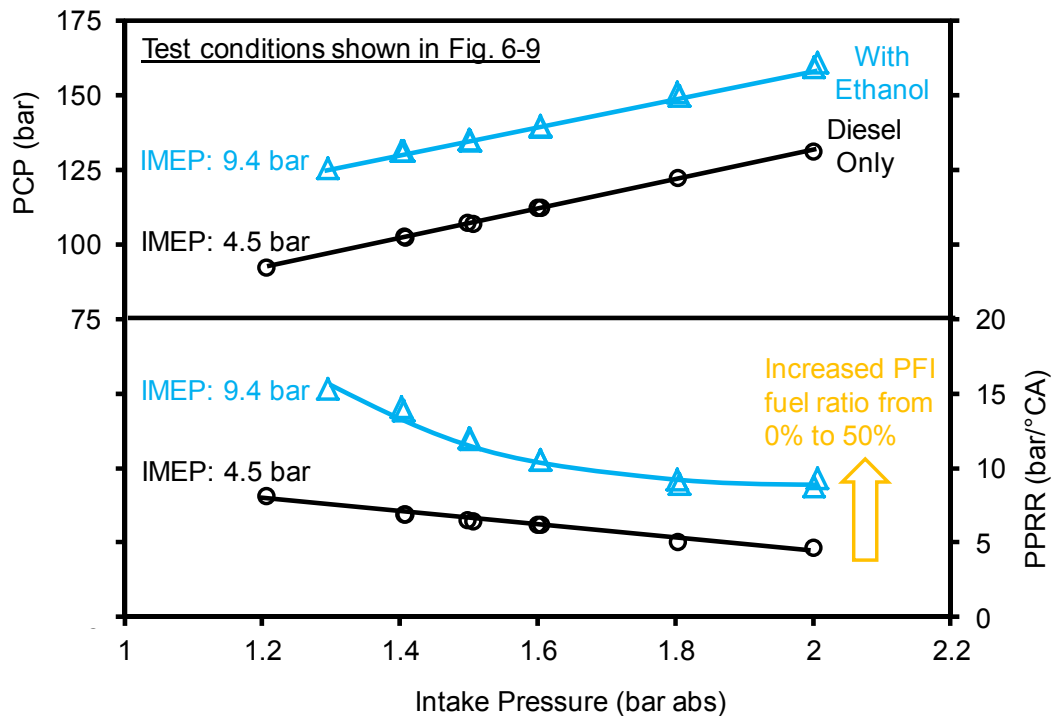
Figure 6-9 Intake pressure effect: PCP and PPRR at various intake pressures

The benefit of using the premixed ethanol fuel is demonstrated in Figure 6-10, together with the emissions of NOx and THC. It is observed that the indicated NOx emissions from the combustion with 50% PFI fuel ratio are significantly lower than that from the combustion with diesel only. The engine load extension with the PFI ethanol can reduce the indicated NOx emissions. Moreover, the NOx emissions from the diesel-only combustion increase with the intake pressure. The increase NOx emission is mainly because of the potentially higher combustion temperature with a shorter ignition delay. In contrast, the NOx emissions remain at the same level for the combustion with 50% ethanol. The NOx emissions become insensitive to the change of intake pressure with the premixed ethanol charge. Meanwhile, the THC emissions drastically increase in the

combustion with the ethanol port injection. This is a common feature with PFI applications. The background fuel often cannot be oxidized completely, especially for the regions close to the cold walls of the combustion chamber. Higher THC emissions are detected at a higher intake pressure because of the potentially leaner premixed charge that is challenging to oxidize.
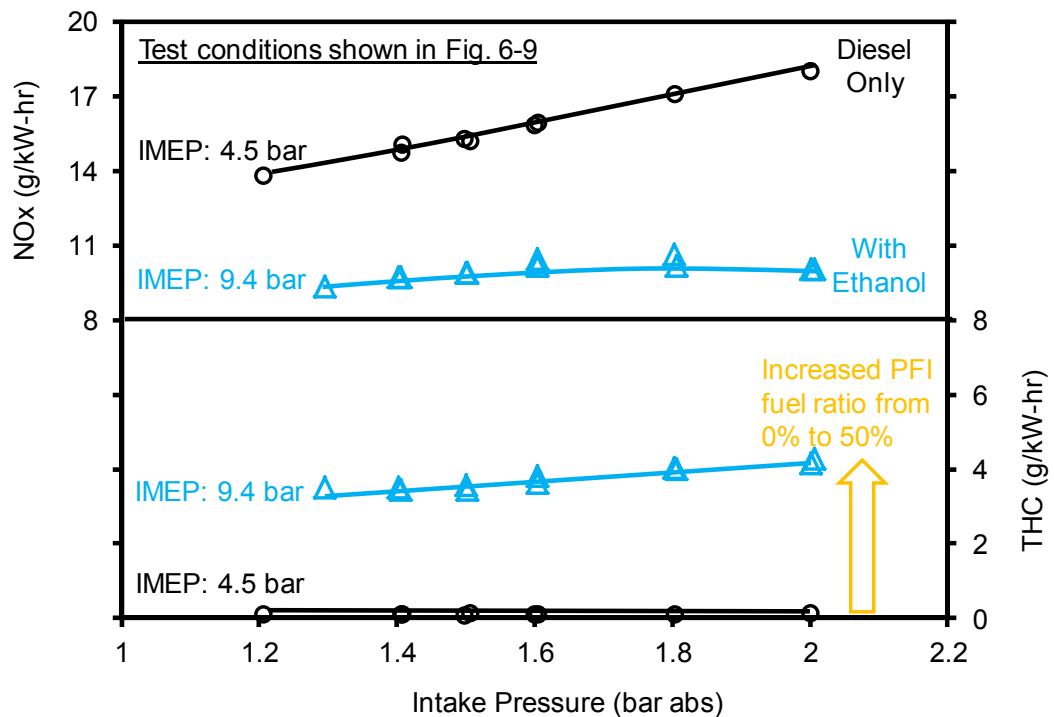
Figure 6-10 Intake pressure effect: NOx and THC at various intake pressures

The mass-based emissions of NOx and THC are shown in Figure 6-11 to compare the absolute formations of NOx and THC with different ethanol fuel ratios. It is observed that the NOx formation in the combustion with 50% ethanol fuel ratio is higher than that with diesel only over the entire range of intake pressures. The higher NOx formation can be attributed to the potentially higher combustion temperature at a higher engine load. However, the increase rate of NOx is less than that of IMEP. Hence, the indicated NOx emissions are lower in the 50% ethanol case.
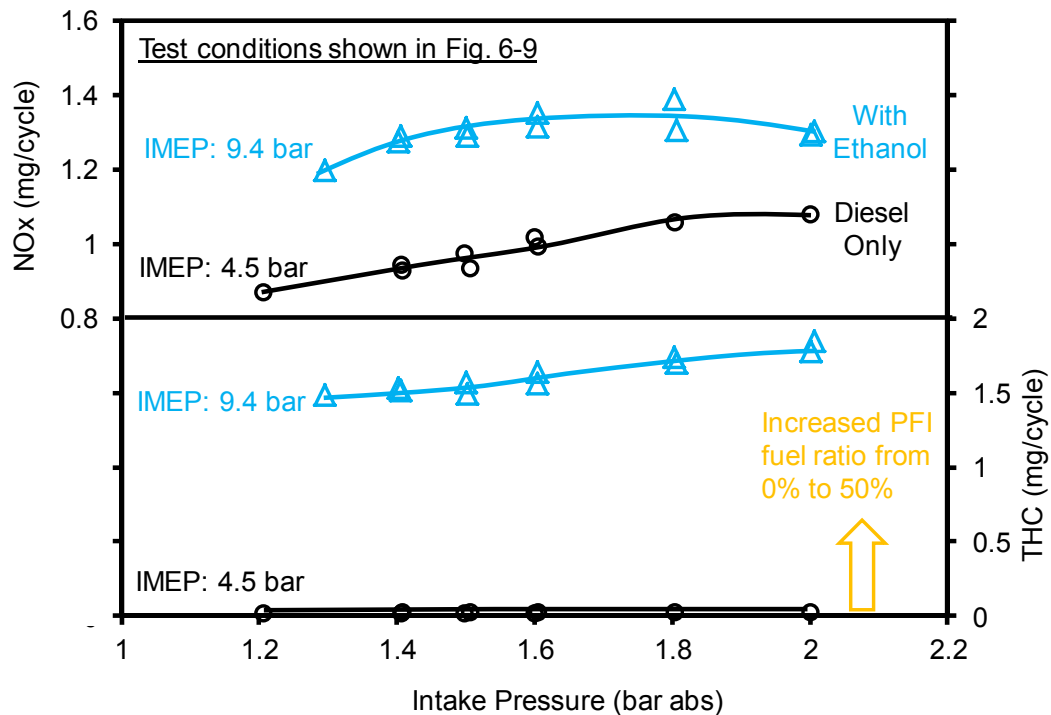
Figure 6-11 Intake pressure effect: absolute emissions of NOx and THC

6.1.4 EGR Effect on NOx and Smoke Emissions

The effects of EGR on the emissions of NOx and smoke are studied at different fuel ratios. The net IMEP is maintained at 10 bar, while the PFI fuel ratio is increased progressively from 24.3% to 79.5%. The CA50 is approximately 369 °CA for all the test points. The constant combustion phasing is achieved by advancing the diesel injection timing during each of the EGR sweeps.

The general trends of lower NOx emissions with reduced intake oxygen concentrations are similar for all the fuel ratios (Figure 6-12). The slopes of the NOx emission curves are steeper when the intake oxygen concentration is higher than 16%, and becomes flatter thereafter. At similar intake oxygen levels, the cases with lower fuel ratios of 24.3% and 38.5%, and the cases with higher fuel ratios of 57.0% and 79.5%, have similar NOx emissions, respectively. Moreover, the combustion with higher fuel ratios (57.0%,

79.5%), produces lower NOx emissions, which is consistent with the observation in Figure 6-5.
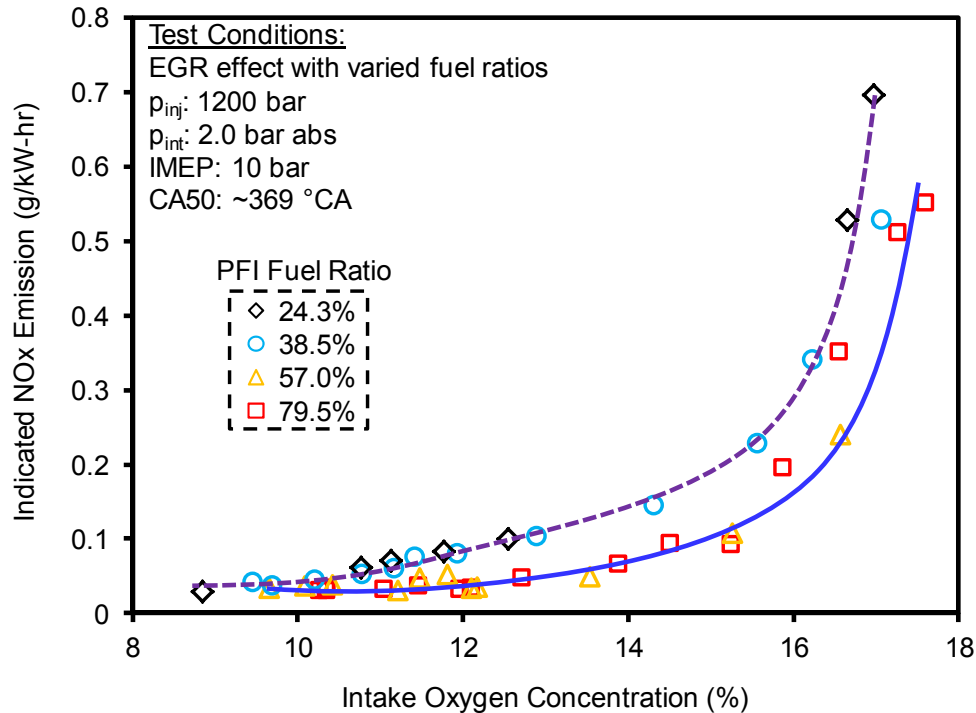
Figure 6-12 EGR effect: NOx emissions at different fuel ratios

The smoke emissions at various fuel ratios are given in Figure 6-13. Similar to the diesel baseline shown in Figure 5-2, the smoke decreasing slope is detected for all the four fuel ratios as the intake oxygen concentration is reduced. The peak smoke emissions in each of the EGR sweeps reduce as the PFI fuel ratio increases. The emissions of smoke are reduced by the increased PFI fuel ratio, instead of the retarded combustion phasing in the diesel baseline. Furthermore, with the high PFI fuel ratio ($\zeta = 79.5\%$), simultaneously low emissions of NOx and smoke are achieved when the intake oxygen is reduced to about 15%. However, the low emissions are achieved within a very narrow range of intake oxygen concentration, which necessitates a precise control of EGR. The EGR rate that is out of this range would result in either high emissions of NOx or smoke.
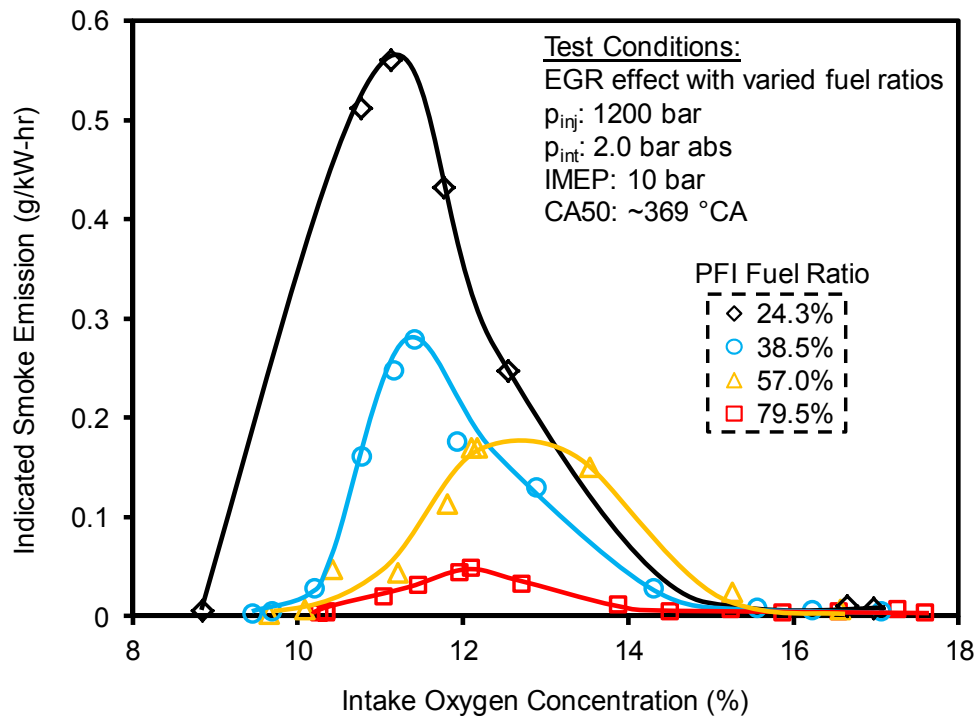
Figure 6-13 EGR effect: smoke emissions at different fuel ratios

Simultaneously low emissions of NOx and smoke can also be achieved when the intake oxygen is reduced to lower than 9% for the four tested fuel ratios. The concept is similar to the diesel LTC enabled with heavy EGR. As shown in Figure 6-14, the normalized IMEP reduces by about 30% when the intake oxygen concentration is decreased to about 9%. The highest IMEP (100% normalized IMEP) is often achieved without EGR or with a low EGR rate. The trends of the normalized IMEP for different fuel ratios are similar. The IMEP starts to drop when the intake oxygen concentration is lower than 14%, at this test condition. When the IMEP drops, the emissions of smoke, CO, and THC are increased. The increased emissions of partially oxidized products are closely related to the combustion temperature that is suppressed with a higher rate of EGR.
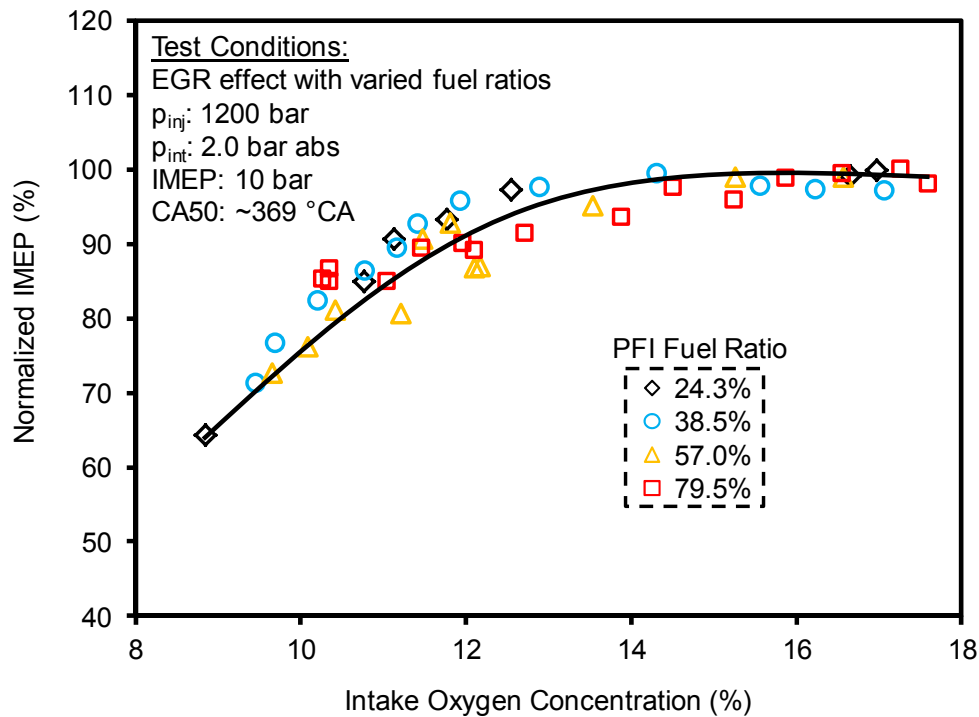
Figure 6-14 EGR effect: normalized IMEP at different fuel ratios

The ignition delays are prolonged for the EGR sweeps with different fuel ratios, as shown in Figure 6-15. At the higher intake oxygen level of 16% to 18%, the fuel ratio has a limited impact on the ignition delay, which is consistent with the observation in Figure 6-7. However, when the intake oxygen is further lowered, the impact of the fuel ratio on the ignition delay becomes pronounced. A higher PFI fuel ratio drastically increases the ignition delay at a lower intake oxygen level.

The effects of EGR on cylinder pressure and HRR are shown in Figure 6-16 using a selected fuel ratio of 57% as an example. As the EGR rate is increased, the intake oxygen concentration is reduced from 18.8% to 9.7%. To maintain the combustion phasing, the diesel injection timing is advanced. The engine efficiency often reduces with a longer combustion duration [104]. This is the potential cause for the IMEP drop in Figure 6-14.

113
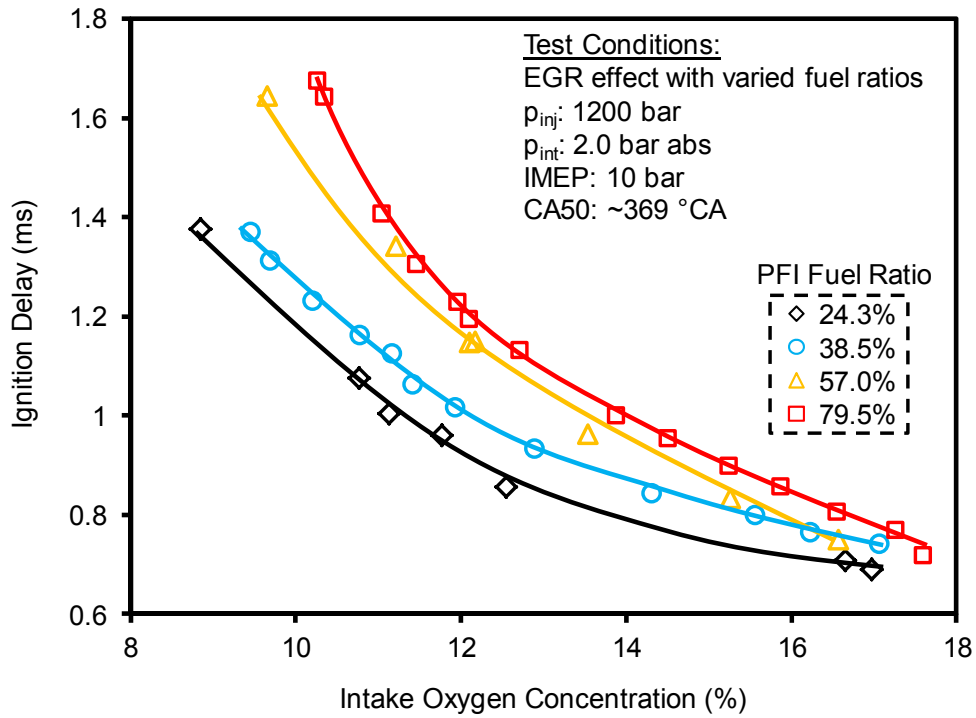
Figure 6-15 EGR effect: ignition delay at different fuel ratios
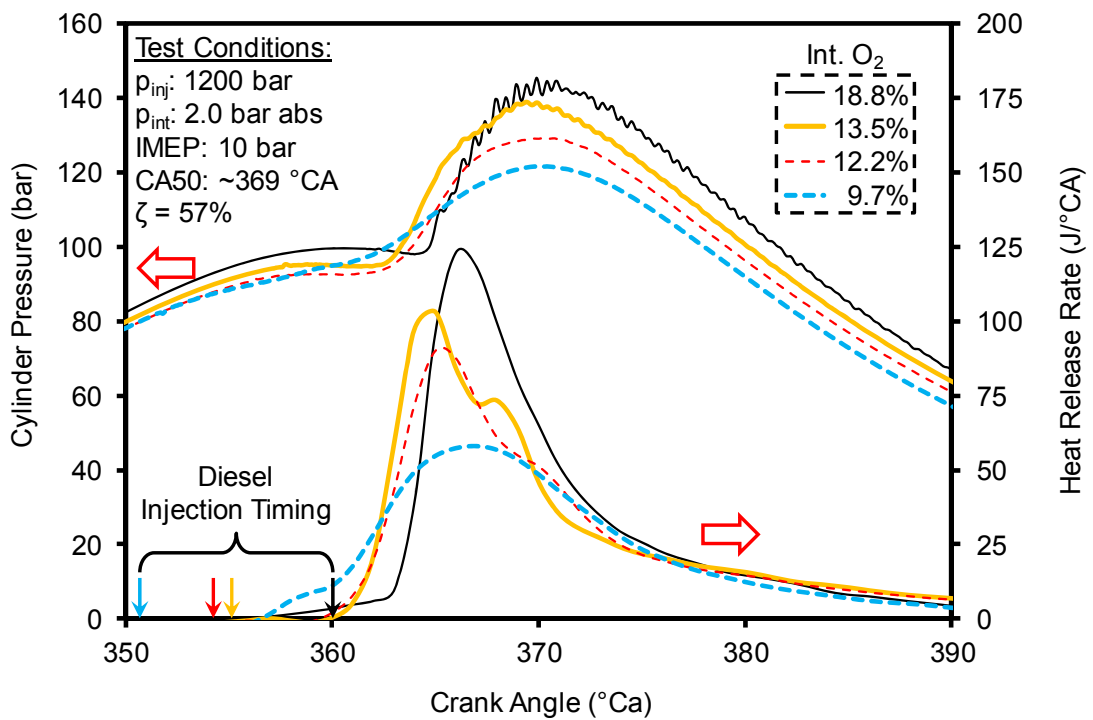
Figure 6-16 EGR effect: cylinder pressure and HRR at a selected fuel ratio

6.1.5 Diesel Micro Pilot to Increase Charge Reactivity

In the previous subsections, it has been discussed that the application of EGR is often essential to suppress the NOx emissions from the combustion with ethanol PFI and diesel DI. However, the smoke emissions are elevated at medium to high EGR levels, at the tested conditions. The further increase of EGR may eventually reduce the smoke emissions, but at the ultra-high rate of EGR, the thermal efficiency often reduces. The combustion efficiency is also reduced as evidenced from the high emissions of THC and CO. The emission results shown in Figure 6-13 suggest that a higher PFI fuel ratio might help to reduce the NOx-smoke trade-off on the PUMA platform.

Two high PFI fuel ratios are tested to demonstrate the need of enhancing the charge reactivity. The emissions of NOx and smoke at 95% fuel ratio are compared to the ones at 79.5% fuel ratio in Figure 6-17. The intake pressure is maintained at 2 bar absolute. The net IMEP is set to 10 bar. The higher PFI fuel ratio is achieved by increasing the PFI fuel amount and reducing the DI fuel amount at the same time. In order to keep the combustion phasing constant, the diesel injection timing is advanced when a higher EGR rate is used for both the fuel ratios.

The differences in NOx emissions between the two PFI fuel ratios are negligible. The general trend is that lower NOx emissions are achieved at a lower intake oxygen concentration. The smoke emissions at a PFI fuel ratio of 95% remain at an ultra-low level when the intake oxygen is reduced from approximately 21% to 13.5%. The NOx and smoke trade-off is overcome at the high fuel ratio of 95%. With the prolonged ignition delay as shown in Figure 6-18, and the reduced diesel DI amount, the mixing of the diesel DI is considerably improved at the high fuel ratio. Hence, the smoke emissions

remain at a low level. However, the normalized IMEP drops drastically when the intake oxygen is reduced to below 14%. The drastic drop of IMEP occurs when the overall charge reactivity is not sufficient to sustain the combustion. This phenomenon shows the benefits of using a high PFI fuel ratio on smoke and NOx emissions. Moreover, the low charge reactivity limits the range of the EGR application for the further reduction of NOx emissions.
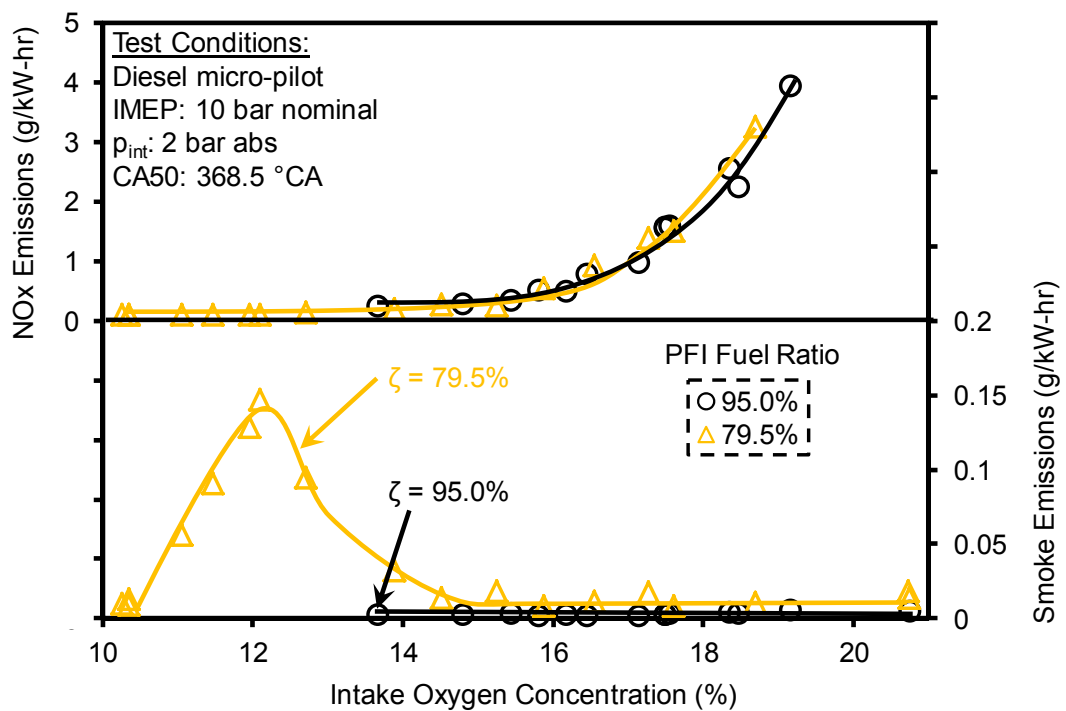
Figure 6-17 Diesel micro-pilot: NOx and smoke emissions at varied fuel ratios
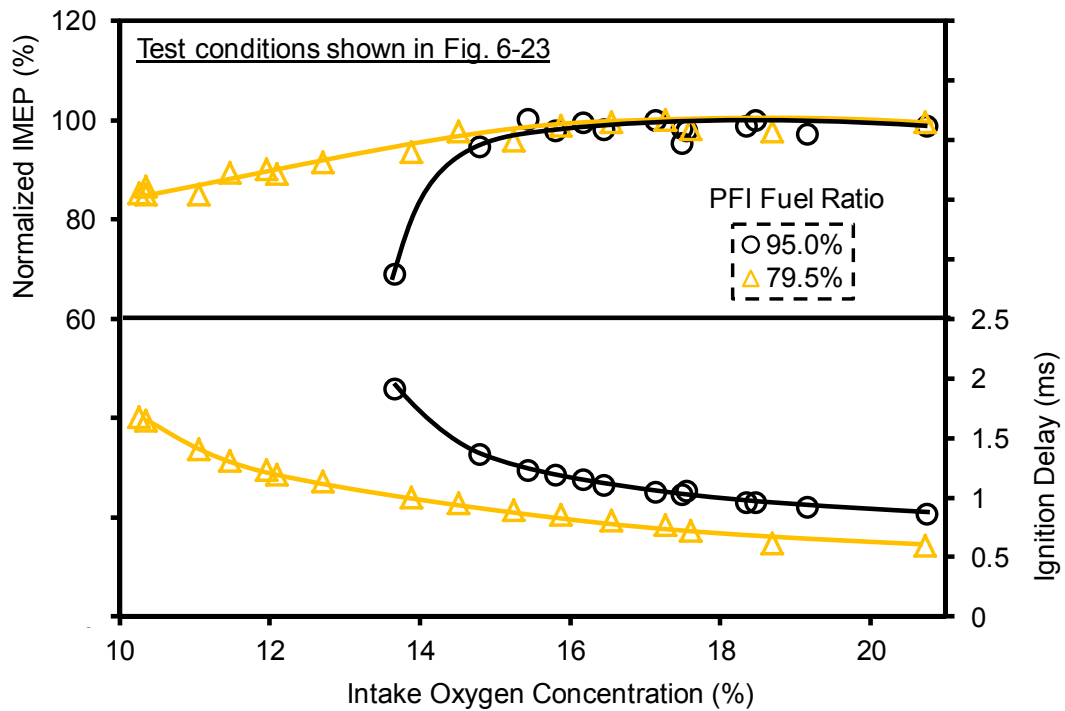
Figure 6-18 Diesel micro-pilot: normalized IMEP and ignition delay

Increasing the diesel DI quantity is an approach to enhance the overall charge reactivity. However, the combustion of the DI with a long injection duration may have the aforementioned trade-off between the emissions of NOx and smoke (Figure 6-17). Therefore, the long duration DI is split into two pilot injections of shorter durations. The first diesel injection is delivered early during the compression stroke. This injection evaporates and blends with the ethanol background to create a region with the reactivity higher than the ethanol premixed charge. Nevertheless, the enhanced charge reactivity is still not sufficient for auto-ignition. Another injection of diesel is supplied to this charge of higher reactivity to initiate the combustion. The pilot injections at short durations are called 'micro pilot' in this dissertation due to the small amount of fuel to distinguish them from the conventional diesel pilot injections.

117

The cylinder pressure and heat release rate curves are shown in Figure 6-19 to investigate the impacts of the double micro-pilot diesel injections on combustion performance. With a single injection of 270 µs injection duration, the combustion duration is long, and the majority of the heat is released after 370 °CA. This observation indicates that the single injection of 270 µs is not sufficient to ignite the premixed charge of ethanol at low reactivity. The diesel single DI is increased to 300 µs at the same injection timing. The heat release rate is considerably enhanced, and the combustion duration is shortened. The double micro-pilot injections, 250 µs at 300 °CA and 270 µs at 355.5 °CA, are then tested. Based on the offline injection rate measurement, the combined fuel mass delivered by the double micro-pilot injections is similar to the mass delivered by a single 300 µs duration pilot injection at 900 bar injection pressure. It is observed that the combustion duration of the double-micro-pilot case is close to the one of 300 µs single pilot injection case.
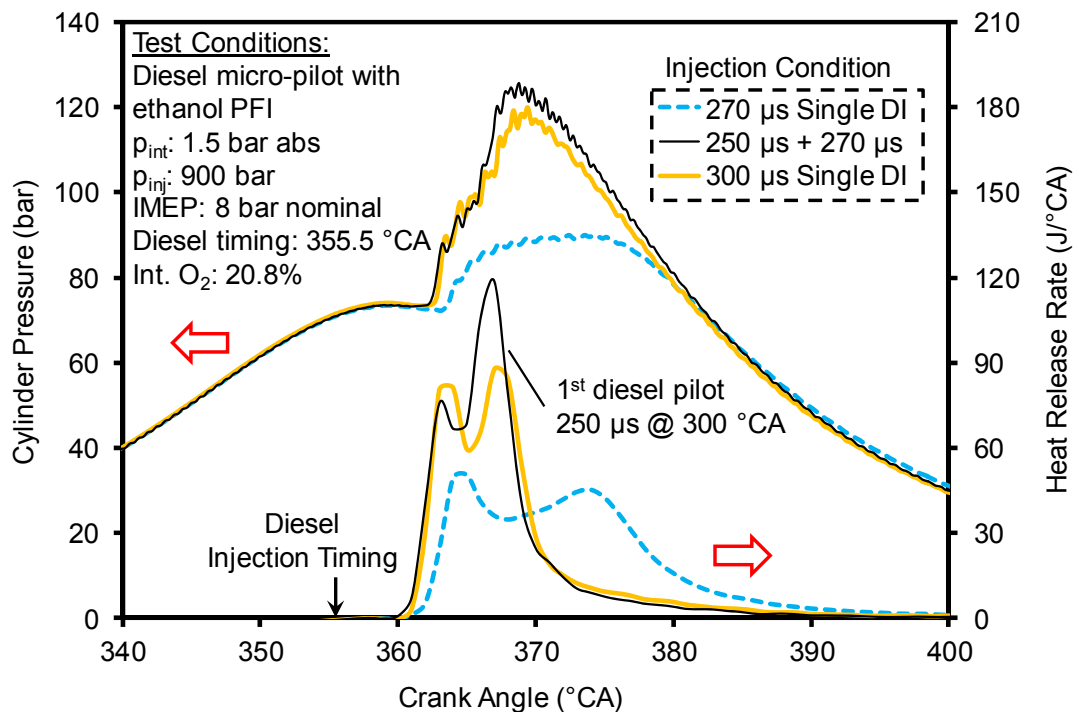
Figure 6-19 Diesel micro-pilot: cylinder pressure and HRR

The heat release rate curves are further analyzed to investigate the impact of the double micro-pilots. The dual-hump heat release is observed for all the three injection strategies. As previously mentioned, the first peak of the heat release is related to the diesel ignition, while the second peak is determined by the reactivity of the premixed charge. It is observed that the heat release rate curve with the single DI of 300 μs has the strongest ignition ability (highest first peak), while the double micro-pilot injections have the strongest premixed combustion (highest second peak). The stronger premixed combustion with double micro-pilot injections suggests that the early diesel pilot effectively enhances the charge reactivity.

The emissions of NOx, CO, and THC with the three different injection strategies are compared in Figure 6-20. The volumetric concentrations of the emissions are reported in this subsection instead of the indicated emissions to eliminate the potential effects from the changes in engine load at different injection timings and intake oxygen levels. The highest CO and THC emissions are detected from the combustion with the 270 μs single injection. The high emissions of the partially oxidized products can be explained by the low combustion temperature caused by the low charge reactivity and long combustion duration. When a longer injection duration of 300 μs is used for ignition, the combustion temperature is increased, which is indicated by the increased NOx emissions. In the double-micro-pilot case, the THC emissions reduce by about 300 ppm, while the CO emissions drop to less than half of that from the single-micro-pilot case. The significant reduction in the CO emissions supports the assumption of enhanced charge reactivity.
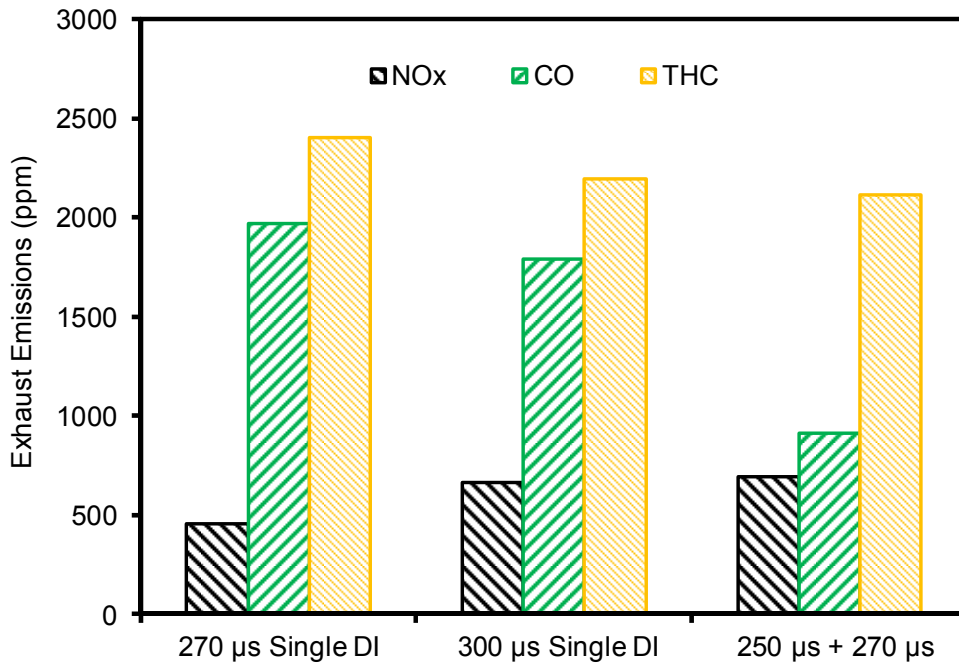
Figure 6-20 Emissions of NOx, CO, and THC with various injection strategies

The comparisons of the smoke and NOx emissions are presented in Figure 6-21. The smoke emissions at various injection and intake oxygen conditions remain at an ultra-low level because the premixed combustion of the ethanol charge forms ultra-low smoke emissions. The NOx emissions show similar trends for both the injection strategies. No clear distinction is observed at the two tested intake oxygen levels. Moreover, the application of EGR is effective in suppressing the NOx emissions for both the injection strategies.
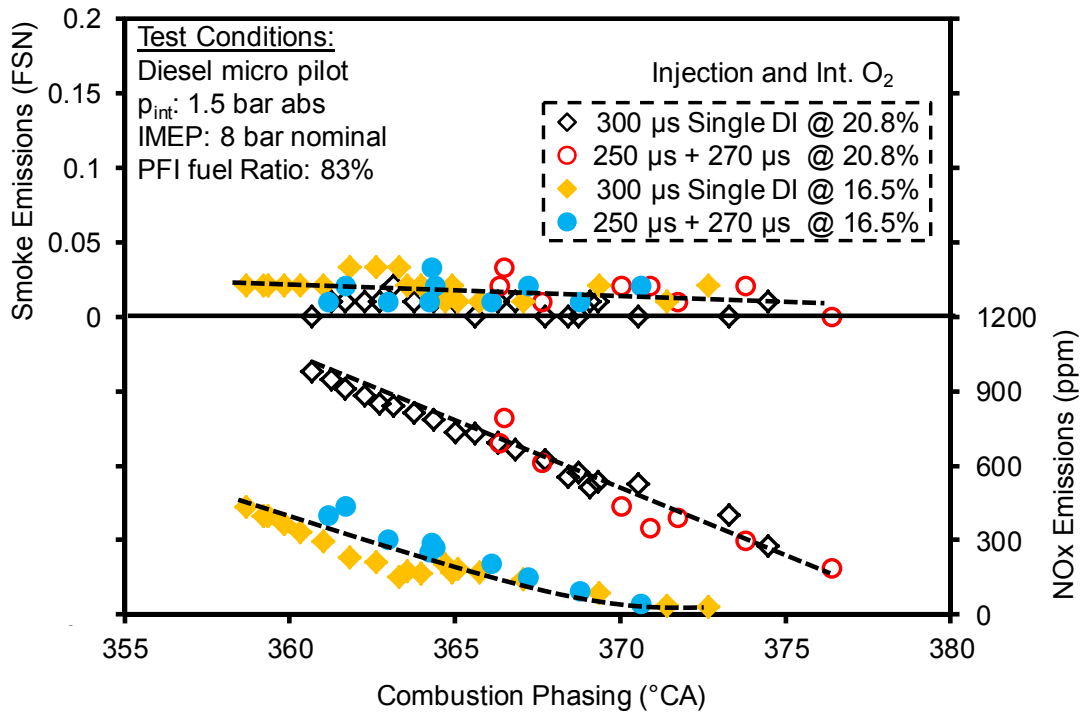
Figure 6-21 Diesel micro pilot: Smoke and NOx emissions

This double-micro-pilot injection strategy is mainly applicable at medium engine loads. When the engine load is low, the premixed ethanol charge is often excessively lean to be effectively oxidized, even if a longer duration of diesel DI is used. High concentrations of THC emissions are commonly detected in the engine exhaust. Therefore, the benefits of using ethanol PFI are limited at low engine loads due to the poor combustion efficiency. On the other hand, when the engine is operated at high engine loads, the ignition often becomes less challenging due to the high residual temperature from the previous engine cycle. A single DI is typically sufficient to generate the ignition.

6.2 Combustion with Butanol Port Fuel Injection

This section describes the results from the use of n-butanol as the port injection fuel. N-butanol has a higher reactivity to compression ignition compared to ethanol. The

121

premixed charge of n-butanol can auto-ignite in the PUMA engine without the need of additional intake heating. Hence, the benefits and challenges of the HCCI combustion of n-butanol are investigated on that platform. The direct injection of diesel is also used with the n-butanol port fuel injection. The impacts of diesel injection timing and PFI fuel ratio on combustion characteristics and emissions are studied at various EGR rates.

6.2.1 Butanol HCCI

The HCCI combustion of n-butanol is presented in this sub-section. N-butanol can auto-ignite without additional intake heating on the PUMA platform, and with intake heating on the SCRE platform. However, the direct application of PFI n-butanol is often unsuccessful to ignite during the initial engine start due to the relatively low temperature in the engine combustion chamber. Although the engine oil and coolant are preheated to 80 °C in this setup, the temperature is still not sufficient for consistent ignition. A promising method is to start the engine with diesel DI and n-butanol PFI. When the engine is fully warmed up, the diesel DI is gradually reduced until it is stopped completely. Stable neat n-butanol HCCI combustion is thereafter achieved with the PFI only.

In the HCCI combustion enabled by n-butanol port fuel injection, the control of mixing and reactivity through direct fuel injection is not available. The primary control methods that can be used on this engine platform to control the HCCI combustion of n-butanol are intake pressure and EGR. A higher intake pressure has been observed to enhance the charge reactivity (Sections 5.2 and 6.1). However, a higher intake pressure may generate two contrary effects in the HCCI combustion. The reactivity may be enhanced as suggested in the previous observations, or it may be suppressed because of the potentially

leaner combustion (more air is charged into the engine at a higher intake pressure, but the PFI injection duration is constant). Therefore, the actual effect of intake pressure on HCCI combustion is examined in detail in this subsection.

The effect of intake pressure on the onset of combustion is illustrated in Figure 6-22 at various engine loads. The SOC timings in this figure are calculated with the 50 Joule threshold. As discussed in Section 6.1.2, a fixed energy amount is more suitable than a fixed percentage (CA5) to indicate the start of combustion when the total energy amounts (engine loads) are varied significantly. The calculated excess AFR values are also overlaid in the same figure. The intake oxygen level is maintained at 20.8% in this set of tests.
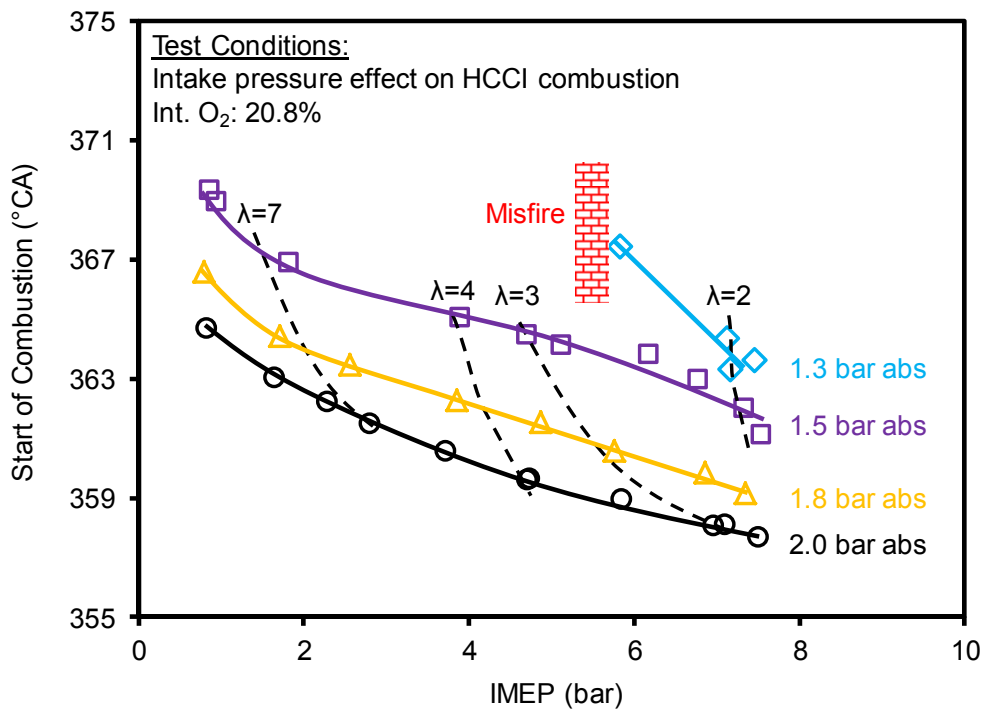
Figure 6-22 Intake pressure effect: SOC at various intake pressures

123

The general trend of SOC is similar at different intake pressures. As the IMEP increases, the SOC advances. A higher level of IMEP is produced from a higher amount of fuel supplied via the PFI application. At the same intake pressure, the mass of the fresh air intake is at a similar level. Therefore, the in-cylinder charge is richer at a higher IMEP. The SOC is advanced due to the relatively higher reactivity for the richer mixture of fuel and air. However, when the SOC values are compared at a similar IMEP level, the in-cylinder charge is richer at a lower intake pressure, but a delayed SOC is still detected. The results suggest that for the HCCI combustion, intake pressure has stronger impacts on the SOC than the AFR. This observation also explains the misfire condition at 1.3 bar absolute intake pressure. When the intake pressure is lower than a certain limit, the charge reactivity becomes more sensitive to the changes in AFR. A slight increase of the excess air ratio (λ) from 2 to 2.3 causes misfire.

The PCP and PPRR are shown in Figure 6-23 for the same set of tests. At the same intake pressure, the PCP reduces as the IMEP is lowered. At a lower IMEP, the total combustion energy is reduced, and the combustion phasing is also retarded. Both the effects suppress the PCP. Similar trends are observed at different intake pressures. The gradient of PPRR is smaller at a higher intake pressure than at a lower intake pressure, with respect to IMEP. When the PPRR increases from 5 bar/°CA to 15 bar/°CA at 2 bar absolute intake pressure, the IMEP difference is about 5 bar (from 2 bar to 7 bar). For the same PPRR increase at 1.5 bar intake pressure, the IMEP difference is only 2 bar (from 5 bar to 7 bar). This observation suggests that it is beneficial to use a lower intake pressure for the lower PCP and PPRR at the same IMEP if the reactivity of the in-cylinder charge is sufficient for reliable ignition. However, when the mixture approaches the stoichiometric

combustion, the increase rate in PPRR accelerates. Therefore, the primary limitation of achieving a higher engine load at a lower intake pressure is the PPRR, while it is often the PCP at a higher intake pressure.
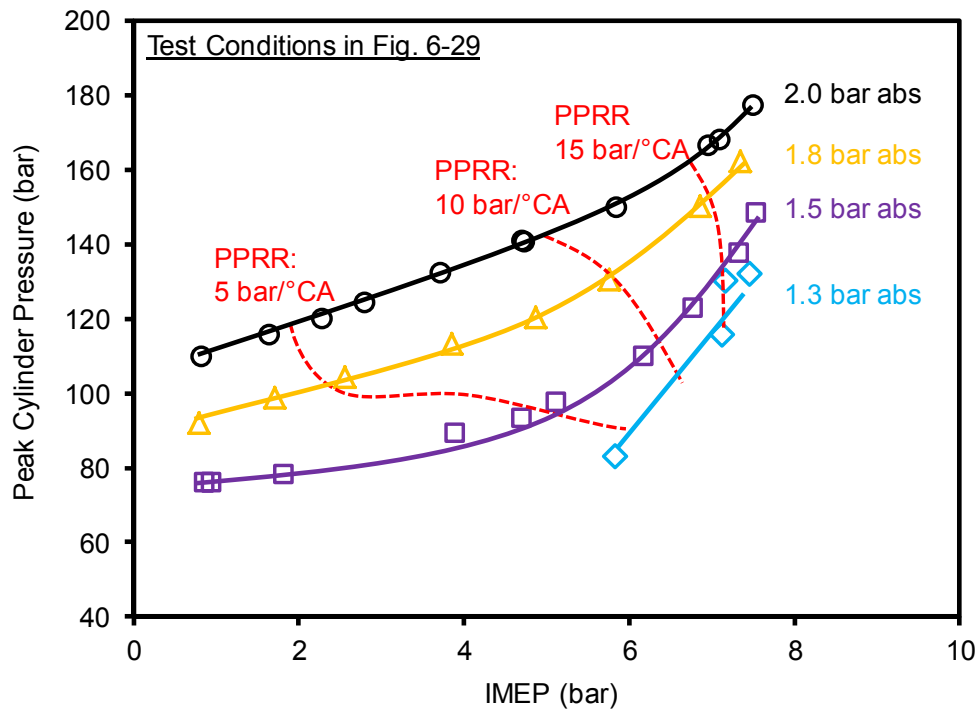
Figure 6-23 Intake pressure effect: PCP and PPRR at various intake pressures

The indicated thermal efficiency and NOx emissions are shown in Figure 6-24 at different intake pressures and IMEP levels. The thermal efficiency comparable to that in conventional diesel combustion can be maintained for IMEP higher than 3 bar in the n-butanol HCCI operation. A lower efficiency is detected for low engine loads (less than 3 bar). At such low loads, the homogeneous in-cylinder charge is typically excessively lean to be effectively oxidized, hence, the combustion efficiency is lower. The combustion phasing is also delayed, which further reduces the thermal efficiency. There are no distinct differences in the thermal efficiency between the different intake pressures.

The NOx emissions at various intake pressures follow similar trends. The absolute volumetric concentrations of the NOx emissions are consistently approximately 10 ppm at different engine loads and intake pressure levels. The indicated NOx emissions are elevated mainly due to the reduction in the engine load. It should be noted that the smoke emissions are always lower than 0.005 g/kW-hr in this set of tests.
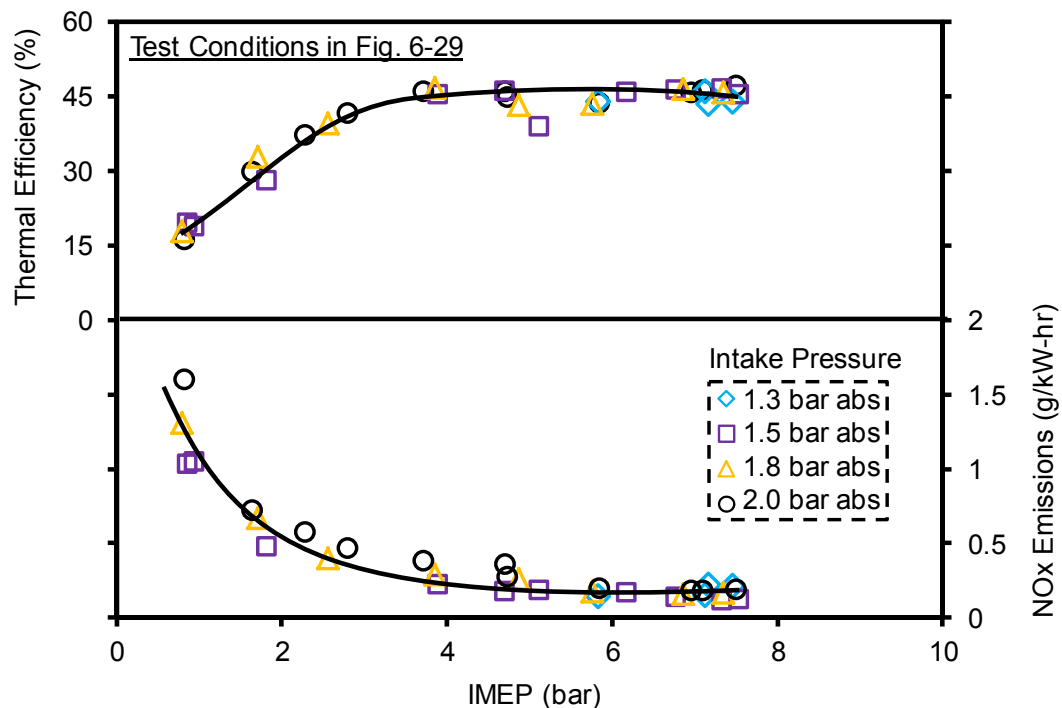
Figure 6-24 Intake pressure effect: efficiency and NOx emissions

The EGR is applied in HCCI combustion mainly to suppress the PCP and the PPRR, as the NOx and smoke emissions are typically low. The EGR effects on PCP, PPRR, and SOC are studied at two IMEP levels and two intake pressure levels. The PFI fuel injection amount is constant during the individual EGR sweep.

The PCP values at various intake oxygen levels are shown in Figure 6-25. The general trends are similar for different intake pressures and IMEP levels. EGR is more effective

to reduce the peak cylinder pressure at a lower intake pressure. As previously discussed, a higher intake pressure increases the charge reactivity, while a higher EGR rate reduces the charge reactivity. The high intake pressure and the high EGR rate counteract each other, and thus reduce their individual effectiveness. A higher IMEP and a higher intake pressure are the two primary causes for the higher PCP values in HCCI combustion. It is critical to match the intake pressure with the desired engine load to explore the potential of load extension. A higher than necessary intake pressure often reduces the efficacy of EGR for the regulation of PCP.
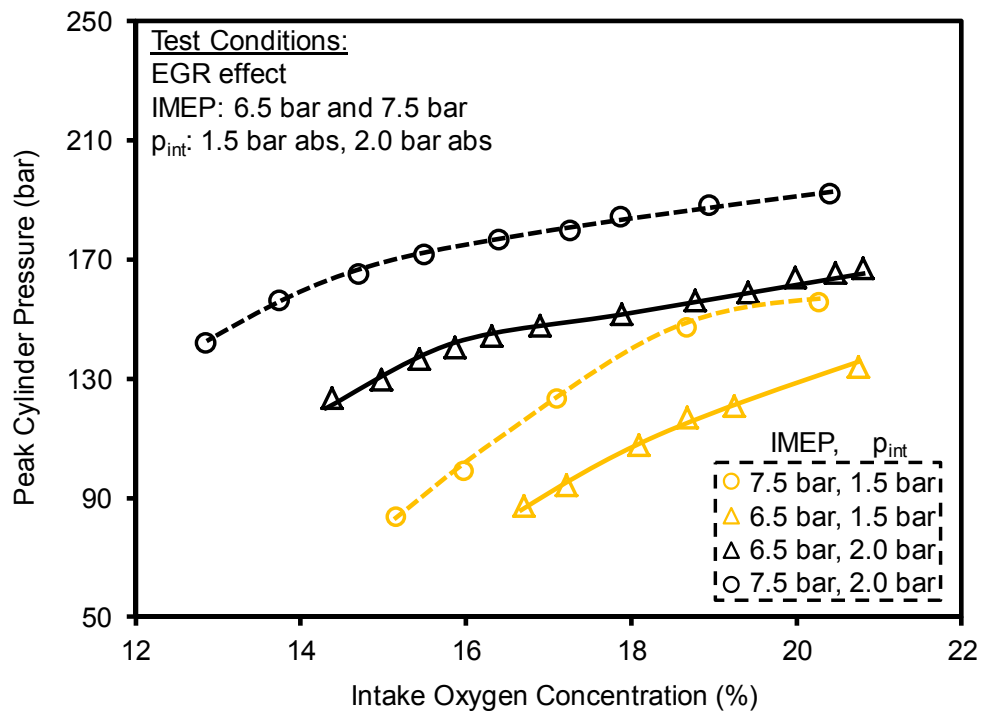
Figure 6-25 EGR effect: peak cylinder pressure at varied intake pressure

The calculated PPRR values are shown in Figure 6-26. When no EGR is applied, the PPRR values are at a similar level at the same IMEP. This suggests that the PPRR is mainly determined by the engine load level without EGR. It is observed that the

application of EGR is effective to decrease PPRR at different IMEP levels and intake pressures. The EGR application is more effective at the lower intake pressure.
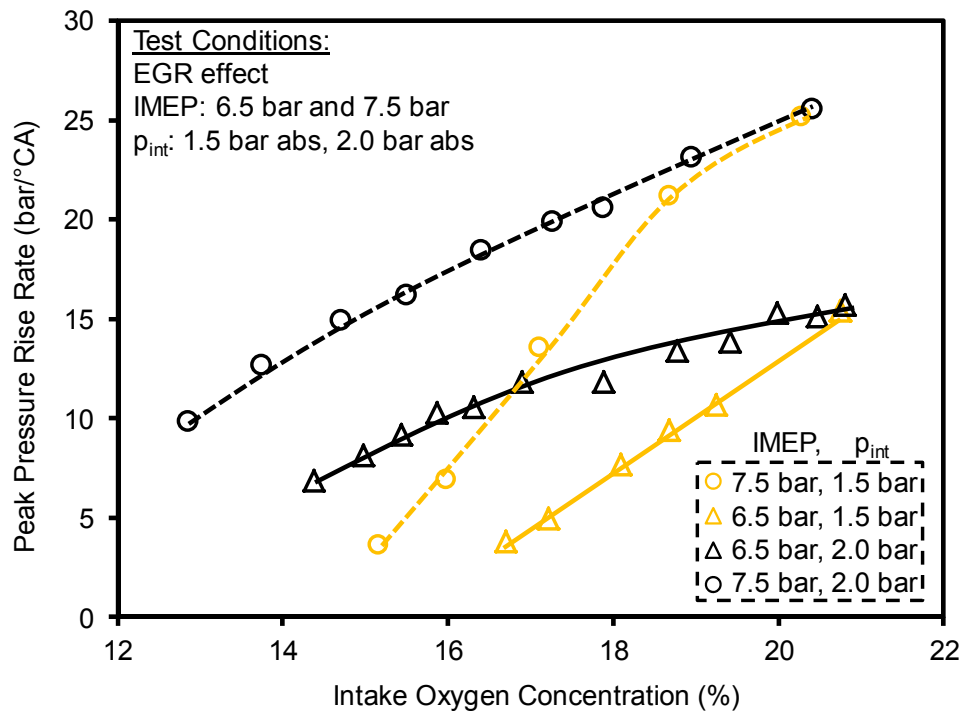
Figure 6-26 EGR effect: PPRR at varied intake pressure

The actual mechanism of suppressing PCP and PPRR with the application of EGR is studied with the cylinder pressure and HRR curves shown in Figure 6-27. The EGR application affects the HRR in two major ways: delaying the combustion phasing and reducing the burning rate. The reduction of PCP can be primarily attributed to the delayed combustion phasing, while the decreased PPRR is more related to the lowered burning rate. When a higher EGR rate is applied to the engine intake, the general charge reactivity is decreased. The combustion tends to initiate later and progress slower. Therefore, the combustion phasing is delayed, and the combustion rate is suppressed.
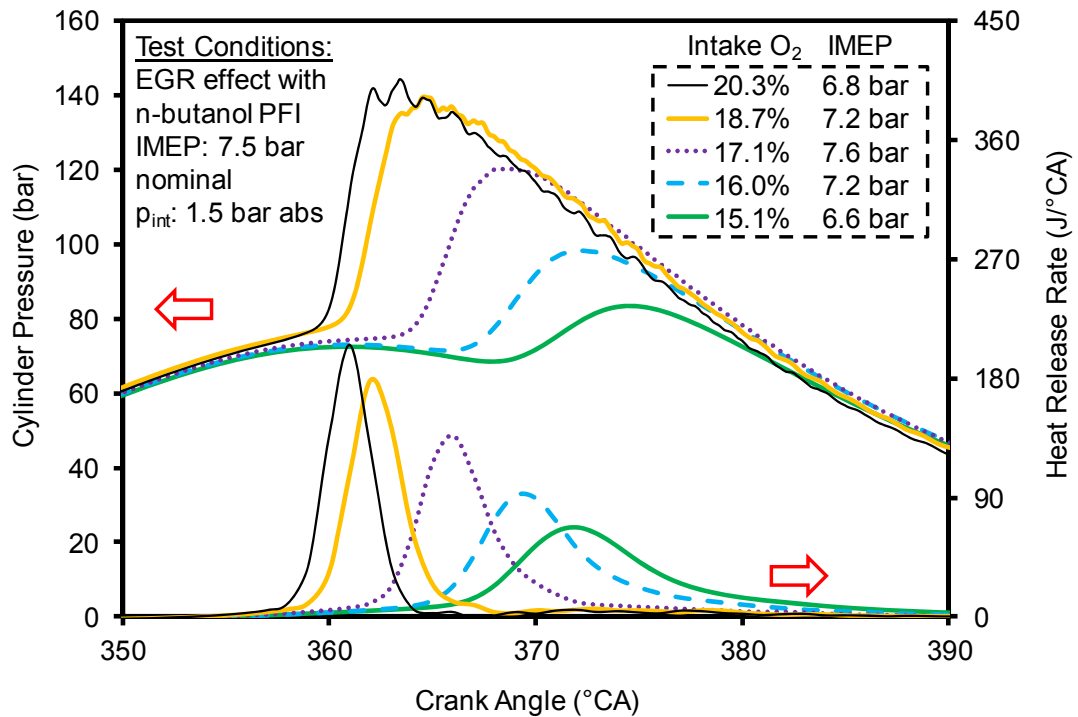
Figure 6-27 EGR effect: cylinder pressure and HRR at varied intake oxygen levels

6.2.2 Diesel DI and Butanol PFI

The direct injection of diesel is applied to the premixed n-butanol charge to study its effect on the modulation of charge reactivity. The reactivity control is mainly achieved via the control of the fuel ratios in this subsection.

Three EGR sweeps are conducted at different n-butanol PFI fuel ratios to study the emission performance. The NOx emissions are shown in Figure 6-28. The general trends of lower NOx emissions at lower intake oxygen levels are observed for all the three fuel ratios. The results also reveal that a higher PFI fuel ratio generates lower NOx emissions at a similar level of intake oxygen concentration. This is consistent with the results from the combustion with the ethanol premixed charge (Figure 6-12). The main cause for the low NOx emissions is the reduced amount of diesel injection.
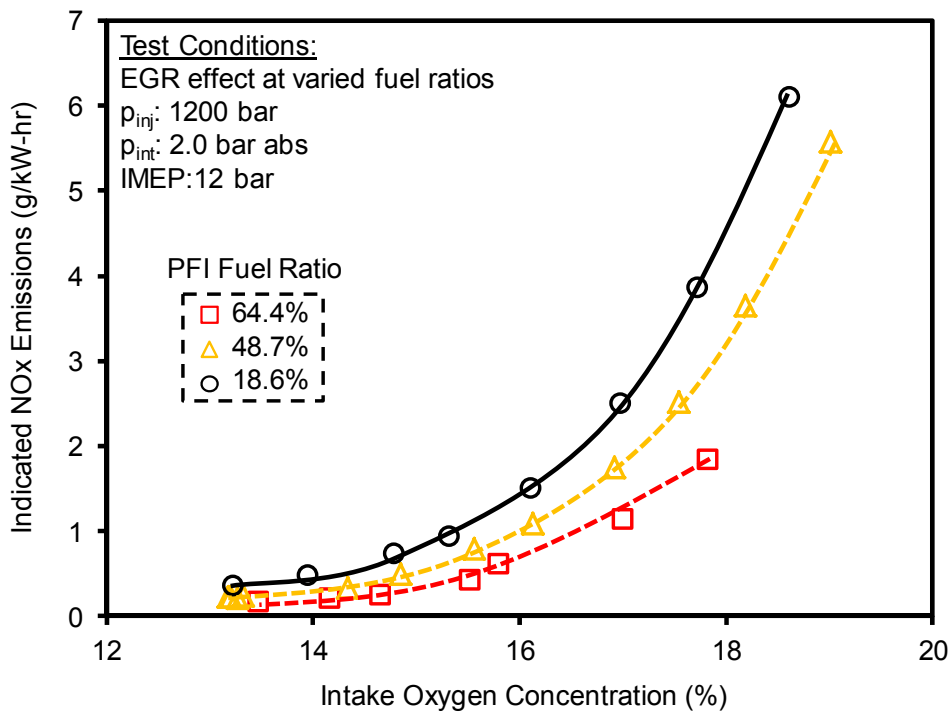
Figure 6-28 EGR effect: NOx emissions at varied fuel ratios

The overall trends for the smoke emissions are also similar between different fuel ratios. As shown in Figure 6-29, the smoke emissions remain at low levels for the intake oxygen concentration from approximately 20% to 16%. The sharp increase of smoke emissions occurs when the intake oxygen concentration is lowered to below 16%. The smoke emissions often reach the predefined threshold (5 FSN) with another 2 to 3% reduction in the intake oxygen concentration. The combustion with the highest PFI fuel ratio (64.4%) generates slightly higher smoke emissions with a lower amount of diesel injection, compared with the other two cases. The high smoke emissions indicate that the diesel combustion with a higher PFI fuel ratio generates considerably more smoke emissions per unit mass of fuel. The in-cylinder temperature is potentially higher, and the oxygen concentration is potentially lower, when more PFI fuel is burnt before the diesel combustion. The diesel injection burns in an environment with a relatively high rate of

internal EGR. Hence, the smoke emissions are elevated under the high temperature and internal EGR.
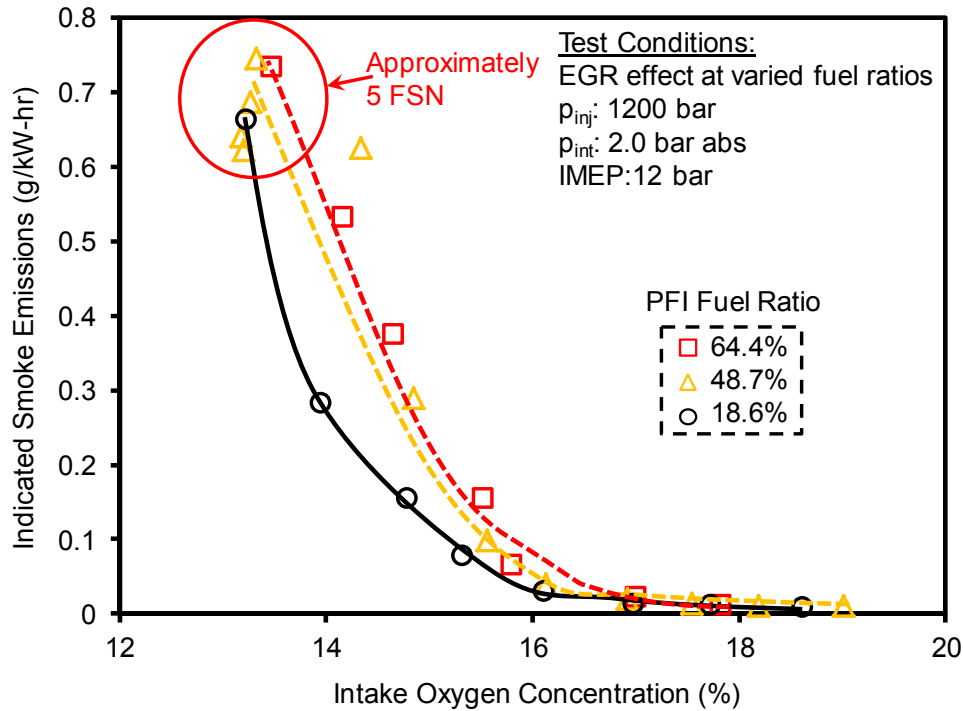
Figure 6-29 EGR effect: smoke emissions at varied fuel ratios

The diesel combustion with n-butanol port fuel injection forms more smoke emissions than the combustion with diesel only. The primary reason is that the mixing timing for diesel is insufficient at the high temperature generated from the first stage of combustion. With the elevated in-cylinder temperature, the diesel injection would start to burn immediately when the oxygen is available. The impact of external EGR is very limited to withhold the combustion of diesel due to its high reactivity at elevated temperatures. Therefore, diesel may not be the optimal fuel to be used after the start of the initial combustion. However, if the DI fuel is replaced with a lower reactivity fuel, the trade-off for NOx and smoke emissions may potentially be improved. The n-butanol DI is thus

tested after the first stage of combustion of the PFI n-butanol. The results will be discussed in Chapter 7.

The normalized IMEP values of the combustion with various PFI fuel ratios are compared in Figure 6-30. The general trend of the combustion with ethanol shown in Figure 6-14 is also included in this figure. The relative IMEP remains in a range of higher than 90% when the intake oxygen concentration is reduced from 20% to 13%. The relative IMEP level is also similar to the one with ethanol PFI in a similar range of intake oxygen concentration. The applicable rate of EGR is mainly limited by the high smoke emissions as shown in Figure 6-29 for the three tested PFI fuel ratios.
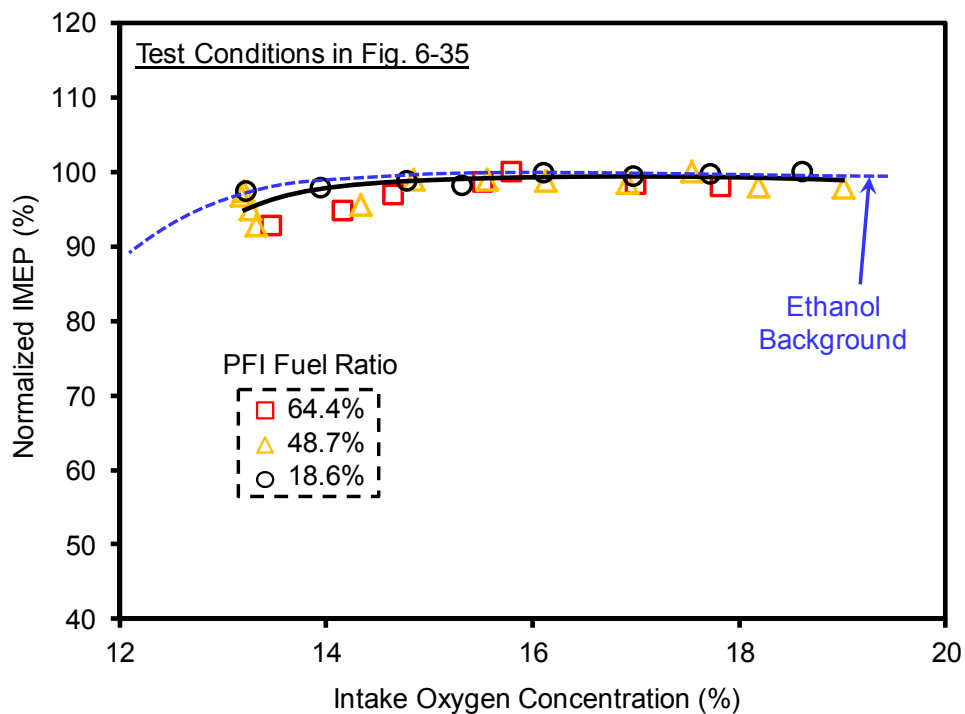
Figure 6-30 EGR effect: normalized IMEP at varied fuel ratios

Three data points are selected from the EGR sweep with a fixed PFI fuel ratio of 64.4% to examine the EGR impact on combustion characteristics. The diesel injection is at a

fixed timing for the three cases. The cylinder pressure and HRR curves are shown in Figure 6-31. The intake oxygen level is gradually reduced in an interval of 2% with the increased EGR rate. The first stage of combustion is drastically retarded at a lower intake oxygen concentration. The peak HRR of the first stage is also reduced. The PCP and PPRR, which are closely related to the first-stage heat release, are also decreased. However, the second stage of combustion only changes slightly in the peak of the HRR. The slightly increased peak HRR is from the burning of partially oxidized products of the previous combustion. The combustion phasing of the second stage remains with the increased EGR rate. This phenomenon suggests that the mixing period of the diesel injection remains in a similar range at different intake oxygen levels. The EGR application has limited impacts to extend the mixing duration for the DI after the initial stage of combustion.
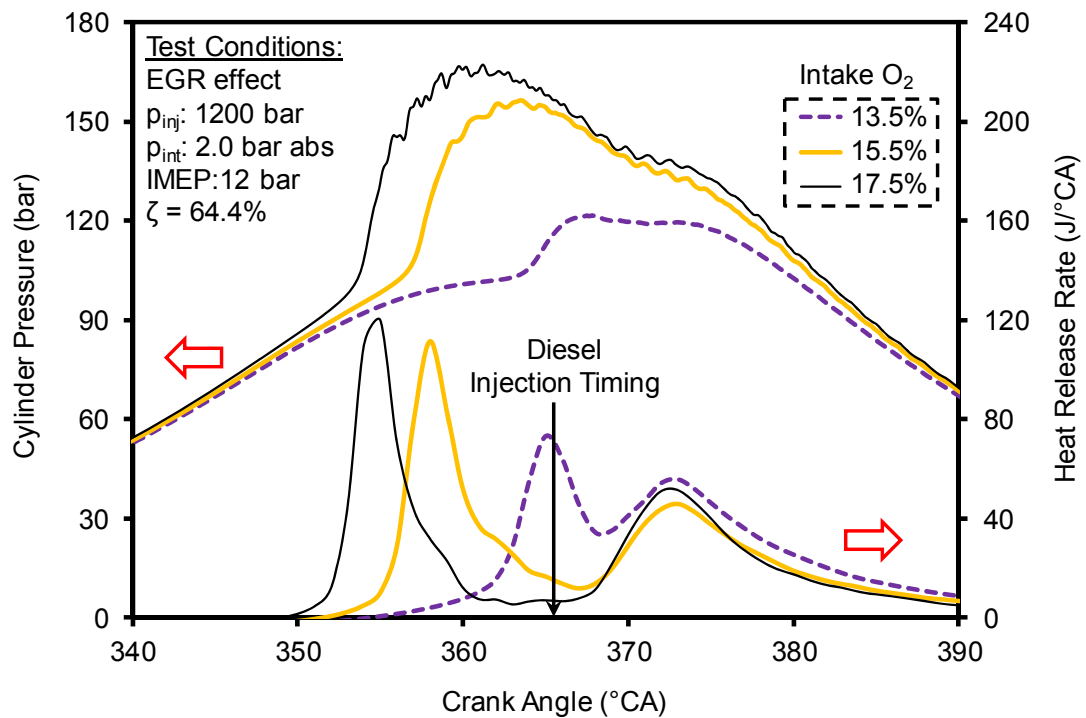
Figure 6-31 EGR effect: cylinder pressure and HRR at fixed fuel ratio

6.3 Summary

The combustion performance and emissions have been studied with ethanol and n-butanol as the port injection fuels. A single DI of diesel has been used as the ignition source for ethanol. The premixed n-butanol fuel generates auto-ignition on the PUMA engine platform with a high compression ratio. However, the single DI of diesel is still added to study the reactivity modulation. The research observations can be summarized as follows:

In the combustion with ethanol port fuel injection:

- The diesel injection timing controls the start of combustion and combustion phasing without using extensive EGR. The ethanol premixed charge marginally contributes to the initial stage of heat release with the fixed close-to-TDC diesel injections.

- The PFI fuel ratio is critical for the combustion with ethanol port fuel injection. A longer ignition delay is often detected at a higher PFI fuel ratio. This effect becomes more significant at lower charge reactivity (with a lower intake pressure and a higher EGR rate), when the diesel injection timing is fixed close to TDC.

- The combustion with a higher PFI fuel ratio often generates lower emissions of NOx and smoke at similar engine operating conditions. The premixed combustion is enhanced by the increase in ethanol and reduction in diesel.

- A high EGR rate and a high ethanol ratio are essential to regulate the emissions of NOx and smoke to below the emission standards. However, the charge reactivity with these conditions is often excessively low to effectively oxidize THC and CO, and thus the combustion efficiency reduces.

- Diesel micro-pilot injections are employed to improve the reactivity of the premixed ethanol charge. The oxidization of CO and THC is considerably enhanced while the ultra-low NOx and smoke emissions can be maintained with the application of EGR.

In the combustion with n-butanol port fuel injection:

- The HCCI combustion enabled with port injection of n-butanol is demonstrated in the PUMA engine. The control of intake pressure is an effective method to regulate the SOC in the HCCI combustion with n-butanol. However, the high intake pressure is often associated with the high PCP and PPRR. The application of EGR can delay the SOC, and reduce the PCP and PPRR. The impact of EGR is more significant at a lower intake pressure.

- A higher n-butanol ratio increases the portion of premixed combustion and is beneficial for low NOx emissions in the combustion with n-butanol PFI and diesel DI. The smoke emissions remain at an ultra-low level without EGR. However, the smoke emissions increase significantly with EGR. The diffusion-dominated diesel burning in the second stage contributes the majority of the smoke emissions. The results suggest that high reactivity fuels, such as diesel, are not optimal to be used in the combustion with pre-ignition due to the insufficient mixing.

CHAPTER VII

PARTIALLY PREMIXED COMBUSTION WITH ALCOHOL FUELS

The results of the partially premixed combustion with alcohol fuels are presented in this chapter. In the first section, the effects of n-butanol injection timing and duration on combustion characteristics are investigated with ethanol port injection and n-butanol port injection. In the next section, multiple injections of n-butanol are employed to enhance the mixing control of the in-cylinder charge. The optimal combustion performance and emissions are demonstrated using selected fuel injection timings and durations. A high intake pressure is used to enhance the charge reactivity for the improved ignition, while EGR is applied to regulate the combustion rate and suppress the NOx emissions.

7.1 Butanol DI with Premixed Charge

The direct injection of n-butanol is used in the premixed charge generated via the port injection of ethanol or n-butanol. The main advantage of such an arrangement is that the combustion energy is supplied entirely by the alcohol fuels that could be produced from renewable resources. Furthermore, the combustion performance and emissions also benefit from the fuel properties of ethanol and n-butanol in compression ignition engines.

7.1.1 Ethanol Port Fuel Injection with Butanol DI

A single injection of n-butanol is typically not sufficient to ignite the bulk premixed charge of ethanol on the PUMA engine platform. The primary cause for that is the IMEP from the combustion of n-butanol DI is closely coupled with the peak pressure rise rate (PPRR), which has been discussed in Section 5.2.2. A lower IMEP is not sufficient to

ignite the ethanol charge of low reactivity, while a higher IMEP may exceed the PPRR limit when the premixed ethanol is ignited.

Therefore, in this research, the double injections of n-butanol are employed to ignite the premixed ethanol charge. The first DI is employed to form the local stratification of reactivity through in-cylinder blending with the premixed ethanol. The gradient of charge reactivity thereafter determines the SOC and the combustion rate at the first stage. The second injection combusts in the heated environment generated from the initial combustion. The high temperature produced from the second stage of combustion is partially retained to the next engine cycle to enhance the charge reactivity and secure the first stage of ignition.

The effects of the injection timings on ignition delay and combustion rate are studied with two independent injection timing sweeps. The test conditions are given in Table 7-1. The injection timings and injection durations shown in the table are command timings and command durations. In the first timing sweep, the second DI timing is kept constant while the first DI timing is changed. In the second timing sweep, the first DI timing is fixed while the second DI timing is changed. The nominal IMEP is 12 bar with a PFI fuel ratio of 35.5%. The injection durations for both the DI injections and the PFI are maintained constant. It should be noted that the ignition delay is defined as the duration from the first direct injection to the onset of combustion. The n-butanol flowrate is measured during both the injection timing sweeps.

Table 7-1 Test conditions of the injection timing sweeps

Injection Timing Effect on Combustion Characteristics Fig. 7-1, Fig. 7-2, Fig. 7-3		
Engine Parameters	Timing Sweep 1	Timing Sweep 2
IMEP (bar)	12.3	12.0
Intake Pressure (bar abs)	2.0	2.0
Intake Temperature (°C)	33.0	32.8
Intake O_2 (%)	20.8	20.8
Injection Pressure (bar)	900	900
First Injection Timing (°CA)	**330-350**	334
First Injection Duration (μs)	340	340
Second Injection Timing (°CA)	366	**360-374**
Second Injection Duration (μs)	650	650
Port Injection Duration (μs)	3200	3200
PFI Fuel Ratio (%)	35.5	35.5

In timing sweep 1, the ignition delay is shortened from 3.6 ms to 1.4 ms, as shown in Figure 7-1. This is mainly caused by the variations in the cylinder temperature during the engine compression stroke. When the timing of the first injection is close to TDC, the tendency of ignition is higher due to the relatively higher compression temperature. Therefore, a shorter ignition delay is observed. The higher peak cylinder pressure (PCP) and PPRR are also observed with the shorter ignition delay.
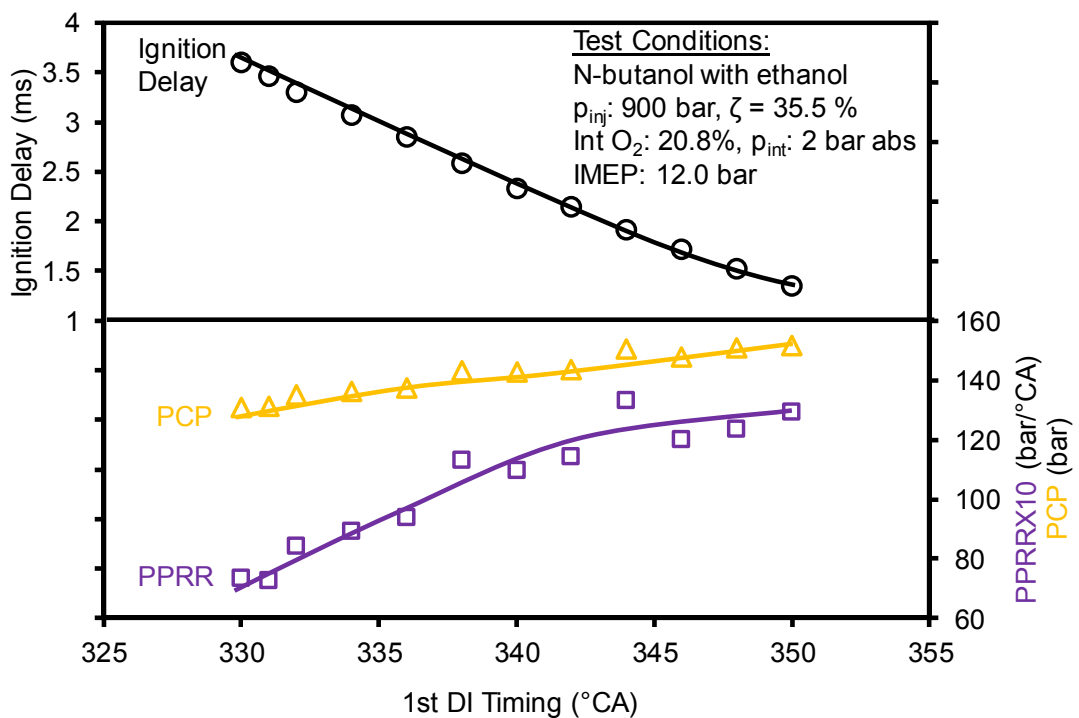
Figure 7-1 Time sweep 1: ignition delay, PPRR, and PCP

The effects of the second injection timing on the ignition delay, PCP, and PPRR are shown in Figure 7-2. When the timing of the second injection is retarded away from TDC, the ignition delay is prolonged from 2.8 ms to 3.0 ms. The impact of the injection timing on the ignition delay is secondary and is mainly achieved through the residual temperature that is partially retained to the next engine cycle. The PCP and PPRR have

similar trends as that in Figure 7-1. Overall, a shorter ignition delay is associated with a higher PCP and a higher PPRR in timing sweep 1 and timing sweep 2.
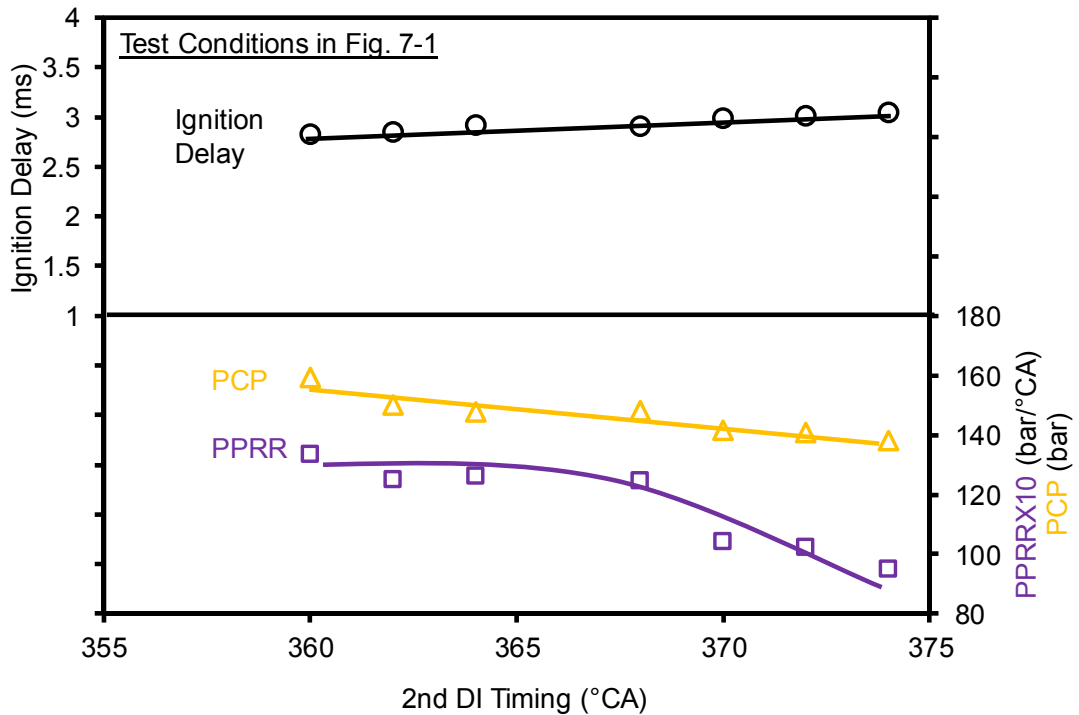
Figure 7-2 Timing sweep 2: Ignition delay, PPRR, and PCP

The injection timing impacts on CA5 and CA50 are shown in Figure 7-3. It is observed that the first DI timing has a limited control over both CA5 and CA50 in timing sweep 1. The changes in CA5 and CA50 are within 2 °CA when the timing of the first injection is delayed for more than 20 °CA. In contrast, the timing of the second injection has a more direct control on CA5 and CA50 in timing sweep 2.
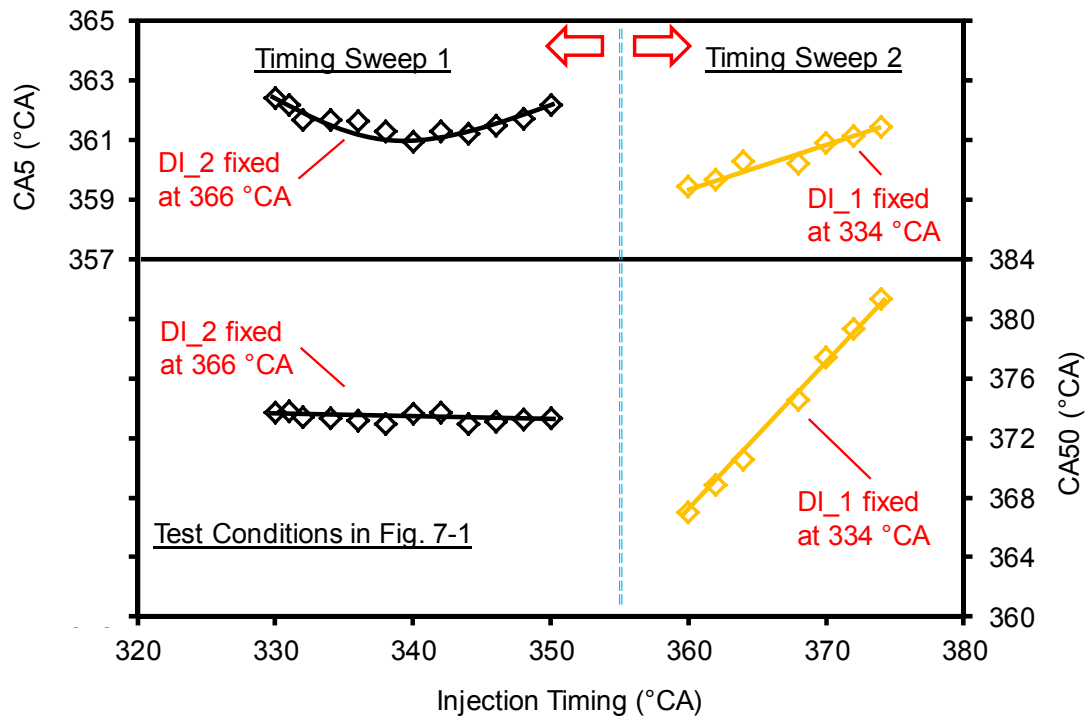
Figure 7-3 Injection timing effects: CA5 and CA50

Three data points are compared in Figure 7-4 to examine the effects of the PFI fuel ratios. When the duration of the port injection is increased, the durations of both the double DI injections are shortened to maintain the same IMEP level. The injection timing for both the DI injections and PFI are kept constant. As the PFI ratio increases, the phasing of the first stage of combustion is retarded, and the combustion intensity is enhanced (higher peak HRR). The increased ethanol ratio reduces the general charge reactivity due to the low Cetane number and thus delays the SOC. Moreover, it also increases the heat release rate during the first stage of combustion. For the second stage of combustion, the peak heat release rate is lowered by the shortened duration of the second injection, while the combustion phasing remains at the same level.
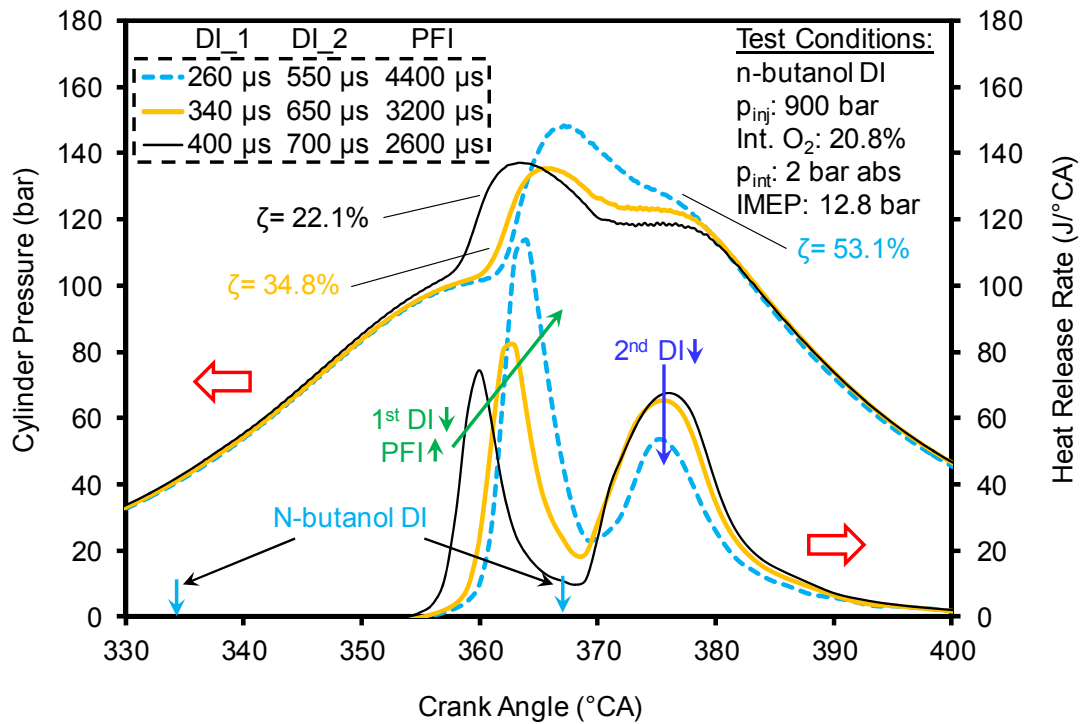
Figure 7-4 Varied PFI fuel ratios: cylinder pressure and HRR

With the experience gained from the previous analysis of injection timings and PFI fuel ratios, the engine load is further extended to 16 bar with a PCP of 159.3 bar and a PPRR of 14.1 bar/°CA. The cylinder pressure and HRR traces are given in Figure 7-5. The ignition delay is prolonged, and the PPRR is suppressed by the advanced timing of the first injection. The duration of the first injection is also reduced to further suppress the PPRR. A longer duration of port injection and a longer duration of the second DI are used to extend the engine load. The timing of the second DI is delayed to potentially reduce the PCP and PPRR.
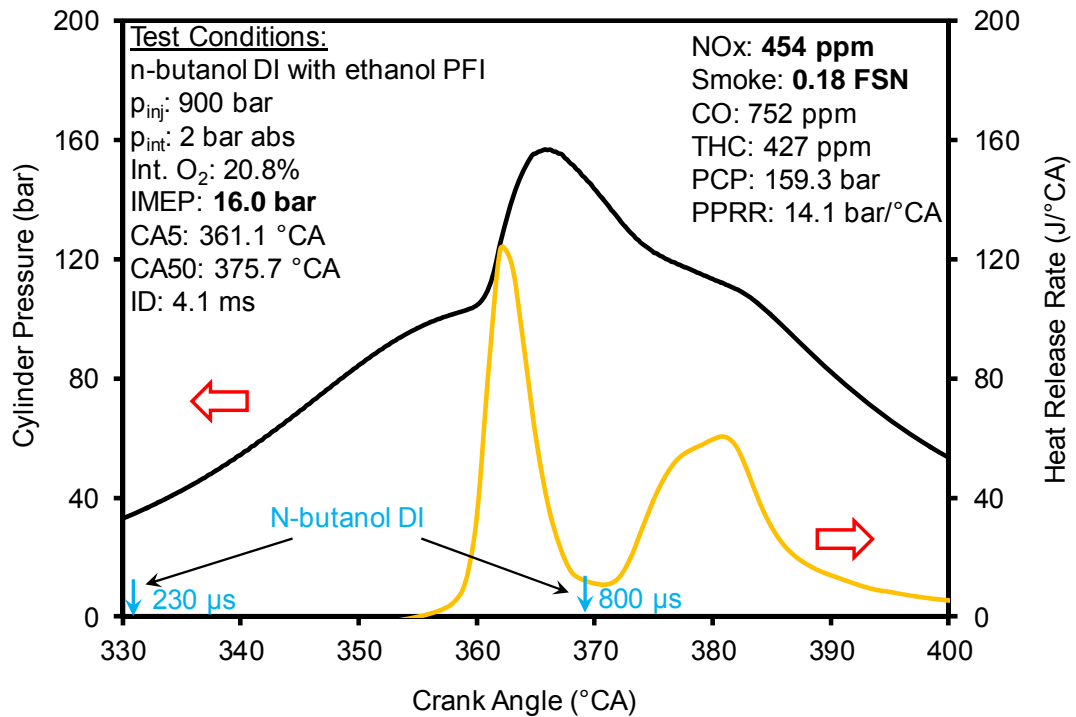
Figure 7-5 N-butanol DI with ethanol background: cylinder pressure and HRR

The result shown in Figure 7-5 demonstrates the basic concept to achieve a high engine load in the partially premixed combustion. The portion of premixed combustion should be limited to constrain the PCP and PPRR. The two methods used in this test to regulate the premixed combustion are the control of the premixed fuel amount and the control of charge reactivity. With the second stage of combustion, the partially oxidized products from the first stage of combustion are oxidized, and thus the combustion efficiency is significantly increased (98.5%), compared to that from the premixed combustion discussed in Chapter 6. It should be noted that the demonstrated condition is only an example of using the control of the PFI fuel ratio to reach a higher engine load.

7.1.2 Butanol Port Fuel Injection with Butanol DI

The combustion characteristics with both n-butanol PFI and DI are reported in this subsection. The fuel handling is easier due to the application with the single fuel,

143

compared with that in dual fuel applications. Moreover, the flexible mixing control in the dual-fuel application is maintained because of the use of port fuel injection and direct injection.

The cylinder pressure and HRR traces are shown in Figure 7-6 for the combustion with a port fuel injection at varied injection durations and a single direct injection at a constant injection duration. The first stage of combustion is generated from the HCCI combustion of the PFI of n-butanol. As the PFI amount increases, the phasing of the first stage of combustion is advanced, and the peak of heat release rate is elevated. The PCP and PPRR, which are closely related to the first stage of combustion, are also increased. The second stage of combustion is marginally affected by the first stage. The partially oxidized products that are formed in the first stage of combustion are combusted in the second stage of combustion. Hence, the HRR curve changes slightly in the second stage of combustion.

The cylinder pressure and HRR curves of the combustion with varied DI durations are shown in Figure 7-7. The timing of the DI, the timing of the PFI, and the duration of the PFI are maintained at the same level. As the DI duration increases, the second stage of heat release becomes wider and higher. The heat release shape is similar to the diesel combustion shown in Figure 5-12, which suggests that the second stage of combustion is dominated by the diffusion combustion. The SOC tends to advance as the injection duration of the DI increases. This advancement may be related to the potentially higher residual temperature from the previous engine cycle.
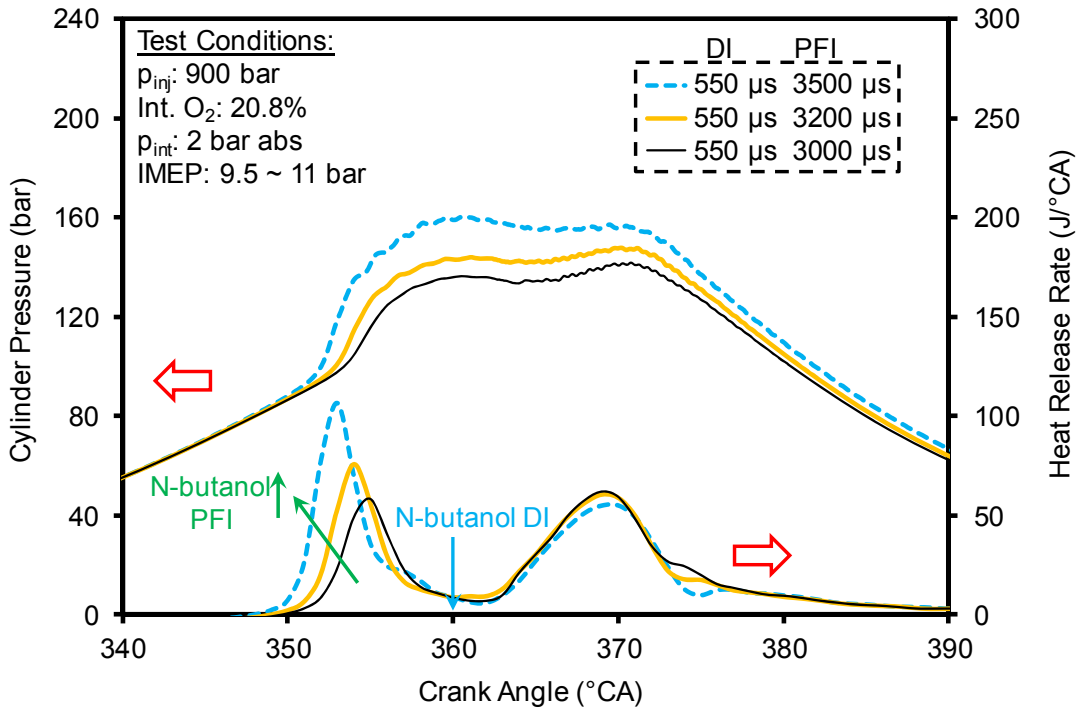
Figure 7-6 N-butanol PFI and DI: cylinder pressure and HRR
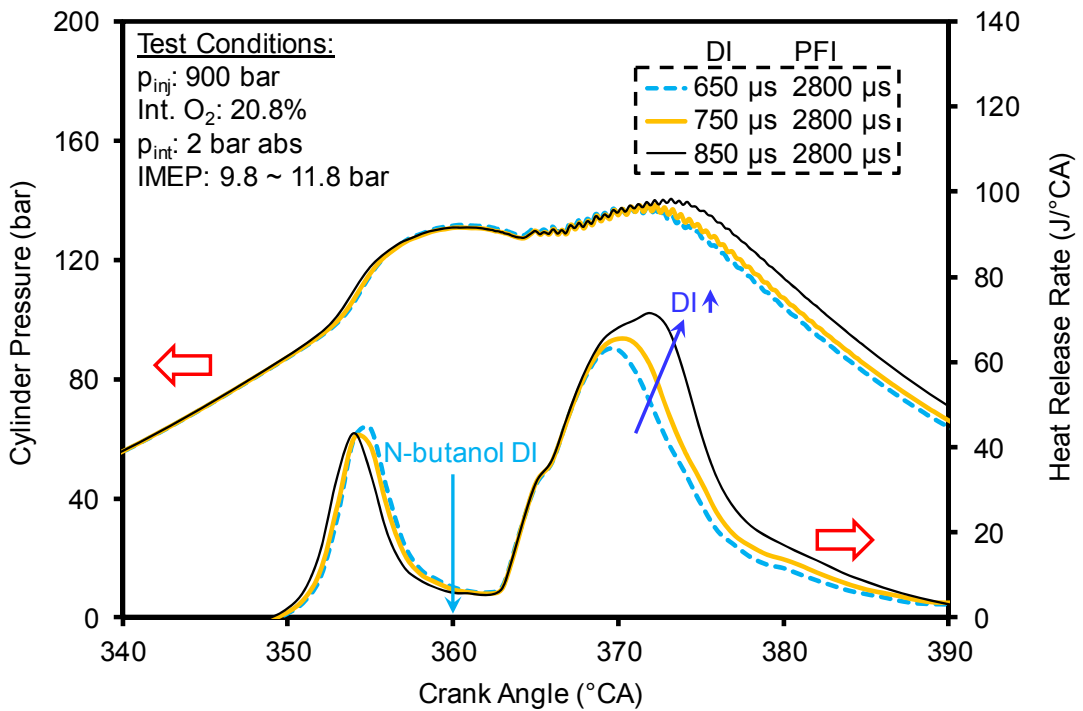
Figure 7-7 N-butanol PFI and DI: cylinder pressure and HRR

The mean cylinder temperatures are calculated in Figure 7-8 to investigate the temperature changes before the first stage of combustion in Figure 7-7. The mean cylinder temperature of the data point with 850 μs DI is about 6 °C higher than the temperature of the data point with 650 μs DI, at approximately 350 °CA before the onset of combustion. The intake temperature differences are within 0.1 °CA for the test in Figure 7-7, which contributes little to the temperature deviations during the engine compression stroke. Therefore, the higher temperature is attributed to the higher temperature in the residual gas and the higher heat transfer rate from the cylinder wall that is at a potentially higher temperature. The change in the first stage of combustion also demonstrates the high sensitivity of the HCCI combustion to the variations of cylinder temperature.
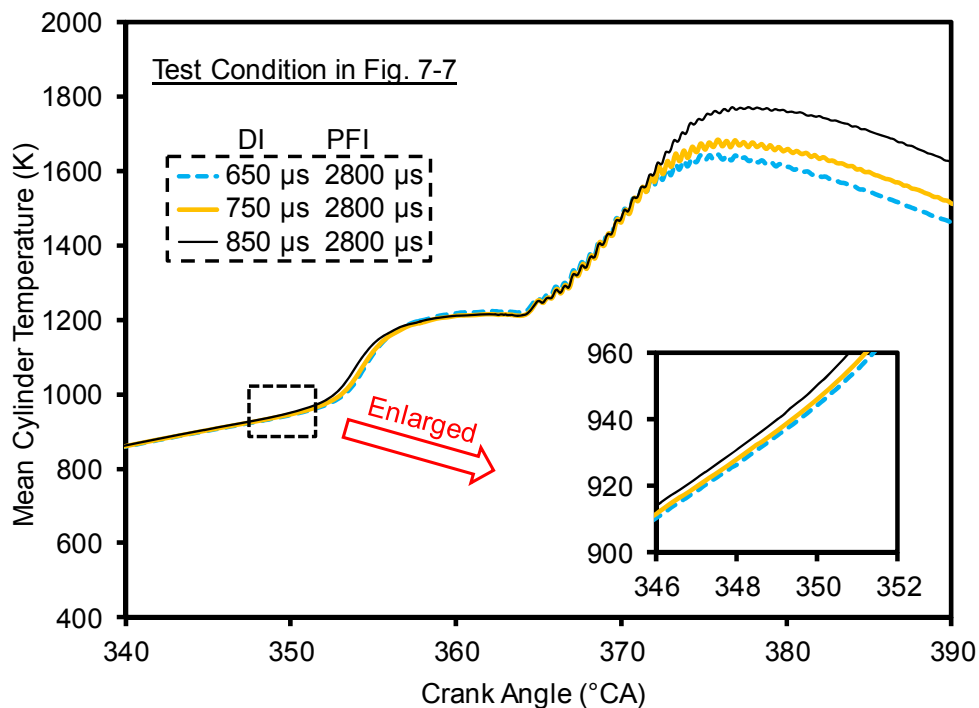
Figure 7-8 N-butanol PFI and DI: mean cylinder temperature

The cylinder pressure and HRR curves with three selected DI timings are shown in Figure 7-9 to study the combustion control with the timing of direct injection. It is observed that the phasing of the second stage of combustion retards with the retarded DI timing. The phasing of the first stage of combustion is also postponed with the delayed DI timing.

The mean cylinder temperatures are shown in Figure 7-10 to explore the mechanism of the indirect control of combustion phasing with the direct injection. With a retarded phasing of the second stage of combustion, the exhaust gas temperature is increased due to the late combustion phasing in the expansion stroke. The temperature in the residual gas is higher. However, the cylinder temperature at approximately 350 °CA is lower for the case with a retarded combustion phasing of the second stage. Hence, the lower rate of heat transfer from the cylinder wall is the primary cause for the lower temperature in this test.
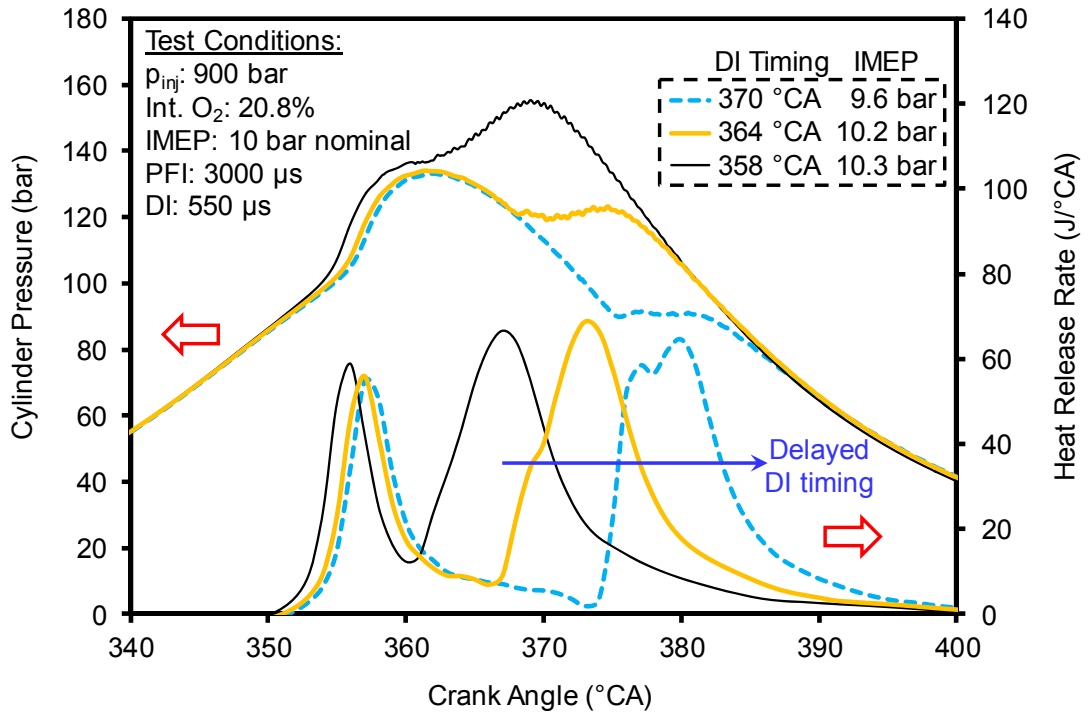
Figure 7-9 N-butanol PFI and DI: cylinder pressure and HRR with varied DI timing
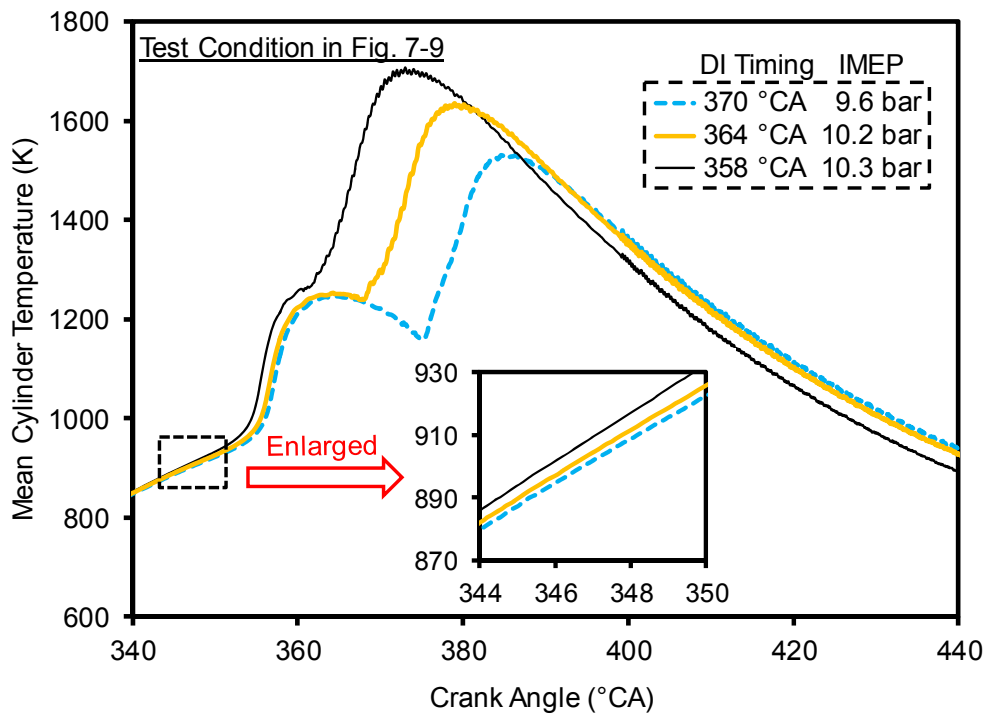
Figure 7-10 N-butanol PFI and DI: mean cylinder temperature

The PCP and PPRR of the same EGR sweep are shown in Figure 7-11. The PCP and PPRR are obtained during the first stage of combustion. With the delayed combustion phasing of the first stage, both the PCP and the PPRR are suppressed. Higher reduction rates of PCP and PPRR are observed when the intake oxygen is lower than 17%.
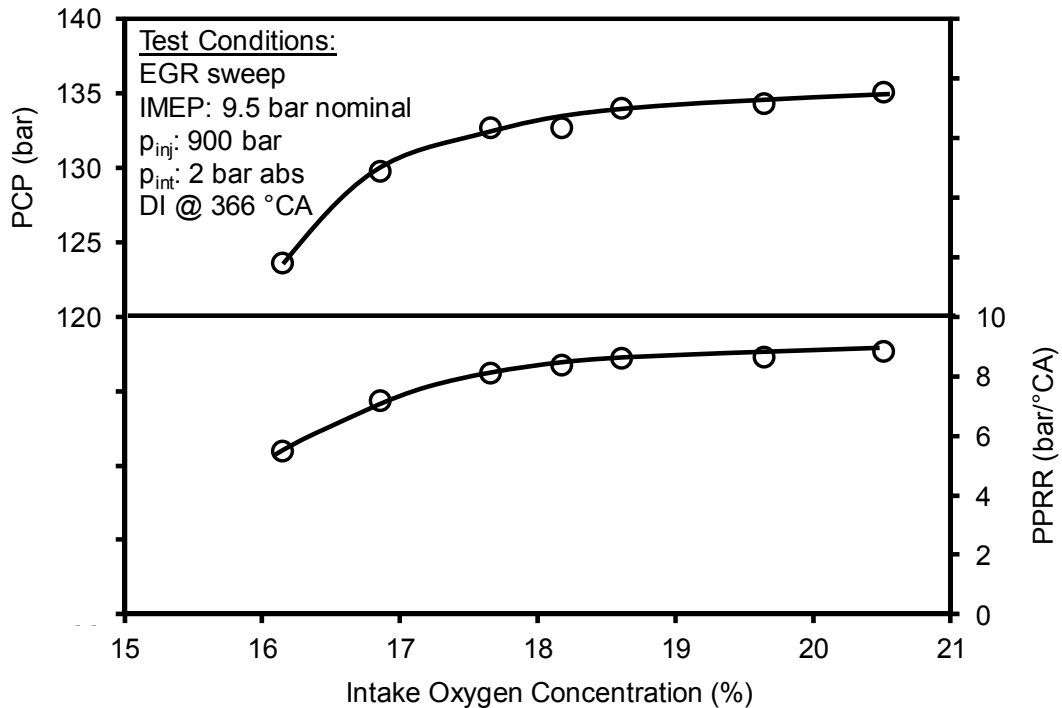
Figure 7-11 N-butanol PFI and DI: PCP and PPRR of an EGR sweep

The NOx and smoke emissions of the EGR sweep are shown in Figure 7-12 denoted by the black markers. The emissions are compared with the ones for the EGR sweep with an earlier DI timing denoted by the yellow markers. The durations of the n-butanol PFI and DI remain constant for both the EGR sweeps. Hence, the characteristics of the first stage of combustion are similar for the two cases. However, when the DI timing is advanced, the phasing of the second stage of combustion is also advanced. The two stages of combustion are closer to each other. The in-cylinder temperature before the n-butanol DI is potentially higher, and thus the ignition delay of the n-butanol DI is reduced. The

reduced mixing duration with an advanced timing of the n-butanol DI increases the smoke emissions when the intake oxygen is lower than 17%. The NOx emissions are also higher with the early DI timing due to the potentially higher combustion temperature.
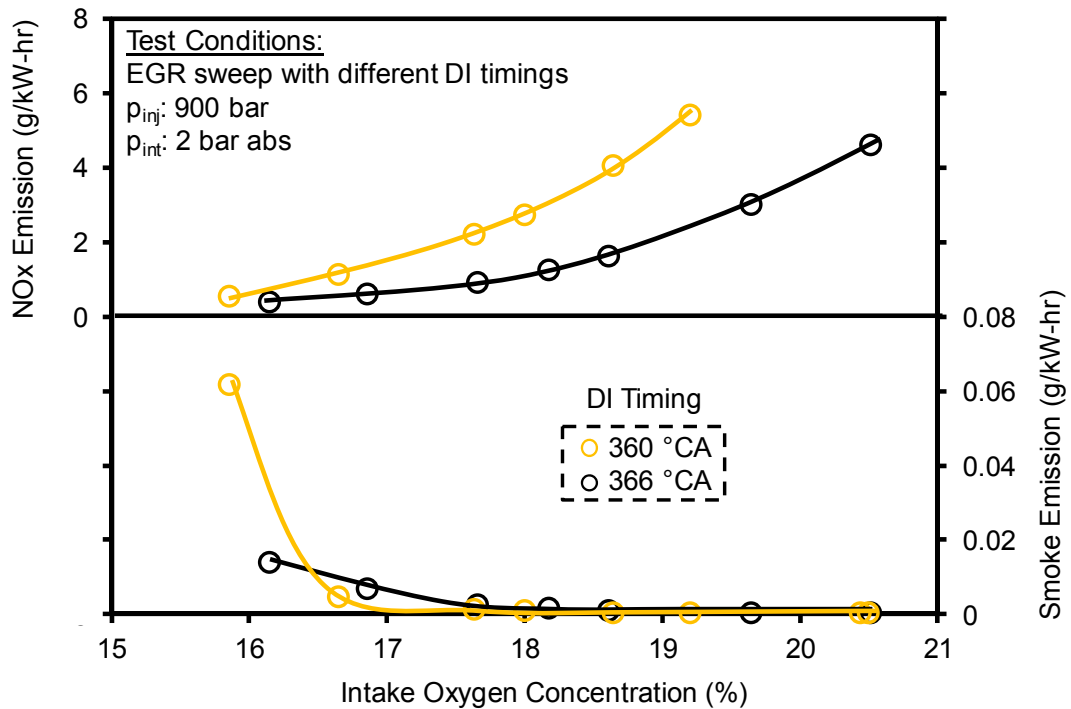
Figure 7-12 N-butanol PFI and DI: NOx and smoke emissions of an EGR sweep

7.2 Butanol Multiple Injections

The combustion with n-butanol single DI in Section 5.2 has shown the low emissions of NOx and smoke. However, the operation range is limited to medium engine load, mainly due to the high PPRR. Although the combustion phasing can be controlled with the DI timing, the late combustion phasing is commonly associated with IMEP losses due to the low fuel reactivity of n-butanol, compared with diesel.

The injection strategy with n-butanol PFI and DI in Section 7.1.2 lacks the direct control over the first stage of combustion. The control of the combustion rate relies on the

indirect impacts from the second stage of combustion and the application of EGR. In this approach, multiple direct injections of n-butanol are used to generate a partially premixed cylinder charge before auto-ignition. A subsequent direct injection is employed after the initial combustion to control the HRR shape and to extend the engine loads. With the multiple direct injections, the control flexibilities on the mixing process and charge reactivity are enhanced. The focus of this subsection is on medium to high engine loads.

The injection timing effects on CA5 and CA50 with a double-injection strategy are shown in Figure 7-13 and Figure 7-14. The test conditions are given in Table 7-2. The injection timings and injection durations shown in the table are command timings and command durations. It is observed that the CA50 is mainly controlled by the second DI timing, while the CA5 is slightly affected by the second DI because of the potential variations in the gas temperature in the previous cycle.
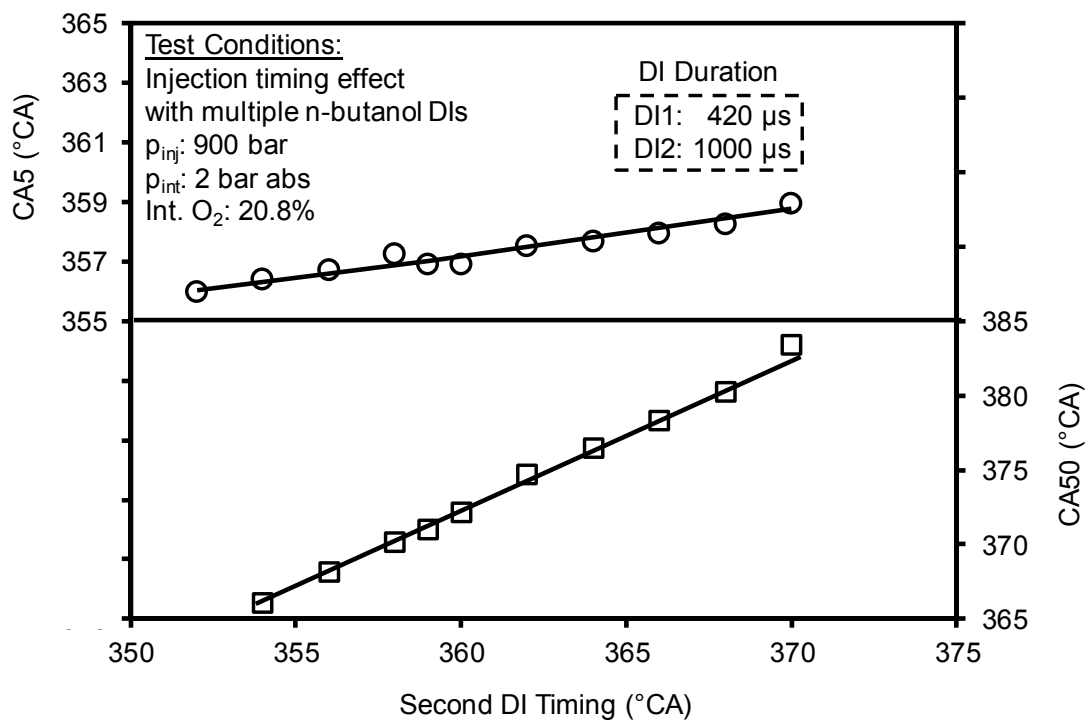
Figure 7-13 N-butanol multiple DIs: CA5 and CA50 of Timing sweep 3

Table 7-2 Test conditions of the injection timing sweeps

Injection Timing Effect on Combustion Characteristics, n-butanol multiple injections Fig. 7-15, Fig. 7-16		
Engine Parameters	Timing Sweep 3	Timing Sweep 4
IMEP (bar)	9.9	10.4
Intake Pressure (bar abs)	2.0	2.0
Intake Temperature (°C)	33.0	33.0
Intake O_2 (%)	20.8	20.8
Injection Pressure (bar)	600	600
First Injection Timing (°CA)	336	**320-350**
First Injection Duration (μs)	420	420
Second Injection Timing (°CA)	**352-370**	359
Second Injection Duration (μs)	1000	1000

With a fixed second direct injection, the CA5 curve appears parabolic when it is plotted against the timing of the first DI. The early CA5 values are achieved with the injection timings in the range from 330 °CA to 340 °CA. The timing of the first DI has a very limited impact on the combustion phasing. This can be attributed to the low percentage of

energy contribution from the first DI, as indicated from the shorter injection duration of 420 μs versus 1000 μs for the second DI. The majority of heat is released from the second DI which is fixed at a constant injection time during the test.

The effects of the ratio between the two injections on HRR are examined at a constant IMEP level. The cylinder pressure and HRR curves are shown in Figure 7-15. The injection timings for the DI injections are fixed. It is observed that the phasing of the first stage of combustion remains in a similar range when the injection duration of the first DI is increased. The higher PCP and PPRR are detected with a longer duration of the first DI.
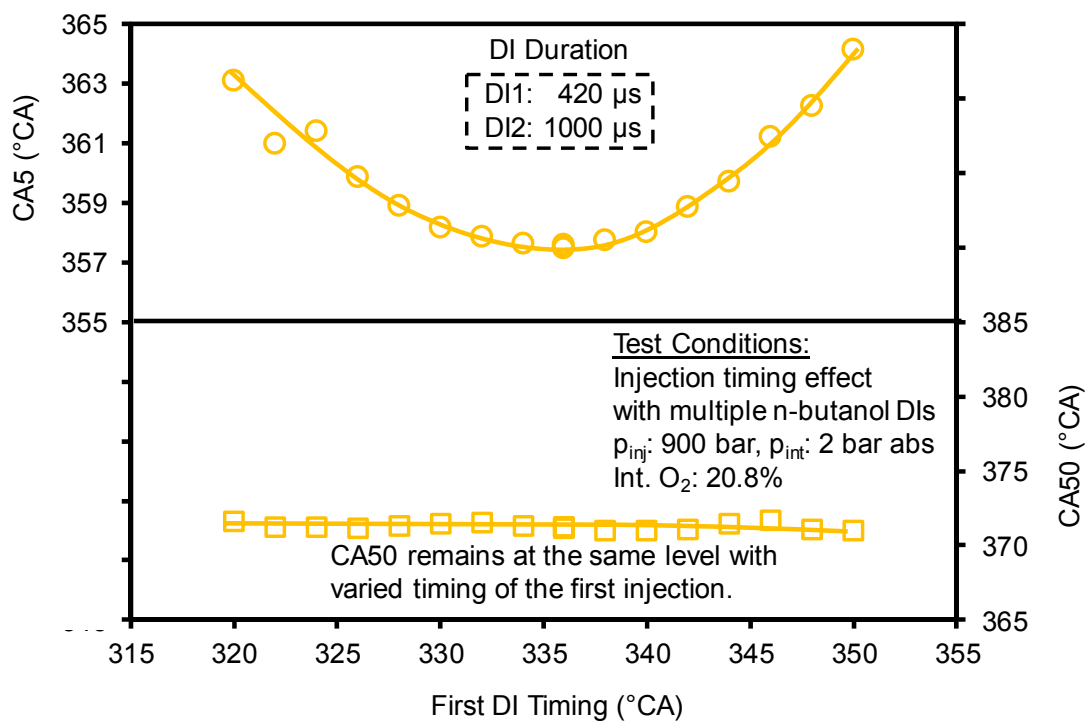
Figure 7-14 N-butanol multiple DIs: CA5 and CA50 of Timing sweep 4
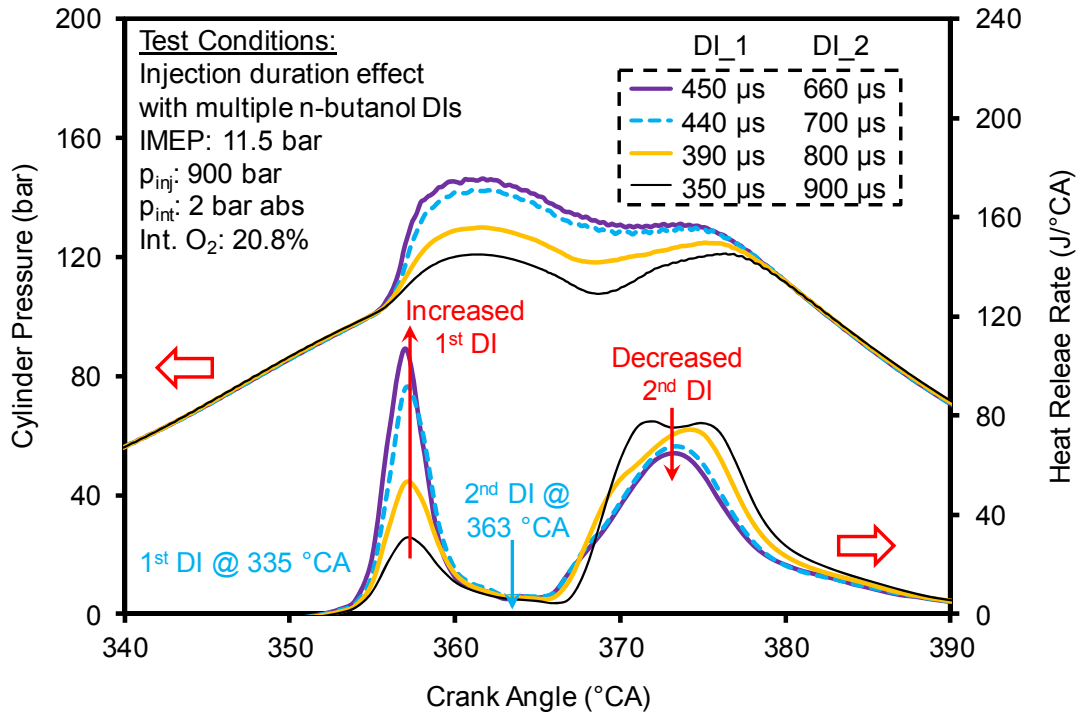
Figure 7-15 N-butanol multiple DIs: cylinder pressure and HRR

Based on the analysis in Figure 7-13, Figure 7-14, and Figure 7-15, the timing and the

duration of the first injection can be employed to control the SOC, PCP, and PPRR, while

the timing and the duration of the second DI are effective to control the combustion

phasing. The SOC and PPRR are coupled in the combustion of n-butanol single DI, as

discussed in Section 5.2.2. In stark contrast, the SOC and PPRR can be regulated

independently with the modulation of the timings and duration of the two direct

injections of n-butanol. According to the observations in Section 7.1.2, the second stage

of combustion is the main source for the NOx and smoke emissions. The separation

between the two combustion events is a critical factor to determine the emissions of NOx

and smoke.

The injection timings of the two direct injections are fixed at 336 °CA and 359 °CA, to

fix an initial separation of the two combustion events. The injection durations are also

maintained for the two injections when the EGR rate is changed. The emissions of NOx and smoke in this EGR sweep are shown in Figure 7-16. A trade-off between NOx and smoke emissions is observed with the EGR application. When the intake oxygen level is lower than 17%, the NOx emissions are lower than 0.2 g/kW-hr, while the smoke emissions are slightly higher than 0.01 g/kW-hr. Further decrease of the intake oxygen increases the smoke emissions.
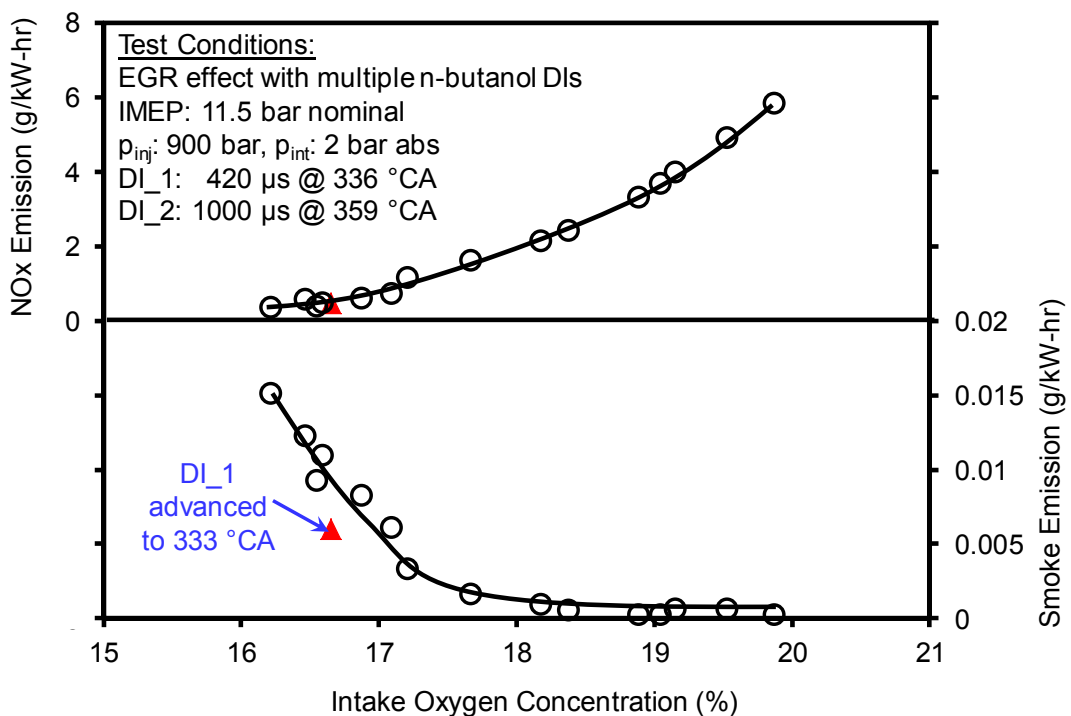
Figure 7-16 N-butanol multiple DIs: NOx and smoke emissions

An early injection timing of the first DI (denoted with the red marker in Figure 7-16) is used to increase the separation duration between the two combustion events. It is observed that the smoke emissions are reduced by approximately 50%, compared with the one with the later DI timing. The NOx emissions remain at a similar level. With the control of the first DI timing, the mixing process of this injection is regulated. The SOC and the in-cylinder temperature before the second stage of combustion are thereafter

controlled. Hence, the mixing of the second DI and the emission formation during the second stage of combustion can be controlled. Nevertheless, it should be noted that this DI advancement might not be the most optimal operating condition.

An example of a high engine load achieved with two direct injections of n-butanol is given in Figure 7-17. An IMEP of 14 bar is obtained with an increased injection duration of the second DI. The duration and timing of the first injection remain at similar levels due to the limitations of PCP and PPRR. The majority of energy is released in the second stage of combustion occurred in the early expansion stroke. A clear diffusion-dominated HRR curve is observed for the second stage of combustion. Low emissions of smoke, CO, and THC but high emissions of NOx are detected. The emission trade-off between NOx and smoke is primarily caused by the high temperature combustion in the second stage with a high intake oxygen concentration (20.8%).
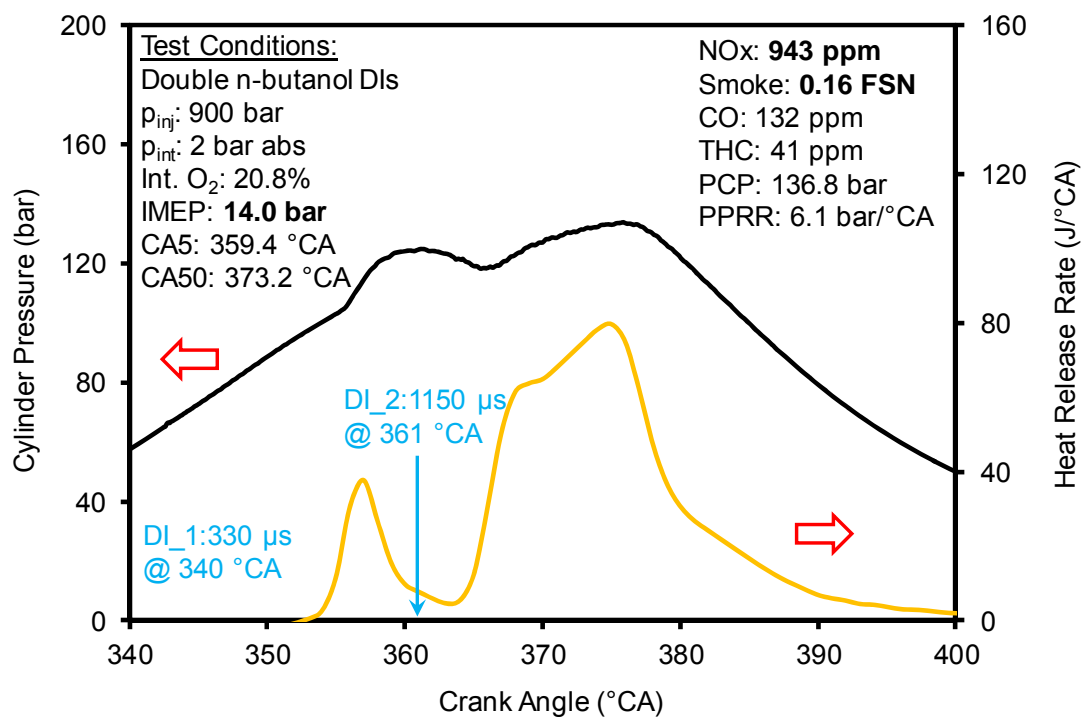
Figure 7-17 N-butanol multiple DIs: cylinder pressure and HRR

The engine load can be further extended to a higher level by using a longer duration of second DI and adding post injections. However, the mixing of the second injection with longer injection duration and the mixing of the post injections are even worse than the combustion in Figure 7-17. High emissions of NOx and smoke would be formed due to the insufficient mixing of the second injection. The high emissions of partially oxidized products, high exhaust temperature, and delayed combustion phasing would reduce the combustion efficiency and thermal efficiency. The high emissions of NOx and smoke are the main challenge for the high load clean combustion enabled with n-butanol multiple injections.

In order to tackle the challenge of NOx and smoke emissions, the mixing process for the second direct injection needs to be optimized. Hence, the injection duration of the second DI should be limited for sufficient mixing. The first stage of combustion has to be increased to maintain the high engine load. Then the challenge shifts to the control of PCP and PPRR of the initial combustion. A lower engine compression ratio produces lower motoring PCP and PPRR. Moreover, the lower compression temperature can potentially lower the combustion temperature after the initial combustion. The lower combustion temperature is also beneficial for a better mixing of the second direct injection after the first stage of combustion.

A strategy of n-butanol multiple DI injections is thereafter explored on the SCRE platform to benefit from the relatively lower compression ratio. The cylinder pressure and HRR curves of a high load operation are shown in Figure 7-18. The net IMEP is 14 bar with three direct injections of n-butanol. The HRR curve still displays the typical two-stage combustion. However, because of the lower compression ratio and larger engine

displacement, a relatively more combustion energy can be released at the first stage. Therefore, two early injections are combined to generate the first stage of combustion. The first injection is used to form a lean premixed charge, while the second injection is employed to trigger the ignition. A relatively short duration of the third injection is added after the first stage of combustion to raise the engine load. Because of the significantly reduced second stage of combustion, the smoke emissions are suppressed at a higher EGR rate. When the intake oxygen is lowered to 14.4%, the NOx emissions are drastically suppressed, while the smoke emissions still remain at a relatively low level.
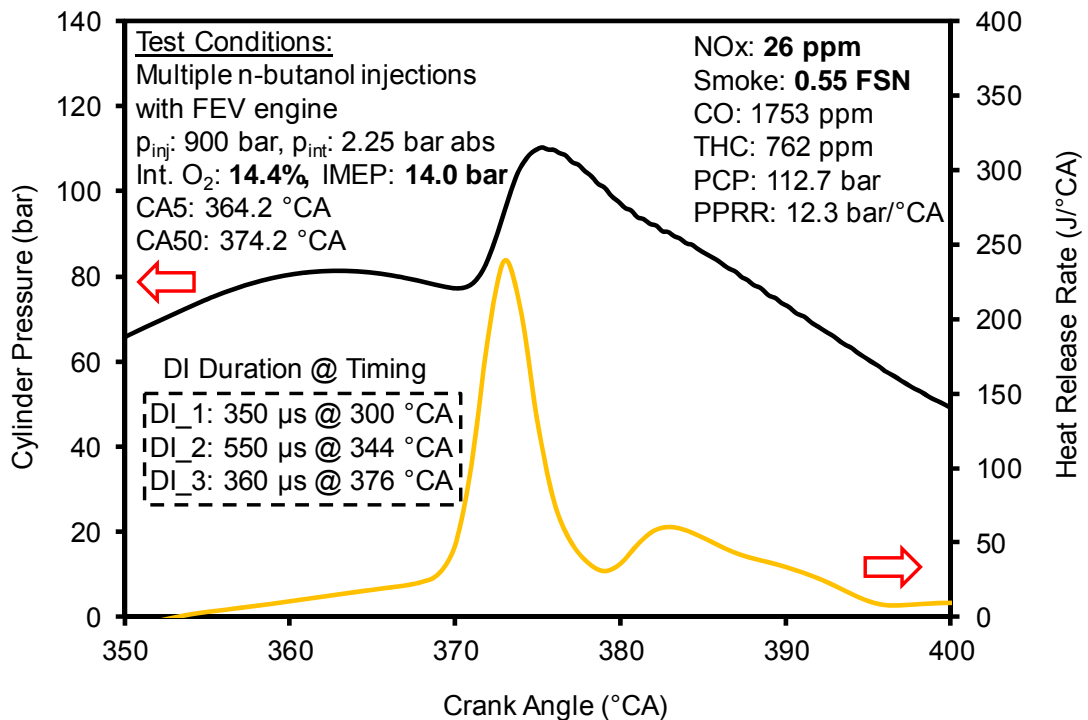
Figure 7-18 N-butanol multiple injections: cylinder pressure and HRR

7.3 Summary

The work reported in this chapter can be summarized as follows:

Ethanol port injection with butanol direct injection:

- The port delivered ethanol can be ignited with double n-butanol injections. A single injection of n-butanol was insufficient for ignition due to closely coupled IMEP with PPRR.

- The CA5 was marginally affected by the injection timing of the first DI, but the mixing process of the first DI was controlled by the injection timing of the first DI. Therefore, the ignition delay of the first DI was used to control the combustion rate in the first stage of combustion.

- The second n-butanol direct injection increased the engine load and the combustion temperature. The high combustion temperature transferred to the following engine cycle and secured the ignition in the cycle. The second injection also had an effective control on the combustion phasing.

- An IMEP of 16 bar was achieved with this combustion strategy. The NOx emission is 454 ppm, and smoke emission is 0.18 FSN, without the application of EGR.

Butanol port injection with butanol direct injection:

- Port injection of n-butanol was used to initiate HCCI type of combustion. The addition of n-butanol DI was used to extend the engine load.

- The ratio between the port injection fuel and direct injection fuel was an effective parameter to control the shape of heat release rate, and thus the peak cylinder pressure (PCP) and peak pressure rise rate (PPRR).

- The emissions of NOx and smoke were mainly generated from the second stage of combustion. The separation between the two stages of combustion was critical for low NOx and smoke emissions.

Multiple direct injections of butanol:

- The strategy with multiple injections of n-butanol was implemented to improve the control of the mixing process. With varied injection scheduling, the in-cylinder fuel distribution and fuel reactivity can be actively modulated in accordance with the requirements at different engine conditions, such as generating a relatively rich local mixture for ignition.

- The two-stage combustion was detected with the n-butanol multiple injections. The control approach was similar to the combustion with n-butanol PFI. The separation between the two stages of combustion was again identified to be critical for low NOx and smoke emissions.

- An engine load of 14 bar IMEP was demonstrated on the SCRE engine platform with NOx emission of 26 ppm and smoke emission of 0.55 FSN. This ultra-clean combustion was achieved with triple fuel injections and approximately 14% intake oxygen concentration.

CHAPTER VIII

CONCLUSIONS AND FUTURE WORK

Empirical investigations on the impacts of mixing and charge reactivity have been conducted using diesel, ethanol, and n-butanol with the objective of clean and efficient combustion in CI engines. The conclusions and the recommendations are presented as follows.

8.1 Mixing Control with Direct Fuel Injection

The mixing process of the fuel and air was enhanced with the n-butanol direct injection in a heterogeneous in-cylinder charge, compared with the baseline results with the diesel direct injection. The empirical observations and analysis are summarized as follows:

- The trade-off between NOx and smoke emissions in diesel combustion was primarily attributed to the insufficient mixing of the in-cylinder charge and the diffusion-dominated burning of the fuel. Varied injection timings, different injection pressures, and the application of EGR had limited effects to prolong the ignition delay due to the low volatility and high reactivity of diesel, at the confined test conditions.

- The mixing process of the in-cylinder charge was enhanced with the n-butanol high pressure direct injection, indicated by the longer ignition delay (higher than 3 ms) compared with the one of diesel (lower than 1 ms). The combustion exhibited simultaneously low emissions of NOx and smoke at low to medium engine load.

- The peak pressure rise rate was increased in the n-butanol combustion due to the high combustion rate with improved homogeneity, which limited the engine load

to moderate levels. The application of EGR was effective to regulate the combustion rate. However, the combustion phasing and CO emissions were also sensitive to the EGR rate.

• The ignition of the n-butanol DI was more demanding than the diesel DI due to the relatively low fuel reactivity and the over-mixed in-cylinder charge. A higher intake pressure was used to enhance the ignition ability. With the lower compression ratio in the SCRE engine, a higher intake temperature was essential to compensate the lower compression temperature for consistent ignition, under the confined testing condition.

8.2 Reactivity Modulation in Premixed Charge

The port fuel injections of ethanol and butanol were employed to generate the premixed in-cylinder mixture, while the direct injection of diesel was applied to modulate the charge reactivity. Under the confined empirical conditions, the results are summarized as follows:

In the combustion with ethanol port fuel injection:

• The diesel injection timing controls the start of combustion and combustion phasing.

• The PFI fuel ratio was critical for the combustion with ethanol port fuel injection. A longer ignition delay was detected at a higher PFI fuel ratio. This effect became more significant at lower charge reactivity (with a lower intake pressure and a higher EGR rate), when the diesel injection timing is fixed close to TDC.

• The combustion with a higher PFI fuel ratio generated lower emissions of NOx and smoke, compared with the combustion with a lower PFI fuel ratio at similar

engine operating conditions. The premixed combustion was enhanced by the increase in ethanol and the reduction in diesel.

- A high EGR rate and a high ethanol ratio were found to be essential to regulate the emissions of NOx and smoke to below the emission standards. However, the charge reactivity with these conditions was excessively low to effectively oxidize THC and CO, and thus the combustion efficiency reduces.

- Diesel micro-pilot injections were employed to improve the reactivity of the premixed ethanol charge. The oxidizations of CO and THC were considerably enhanced while the ultra-low NOx and smoke emissions can be maintained with the application of EGR.

In the combustion with n-butanol port fuel injection:

- The HCCI combustion enabled with port injection of n-butanol was demonstrated in the PUMA engine. The control of intake pressure was an effective method to regulate the SOC in the HCCI combustion with n-butanol. However, the high intake pressure was associated with the high PCP and PPRR. The application of EGR delayed the SOC, and reduced the PCP and PPRR. The impact of EGR was more significant at a lower intake pressure.

- In the combustion with n-butanol PFI and diesel DI, a higher n-butanol ratio increased the portion of premixed combustion and was beneficial for low NOx emissions. The smoke emissions remained at an ultra-low level without EGR, while the smoke emissions increased significantly with EGR. The diffusion-dominated diesel burning in the second stage contributed the majority of the smoke emissions.

8.3 Partially Premixed Combustion with Alcohol Fuels

The partially premixed combustion with ethanol and n-butanol was formulated with accordance to the observations in the mixing and reactivity control with different fuel delivery methods assisted with intake boosting and EGR. The significant findings are concluded as follows:

Ethanol port injection with butanol direct injection:

- The port delivered ethanol was ignited with two direct injections of n-butanol. A single injection of n-butanol was insufficient for ignition due to closely coupled IMEP with PPRR.

- The CA5 was marginally affected by the injection timing of the first DI, but the mixing process of the first DI was controlled by the injection timing of the first DI. Therefore, the ignition delay of the first DI was regulated to control the combustion rate in the first stage of combustion.

- The second n-butanol direct injection increased the engine load and the combustion temperature. The high combustion temperature was transferred to the following engine cycle to secure the ignition in the cycle. The second injection also had an effective control on the combustion phasing.

- An IMEP of 16 bar was achieved with this combustion strategy. The NOx emission was 454 ppm, and smoke emission was 0.18 FSN, without the application of EGR.

Butanol port injection with butanol direct injection:

- Port injection of n-butanol was used to initiate HCCI type of combustion. The addition of n-butanol DI was used to extend the engine load.

- The ratio between the port injection fuel and direct injection fuel was an effective parameter to control the shape of heat release rate, and thus the peak cylinder pressure and peak pressure rise rate.

- The emissions of NOx and smoke were mainly generated from the second stage of combustion. The separation between the two stages of combustion was critical for low NOx and smoke emissions.

Multiple direct injections of butanol:

- The strategy with multiple injections of n-butanol was implemented to improve the control of the mixing process. With varied injection scheduling, the in-cylinder fuel distribution and fuel reactivity were actively modulated in accordance with the requirements at different engine conditions.

- The two-stage combustion was observed with the n-butanol multiple injections. The control approach was similar to the combustion with n-butanol PFI. The separation between the two stages of combustion was identified to be critical for low NOx and smoke emissions.

- An engine load of 14 bar IMEP was demonstrated on the SCRE engine platform with NOx emission of 26 ppm and smoke emission of 0.55 FSN. This ultra-clean combustion was achieved with triple fuel injections and approximately 14% intake oxygen concentration.

8.4 Butanol High Pressure Injection

The n-butanol high pressure fuel injection was characterized with the EFS injection bench and the Bosch type long-tube bench at various injection conditions. High speed camera and laser PDA were also employed for the optical measurement of the fuel spray. This study provided an essential guidance for understanding the combustion performance with n-butanol high pressure injection. The observations are summarized as follows:

- The volumetric injection rate of n-butanol was similar to that of diesel at the same injection duration and injection pressure.

- The injection opening delays with n-butanol were at the same level as the ones with diesel, while the injection closing delays were slightly longer, evaluated over various injection pressures and injection durations.

- The dwell time between multiple DI injections was important for the total injection volume and injection rate. Closely scheduled injection events tended to merge into a single event, and the injection volume may increase drastically.

- The macro n-butanol spray had similar penetration and cone angle as the one with diesel. The close-to-nozzle droplets had the velocity of approximately 330 m/s detected by PDA. The diameters of the droplets were primarily in a range from 10 μm to 20 μm.

8.5 Future Work

The following recommendations are for the future work:

- The fuel injector could be optimized for the application of early and small fuel pilots. For example, the spray umbrella angle could be narrowed to reduce the

166

wall impingement for the early injections; the nozzle-hole diameter could be reduced to enhance the repeatability of small pilots. With the improved injector hardware, the diesel micro-pilot strategy would extend its applicable load range.

- The SCRE platform with a lower compression ratio has shown some promising results. However, it could be possible to further improve the combustion with the engine hardware refinements, such as different compression ratios and piston bowl geometries, variable valve timing, and intake air management.

- Advanced optical investigations are recommended to reveal the in-cylinder interaction between the fuel spray and the environment (*e.g.* background gas composition, temperature, and the combustion chamber geometry). The detailed injection and combustion processes may provide some more insights on the process of emission formation, compared with the heat release analysis.

- The control of charge stratification is critical to maintain the required reactivity for ignition, especially at a high intake pressure level. The with-in-the-cycle ignition feedback and injection control could be beneficial to reduce the misfire possibility and improve the smoothness of engine operation.

- The n-butanol direct injection with ethanol or butanol port injection would be further explored on the SCRE engine platform with carefully designed fuel ratios and injection scheduling. The impact of injection pressure with the n-butanol fuel should be further studied.

REFERENCES

1. UNECE, "Diesel Engine Exhausts: Myths and Realities, Discussion Paper," Report, United Nations Economic Commission for Europe, New York and Geneva, 2014.

2. Pedersen, P., "The Effect of Exhaust Gas Recirculation (EGR) on The Emission from a Lean-Bum Gas Engine," Project Report, 1998.

3. Hiroyasu, H. and Arai, M., "Structures of Fuel Sprays in Diesel Engines," SAE Technical Paper 900475, 1990, doi:10.4271/900475.

4. Chevron, "Diesel Fuel Technical Review," https://www.chevron.com/-/media/chevron/operations/documents/diesel-fuel-tech-review.pdf, cited on November 9th, 2016.

5. ASTM D975, "Standard Specification for Diesel Fuel Oils," https://compass.astm.org/download/D975.40016.pdf, cited on November 9th, 2016.

6. Heywood, J., "Internal Combustion Engine Fundamentals," New York: McGraw-Hill, 1988.

7. US EPA, "Emission Standards Reference Guide for On-road and Nonroad Vehicles and Engines," https://www.epa.gov/emission-standards-reference-guide, cited on November 9th, 2016.

8. US EPA, "Technical Bulletin, Nitrogen Oxides (NOx), Why and How They Are Controlled," EPA 456/F-99-006R, November 1999.

9. Mellor, A., Mello, J., Duffy, K., Easley, W. et al., "Skeletal Mechanism for NOx Chemistry in Diesel Engines," SAE Technical Paper 981450, 1998, doi:10.4271/981450.

10. US EPA, "Overview of Greenhouse Gases," https://www.epa.gov/ghgemissions/overview-greenhouse-gases#nitrous-oxide, Cited on November 14th, 2016.

11. Idicheria, C. and Pickett, L., "Soot Formation in Diesel Combustion under High-EGR Conditions," SAE Technical Paper 2005-01-3834, 2005, doi:10.4271/2005-01-3834.77.

12. Wang, Y., Yao, M., Li, T., Zhang, W., et al., "A Parametric Study for Enabling Reactivity Controlled Compression Ignition (RCCI) Operation in Diesel Engines at Various Engine Loads," Applied Energy 175 (2016) 389–402, https://doi.org/10.1016/j.apenergy.2016.04.095.

13. Kodavasal, J., Lavoie, G., Assanis, D., Martz, J., "Reaction-space Analysis of Homogeneous Charge Compression Ignition Combustion with Varying Levels of Fuel Stratification Under Positive and Negative Valve Overlap Conditions," International J of Engine Research, 2016, Vol. 17(7) 776–794, DOI: 10.1177/1468087415613208.

14. Splitter, D., Reitz, R., "Fuel Reactivity Effects on the Efficiency and Operational Window of Dual-Fuel Compression Ignition Engines," Fuel 118 (2014) 163–175, http://dx.doi.org/10.1016/j.fuel.2013.10.045.

15. Omae, K., Watanabe, Y., Matsushita, S., and Sakata, I., "Reduction of HC Emission for Passenger Car Diesel Engine," SAE Technical Paper 2007-01-0663, 2007, doi:10.4271/2007-01-0663.

16. Lu, X., Han, D., and Huang, Z., "Fuel Design and Management for The Control of Advanced Compression-Ignition Combustion Modes," Progress in Energy and Combustion Science 37 (2011) 741-783, doi:10.1016/j.pecs.2011.03.003.

17. Bosch Auto Parts, "PFI (Port Fuel Injection)," https://www.boschautoparts.com/en/auto/fuel-injectors/port-fuel-injection, cited on November 14th, 2016.

18. Wissink, M. and Reitz, R., "Direct Dual Fuel Stratification, a Path to Combine the Benefits of RCCI and PPC," SAE Int. J. Engines 8(2):878-889, 2015, doi:10.4271/2015-01-0856.

19. Aroonsrisopon, T., Werner, P., Waldman, J., Sohm, V. et al., "Expanding the HCCI Operation With the Charge Stratification," SAE Technical Paper 2004-01-1756, 2004, doi:10.4271/2004-01-1756.

20. Sjöberg, M., Edling, L., Eliassen, T., Magnusson, L. et al., "GDI HCCI: Effects of Injection Timing and Air Swirl on Fuel Stratification, Combustion and Emissions Formation," SAE Technical Paper 2002-01-0106, 2002, doi:10.4271/2002-01-0106.

21. Su, H., Mosbach, S., Kraft, M., Bhave, A. et al., "Two-stage Fuel Direct Injection in a Diesel Fuelled HCCI Engine," SAE Technical Paper 2007-01-1880, 2007, doi:10.4271/2007-01-1880.

22. Hwang, W., Dec, J., and Sjöberg, M., "Fuel Stratification for Low-Load HCCI Combustion: Performance & Fuel-PLIF Measurements," SAE Technical Paper 2007-01-4130, 2007, doi:10.4271/2007-01-4130.

23. Bakker, P., De Abreu Goes, J., Somers, L., and Johansson, B., "Characterization of Low Load PPC Operation using RON70 Fuels," SAE Technical Paper 2014-01-1304, 2014, doi:10.4271/2014-01-1304.

24. Splitter, D., Hanson, R., Kokjohn, S., Wissink, M. et al., "Injection Effects in Low Load RCCI Dual-Fuel Combustion," SAE Technical Paper 2011-24-0047, 2011, doi:10.4271/2011-24-0047.

25. Tong, L., Wang, H., Zheng, Z., Reitz, R., et al., "Experimental Study of RCCI Combustion and Load Extension in a Compression Ignition Engine Fueled with Gasoline and PODE," Fuel 181 (2016) 878–886, http://dx.doi.org/10.1016/j.fuel.2016.05.037.

26. Bergin, M., Reitz, R., Rutland, C., Dempsey, A. et al., "Load Limit Extension in Pre-Mixed Compression Ignition Using a 2-Zone Combustion System," SAE Int. J. Engines 8(2):903-920, 2015, doi:10.4271/2015-01-0860.

27. Sjöberg, M. and Dec, J., "Smoothing HCCI Heat-Release Rates Using Partial Fuel Stratification with Two-Stage Ignition Fuels," SAE Technical Paper 2006-01-0629, 2006, doi:10.4271/2006-01-0629.

28. Dec, J., "A Conceptual Model of DI Diesel Combustion Based on Laser-Sheet Imaging," SAE Technical Paper 970873, 1997, doi:10.4271/970873.

29. Dec, J., "Advanced Compression-Ignition Engines—Understanding the In-Cylinder Processes," Proceedings of the Combustion Institute 32 (2009) 2727–2742, doi:10.1016/j.proci.2008.08.008.

30. Kamimoto, T. and Bae, M., "High Combustion Temperature for the Reduction of Particulate in Diesel Engines," SAE Technical Paper 880423, 1988, doi:10.4271/880423.

31. Kumar, R. and Zheng, M., "Fuel Efficiency Improvements of Low Temperature Combustion Diesel Engines," SAE Technical Paper 2008-01-0841, 2008, doi:10.4271/2008-01-0841.

32. Asad, U., Han, X., and Zheng, M., "An Empirical Study to Extend Engine Load in Diesel Low Temperature Combustion," SAE Int. J. Engines 5(3):709-717, 2012, doi:10.4271/2011-01-1814.

33. Kokjohn, S., Hanson, R., Splitter, D., and Reitz, R., "Experiments and Modeling of Dual-Fuel HCCI and PCCI Combustion Using In-Cylinder Fuel Blending," SAE Int. J. Engines 2(2):24-39, 2010, doi:10.4271/2009-01-2647.

34. Olsson, J., Tunestål, P., Haraldsson, G., and Johansson, B., "A Turbo Charged Dual Fuel HCCI Engine," SAE Technical Paper 2001-01-1896, 2001, doi:10.4271/2001-01-1896.

35. Dec, J., Yang, Y., and Dronniou, N., "Boosted HCCI - Controlling Pressure-Rise Rates for Performance Improvements using Partial Fuel Stratification with Conventional Gasoline," SAE Int. J. Engines 4(1):1169-1189, 2011, doi:10.4271/2011-01-0897.

36. Han, X., Zheng, M., and Wang, J., "Fuel Suitability for Low Temperature Combustion in Compression Ignition Engines", Fuel 109 (2013) 336–349, doi:10.1016/j.fuel.2013.01.049.

37. Gao, T., Divekar, P., Asad, U., and Han, X. et al, "An Enabling Study of Low Temperature Combustion with Ethanol in A Diesel Engine," Journal of Energy Resources Technology, Vol. 135/042203-1, 2013, doi:10.1115/1.4024027.

38. Busch, S., Zha, K., Miles, P., Warey, A. et al., "Experimental and Numerical Investigations of Close-Coupled Pilot Injections to Reduce Combustion Noise in a Small-Bore Diesel Engine," SAE Int. J. Engines 8(2):2015, doi:10.4271/2015-01-0796.

39.   Knox, B., Franze, M., and Genzale, C., "Diesel Spray Rate-of-momentum Measurement Uncertainties and Diagnostic Considerations," ICEF2014-5566, ICEF2014, October 19-22, 2014, Columbus, IN, USA.

40.   Montajir, R., Tsunemoto, H., Ishitani, H., and Minami, T., "Fuel Spray Behavior in a Small DI Diesel Engine: Effect of Combustion Chamber Geometry," SAE Technical Paper 2000-01-0946, 2000, doi:10.4271/2000-01-0946.

41.   Payri, F., Payri, R., Salvador, F., and Gimeno, J., "Influence of Nozzle Geometry on Spray Characteristics in Non-evaporative and Evaporative Conditions," SAE Technical Paper 2007-24-0023, 2007, doi:10.4271/2007-24-0023.

42.   Siebers, D., "Liquid-Phase Fuel Penetration in Diesel Sprays," SAE Technical Paper 980809, 1998, doi:10.4271/980809.

43.   Hiroyasu, H. and Arai, M., "Structures of Fuel Sprays in Diesel Engines," SAE Technical Paper 900475, 1990, doi:10.4271/900475.

44.   Koo, J. and Martin, J., "Droplet Sizes and Velocities in a Transient Diesel Fuel Spray," SAE Technical Paper 900397, 1990, doi:10.4271/900397.

45.   Bosch, W., "The Fuel Rate Indicator: A New Measuring Instrument For Display of the Characteristics of Individual Injection," SAE Technical Paper 660749, 1966, doi:10.4271/660749.

46.   Desantes, J., Payri, R., Salvador, F., and Gimeno, J., "Prediction of Spray Penetration by Means of Spray Momentum Flux," SAE Technical Paper 2006-01-1387, 2006, doi:10.4271/2006-01-1387.

47.   de Ojeda, W., Bulicz, T., Han, X., Zheng, M. et al., "Impact of Fuel Properties on Diesel Low Temperature Combustion," SAE Int. J. Engines 4(1):188-201, 2011, doi:10.4271/2011-01-0329.

48. Lu, X., Shen, Y., Zhang, Y., Zhou, X., et al. "Controlled Three-stage Heat Release of Stratified Charge Compression Ignition (SCCI) Combustion with a Two-Stage Primary Reference Fuel Supply," Fuel 90 (2011) 2026–2038, doi:10.1016/j.fuel.2011.01.026.

49. Alptekin, E., "Emission, Injection and Combustion Characteristics of Biodiesel and Oxygenated Fuel Blends in a Common Rail Diesel Engine," Energy 119 (2017) 44-52, http://dx.doi.org/10.1016/j.energy.2016.12.069.

50. Sjoberg, M., Dec, J., "Comparing Late-cycle Autoignition Stability for Single- and Two-Stage Ignition Fuels in HCCI Engines," Proceedings of the Combustion Institute 31 (2007) 2895–2902, doi:10.1016/j.proci.2006.08.010.

51. Zheng, M., Li, T., Han, X., "Direct Injection of Neat N-Butanol for Enabling Clean Low Temperature Combustion in a Modern Diesel Engine," Fuel 142 (2015) 28–37, http://dx.doi.org/10.1016/j.fuel.2014.10.075.

52. McTaggart-Cowan, G., Rogak, S., Munshi, S., Hill., P., et al. "The Influence of Fuel Composition on a Heavy-Duty, Natural-Gas Direct-Injection Engine," Fuel 89 (2010) 752–759, doi:10.1016/j.fuel.2009.10.007.

53. McTaggart-Cowan, G., Bushe, W., Hill, P., Munshi, S., "A Supercharged Heavy Duty Diesel Single-Cylinder Research Engine for High-Pressure Direct Injection of Natural Gas," International Journal of Engine Research Vol 4, Issue 4, pp. 315 - 330, doi: 10.1243/146808703322743912.

54. Wissink, M. and Reitz, R., "Exploring the Role of Reactivity Gradients in Direct Dual Fuel Stratification," SAE Int. J. Engines 9(2):1036-1048, 2016, doi:10.4271/2016-01-0774.

55. Dec, J., "Advanced Compression-Ignition Engines—Understanding the In-Cylinder Processes," Proceedings of the Combustion Institute 32 (2009) 2727–2742, doi:10.1016/j.proci.2008.08.008.

56. Zhu, J., Kuti, O., and Nishida, K., "Effects of Injection Pressure and Ambient Gas Density on Fuel - Ambient Gas Mixing and Combustion Characteristics of D.I. Diesel Spray," SAE Technical Paper 2011-01-1819, 2011, doi:10.4271/2011-01-1819.

57. Han, S. and Bae, C., "The Influence of Fuel Injection Pressure and Intake Pressure on Conventional and Low Temperature Diesel Combustion," SAE Technical Paper 2012-01-1721, 2012, doi:10.4271/2012-01-1721.

58. Gao, T., Reader, G., Tjong, J., and Zheng, M., "Energy Efficiency Comparison between Butanol and Ethanol Combustion with Diesel Ignition," SAE Technical Paper 2015-01-0859, 2015, doi:10.4271/2015-01-0859.

59. Sjöberg, M., Zeng, W., Singleton, D., Sanders, J. et al., "Combined Effects of Multi-Pulse Transient Plasma Ignition and Intake Heating on Lean Limits of Well-Mixed E85 DISI Engine Operation," SAE Int. J. Engines 7(4):1781-1801, 2014, doi:10.4271/2014-01-2615.

60. Zheng, M., Reader, G., Hawley, G., "Diesel Engine Exhaust Gas Recirculation—a Review on Advanced and Novel Concepts," Energy Conversion and Management 45 (2004) 883–900, doi:10.1016/S0196-8904(03)00194-8.

61. Sjoberg, M., Dec, J., "Effects of EGR and Its Constituents on HCCI Autoignition of Ethanol," Proceedings of the Combustion Institute 33 (2011) 3031–3038, doi:10.1016/j.proci.2010.06.043.

62. Gao, T., Divekar, P., Asad, U., Han, X., et al. "An Enabling Study of Low Temperature Combustion with Ethanol in A Diesel Engine", Journal of Energy Resources Technology, Vol. 135/042203-1, 2013, doi:10.1115/1.4024027.

63. Asad, U., Tjong, J., Zheng, M., "Exhaust Gas Recirculation – Zero Dimensional Modelling and Characterization for Transient Diesel Combustion Control," Energy Conversion and Management 86 (2014) 309–324, http://dx.doi.org/10.1016/j.enconman.2014.05.035.

64. Agarwal, A., Ravishankar, S., and Arvind, R., "Hardware and Combustion Optimization Strategy to Reduce Engine Out Emissions for BS V Limits," SAE Technical Paper 2015-26-0018, 2015, doi:10.4271/2015-26-0018.

65. Kitabatake, R., Shimazaki, N., and Nishimura, T., "Expansion of Premixed Compression Ignition Combustion Region by Supercharging Operation and Lower Compression Ratio Piston," SAE Technical Paper 2007-01-3614, 2007, doi:10.4271/2007-01-3614.

66. Hanson, R., Curran, S., Wagner, R., Kokjohn, S. et al., "Piston Bowl Optimization for RCCI Combustion in a Light-Duty Multi-Cylinder Engine," SAE Int. J. Engines 5(2):286-299, 2012, doi:10.4271/2012-01-0380.

67. de Ojeda, W., Zoldak, P., Espinosa, R., and Kumar, R., "Development of a Fuel Injection Strategy for Diesel LTC," SAE Technical Paper 2008-01-0057, 2008, doi:10.4271/2008-01-0057.

68. Henein, N., Bhattacharyya, A., Schipper, J., and Bryzik, W., "Combustion and Emission Characteristics of a Small-Bore HSDI Diesel Engine in the Conventional and LTC Combustion Regimes," SAE Technical Paper 2005-24-045, 2005, doi:10.4271/2005-24-045.

69. Musculus, M., Miles, P., Pickett, L., "Conceptual Models for Partially Premixed Low-Temperature Diesel Combustion," Progress in Energy and Combustion Science 39 (2013) 246-283, http://dx.doi.org/10.1016/j.pecs.2012.09.001.

70. Johnson, T., "Diesel Emission Control - Last 12 Months in Review," SAE Technical Paper 2000-01-2817, 2000, doi:10.4271/2000-01-2817.

71. Kumar, R., "Modeling, Control, and Implementation of Enhanced Premixed Combustion in Diesel Engines," Phd Dissertation, 2008, University of Windsor (Canada).

72. Kimura, S., Aoki, O., Ogawa, H., Muranaka, S. et al., "New Combustion Concept for Ultra-Clean and High-Efficiency Small DI Diesel Engines," SAE Technical Paper 1999-01-3681, 1999, doi:10.4271/1999-01-3681.

73. Hasegawa, R. and Yanagihara, H., "HCCI Combustion in DI Diesel Engine," SAE Technical Paper 2003-01-0745, 2003, doi:10.4271/2003-01-0745.

74. Takeda, Y., Keiichi, N., and Keiichi, N., "Emission Characteristics of Premixed Lean Diesel Combustion with Extremely Early Staged Fuel Injection," SAE Technical Paper 961163, 1996, doi:10.4271/961163.

75. Yokota, H., Kudo, Y., Nakajima, H., Kakegawa, T. et al., "A New Concept for Low Emission Diesel Combustion," SAE Technical Paper 970891, 1997, doi:10.4271/970891.

76. Aoyama, T., Hattori, Y., Mizuta, J., and Sato, Y., "An Experimental Study on Premixed-Charge Compression Ignition Gasoline Engine," SAE Technical Paper 960081, 1996, doi:10.4271/960081.

177

77.   Onishi, S., Jo, S., Shoda, K., Jo, P. et al., "Active Thermo-Atmosphere Combustion (ATAC) - A New Combustion Process for Internal Combustion Engines," SAE Technical Paper 790501, 1979, doi:10.4271/790501.

78.   Ryan, T. and Matheaus, A., "Fuel Requirements for HCCI Engine Operation," SAE Technical Paper 2003-01-1813, 2003, doi:10.4271/2003-01-1813.

79.   Hashimoto, K., "Effect of Ethanol on the HCCI Combustion," SAE Technical Paper 2007-01-2038, 2007, doi:10.4271/2007-01-2038.

80.   Tanaka, H., Somezawa, S., Sako, T., Sakai, Y. et al., "Fuel Design Concept for Robust Ignition in HCCI Engine and Its Application to Optimize Methane-Based Blend," SAE Int. J. Engines 7(2):807-819, 2014, doi:10.4271/2014-01-1286.

81.   Andreae, M., Cheng, W., Kenney, T., and Yang, J., "On HCCI Engine Knock," SAE Technical Paper 2007-01-1858, 2007, doi:10.4271/2007-01-1858.

82.   Inagaki, K., Fuyuto, T., Nishikawa, K., Nakakita, K. et al., "Dual-Fuel PCI Combustion Controlled by In-Cylinder Stratification of Ignitability," SAE Technical Paper 2006-01-0028, 2006, doi:10.4271/2006-01-0028.

83.   Klos, D., Janecek, D., and Kokjohn, S., "Investigation of the Combustion Instability-NOx Tradeoff in a Dual Fuel Reactivity Controlled Compression Ignition (RCCI) Engine," SAE Int. J. Engines 8(2):821-830, 2015, doi:10.4271/2015-01-0841.

84.   Li, J., Yang, W., Zhou, D., "Review on the Management of RCCI Engines," Renewable and Sustainable Energy Reviews 69 (2017) 65–79, http://dx.doi.org/10.1016/j.rser.2016.11.159.

85.   Ingesson, G., Yin, L., Johansson, R., Tunestål, P., "A Double-Injection Control Strategy For Partially Premixed Combustion," IFAC-PapersOnLine, Volume 49, Issue 11, 2016, Pages 353-360, doi: 10.1016/j.ifacol.2016.08.053.

86.   Kalghatgi, G., Hildingsson, L., Harrison, A., Johansson, B., "Autoignition Quality of Gasoline Fuels in Partially Premixed Combustion in Diesel Engines," Proceedings of the Combustion Institute, Volume 33, Issue 2, 2011, Pages 3015-3021, doi:10.1016/j.proci.2010.07.007.

87.   Manente, V., Johansson, B., and Tunestal, P., "Partially Premixed Combustion at High Load using Gasoline and Ethanol, a Comparison with Diesel," SAE Technical Paper 2009-01-0944, 2009, doi:10.4271/2009-01-0944.

88.   Noehre, C., Andersson, M., Johansson, B., and Hultqvist, A., "Characterization of Partially Premixed Combustion," SAE Technical Paper 2006-01-3412, 2006, doi:10.4271/2006-01-3412.

89.   Gao, T., "Implementation and Preliminary Study of Low Temperature Combustion with Assorted Biofuels in a Ford Diesel Engine," Thesis of M. Sc., 2012, University of Windsor (Canada).

90.   Asad, U., Kumar, J., Han, X., Zheng, M., "Precise Instrumentation of A Diesel Single-Cylinder Research Engine," Measurement 44 (2011) 1261–1278, doi:10.1016/j.measurement.2011.03.028

91.   Bosch, W., "The Fuel Rate Indicator: A New Measuring Instrument for Display of The Characteristics of Individual Injection," SAE Tech paper, 660749; 1966.

92.   User's Manual, "Stabilite 2017, Ion Laser," http://www.spectra-physics.com/assets/client_files/files/documents/service/user-manuals/2017%20User%20Manual.pdf, cited on January 20th, 2017.

93. "Diesel Fuel Properties Data Sheet For Research Grade Diesel", Clean Diesel Engine Lab Internal Database.

94. Tat, M., Gerpen, J., "Measurement of Biodiesel Speed of Sound and Its Impact on Injection Timing," Final Report, Report 4 in a series of 6, February 2003, NREL/SR-510-31462, National Renewable Energy Laboratory.

95. Romani, L., "Temperature Dependence of Densities and Speeds of Sound of Nitromethane + Butanol Isomers in the Range (188.15 - 308.15) K," J.Chem.Eng.Data 46 (2001) 312-316.

96. Tojo, J., "Thermodynamic Properties of the Ternary Mixture Acetone + Methanol + Ethanol at 298.15 K," J.Chem.Eng.Data 43 (1998) 776-780.

97. Lapuerta, M., Contreras, R., Fernadez, J., Dorado, M., "Stability, Lubricity, Viscosity, and Cold-Flow Properties of Alcohol-Diesel Blends," Energy Fuels 2010, 24, 4497–4502 : DOI:10.1021/ef100498u.

98. Sigma-Alorich, "1-Butanol, HPLC grade", http://www.sigmaaldrich.com/catalog/product/sigald/34867?lang=en&region=CA, Cited on June 15th, 2017.

99. Sigma-Alorich, " Ethyl alcohol, Pure, Anhydrous", http://www.sigmaaldrich.com/catalog/product/sial/459836?lang=en&region=CA, Cited on June 15th, 2017.

100. Gao, T., Xie, K., Yu, S., Han, X., Wang, M., Zheng, M., "Characterization of N-Butanol High Pressure Injection From Modern Common Rail Injection System," ICEF2015-1129, ICEF, November 8-11, 2015, Houston, TX, USA.

101. Gao, T., Jeftic, M., Bryden, G., Reader, G. et al., "Heat Release Analysis of Clean Combustion with Ethanol Ignited by Diesel in a High Compression Ratio Engine," SAE Technical Paper 2016-01-0766, 2016, doi:10.4271/2016-01-0766.

102. Wu, Y., Reitz, R., "Effects of EGR And Boost Pressure on Reactivity Controlled Compression Ignition (RCCI) Engine at High Load Operating Conditions," ICEF2014-5485, Proceedings of the ASME 2014 Internal Combustion Engine Division Fall Technical Conference, ICEF2014, October 19-22, 2014, Columbus, IN, USA.

103. Asad, U., Kumar, R., Han, X., Zheng, M., "Precise Instrumentation of a Diesel Single-Cylinder Research Engine," Measurement 44 (2011) 1261–1278, doi:10.1016/j.measurement.2011.03.028.

104. Zheng, M., Tan, Y., Mulenga, M., and Wang, M., "Thermal Efficiency Analyses of Diesel Low Temperature Combustion Cycles," SAE Technical Paper 2007-01-4019, 2007, doi:10.4271/2007-01-4019.

105. DieselNet, "Diesel Fuel Injection," https://www.dieselnet.com/tech/diesel_fi.php, Cited on June 15th, 2017.

106. Gao, T., "Progress Report to Clean Diesel Engine Lab," 2013-09-06.

107. The Engineering Toolbox, "Fuels and Chemicals - Auto Ignition Temperatures," http://www.engineeringtoolbox.com/fuels-ignition-temperatures-d_171.html, Cited on July 20th, 2017.

APPENDICES

APPENDIX A

Image Processing for Injector Opening/Closing Delay

A LabVIEW program is developed to process the large quantity of images from the high speed imaging test for injector opening/closing delay detection. The critical steps in the image processing are the image enhancement and the interested region definition in the image. The image enhancement is the process which converted the image to black and white according to a predefined threshold. The threshold value selection is critical to eliminate the image noise, maintain the useful information as well, and is highly dependent on the illumination status when the images are captured. A universal threshold for all data sets is often not feasible. The selection required a trail run for each set of images to find a reasonable value.

The image interested region definition is a process to choose a region on the image to count the plume quantity of the sprays. As shown in Figure A-1, an annulus band is selected as the image interested region. The inner circle of the annulus is the projection circle of all the nozzle holes. The width of the annulus is 3 pixels. The plume quantity inside the annulus is the detection parameter used for identifying the images for injector opening and closing. The image processing is demonstrated in Figure A-2. In the calculations in this paper, the first image in which the plume quantity increases from 0 to more than 4 in the annular region is identified as the injector opening image, while the first image in which the plume quantity reduced from 8 to less than 4 is identified as the

182

injector closing image. By comparing the time step of these images to the injection command, the injector opening and closing delay can be calculated.
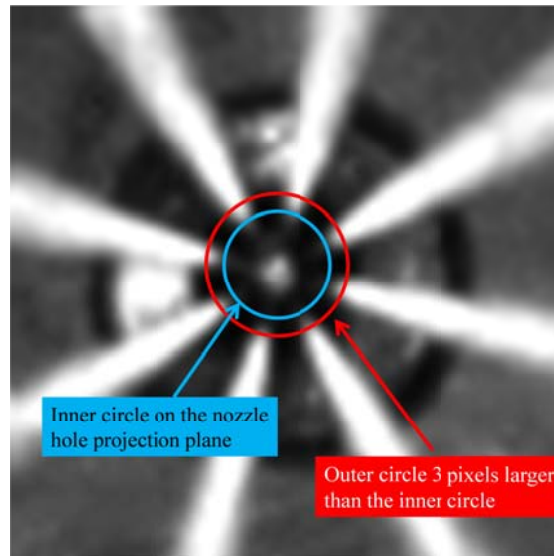

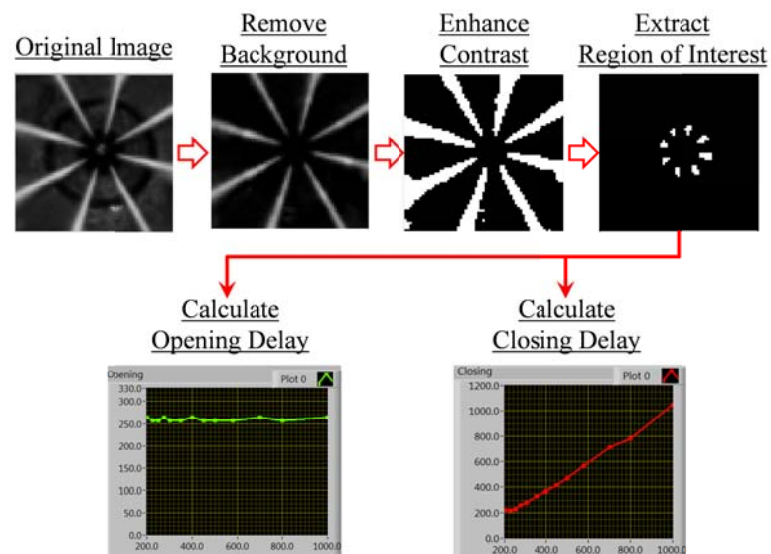Figure A-1 Illustration of the image interested range definition

Figure A-2 Image processing for injector opening and closing

APPENDIX B

Gas Supply System for Constant Volume Chamber

The gas supply system of the constant volume chamber is demonstrated in Figure B-1. In the preliminary state, three gases are used for the chamber test, which are compressed air, methane (CH_4), and N_2. Two pneumatic valves are used for the gas inlet and outlet, which can be operated remotely with solenoid valves. A check valve is installed in the intake gas line to prevent gas backflow. Several pressure and temperature sensors are used to monitor the chamber internal pressure and temperature. A rupture disc set to burst at 68 bar is used to prevent the possible high pressure causing optical damages.
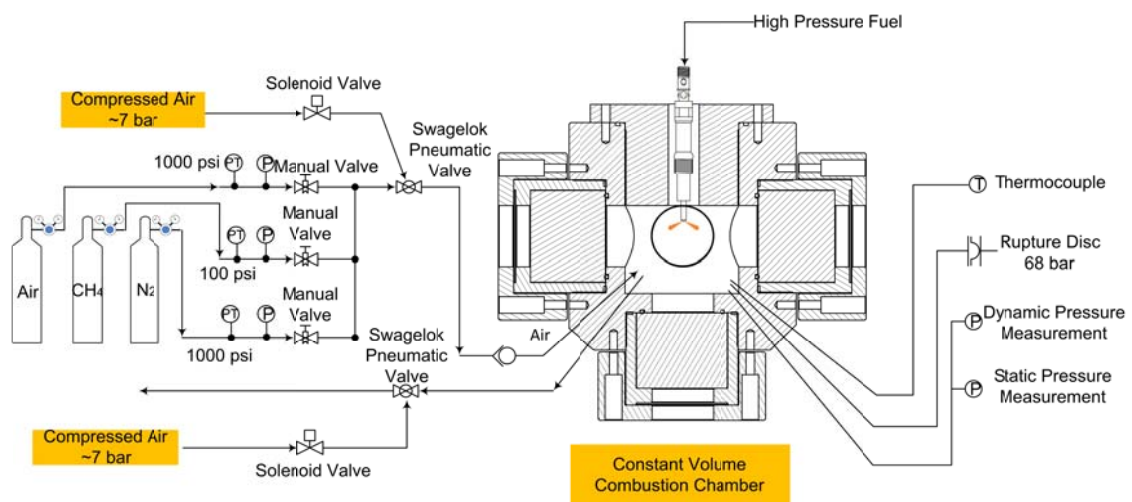

Figure B-1 Gas supply system of the constant volume chamber

APPENDIX C

Injection Volume with Varied Dwell Time

The supplemental data and analysis for sub-Section 4.4.2 are provided in APPENDIX C. The injection rate profile with relatively long dwell time is shown in Figure C-1. The repeatability of the first injection is high that the injection rate overlaps on each other. The variation of the second injection is mainly due to rail pressure fluctuation caused by the first injection.
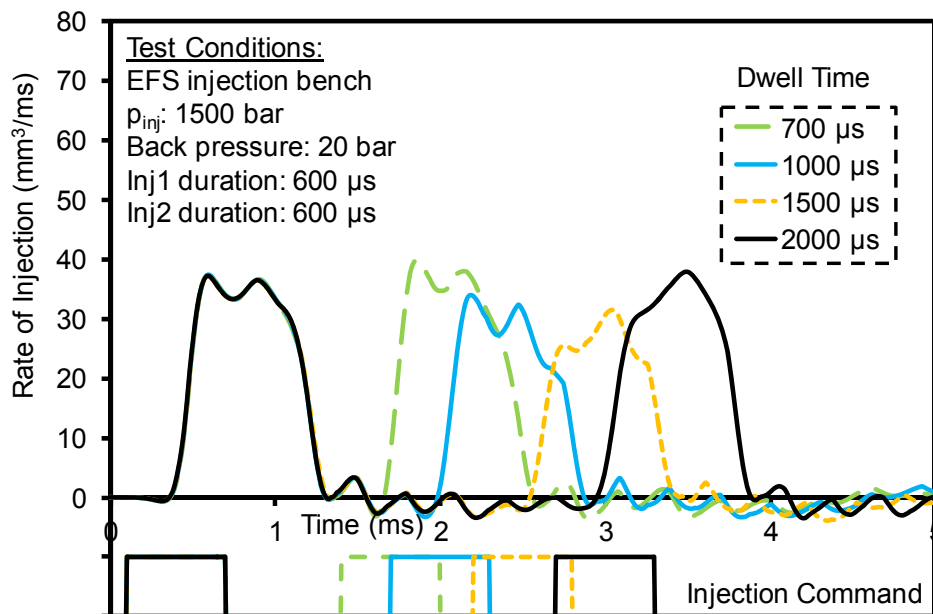
Figure C-1 Injection rate profile with relatively long dwell time

185

APPENDIX D

Diesel Injection Rate Measurement

D.1 Injection Duration Effect

The injection volumes of different injection durations are measured with the EFS injection bench at different injection pressures, as shown in Figure D-1. The fuel injector delivers more fuel at a higher injection pressure with the same injection command duration, as expected. The fuel injector operated at a higher injection pressure also requires a shorter commanded duration to deliver the same amount of fuel. For example, to supply 40 mm^3 of fuel which is equivalent to about 11 bar indicated mean effective pressure (IMEP) in the Ford PUMA engine, requires the injection command to be approximately 1050 μs for 1500 bar injection pressure, and about 1700 μs for 600 bar injection pressure.
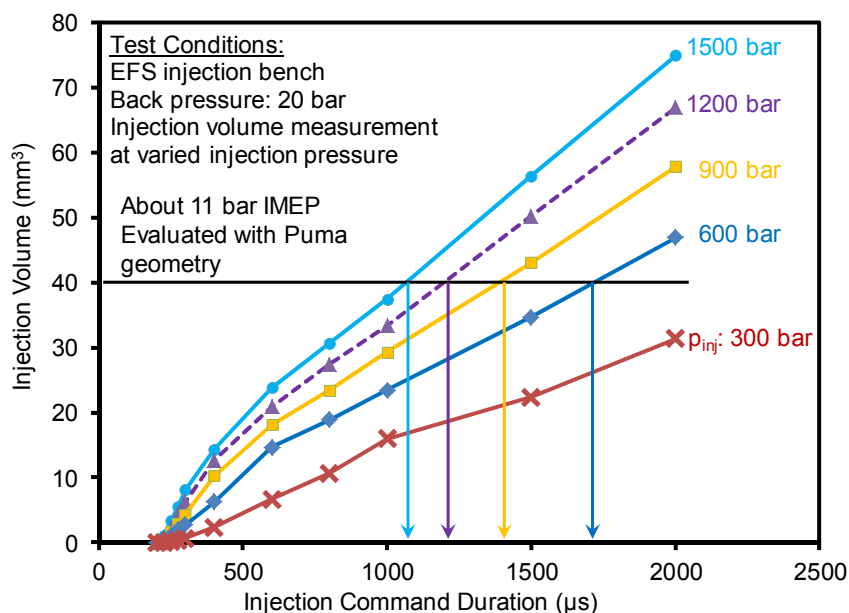
Figure D-1 Injection volumes at varied injection pressures

The use of too long injection duration is often disadvantageous in CI engines. First of all, it is challenging to prevent the potential wall impingement which tends to reduce the combustion efficiency and dilute lubrication oil. It is also demanding, *e.g.* requiring more EGR to withhold the combustion, to separate the combustion event from the injection event, which is critical for certain advanced combustion modes (*e.g.* partially premixed combustion [85]). Therefore, the increase of injection pressure is potentially beneficial to improve combustion efficiency, enhance the performance of combustion control, and extend engine operational load.

D.2 Injection Timing Effect

The injection timing is supposed to have a minimal effect on the fuel injection amount if the pressure remained constant in the fuel rail. An example of injection timing sweep is conducted with the EFS injection bench. The injection volumes and the selected rail pressures are shown in Figure D-2. The injection volume shows a negligible difference at varied injection timings. The primary reason is the consistent rail pressure before the injection event. However, a significantly increased variation in rail pressure is detected after the injection event. This pressure fluctuation is compensated with the dynamic close-loop control of the rail pressure before the next injection event. The injection frequency used is 10 Hz, which is equal to the injection frequency of 1200 revolution per minute (rpm) with a single injection per cycle. If a higher injection frequency is employed or multiple injections are used, the rail pressure fluctuation may affect the actual injection amount. The impacts of multiple fuel injections have been discussed in details in Section 4.3.

187

The EFS injection bench test condition is slightly different from the actual engine conditions. The background pressure of the injector is constant in the EFS injection bench, rather than varied with different crank angles as in engines. However, the variations in the pressure difference are still in a negligible range (< 2%) owing to the high fuel injection pressure. Therefore, the injection timing effect analyzed with EFS injection bench is relevant to the actual conditions in CI engines.
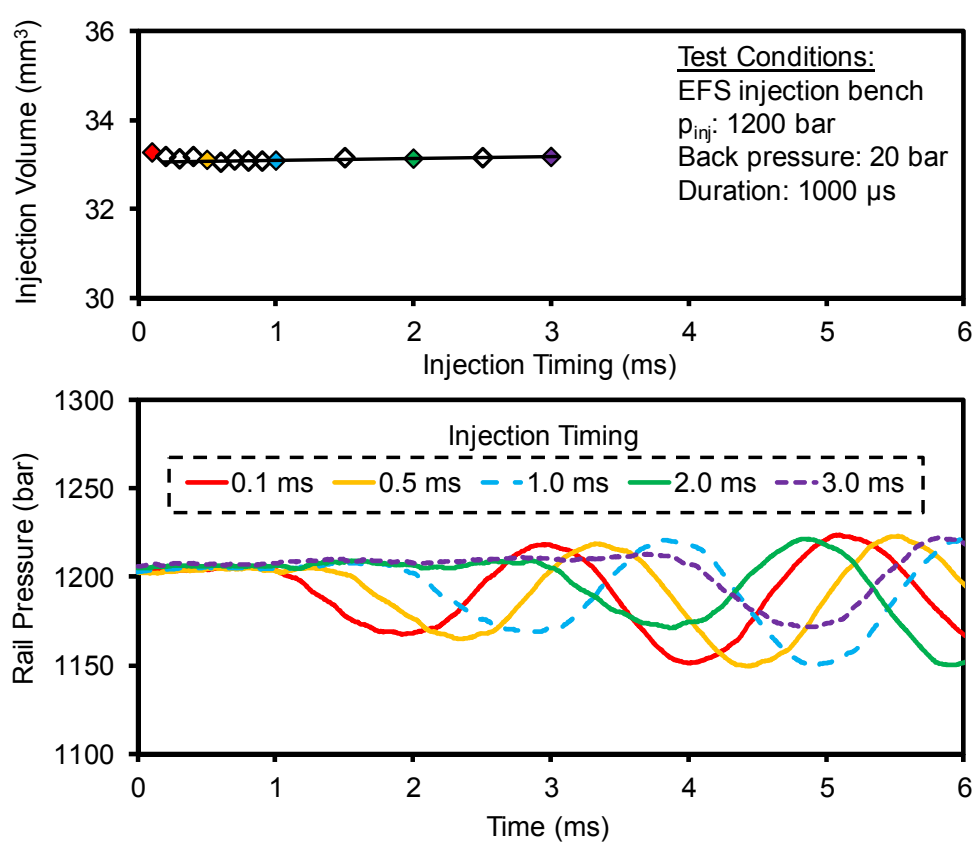

Figure D-2 Injection volumes at varied injection timings

APPENDIX E

Emission Comparison between Engine Platforms

A series of EGR sweeps are conducted with the SCRE to compare the results to that with the PUMA engine platform. The test conditions are similar to the ones in Figure 6-12. The NOx emissions with different PFI fuel ratios are demonstrated in Figure E-1. The trend line of the NOx emissions (Figure 6-12) from the PUMA platform is shown as a dashed line in the figure for comparison. Lower NOx emissions are observed at lower intake oxygen levels, which is consistent with the trend from the PUMA platform. There are no distinct differences between the varied PFI fuel ratios. The NOx emissions from the SCRE platform are generally higher than the ones from PUMA at a similar intake oxygen concentration. With the increased PFI fuel ratio, the overall homogeneity is considerably enhanced (increased ethanol PFI, reduced diesel DI). However, the ignition of the premixed ethanol still relies on the diesel injection that is not uniformly distributed over the entire cylinder.
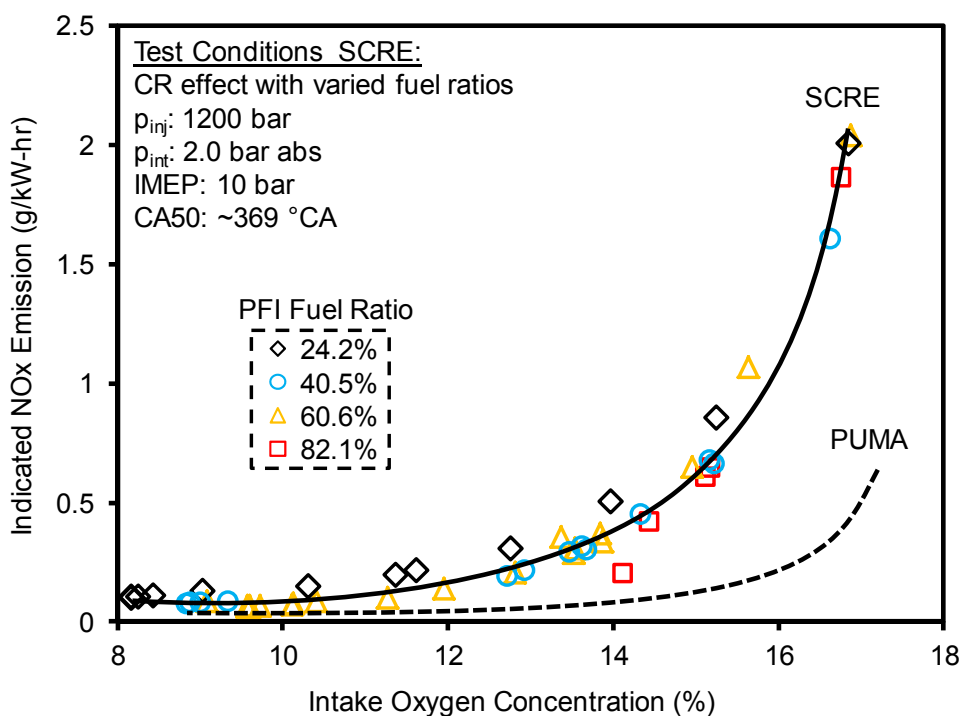
Figure E-1 Engine platform comparison: NOx emissions

The smoke emissions from the SCRE platform are shown in Figure E-2 for the PFI fuel ratios of 24.2% and 40.5%. As the intake oxygen concentration is decreased, the smoke emissions show similar trends as the ones from the PUMA platform (Figure 6-13) for both the fuel ratios. Lower smoke emissions are detected for the case with a higher fuel ratio at a similar intake oxygen level. The smoke emissions from the SCRE platform are lower than the ones from the PUMA platform at similar fuel ratios. The peak smoke emissions of the SCRE platform are achieved at a lower intake oxygen concentration compared with that from the PUMA platform. This phenomenon may be related to the potentially higher local temperature on the SCRE platform, which requires a lower intake oxygen level to enable the low temperature combustion.
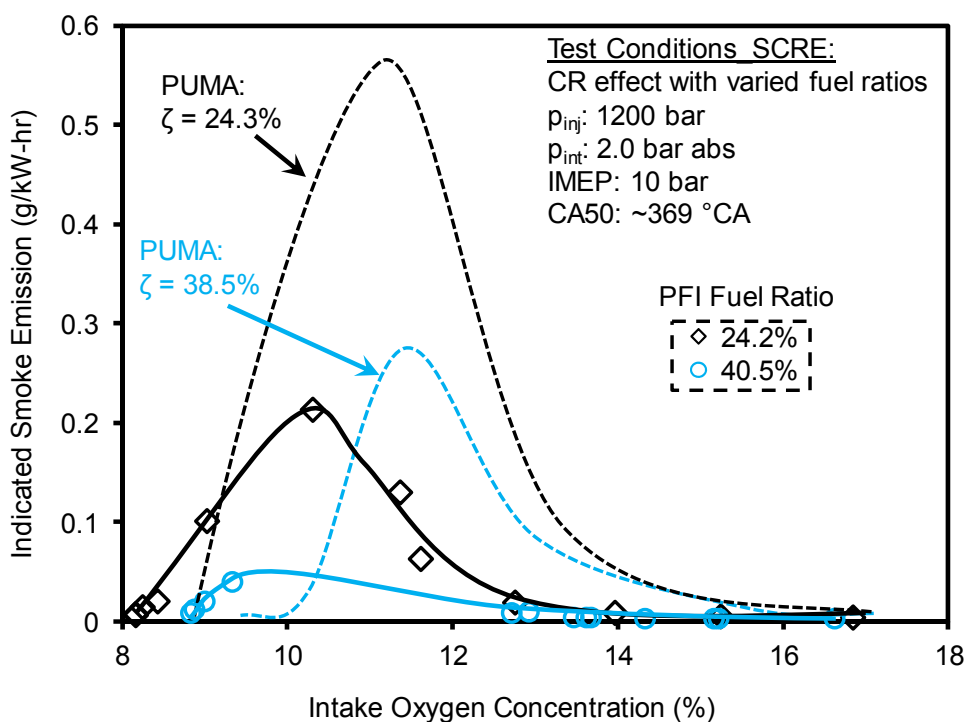
Figure E-2 Engine platform comparison: smoke emissions, part 1

The smoke emissions for the PFI fuel ratios of 60.6% and 82.1% are shown in Figure E-3. The smoke emissions remain at an ultra-low level during the EGR sweep for the two fuel ratios. The trade-off of NOx and smoke emissions is eliminated by the application of ethanol PFI in the SCRE at the two cases with high PFI fuel ratios. Therefore, the EGR rate can be regulated to suppress the emissions of NOx and to control the PPRR, without the concern of the high smoke emissions as in the combustion on the PUMA platform. The smoke emissions at similar fuel ratios from the PUMA platform are also given in this figure as a reference. Even the combustion with a PFI fuel ratio of as high as 79.5% still has relatively high smoke emissions. The results indicate that it may be beneficial to further increase the PFI ratio to reduce the smoke emissions in the PUMA engine. However, for the SCRE, there is only a marginal reduction in the smoke emissions when the PFI fuel ratio is increased from 60.6% to 82.1%.
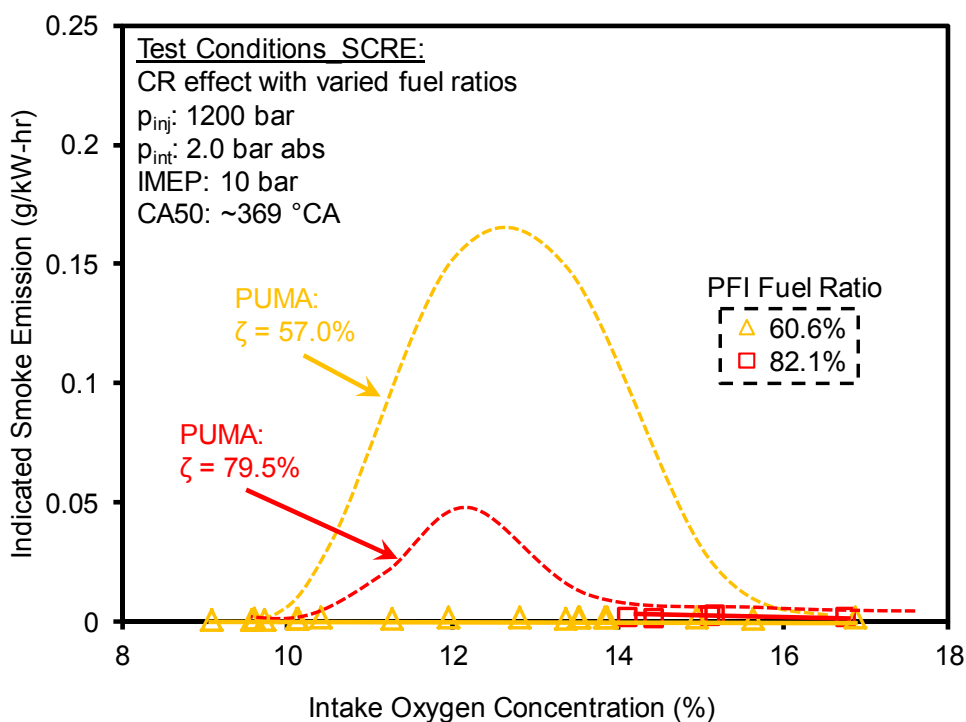
191

Figure E-3 Engine platform comparison: smoke emissions, part 2

The normalized IMEP is shown in Figure E-4 for different fuel ratios. For the two lower fuel ratios (ζ = 24.2% and 40.5%), the normalized IMEP decreases gradually as the intake oxygen is diluted with more EGR. The results from the PUMA platform show a similar trend (Figure 6-14). The reduction in IMEP is an indication of lower indicated thermal efficiency. When EGR is applied to regulate the NOx emissions, the thermal efficiency often reduces. However, when the fuel ratio is further increased to 60.6% and 82.1%, the IMEP remains at a high level (more than 95%) with the reduced intake oxygen concentration. This suggests that the NOx emissions can be suppressed without the penalty of efficiency at these engine conditions. However, the IMEP decreases sharply when the intake oxygen concentration is slightly lower than a threshold. This sharp drop in IMEP is caused by the partial misfire. The combustion phasing is also significantly

192

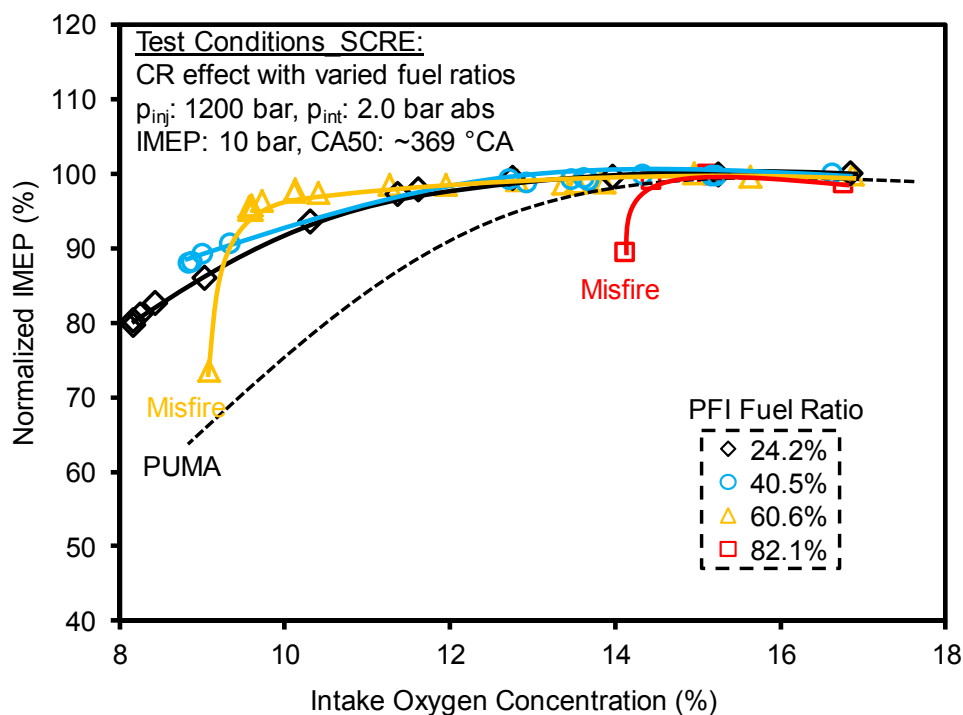retarded at these points, and cannot be maintained constant with the advanced diesel injection timing.

Figure E-4 Engine platform comparison: normalized IMEP

The different impact of EGR on IMEP and the lack of the trade-off between NOx and smoke emissions suggest that the combustion of the high PFI fuel ratio cases on the SCRE platform is similar to the RCCI combustion. The ignition delays of the four fuel ratios are shown in Figure E-5. The ignition delays of the two low fuel ratios (ζ = 24.2% and 40.5%) are in a similar range for both the SCRE platform and PUMA platform. However, the ignition delays of the two high PFI ratios are significantly longer. The longer ignition delay provides more time for the diesel fuel to mix with the premixed ethanol charge. The reactivity of this premixed charge is increased by the diesel injection via in-cylinder blending. The ignition of the mixture is mainly determined by the fuel ratio and the intake oxygen concentration. It is observed that the ignition becomes

unstable when the intake oxygen is lower than 15% for the case of 82.1% PFI fuel ratio. This unstable combustion further reduces the in-cylinder temperature and eventually leads to misfire.
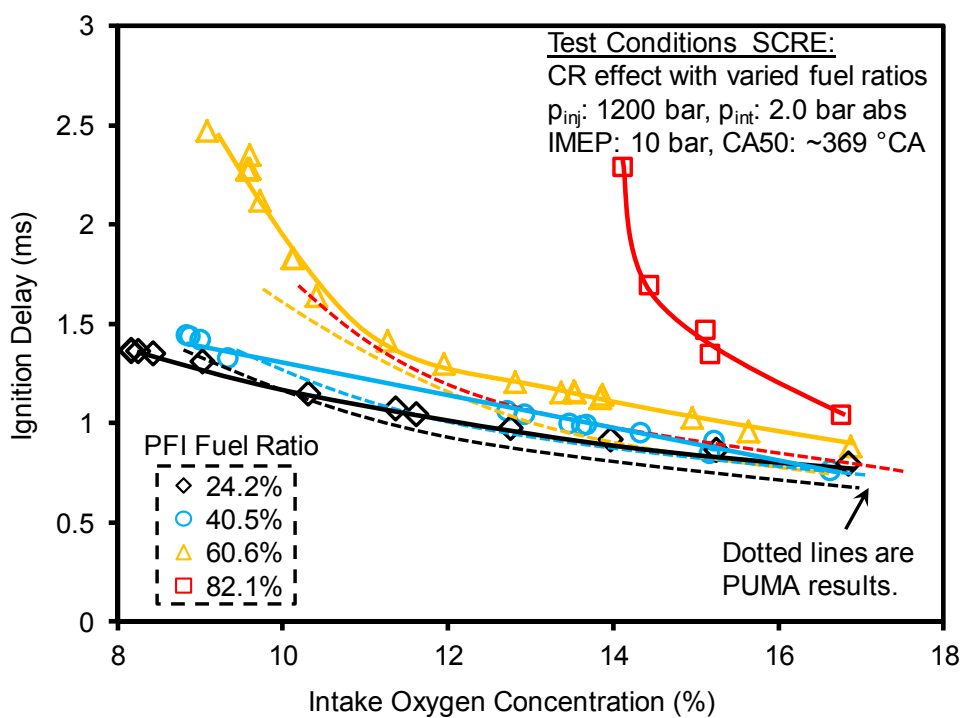

Figure E-5 Engine platform comparison: ignition delay

LIST OF PUBLICATIONS

Refereed Journals:

1. **Tongyang Gao**, Prasad Divekar, Usman Asad, Xiaoye Han, Graham T. Reader, Meiping Wang, Ming Zheng and Jimi Tjong, "An Enabling Study of Low Temperature Combustion with Ethanol in A Diesel Engine," Journal of Energy Resources Technology, Volume 135, Issue 4, 8 pages, 2013.

2. Shui Yu, **Tongyang Gao**, Meiping Wang, Liguang Li, Ming Zheng, "Ignition Control for Liquid Dual-Fuel Combustion in Compression Ignition Engines," Fuel 197 (2017) 583–595.

3. **Tongyang Gao**, Shui Yu, Tie Li, Ming Zheng, "Impact of Multiple Diesel Pilots on Premixed Combustion of Ethanol Fuel," Proc IMechE Part D: J Automobile Engineering, 1–17. First Published 3 Jul 2017.

Refereed Conference Proceedings

4. **Tongyang Gao**, Shui Yu, Kelvin Xie, Marko Jeftic, Meiping Wang, Ming Zheng, "The Estimation of Nitrogen Oxides Reduction Potential through Enhanced Heat Release Analysis," Proceedings of the ASME 2016 Internal Combustion Engine Fall Technical Conference, ICEF2016, October 9-12, 2016, Greenville, SC, USA.

5. Kelvin Xie, Shui Yu, **Tongyang Gao**, Xiao Yu, Ming Zheng, Liguang Li, "Investigation of Multi-Pole Spark Ignition on Flame Kernel Development and in Engine Operation," Proceedings of the ASME 2016 Internal

Combustion Engine Fall Technical Conference, ICEF2016, October 9-12, 2016, Greenville, SC, USA.

6. **Tongyang Gao**, Kelvin Xie, Shui Yu, Xiaoye Han, Meiping Wang, Ming Zheng, "Characterization of N-Butanol High Pressure Injection From Modern Common Rail Injection System," Proceedings of the ASME 2015 Internal Combustion Engine Division Fall Technical Conference, ICEF2015, November 8-11, 2015, Houston, TX, USA.

7. **Tongyang Gao**, Prasad Divekar, Usman Asad, Xiaoye Han, Graham T. Reader, Meiping Wang, Ming Zheng, Jimi Tjong, "An Enabling Study of Low Temperature Combustion With Ethanol in a Diesel Engine," Proceedings of the ASME 2012 Internal Combustion Engine Division Fall Technical Conference, ICEF2012, September 23-26, 2012, Vancouver, BC, Canada.

8. Xiaoye Han, **Tongyang Gao**, Usman Asad, Kelvin Xie, and Ming Zheng, "Empirical Study of Simultaneously Low NOx and Soot Combustion With Diesel and Ethanol Fuels in Diesel Engine," Proceedings of the ASME 2012 Internal Combustion Engine Division Spring Technical Conference, ICES2012, May 6-9, 2012, Torino, Piemonte, Italy.

9. Shui Yu, Kelvin Xie, Xiaoye Han, Marko Jeftic, **Tongyang Gao**, Ming Zheng, "A Preliminary Study of the Spark Characteristics for Unconventional Cylinder Charge With Strong Air Movement," Proceedings of the ASME 2011 Internal Combustion Engine Division Fall Technical Conference, ICEF2011, October 2-5, 2011, Morgantown, West Virginia, USA.

10. **Tongyang Gao**, Graham Reader, Jimi Tjong, Ming Zheng, "Energy Efficiency Comparison between Butanol and Ethanol Combustion with Diesel Ignition," SAE Technical Paper 2015-01-0859, 2015.

11. **Tongyang Gao**, Marko Jeftic, Geraint Bryden, Graham Reader, Jimi Tjong, Ming Zheng, "Heat Release Analysis of Clean Combustion with Ethanol Ignited by Diesel in a High Compression Ratio Engine," SAE Technical Paper 2016-01-0766, 2016.

12. **Tongyang Gao**, Shui Yu, Hua Zhu, Tie Li, Jimi Tjong, Graham Reader, Ming Zheng, "A Feasibility Study of Using DI Butanol as an Ignition Source for Dual-Fuel Combustion," SAE Technical Paper 2017-01-0770, 2017.

13. Xiaoye Han, **Tongyang Gao**, Ming Zheng and Jimi Tjong, "Fuel Injection Strategies to Enable Low Temperature Combustion in a Light-Duty Diesel Engine," Global Powertrain Congress, Troy, Michigan, November, 2010.

Non-refereed Conference Proceedings

14. **Tongyang Gao**, Xiaoye Han, Meiping Wang, Jimi Tjong, Ming Zheng, "Effect of Port Delivered Ethanol on The Heat Release Rate and Combustion Performance of a High Compression Ratio Diesel Engine," Proceedings of Combustion Institute – Canadian Section, Spring Technical Meeting, University of Windsor, May 12-15, 2014.

15. Marko Jeftic, **Tongyang Gao**, Ming Zheng, "Post Injection Strategies for Increased Power Output of Neat n-Butanol Combustion in a Compression Ignition Engine," Proceedings of Combustion Institute – Canadian Section Spring Technical Meeting, 6 Pages, 2016, Waterloo, ON.

Selected Poster Publications

16. **Tongyang Gao**, Prasad Divekar, Marko Jeftić, Kelvin Xie, Xiaoye Han, Shui Yu, Usman Asad, Dale Haggith, Meiping Wang, "Flexible Operation of HCCI Combustion using Intelligent Control," Auto21 Annual Conference, 2011, Ottawa, ON.

17. **Tongyang Gao**, "Engine Efficiency Improvement for Biofuels in Low Temperature Combustion Application - n-Butanol High Pressure Spray Characterization," BIOFUELNET Annual Conference, 2015, Montreal, QC.

18. Marko Jeftić, **Tongyang Gao**, Kelvin Xie, "Diesel Injector Characterization", NSERC CREATE Program for Clean Combustion Engines, Combustion Summer School, 2014, Toronto, ON.

19. Marko Jeftić, **Tongyang Gao**, Shui Yu, "Theme 2: Diesel and Diesel-Electric Power Train," Annual General Meeting: ORF-RE: Green Auto Powertrain, 2010, Waterloo, ON.

20. **Tongyang Gao**, Xiaoye Han, "Clean Combustion of Renewable Ethanol in Diesel Engines, Theme 2: Diesel and Diesel-Electric Power Train," Annual General Meeting: ORF-RE: Green Auto Powertrain, 2012, Windsor, ON.

21. Prasad Divekar, Fangfang Lin, **Tongyang Gao**, Qiaochu Han, Marko Jeftić, Arturo Mendoza, Kelvin Xie, Xiaoxi Zhang, Usman Asad, Raj Kumar, Clarence Mulenga, Meiping Wang, Shui Yu, "Clean Diesel Engine Technologies: Past, Present, Future and Beyond," 10th Year Canada Research Chairs - Thinking Ahead for a Strong Future Conference Series: Ontario Region, 2010, Toronto, ON.

VITA AUCTORIS

NAME: Tongyang Gao

PLACE OF BIRTH: Changchun, Jilin, China

YEAR OF BIRTH: 1983

EDUCATION: Tsinghua University, B.Sc., Beijing, China, 2006

                         University of Windsor, M.Sc., Windsor, ON, Canada, 2012

                         University of Windsor, Ph.D., Windsor, ON, Canada, 2017